On-Shell Methods for Perturbative QCD

A thesis presented for the degree of

Doctor of Philosophy

by

Simon D. Badger

Institute for Particle Physics Phenomenology

University of Durham

August 2006

Durham University

Abstract

We present new on-shell techniques for the calculation of colour ordered helicity amplitudes in QCD. We review the methods of on-shell recursion and the MHV rules before applying them to tree-level processes within the Standard Model. The MHV rules are applied to QCD corrections to Higgs amplitudes in the heavy top quark limit at tree-level, generating simple n-point expressions for specific helicity configurations as well as developing more generally applicable recursion relations. We then generalise the on-shell recursion relations for massless QCD to include massive propagating particles and apply them to amplitudes with massive scalar particles, vector bosons and fermions. We then apply on-shell methods to compute the cut-constructible parts of 1-loop Higgs plus multi-gluon amplitudes fixing the remaining rational terms through Feynman diagrams. In all cases we find that the on-shell methods generate simpler analytic expressions than the traditional off-shell methods.

Acknowledgements

Thanks must firstly go to my supervisor Nigel Glover whose guidance and advice has been invaluable throughout the course of my time at Durham. Thanks also go to Valya Khoze who has always been there to help discuss problems and offer advice and to Peter Svrček for his input into the work on recursion relations for massive particles.

Thanks also to my family and friends for all the help and support they have offered over the last three years.

The work presented here was supported by the award of a PPARC studentship.

Declaration

I declare that no material presented in this thesis has previously been submitted for a degree at this or any other university.

The research described in this thesis was carried out in collaboration with Professor E.W.N. Glover, Professor V.V. Khoze and Dr P. Svrček. Aspects of chapters 3,4 and 5 are based on the following published works:

- S. D. Badger, E. W. N. Glover and V. V. Khoze, *MHV rules for Higgs plus multi-parton amplitudes*, *JHEP* **03** (2005) 023 [`hep-th/0412275`].
- S. D. Badger, E. W. N. Glover, V. V. Khoze and P. Svrček, *Recursion relations for gauge theory amplitudes with massive particles*, *JHEP* **07** (2005) 025 [`hep-th/0504159`].
- S. D. Badger, E. W. N. Glover and V. V. Khoze, *Recursion relations for gauge theory amplitudes with massive vector bosons and fermions*, *JHEP* **01** (2006) 066 [`hep-th/0507161`].
- S. D. Badger and E. W. N. Glover, *One-loop helicity amplitudes for $H \to$ gluons: the all minus configuration*, Talk presented at Loops and Legs 2006, Zinnowitz, Germany [`hep-ph/0607139`].

"The theory of general relativity describes the theory of gravity and the large scale structures of the universe, that is structures on scales from only a few miles to as large as a million million million million miles, the size of the observable universe." - A Brief History of Time, Stephen Hawking

"A million million million million things! I get to about 12 or 13 things, my eyes start to glaze over and I have to sit down and eat a Pringle™ sandwich, crush-crush-crush, yum-yum-yum-yum." - Bill Bailey

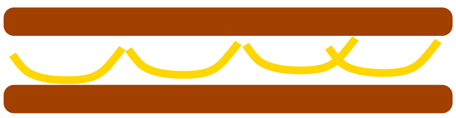

"crush-crush-crush, yum-yum-yum-yum"

Contents

List of Figures

List of Tables

1. Introduction

Quantum Mechanics and Relativity have been the most influential ideas in our understanding of the physical world over the last 100 years. Modern particle physics applies in a regime where we need to use both of these theories together and formulate so called *Quantum Field Theories* to describe the observations we see in nature. Currently the best model describing the dynamics of the fundamental particles of nature is the Standard Model: an interacting quantum field theory invariant under local transformations of the gauge group $SU(3) \times SU(2) \times U_Y(1)$.

The strong interaction of nuclear particles is described by the $SU(3)$ sector and is known as QCD. The electro-weak sector of the standard model ($SU(2) \times U_Y(1)$) describes the electro-magnetic and weak forces. This sector of the Lagrangian is predicted to be broken spontaneously by the Higgs potential. The scalar field associated with this potential is the Higgs boson - the only particle yet to be observed in the standard model.

The standard model has been extremely successful and has resulted in the most accurate predictions ever made by a physical model. Processes in high energy physics are generally studied through collider experiments which have either been in the form of linear colliders or circular, synchrotron colliders. At the present time the most important colliders for probing the Higgs sector and searching for new physics are the Tevatron at Fermilab and the LHC (Large Hadron Collider) at CERN (from around summer 2007). Both of these machines are synchrotron hadron-hadron colliders, with a centre of momentum energies of 2 Tev (Tevatron) and 14 Tev (LHC). The advantage of colliding massive nuclear particles is that these high energies can be achieved, however the proton is not an elementary particle and therefore signals from such machines are usually extremely complicated.

Observations at hadron colliders involve collisions of composite particles. In order to link these collisions with the matrix elements of the elementary fields, one introduces a factorisation scale which splits the interaction into long range effects concerned with the hadron structure and short range effects which can be calculated perturbatively since QCD is asymptotically free. The total cross section is therefore written as:

$$\sigma(h_1 h_2 \to X) = \sum_{p_1=\{g,u,d,\dots\}} \sum_{p_2=\{g,u,d,\dots\}} \int_0^1 d\xi_1 \int_0^1 d\xi_2$$
$$f_{h_1}^{(p_1)}\left(\xi_1, \mu_F^2\right) f_{h_2}^{(p_2)}\left(\xi_2, \mu_F^2\right) \widehat{\sigma}(p_1 p_2 \to X; \frac{\mu_F^2}{Q^2}, \frac{\mu_R^2}{Q^2}, Q^2) \qquad (1.1)$$

where h_1 and h_2 are the two initial state hadrons and X is some generic (infra-red safe) final state.

A schematic picture of this factorisation is shown in figure 1.1. $f_h^{(p)}(\xi, \mu_F^2)$ are the parton distribution functions (PDFs) which give the probability of finding the parton p within the hadron, h, at a given momentum fraction ξ and factorisation scale μ_F^2. The partons p_1 and p_2 then enter the hard scattering cross section with a momentum $p_1 = \xi_1 P_1$ and $p_2 = \xi_2 P_2$ respectively. The PDFs are non-perturbative objects which must be determined experimentally. The factorisation scale μ_F is such that the evolution of the parton densities can be calculated perturbatively. Much of the work to determine the precise structure of the PDFs has been done at the eP collider HERA using deep inelastic scattering, global analyses of all data are available to NNLO accuracy from MRST [1, 2] and the CTEQ [3] collaborations. The dependence of the PDFs on μ_F^2 however is understood perturbatively and is governed by the Altarelli-Parisi splitting kernels [4]. Recently these kernels have been computed to 3-loop accuracy by Moch, Vogt and Vemaseren [5, 6] which is vital when evolving the PDFs from the relatively low energies at HERA to the high energies at the LHC.

The confinement property of the strong interaction ensures observed final states will always be in the form of colourless hadrons which form through a complicated non-

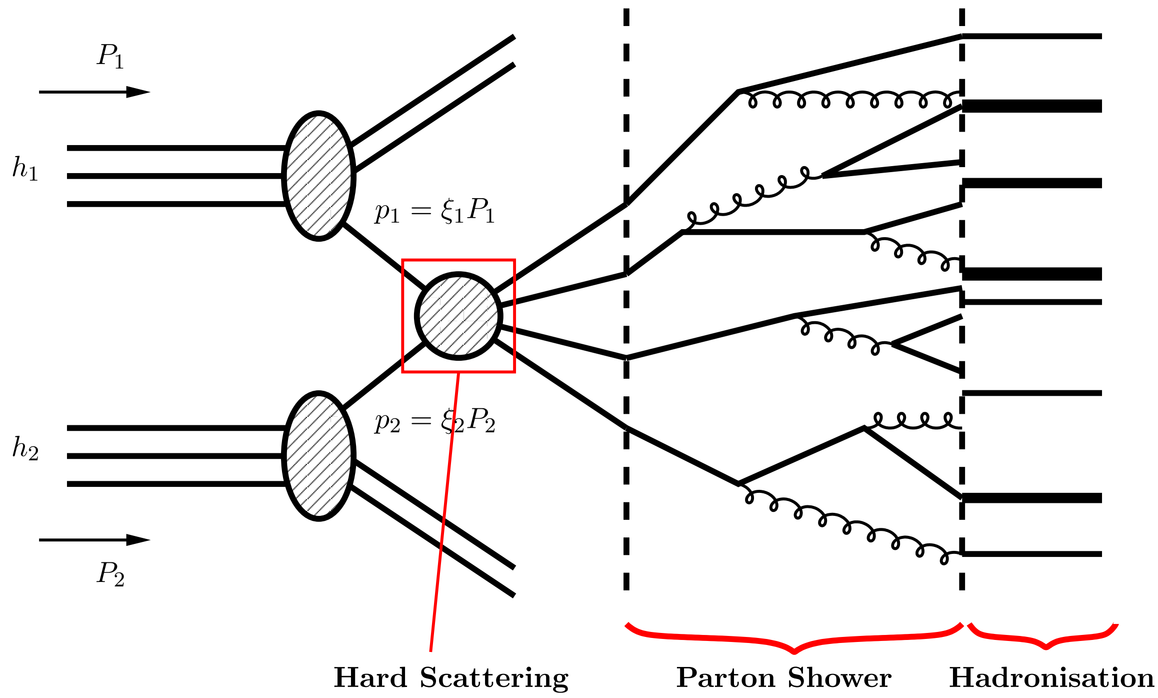

Figure 1.1: Schematic depiction of the factorisation of hadron/hadron collisions.

perturbative process known as *hadronisation*. The energetic, "hard", scattering process therefore results in the final state fragmenting into hadrons with high transverse momentum forming *jets*. Fragmentation of the hard partons occurs through the emission of soft radiation away from the hard interaction point and this stage of the scattering process is modelled by parton showering Monte Carlo (MC) algorithms. Examples of such MC event generators are SHERPA, PYTHIA and HERWIG, which take the hard matrix elements and interface them with parton showers and hadronisation. One extremely important area of research is to extend these MC programs to NLO accuracy where the problem of matching the matrix elements to the parton shower becomes highly non-trivial. MC@NLO is currently the only MC event generator to address such problems and has been applied successfully to a small number of processes.

This is in fact a much simplified picture of what is really happening. Real MC event generators must model the part of the final state coming from the hadron remnants (called the underlying event) and account for initial state radiation and subsequent parton showering where the parton from the incoming hadron loses some energy by radiating collinear partons before the hard scattering. The underlying event is generally made of low energy soft hadrons and so, as with the parton distribution functions, is modelled using experimental data. The factorisation (1.1) is actually only the leading order contribution to the expansion in Q^2. One can imagine events where two partons from each hadron would separately interact and we could have a double scattering process. Such terms are called *higher twist* contributions and are suppressed by a factor of $\frac{1}{Q^2}$ or more with respect to the leading twist term, although they can be extremely important at low values of ξ and Q^2.

The parton level cross section is related to the square of the matrix element:

$$\begin{aligned}\widehat{\sigma}(p_1p_2 \to q_3 \dots q_n) =& \frac{\mathcal{S}}{2\widehat{s}} \int \prod_{i=3}^{n} \frac{d^3 q_i}{2(2\pi)^3 E_i} \\ & (2\pi)^4 \delta^{(4)}(p_1 + p_2 - \sum_{i=3}^{n} q_i) |\mathcal{M}(p_1p_2 \to q_3 \dots q_n)|^2, \end{aligned} \tag{1.2}$$

where p_1 and p_2 are the two incoming partons and $q_3, \dots, q_n$ are the $n-2$ particles in the final state. $\widehat{s}$ is the centre of mass energy of the hard interaction and $\mathcal{S}$ is a symmetry factor associated with identical particle in the final state. Both the matrix element and the phase space are invariant under Lorentz transformations.

In this thesis we will be concerned with calculating the matrix elements $\mathcal{M}$ rather than its integration over the phase space. The need for accurate predictions for QCD scattering cannot be over stated. If we hope to disentangle any new physics from LHC experiments one must predict the large backgrounds to the relevant processes. However the problem of calculating QCD accurately is an extremely difficult one. Calculations in perturbation theory beyond leading order are plagued with ultraviolet and infrared divergent loop integrals. Calculating these matrix elements with a high number of external particles has been very difficult as the traditional methods are cumbersome and produce extremely large intermediate expressions which must be dealt with analytically in order to handle the divergent terms consistently. The purpose of studying on-shell methods in QCD is therefore to try and find a workable algorithm for automating the calculations of NLO matrix elements which could then be interfaced with some MC parton shower/hadronisation program to produce accurate predictions of the large QCD backgrounds.

In the first chapter we will briefly introduce the central concepts of QCD as a non-abelian gauge theory and quantum field theory, describing the divergences that occur and how one can get around them. We will also review some of the on-shell techniques, namely the on-shell recursion relations and MHV rules.

The second and third chapters are devoted to two specific applications of the on-shell methods to SM tree level amplitudes with large numbers of external legs. Chapter 3 shows how to accommodate Higgs bosons into the MHV formalism and calculate LO predictions important for decay of Higgs bosons to many jets. Chapter 4 makes an important generalisation of the on-shell recursion relations to accommodate massive particles. This is done for particles with either spin 0,1 or 1/2. Clearly amplitudes involving massive fermions and vector bosons are extremely important in SM processes where the top quark and electro-weak bosons $W^{\pm}, Z$ have very large masses. Since the coupling of the Higgs boson to SM particles is proportional the mass of the particular particle these processes will be very important in channels for Higgs discovery at the LHC. Chapter 5 is concerned with applying the on-shell methods at 1-loop to calculate all multiplicity results for the "cut-constructible" components of amplitudes with a single Higgs boson coupling to gluons. The full amplitudes for up to 4 partons are given by computing the remaining rational terms using a Feynman diagram approach.

2. Background

2.1. Basics of Perturbative QCD

QCD is an $SU(N_C)$ gauge theory of quarks and gluons with quarks transforming in the fundamental representation and the gluons transforming in the adjoint representation. The most general renormalisable Lagrangian is written as,

$$\mathcal{L} = -\frac{1}{4} G^a_{\mu\nu} G^{a,\mu\nu} + \sum_{f=1}^{n_f} \bar{\psi}_f (i\not{\mathbf{D}} - \mathbb{1} m)\psi_f + \mathcal{L}_{gauge} - \frac{N_F \theta_s}{32\pi^2} G^a_{\mu\nu} \tilde{G}^{a,\mu\nu} \tag{2.1}$$

where ψ_f are the quark fields and the $N_c^2 - 1$ gluon fields, A^a_μ, appear in the covariant derivative,

$$\begin{aligned} \mathbf{D}_\mu &= \mathbb{1}\partial_\mu - ig\mathbf{T}^a A^a_\mu \\ -ig\mathbf{T}^a G^a_{\mu\nu}\psi &= [\mathbf{D}_\mu, \mathbf{D}_\nu]\psi. \end{aligned} \tag{2.2}$$

The final term in the Lagrangian is permitted since it is both gauge invariant and renormalisable, however it violates CP symmetry and is the origin of the so-called strong CP problem as experimentally θ is observed to be extremely close to zero. This term plays no role in perturbative studies since the Feynman expansion of the vertex vanishes, and hence will not contribute to the calculations presented in this thesis.

The gauge dependent part of the Lagrangian is quite complicated for non-abelian gauge theories. The problem is that in quantising the theory one assumes that the gauge fields have four degrees of freedom whereas gauge invariance actually constrains two of these degrees of freedom. The result is that the over counting in the degrees of freedom must be compensated by the addition of a gauge fixing term and, particular to non-Abelian theories, terms involving a ghost field c,

$$\mathcal{L}_{gauge} = -\frac{1}{2\xi}(\partial^\mu A^a_\mu)^2 - c^a \partial^\mu D^{ab}_\mu c^b. \tag{2.3}$$

For the calculations in chapters 3 and 4 we will choose to work in a gauge where such terms are irrelevant and we do not need to worry about the ghost fields. This gauge is defined by the choice of spinor representation of the polarisation vectors as discussed in section 2.2. To be precise one needs to consider these terms carefully when renormalising QCD and computing the running coupling. However, for the sake of simplicity, these terms will be dropped in all subsequent discussions.

In this thesis we will be concerned with calculating matrix elements perturbatively as an expansion in $\alpha_s = g^2/4\pi$. Traditionally this means decomposing each scattering amplitude into Feynman diagrams and applying the associated computation rules. This is a diagrammatic application of Wick's theorem which helps to reduce the correlation functions to a sum of all possible connection of propagators and vertices. This approach is termed *off-shell* as the correlation functions are related to the cross-section via the LSZ reduction formula which strips off the external wave-functions. Momentum conservation is therefore applied after the evaluation of the individual diagrams and large cancellations often occur between diagrams. The Feynman rules for QCD in momentum space can be found in many places, for instance see p.801-803 of reference [7].

2.1.1. Renormalisation of UV divergences and the running coupling

When calculating scattering amplitudes perturbatively in an interacting quantum field theory past leading order we often encounter UV divergences due to loop integrals of the form:

$$\int_0^\Lambda \frac{d^4 l}{(l^2 - m^2)((l+k)^2 - m^2)} \sim \log(\Lambda) \underset{\Lambda\to\infty}{\to} \infty \tag{2.4}$$

Although this feature appears to be a serious failure, as long as physical observables are finite this is not really a problem at all. In fact it turns out that in interacting field theories the parameters in the Lagrangian are not the physical ones and by rescaling these parameters we can remove all such UV singularities. This procedure is known as *Renormalisation* and is only possible when a finite number of sub-processes diverge, even though divergences may occur at every order in the perturbative series. In particular there cannot be more divergent processes than there are parameters in the Lagrangian in which to absorb them.

To understand this problem in QCD it is necessary to study quantum corrections to both the fermion and gluon propagators as well as the interaction vertices. For a free field theory we know that the 2-point correlation function can be directly interpreted as the amplitude for a particle to travel from a point x to a point y. So a free theory of fermions would have the following relation:

$$\int d^4x e^{ip\cdot x} \langle 0|\mathrm{T}\{\psi(x)\bar{\psi}(0)\}|0\rangle = \frac{i(\not{p} + m_0)}{p^2 - m_0^2 + i\epsilon} \tag{2.5}$$

where m_0 is the mass parameter in the Lagrangian. If we introduce interactions into the theory this interpretation no longer applies as the propagator receives radiative corrections from interactions with virtual gluons. In this situation we find that the 2-point correlation function is now modified to have the form [7],

$$\int d^4x e^{ip\cdot x} \langle 0|\mathrm{T}\{\psi(x)\bar{\psi}(0)\}|0\rangle = \frac{iZ_2(\not{p} + m)}{p^2 - m^2 + i\epsilon} + (\text{branch cuts and bound states}). \tag{2.6}$$

The effect of such corrections is to shift the pole of the propagator, i.e. the mass, to that of its physical value, m. The residue of this pole, Z_2, is the *wave function renormalisation* and it is this quantity we will need to compute if we hope to cancel UV divergences.

Let us now consider the perturbative contributions to the fermion propagator in momentum space. We can write this in terms of 1-particle irreducible diagrams, which are diagrams which cannot be split into two distinct diagrams by cutting a single propagator. Examples of diagrams in this class are shown in figure 2.1. Denoting the sum of

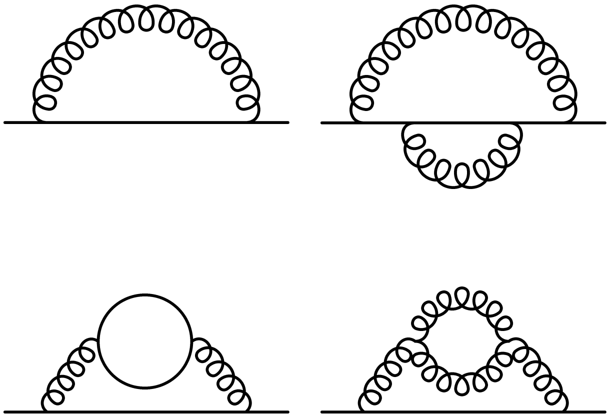

Figure 2.1: Examples of 1-particle irreducible diagrams contributing to the full fermion propagator.

such diagrams as $-i\Sigma(p)$, then the fermion propagator becomes:

$$\begin{aligned}\int d^4x \langle 0|\psi(x)\bar{\psi}(0)|0\rangle e^{ip\cdot x} &= i\frac{\not{p}+m_0}{p^2-m_0^2} + i\frac{\not{p}+m_0}{p^2-m_0^2}(-i\Sigma(p))i\frac{\not{p}+m_0}{p^2-m_0^2} + \dots \\ &= \frac{i}{\not{p}-m_0}\sum_{k=0}^{\infty}\left(\frac{\Sigma(\not{p})}{\not{p}-m_0}\right)^k \\ &= \frac{i}{\not{p}-m_0-\Sigma(\not{p})} \end{aligned} \tag{2.7}$$

so we define the physical mass by the pole of the full propagator,

$$\left[\not{p}-m_0-\Sigma(\not{p})\right]_{\not{p}=m} = 0 \tag{2.8}$$

and by computing the residue* of the propagator we can identify the wave function renormalisation as defined in equation (2.6),

$$Z_2 = \frac{1}{1-\Sigma'(m)}. \tag{2.9}$$

This rescaling of the propagator manifests itself in all amplitude calculations so that in order to find the physical scattering amplitude we must re-scale all the correlation

*Given a function $f(z) = h(z)/g(z)$ where $g(z)$ and $h(z)$ are analytic functions with $h(z_0) \neq 0, g(z_0) = 0$ and $g'(z_0) \neq 0$ then $\mathrm{Res}(z = z_0; f(z) = h(z_0)/g'(z_0))$ [8]

functions by this factor. Z_2 will absorb UV divergences like the ones seen in eq. (2.4) and must be computed at each order in the perturbation series.

Other divergences are absorbed in the re-scaling of the gluon propagator, Z_3, and vertex contribution Z_1 (for the qqg vertex) and Z_{3g}, Z_{4g} for the self interaction vertices. In order to be completely general we would also need to re-scale the ghost fields and associated couplings as well as the gauge fixing parameter. As we have seen in the analysis of the fermion propagator the physical values of the parameters m and g can be determined from these re-scalings and the bare quantities themselves.

To see how the coupling is shifted with the re-scaling one must consider the gluon propagator in a similar fashion to the analysis of the fermion propagator given above. Defining the 1-particle irreducible contributions as[†] $-i\Pi^{\mu\nu}(p) = -i(p^2 g^{\mu\nu} - p^\mu p^\nu)\Pi(p^2)$ we can write (omitting colour factors),

$$\begin{aligned}\int d^4x e^{ip\cdot x}\langle 0|A^\mu(x)A^\nu(0)|0\rangle &= \frac{-ig^{\mu\nu}}{p^2} + \frac{-ig^{\mu\rho}}{p^2}\left[-i(p^2 g_{\rho\sigma} - p_\rho p_\sigma)\right]\Pi(p^2)\frac{-ig^{\sigma\nu}}{p^2} + \dots \\ &= \frac{-ig^{\mu\nu}}{p^2}\frac{1}{1-\Pi(p^2)} \end{aligned} \tag{2.10}$$

The renormalisation of the gluon field strength is then defined by the residue of the propagator at $p^2 = 0$,

$$Z_3 = \frac{1}{1-\Pi(0)}. \tag{2.11}$$

Importantly (2.10) shows that the gluon remains massless at all orders in perturbation theory. Since the gluon propagator will always be present in association with two interaction vertices we can consider that Z_3 can be interpreted as a rescaling of the coupling g_0 at low energies:

$$\frac{Z_2^2}{Z_1^2}\alpha_0 \frac{g^{\mu\nu}}{p^2(1-\Pi(p^2)} \underset{p^2\to 0}{\to} \frac{Z_2^2 Z_3}{Z_1^2}\alpha_0\frac{g^{\mu\nu}}{p^2} \tag{2.12}$$

so we can write the renormalised coupling as $\alpha_R(p^2 = 0) = Z_3 Z_2^2/Z_1^2\alpha_0$. At finite energies we can identify a very important property of interacting quantum field theory

[†]The allowed tensor structures are restricted by the Ward identity

namely the running of the coupling constant:

$$\alpha(p^2) = \alpha(0)\frac{Z_3}{1-\Pi(p^2)} \overset{\mathcal{O}(\alpha)}{\approx} \frac{\alpha(0)}{1-[\Pi_2(p^2)-\Pi_2(0)]}, \tag{2.13}$$

where Π_2 is the leading order contribution to Π. This implies that the coupling constant changes with energy which will have a serious effect on the validity of perturbative expansions.

The renormalised Lagrangian

Re-defining the parameters and fields in the Lagrangian to account for the effect radiative corrections results in a modified set of Feynman rules, which will result in UV finite scattering amplitudes. We take the bare QCD Lagrangian as,

$$\mathcal{L}_0 = -\frac{1}{2}\mathrm{tr}(G_0^{\mu\nu}G_{0;\mu\nu}) + \bar{\psi}_0(i\not{D}_0 - m_0)\psi_0 \tag{2.14}$$

where $D_{0;\mu} = \partial_\mu - ig_0T^aA^a_{0;\mu}$ and $G_{0;\mu\nu} = -\frac{i}{g}[D_{0;\mu}, D_{0;\nu}]$. We now re-define the fields and parameters according to,

$$\begin{aligned}
\psi_0 &= \sqrt{Z_2}\psi = (1+\delta_2)^{1/2}\psi \\
A_0^\mu &= \sqrt{Z_3}A^\mu = (1+\delta_3)^{1/2}A^\mu \\
Z_2\sqrt{Z_3}g_0 &= Z_1 g = (1+\delta_1)g \\
Z_2 m_0 &= m + \delta_m
\end{aligned} \tag{2.15}$$

where the re-scaling of the coupling is defined through the exact gluon-fermion vertex . Substituting these relations into the bare Lagrangian results in a renormalised Lagrangian which includes extra *counter-terms* which compensate the UV divergences found in the higher order corrections,

$$\begin{aligned}
\mathcal{L} = &-\frac{1}{2}\mathrm{tr}(G^{\mu\nu}G_{\mu\nu}) + \bar{\psi}(i\not{D} - m)\psi \\
&+ \bar{\psi}(i\delta_2\not{\partial} - \delta_m)\psi - \frac{1}{4}\delta_3(\partial_\mu A^a_\nu - \partial_\nu A^a_\mu) \\
&+ g\delta_1\bar{\psi}T^a\not{A}^a\psi - g\delta_1^{3g}f^{abc}\partial_\mu A^a_\nu A^{b,\mu}A^{c,\nu} - g\delta_1^{4g}f^{abc}f^{cde}A^a_\mu A^b_\nu A^{d,\mu}A^{e,\mu}
\end{aligned} \tag{2.16}$$

Each of these counter-terms, δ_i, must be evaluated at each order in the perturbation series. They are evaluated using renormalisation conditions which fix the residues of the propagators, the fermion mass and the colour charge at their physical values.

It is here that we need to be a little more careful. Throughout the course of this thesis we will consider QCD with massless fermions, in this case the residues of the fermion propagator are not well defined on shell, at $p^2 = 0$, so we are forced to choose an arbitrary scale, say μ^2, at which to evaluate the residues. This appears to be a rather strange definition of the masses and couplings but as long as the correlation functions are independent of this *renormalisation scale* then this as good a choice as was made in equations (2.8) and (2.11). The renormalisation conditions are now written as:

$$\begin{aligned} \Sigma(\mu^2) &= 0 \\ \frac{d\Sigma}{dp^2}(\mu^2) &= 0 \\ \Pi(\mu^2) &= 0 \\ -ig\Gamma^\mu((p-p')^2 = \mu^2) &= -ig\gamma^\mu \end{aligned} \tag{2.17}$$

where the 1-particle irreducible diagrams include contributions from the counter-terms.

The condition that this renormalised perturbation theory is independent of the renormalisation scale is encompassed in the Callan-Symanzik equation which looks at the infinitesimal changes of the Green's functions with the choice of scale. This can be written as:

$$\left(\mu\frac{\partial}{\partial\mu} + \beta(g)\frac{\partial}{\partial g} + n\gamma_q(g) + m\gamma_g(g)\right) G^{(n,m)}(\{x_i\}, \mu, g) = 0 \tag{2.18}$$

where $G^{(n,m)}$ are the renormalised Green's functions of n fermion fields and m gluon fields. The functions $\beta(g)$ and $\gamma_x(g)$ are extremely important and govern the running coupling and anomalous dimensions respectively. Solving the Callan-Symanzik equation for the two point function leads to the following interpretation of the β function,

$$\beta(\bar{g}) = 2\frac{d\bar{g}}{d(\log p^2/\mu^2)} \tag{2.19}$$

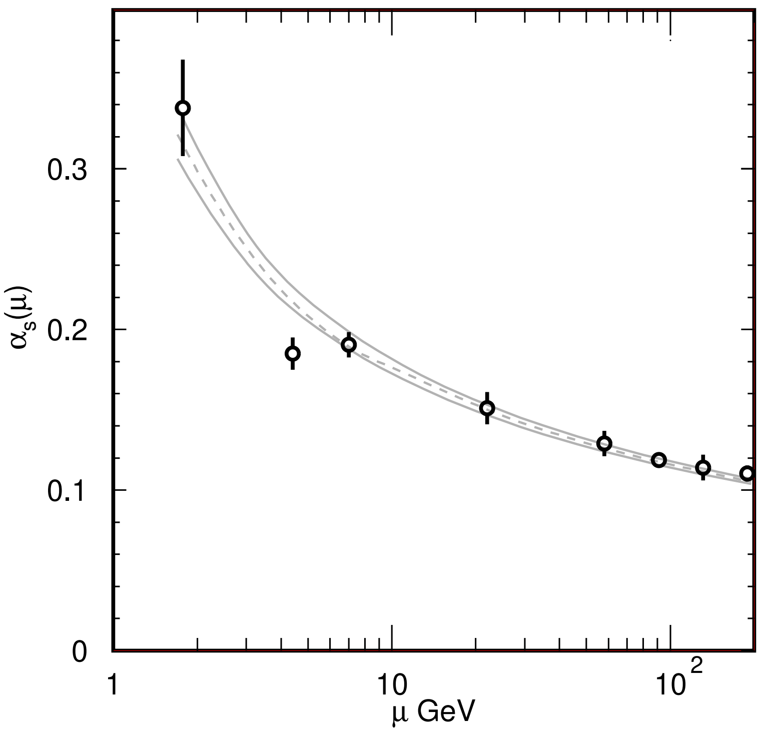

Figure 2.2: The running of the QCD coupling constant taken from the PDG review 2004 [9]. α_s is measured at M_Z and the running coupling is determined by solving the renormalisation group equation to two loop order, shown by the dashed line. The latest world average gives $\alpha_s(M_Z) = 0.1187(20)$.

where $\bar{g}$ is a modified coupling constant which satisfies $\bar{g}(\mu^2) = g$. This is known as the renormalisation group equation and it determines precisely the dependence of the coupling on energy scale which we pointed out in equation (2.13). Expanding $\beta(g)$ in the coupling we can then solve (2.19) to leading order as:

$$\bar{\alpha}_s(p^2) = \frac{\alpha_s(\mu^2)}{1 - \beta_0 \alpha_s(\mu^2)/(2\pi) \log(p^2/\mu^2)} \tag{2.20}$$

where $\beta(g) = -g^3/(4\pi)^2\beta_0 - g^5/(4\pi)^4\beta_1 + \ldots$ and $\alpha_s = g^2/4\pi$

The beta function can be evaluated by computing the coefficients of the counter-terms. In order to do this one needs to introduce a regulator to handle the cancellation of UV divergences in the various diagrams. By far the most common of these is to use a dimensional regularisation where one notices that, although the integral (2.4) diverges in 4 dimensions, if we compute it in d dimensions the integral is finite. After all divergent integrals have been computed and the counter terms subtracted the expression will be finite as $d \to 4$. This is normally achieved by setting $d = 4 - 2\epsilon$ and looking at the poles in ϵ. Details of dimensional regularisation can be found in Appendix A. Such techniques result in,

$$\beta_0 = \frac{11N_c - 2N_F}{3}. \tag{2.21}$$

In the standard model where $N_F = 6$ and $N_c = 3$ we see that β_0 is negative in stark contrast to a similar analysis of QED. This results in the coupling in QCD becoming weaker as the energy is increased, a phenomenon known as *asymptotic freedom*, shown in figure 2.2. Clearly this is an extremely important result for perturbative studies of QCD. Although at low energies the coupling constant is large and the perturbation series is not defined, we can use perturbative techniques to compute the hard scattering processes relevant for high energy interactions.

2.1.2. Cancellation of Infra-Red divergences

Loop integrals also suffer from infra-red divergences. This occurs when massless propagators appear in the integral:

$$\int_{\Lambda_{\mathrm{IR}}}^{\Lambda_{\mathrm{UV}}} \frac{d^4k}{k^2} \underset{\Lambda_{\mathrm{IR}} \to 0}{\longrightarrow} \infty. \tag{2.22}$$

The origin of such singularities lies in the incorrect definition of asymptotic states in the S-matrix which are considered to be free states. Infra-red singularities also occur in tree matrix elements at extreme points in the phase space where one of the invariant masses in the propagators vanishes. For example consider a process where a massless quark couples to a gluon as shown in figure 2.3. The invariant mass of the off-shell quark can be written as,

$$s_{qg} = (p_q + p_g)^2 = 2p_q \cdot p_g. \tag{2.23}$$

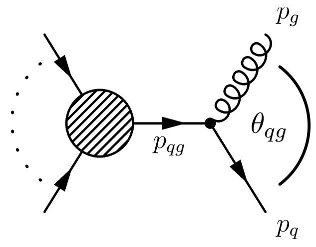

Figure 2.3: Sub-diagram contributing in the IR limit $s_{qg} \to 0$.

Parameterising p_q and p_g as,

$$p_q = E_q(1, \widehat{\mathbf{p}}_q), \quad p_g = E_g(1, \widehat{\mathbf{p}}_g) \quad \Rightarrow \quad s_{qg} = 2E_g E_q(1 - \cos\theta_{qg}) \tag{2.24}$$

Therefore the matrix element will diverge either when,

- $\theta_{gq} \to 0$, i.e. emitted partons are *collinear*
- $E_g \to 0$, i.e. the gluon is emitted *soft* (soft emission cannot occur for quarks).

These IR divergences are classified as virtual (from loop integrals) and real emission (from soft and collinear divergences). In any observed cross section these divergences must cancel and give a finite result. The physical interpretation of this is the fact that a detector will always have some minimum resolution below which the two processes are indistinguishable hence the observed n-particle cross section is:

$$\sigma^n_{\text{obs}} = \sigma^n_{\text{virtual}} + \lim_{\substack{m \text{ soft or} \\ \text{collinear}}} \left(\sigma^{n+m}_{\text{real}}\right). \tag{2.25}$$

Theorems due to Bloch and Nordsieck [10] and Kinoshita [11], Lee and Nauenberg [12] prove that the IR divergences present in each component must cancel to all orders in perturbation theory. Clearly we still need to regulate the divergent integrals but luckily the dimensional regularisation scheme works equally well for IR divergences.

We must include unresolved contributions up to the order in perturbation theory which we wish to calculate. For instance, at one loop, one must include all real emission diagrams which are *single unresolved*. This includes single soft emission and double collinear emission which is at equivalent order in α_s to the loop corrections. The real emission diagrams must be integrated over the unresolved phase space:

$$\sigma_n^{\rm NLO} = \sigma_{n,\rm virtual}^{(1)} + \int dLIPS(1)\sigma_{n+1,\rm real}^{(0)}. \tag{2.26}$$

At two loops the situation is more complicated as we must include single unresolved contributions at 1-loop and double unresolved contributions at tree level,

$$\sigma_n^{\rm NNLO} = \sigma_{n,\rm virtual}^{(2)} + \int dLIPS(1)\sigma_{n+1,\rm real}^{(1)} + \int dLIPS(2)\sigma_{n+2,\rm real}^{(0)}. \tag{2.27}$$

The behaviour at the amplitude level in the various soft/collinear limits can be categorised by splitting functions. These functions contain all the divergent quantities in the given limit and we see the extremely important factorisation of scattering amplitudes. For example, collinear limits at tree level are described by,

$$\begin{aligned}\mathcal{A}_n^{(0)}&(p_1^{\lambda_1},\ldots,p_j^{\lambda_j},p_{j+1}^{\lambda_{j+1}},\ldots,p_n^{\lambda_2})\\ &\underset{j||j+1}{\longrightarrow} \sum_{h=\pm} {\rm Split}^{(0)}(P^{-h};p_j^{\lambda_j},p_{j+1}^{\lambda_{j+1}})\mathcal{A}_{n-1}^{(0)}(p_1,\ldots,P^h,\ldots,p_n)\end{aligned} \tag{2.28}$$

where $p_j + p_{j+1} \to P$ in the collinear limit. This is the indication of quite an important result, because real emission divergences are proportional to the tree level amplitude, the IR divergences from the virtual contributions must also be proportional to the tree level amplitude in order for the cancellation to proceed as expected [13, 14],

$$\mathcal{A}_n^{(1)} = \mathcal{A}_n^{(0)} I_n^{(1)} + \mathcal{O}(\epsilon^0) \tag{2.29}$$

where ϵ is the dimensional regularisation parameter. $I^{(1)}$ contains all of the poles in ϵ and can be written down in many cases for generic processes. This feature has been generalised to two and three loops by appealing to exponentiation of the soft factors of the scattering amplitude [15].

2.1.3. Unitarity techniques for loop amplitudes

Exploiting the unitarity of scattering amplitude has been an extremely useful tool in many areas of quantum field theory. The Cutkosky rules [16] provide a way to calculate discontinuities in amplitudes by performing simple phase space integrals of the products of two tree amplitudes. The fact that the tree amplitudes are on-shell rather than off-shell Feynman diagrams means that we can exploit the large cancellations that occur between tree level Feynman diagrams and derive more compact loop amplitudes.

Using the Cutkosky rules we can write the discontinuity of an amplitude $\mathcal{A}_n^{(1)}$ across the $s_{i,j} = (p_i + \ldots + p_j)^2$ branch cut as:

$$\text{Disc}\mathcal{A}_n^{(1)} = (2\pi)^2 i \int \frac{d^D l_1}{(2\pi)^D} \delta^{(+)}(l_1^2)\delta^{(+)}(l_2^2)\mathcal{A}(-l_1, p_i, \ldots, p_j, l_2)\mathcal{A}(-l_2, p_{j+1}, \ldots, p_{i-1}, l_1), \tag{2.30}$$

where $\delta^{(+)}$ represents the positive energy branch of the delta function and momenta are labelled cyclically. l_2 is given by $l_2 = l_1 + p_{i,j}$. Figure 2.4 gives a diagrammatic representation of this cut. This discontinuity will only reproduce the imaginary part of any terms in the amplitude that have branch cuts such as logarithms, i.e. $\ln(z) = \ln(|z|) - i\pi$. In order to reproduce the full logarithm we replace the cut propagators with the full $1/l^2$ propagator [17]:

$$\mathcal{A}_n^{(1)}|_{p_{i,j}\text{ cut}} = \int \frac{d^D l_1}{(2\pi)^D} \frac{1}{l_1^2}\mathcal{A}(-l_1, p_i, \ldots, p_j, l_2)\frac{1}{l_2^2}\mathcal{A}(-l_2, p_{j+1}, \ldots, p_{i-1}, l_1), \tag{2.31}$$

Unitarity based methods for computing helicity amplitudes have been extremely successful, particularly in supersymmetric theories where entire amplitudes can be reconstructed from the cuts (in 4 dimensions) [18, 19]. Surprisingly simple expressions for amplitudes in $\mathcal{N} = 4$ [17, 20, 21] and $\mathcal{N} = 1$ [18] have been derived. Indeed it is possible to show that in the case of $\mathcal{N} = 4$ SYM amplitudes 1-loop amplitudes must be of the form:

$$\mathcal{A}_n^{\mathcal{N}=4,(1)} = \sum_i c_i I_{4,i} \tag{2.32}$$

where I_4 are scalar box integrals. For $\mathcal{N} = 1$ supersymmetric amplitudes we also find terms proportional scalar triangle and bubble integrals.

For non-supersymmetric amplitudes the situation is more difficult as the cuts must be evaluated to higher order in the dimensional regularisation parameter ϵ in order that

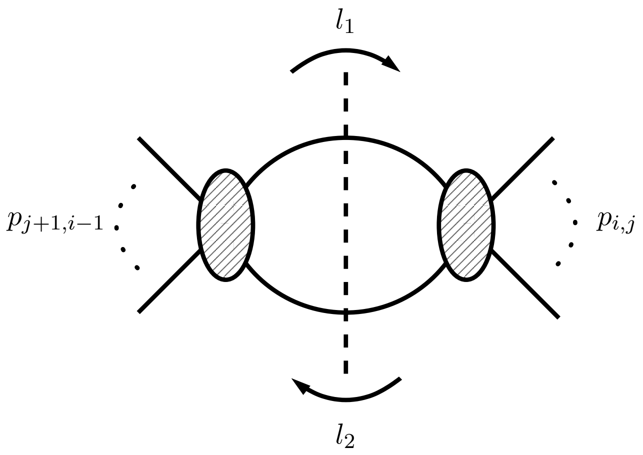

Figure 2.4: Computing the discontinuity in the $s_{i,j}$ channel of an n point, 1-loop amplitude. Momenta are labelled cyclically.

certain rational functions are not missed [22, 23]. In some cases it has been possible to fix these rational functions by using the universal collinear factorisation as an additional constraint. Using these improvements many 1-loop amplitudes in QCD have been derived [24] and it has also been possible to derive some results at 2-loops [25–30].

Cut-constructibility of gauge theory amplitudes.

A proof of the cut-constructibility of 1-loop supersymmetric amplitudes was presented by Bern, Dixon, Dunbar and Kosower in references [17, 18]. The proof requires that we look at colour ordered amplitudes where the kinematic invariants appear only as consecutive sums of the external momentum. The basic object which we need to consider when evaluating 1-loop amplitudes are the tensor integrals,

$$I_m[P(l^\mu)](K_1,\ldots,K_m) = \int \frac{d^D l}{(2\pi)^D} \frac{P(l^\mu)}{l^2(l-K_1)^2(l-K_{12})^2\cdots(l+K_m)^2}, \tag{2.33}$$

where K_i are the momenta, massless or otherwise, entering at each vertex. The function $P(l^\mu)$ is a polynomial in the loop momenta. The proof of cut-constructibility stems from the fact that any m-point tensor integral[‡] which contains at most $m-2$ powers of the loop momentum can be reduced to a set of integral functions which are uniquely determined

[‡]For 2-point, bubble integrals the numerator may have one power of the loop momentum

from their cuts. We are then left to show that all loop integrals in super-symmetric theories obey this simple *power counting* criterion.

In order to evaluate the tensor integrals we can apply conventional reduction techniques, e.g. Passarino-Veltman reduction, to reduce all tensor integrals with $m > 4$ to scalar box integrals. In turn the tensor box integrals are reduced to triangle and bubble integrals with at most one power of the loop momentum. The linear triangles and bubbles can be written as linear combinations of scalar triangles and bubbles leaving a final basis of integral functions for any 1-loop amplitude which obey the power-counting criterion,

$$\mathcal{F} = \{I_{4,4m}, I_{4,3m}, I_{4,2mh}, I_{4,2me}, I_{4,1m}, I_{3,3m}, I_{3,2m}, I_{3,1m}, I_2\}, \tag{2.34}$$

where $I_{i,(j)m}$ is a scalar integral with i propagators and j massive legs (the 2-mass boxes appear in two configurations which are labelled 'easy' and 'hard' reflecting the difficulty of evaluating each integral). It turns out that for $\mathcal{N} = 4$ amplitudes the power counting criterion is even stronger and m-point integrals appear with a maximum $m - 4$ powers of the loop momentum in the numerator. In this case we have at most scalar box integrals as no triangle, bubble or tensor box fit the criterion. As a result we have a much simplified basis for $\mathcal{N} = 4$ amplitudes,

$$\mathcal{F}' = \{I_{4,4m}, I_{4,3m}, I_{4,2mh}, I_{4,2me}, I_{4,1m}\}. \tag{2.35}$$

In order to show that an amplitude made from the basis of functions, $\mathcal{F}$, is cut-constructible in 4-dimensions we need to show that there is no possibility of missing any rational functions. Such a situation would arise if the cuts were not unique and we could find two representations of the cuts of the amplitudes in terms of the integral basis. i.e. a linear combination with (4-dimensional) coefficients c_i and another with coefficients c_i' such that,

$$\sum_{I_i \in \mathcal{F}} c_i I_i|_{\rm cuts} = \sum_{I_i \in \mathcal{F}} c_i' I_i|_{\rm cuts}. \tag{2.36}$$

When reconstructing the full amplitude this could result in the two representations differing by some rational function, R,

$$\sum_{I_i \in \mathcal{F}} (c_i - c_i')I_i = R. \tag{2.37}$$

So if one can show that for the basis $\mathcal{F}$ that no linear combination of the integrals is equal to a rational function then the amplitude will be cut-constructible. This can be shown to be true by looking at the finite parts for each of the integral functions and showing that the logarithms that appear in each case are unique and hence no cancellation in the form of (2.37) is possible. The details of this can be found in reference [18].

If we break the power counting criterion then the basis of integrals changes and we can find combinations of the integral functions which fit the form of (2.37). For instance the appearance of 2-rank tensor bubbles allows the following combination:

$$\left(\frac{K^\mu K^\nu}{3} - \frac{g^{\mu\nu}K^2}{12}\right) I_2[1](K) - I_2[l^\mu l^\nu](K) = -\frac{\Gamma(1+\epsilon)\Gamma(1-\epsilon)^2}{18\Gamma(1-2\epsilon)} \left(K^\mu K^\nu - g^{\mu\nu}K^2\right) \tag{2.38}$$

Very recently it has been suggested that one could exploit the power counting theorem to find any missing rational pieces in non-supersymmetric theories by noticing that the set of integrals contributing to the rational part is fixed by the power counting theorem and performing a simplified calculation [31]. This method has been applied to all helicity configurations for 5 and 6 point gluon amplitudes [32, 33].

The final ingredient necessary to prove the cut-constructibility of super-symmetric amplitudes is to prove that all loop integrals will obey the power counting criterion. In any gauge theory the maximum power of the loop polynomial is m for an m-point integral, the extra cancellations required to meet the condition of a maximum of $m-2$ can be shown by computing the 1-loop effective action and showing that the most dangerous terms cancel. Again I refer the reader to reference [18] for details of the computation.

2.2. The spinor helicity formalism

Helicity amplitudes have been used successfully as an efficient way to organise cross section calculations as well as being essential for detailed spin analyses [34–38]. By fixing the spin alignment of all particles in a particular process we can reduce the cost of computing the squared matrix elements as all cross terms will vanish. The fermion wave functions have helicity states defined by,

$$\frac{1}{2}(1 \pm \gamma_5)|\psi(p)\rangle = |\psi(p)\pm\rangle = |p\pm\rangle \tag{2.39}$$

$$\langle p \pm |p\pm\rangle = 0. \tag{2.40}$$

The projectors, $\frac{1}{2}(1 \pm \gamma_5)$, pick out 2-component spinors from the 4-component Dirac spinors $|\psi\rangle$. Thus the positive and negative helicity wave-functions can be written as 2-component spinors:

$$|p+\rangle = \begin{pmatrix} |p] = \tilde{\lambda}_{\dot{\alpha}} \\ 0 \end{pmatrix} \qquad |p-\rangle = \begin{pmatrix} 0 \\ |p\rangle = \lambda_\alpha \end{pmatrix} \tag{2.41}$$

Massless momenta can be decomposed into 2-component spinors as follows,

$$2p^\mu = \sigma^\mu_{\alpha\dot{\alpha}}|p\rangle^\alpha |p]^{\dot{\alpha}}. \tag{2.42}$$

Using these conventions it is useful to write helicity amplitudes in terms of spinor products,[§]

$$\lambda^\alpha(p)\lambda_\alpha(q) = \langle pq\rangle \qquad \tilde{\lambda}_{\dot{\alpha}}(p)\tilde{\lambda}^{\dot{\alpha}}(q) = [pq]. \tag{2.43}$$

The indices on the spinors λ and $\tilde{\lambda}$ are raised and lowered using $\epsilon_{\alpha\dot{\alpha}}$ hence the spinor products are anti-symmetric. We can use these spinor products to write the usual momentum invariants using,

$$\langle pq\rangle[qp] = (p+q)^2 = s_{pq} \tag{2.44}$$

[§]These conventions differ from the conventions in some of the literature by the sign of the anti-holomorphic spinor product.

It is also possible to write the polarisation vectors of the gluons in terms of the 2-component spinors. The polarisation vectors used to describe spin 1 particles are usually written in terms of the momentum, say p, and a gauge vector. We can use the decomposition of momenta into spinors (2.42) to write the polarisation vectors as:

$$\epsilon_\mu^\pm(p,\eta) = \pm\frac{\langle p\pm|\gamma_\mu|\eta\pm\rangle}{\sqrt{2}\langle\eta\mp|p\pm\rangle} \tag{2.45}$$

where η is an arbitrary, light-like, vector orthogonal to p. It is then easy to see that

$$\epsilon_p^\pm\cdot\epsilon_q^\pm = 0 \tag{2.46}$$

where $\epsilon_{p,\mu}^\pm \equiv \epsilon_\mu^\pm(p)$. This choice of representation for the polarisation vectors corresponds to working in a light like axial gauge:

$$\sum_{\lambda=\pm}\epsilon_\lambda^\mu(p,q)(\epsilon_\lambda^\nu(p,q))^* = -g^{\mu\nu} + \frac{p^\mu q^\nu + q^\mu p^\nu}{p\cdot q} \tag{2.47}$$

Useful Spinor Identities

The spinor products defined above satisfy a number of identities which are extremely useful when calculating scattering amplitudes. One of the most important of these is the Schouten identity

$$\langle ab\rangle\langle cd\rangle = \langle ac\rangle\langle bd\rangle + \langle ad\rangle\langle cb\rangle \tag{2.48}$$

We can also contract gamma matrices through:

$$\langle a|\gamma_\mu|b]\langle c|\gamma^\mu|d] = -2\langle ac\rangle[bd]. \tag{2.49}$$

When looking at spinor strings it is useful to note that:

$$\langle a|p_1\cdots p_{2m+1}|b] = [b|p_{2m+1}\cdots p_1|a\rangle \tag{2.50}$$

$$\langle a|p_1\cdots p_{2m}|b\rangle = -\langle b|p_{2m}\cdots p_1|a\rangle \tag{2.51}$$

$$\langle a|p_1\cdots p_{2m+1}|a] = \frac{1}{2}\mathrm{tr}((1-\gamma_5)p_a p_1\cdots p_{2m+1}) = \mathrm{tr}_-(p_a p_1\cdots p_{2m+1}) \tag{2.52}$$

2.3. Colour ordering in gauge theories

A useful technique to organise calculations in non-Abelian gauge theories is colour ordering. This involves stripping the colour factors associated with the gauge group from the amplitude leaving partial amplitudes which are only functions of the kinematic invariants. These partial amplitudes are subject to the group symmetries and therefore we can reduce the amount of computation that needs to be performed. The technique has been used widely in perturbative calculations for many years [39, 40] and a good review can be found in reference [41].

For the $SU(n)$ gauge group there are 8 traceless generators $T^a_{i,j}$, which are 3×3 matrices obeying the following commutation and normalisation conditions,

$$[T^a, T^b]_{ij} = if^{abc}T^c_{ij} \tag{2.53}$$

$$\mathrm{tr}(T^a T^b) = \delta^{ab}, \tag{2.54}$$

By applying the commutation relation (2.53) to all structure constants, a tree level amplitude of n gluons may be written as:

$$A^{(0)}_n(\{p_i, h_i, a_i\}) = ig^{n-2} \sum_{\sigma \in S_n/\mathbb{Z}_n} \mathrm{tr}(T^{a_{\sigma(1)}} \dots T^{a_{\sigma(n)}})\mathcal{A}^{(0)}_n(\{p_i, h_i\}), \tag{2.55}$$

where a_i are the colour indices for the adjoint representation with p_i and h_i the momenta and helicities respectively. The amplitude $\mathcal{A}_n$ is colour ordered and obeys the following relations,

1. cyclic symmetry: $\mathcal{A}_n(p_1, p_2, \dots, p_n) = \mathcal{A}_n(p_2, p_3, \dots, p_1) = \dots$
2. reflection symmetry: $\mathcal{A}_n(p_1, p_2, \dots, p_n) = (-1)^n \mathcal{A}_n(p_n, p_{n-1}, \dots, p_1)$
3. dual ward identity:

$$\mathcal{A}_n(p_1, p_2, p_3 \dots, p_n) + \mathcal{A}_n(p_2, p_1, p_3 \dots, p_n) + \dots + \mathcal{A}_n(p_2, p_3, \dots, p_1, p_n) = 0$$

Most importantly however the sub-amplitudes are all separately gauge invariant. This allows us to choose a gauge which simplifies the calculation for each colour ordered amplitude independently.

For amplitudes involving fundamental fermions the decomposition is a little more complicated. In general, a particular colour factor for an amplitude with m quark pairs and n gluons would be,

$$(T^{a_1}\dots T^{a_{l_1}})_{i_1 j_1}(T^{a_{l_1+1}}\dots T^{a_{l_2}})_{i_2 j_2}\times\dots\times(T^{a_{l_2+1}}\dots T^{a_n})_{i_m j_m}, \tag{2.56}$$

where a_x are the gluon colour indices and i_x,j_x are the quark and anti-quark indices respectively. The full amplitude would be the sum over all permutations and partitions of the gluons between the quark strings. For a single quark pair this reduces to:

$$\begin{aligned}&A_n(\{p_i,\lambda_i,a_i\},\{p_j,\lambda_j,i_j\})\\&=ig^{n-2}\sum_{\sigma\in S_{n-2}}(T^{a_{\sigma(2)}}\cdots T^{a_{\sigma(n-1)}})_{i_1 i_n}\,\mathcal{A}_n(1^{\lambda},\sigma(2^{\lambda_2},\dots,(n-1)^{\lambda_{n-1}}),n^{-\lambda}).\end{aligned} \tag{2.57}$$

The explicit decomposition for two quark pairs is considered in the context of Higgs amplitudes in section 3.8.

As will be relevant in chapter 3 it is useful to point out that particles that are not coloured under the gauge group play no part in the colour factors. For amplitudes with Higgs bosons equations (2.55) and (2.57) are easily modified by multiplying by the effective Hgg coupling, C, and adding the extra particle into the kinematic amplitude. For example amplitudes with a Higgs and n gluons the decomposition reads,

$$A_n^{(0)}(H;\{p_i,h_i,a_i\})=iCg^{n-2}\sum_{\sigma\in S_n/\mathbb{Z}_n}\mathrm{tr}(T^{a_{\sigma(1)}}\dots T^{a_{\sigma(n)}})\mathcal{A}_n^{(0)}(H;\{p_i,h_i\}). \tag{2.58}$$

Details of the coupling C and the effective interaction are given in chapter 3.

Colour Structures at higher orders

The colour decompositions given above apply only at tree level. To find decompositions for higher loop amplitudes many more colour structures appear. In general these new structures will be colour suppressed, i.e. proportional to $1/N_c$ in comparison to the leading term. For instance one may consider one loop amplitudes of gluons which may now contain delta functions as well as traces of generators. The decomposition then reads [17]:

$$A_n^{(1)}(\{p_i, h_i, a_i\}) = ig^n \sum_{c=1}^{[n/2]+1} \sum_{\sigma \in S_n/S_{n;c}} G_{n;c}(\sigma) \mathcal{A}_{n;c}^{(1)}(\{p_i, h_i\}) \tag{2.59}$$

where,

$$G_{n;c} = \begin{cases} N_c \text{tr}(T^{a_{\sigma(1)}} \dots T^{a_{\sigma(n)}}), & c = 1 \\ \text{tr}(T^{a_{\sigma(1)}} \dots T^{a_{\sigma(c-1)}}) \text{tr}(T^{a_{\sigma(c)}} \dots T^{a_{\sigma(n)}}), & c > 1. \end{cases} \tag{2.60}$$

Clearly as the generators of $SU(n)$ are traceless $G_{n;2} = 0$. We see that due to the extra delta function occurring in the loop, the leading order contribution is just N_c times the tree level factor, (2.55). It has been shown that by performing various summations over the leading order contribution $\mathcal{A}_{n;1}^{(1)}$ one can obtain the sub-leading contributions $\mathcal{A}_{n;c}^{(1)}$ $(c > 2)$ [17] hence it is usually sufficient to drop the colour ordering subscript and compute the cyclic leading order contribution $\mathcal{A}_{n;1}^{(1)} = \mathcal{A}_n^{(1)}$.

2.4. Twistor Inspired Methods

Following the remarkable paper by Witten [42], which pointed out a duality between $\mathcal{N} = 4$ Supersymmetric Yang-Mills theory and a topological string theory on Twistor space, there have been huge advances in new techniques for calculating scattering amplitudes in both supersymmetric and non-supersymmetric gauge theories. These methods have been termed "twistor inspired methods" although in hindsight on-shell methods would seem a more appropriate description. At the present time these methods have been mostly applied at tree level where all gauge theories are essentially super-symmetric, though much progress has also been made at the one loop level.

In this section we will outline the three main methods: The MHV rules, on-shell recursion relations and generalised unitarity.

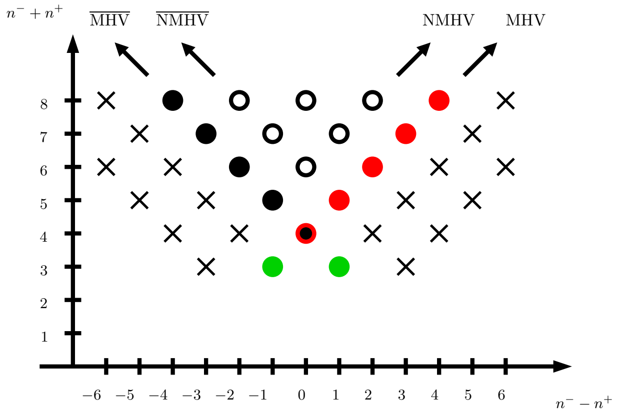

Figure 2.5: Structure of tree level gluonic helicity amplitudes.

2.4.1. MHV Rules

"Maximally Helicity Violating" or MHV amplitudes refer to the rather special structure of helicity amplitudes within QCD. It has been known for some time that gluonic amplitudes with fewer than two negative or positive helicities vanish at tree level irrespective of the number of particles in the amplitude:

$$\mathcal{A}_n^{(0)}(p_1^{\pm}, p_2^{\mp}, p_3^{\mp}, \dots, p_n^{\mp}) = 0. \tag{2.61}$$

This can be proved using supersymmetric Ward identities [41, 43]. The first non-zero amplitudes are those with two negative helicities:

$$\mathcal{A}_n^{(0)}(\dots, i^-, \dots, j^-, \dots) = \frac{\langle ij\rangle^4}{\langle 12\rangle\langle 23\rangle \dots \langle n1\rangle}. \tag{2.62}$$

These are the MHV amplitudes, amplitudes with two positive helicities, related by parity symmetry, are known as the $\overline{\text{MHV}}$ amplitudes. Figure 2.5 shows the structure of the helicity amplitudes as the number of negative/positive helicities increases. A similar picture emerges for amplitudes involving fermions as will be discussed later in chapter 3.

This simplicity is remarkable and shows that simple analysis of such amplitudes using Feynman diagrams is insufficient to uncover the reason for the underlying helicity structure since, in this approach, all helicity amplitudes are treated equally and the structure only emerges after large cancellations occur between diagrams. Indeed the number of Feynman diagrams for a 10 gluon process comes to over 10 million whereas the final result is just one term.

A reason for this simplicity was noticed by Witten [42] who showed that the MHV amplitudes where conformally invariant, as indeed they must be since at tree level QCD is equivalent to $\mathcal{N} = 4$ SYM. In showing this property explicitly, he uncovered the fact that these amplitudes had a very simple structure in Twistor space, since the amplitudes are completely holomorphic (i.e. made entirely of $\langle pq \rangle$ type spinor products).

Twistor space was proposed by Penrose [44] in 1967 as a way to study conformal invariance within Minkowski space. The theory is by now extremely well developed and a full review of the subject is beyond the scope of this thesis, instead it will be sufficient to outline a few facts about the theory which will allow us to see some geometric structure within the QCD helicity amplitudes.

Twistor space is a complex projective space whose co-ordinates are constructed of the two-component spinors discussed in section 2.2,

$$Z^A = (\lambda_\alpha, \mu_{\dot{\alpha}}), \tag{2.63}$$

where $\mu_{\dot{\alpha}} = \frac{\partial}{\partial \tilde{\lambda}^{\dot{\alpha}}}$. These points are related to points in Minkowski space, x, via the Penrose-Ward transform

$$\lambda_\alpha + x_{\alpha\dot{\alpha}} \mu^{\dot{\alpha}} = 0. \tag{2.64}$$

Interesting consequences of this transform are that points in Minkowski space are mapped

n	4	5	6	7	8	9	10
$0 \to ng$	4	25	120	2485	34300	559405	10525900
$q\bar{q} \to (n-2)g$	3	16	123	1240	15495	231280	4016775

Table 2.1: A Table showing the numbers of Feynman diagrams contributing to various tree level processes.

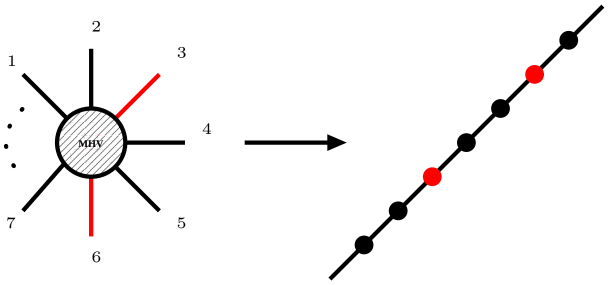

Figure 2.6: MHV amplitudes map onto straight lines in twistor space. Red lines/points correspond to negative helicities.

to lines in Twistor space and points in Twistor space are mapped to null planes in Minkowski space.

Transforming the MHV amplitudes, (2.62), into Twistor space involves performing a Fourier transform on the $\tilde{\lambda}$ co-ordinates. Notice that it is arbitrary whether we choose to Fourier transform the λ or $\tilde{\lambda}$ coordinates which corresponds to working with either MHV or $\overline{\text{MHV}}$ rules respectively.

The result of such an analysis [42] is quite remarkable. It turns out that the MHV amplitudes are supported on degree one curves in Twistor space, i.e. all the external momenta lie in a straight line in twistor space as shown in figure 2.6. This tells us that the MHV amplitudes are localised in Minkowski space and it is this fact that motivates a new scalar perturbation theory where the MHV amplitudes, with a certain off-shell continuation, are the interaction vertices [45].

This leads us to ask whether helicity amplitudes with more complicated helicity assignments also have simple twistor space interpretations. Known expressions for such amplitudes, i.e. NMHV, NNMHV, are extremely long and complicated so direct evaluation of the Fourier transform is not a good idea. However, by applying differential operators to test for co-planarity and collinearity it has been possible to deduce [42] that the 6-point amplitudes with three negative helicities, the first non trivial NMHV amplitudes, lie on degree 2 curves in twistor space. In fact the situation is even better as it turns out that these degree 2 curves are consistent with a picture of intersecting lines as shown in figure 2.7. From this point it has been conjectured that scattering amplitudes in $\mathcal{N} = 4$ SYM are supported on degree d curves where,

$$d = m - 1 + l \tag{2.65}$$

where m is the number of negative helicity and l is the number of loops. This relation has been checked directly for many tree level amplitudes, indeed by virtue of a proof of the MHV rule formalism [46] this relation must hold for all $l = 0$.

This information about the twistor space structure of tree level helicity amplitudes leads to the postulation of a completely new way to calculate scattering amplitudes in $\mathcal{N} = 4$ SYM. At tree level this is equivalent to calculating amplitudes in QCD as, once the colour factors have been removed, the two theories are identical since supersymmetric particles can only propagate via loop corrections. Using the MHV amplitudes as vertices we connect them together using scalar propagators to form amplitudes with more negative helicities. The MHV rules are as follows:

(1) Connect vertices using scalar propagators, $\frac{1}{P^2}$.

(2) Propagating momentum, P, enters the MHV vertex via its spinor component. Being an on-shell object this needs to be continued off-shell in order to make it well defined. This is done by defining a reference spinor ξ: $|P\rangle \to |P|\xi]$. All amplitudes will be independent of the choice for ξ.

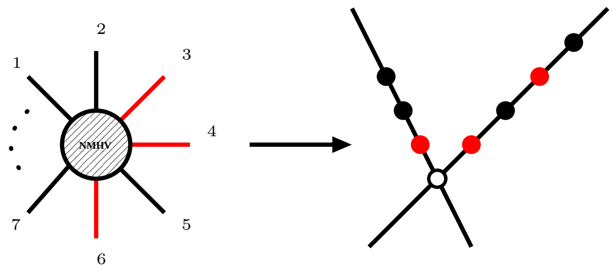

Figure 2.7: NMHV amplitudes map to a pair of intersecting lines in twistor space. Red lines/points correspond to negative helicities.

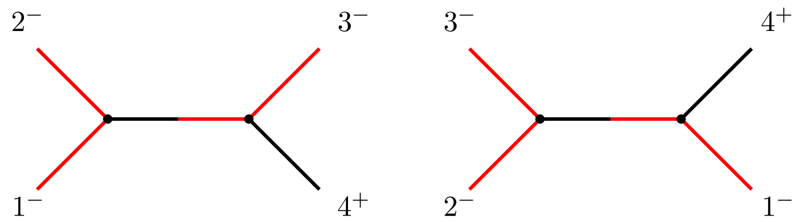

Figure 2.8: The two MHV diagrams contributing to the vanishing $\mathcal{A}(1^-, 2^-, 3^-, 4^+)$ amplitude.

(3) Sum over all the possible ways of connecting the MHV vertices.

The simplest way to understand these rules is by example so we will use the MHV rules to calculate the 4-point amplitude $\mathcal{A}_4(1^-, 2^-, 3^-, 4^+)$. This amplitude must vanish as although it has three negative helicities it falls into the category of (2.61).

There are two MHV diagrams, shown in figure 2.8. Notice that we define an "off-shell continued" 3-point MHV vertex. Although this amplitude vanishes on-shell for real momenta here we can take it to be defined by (2.62) with the continuation ensuring that it doesn't vanish. Applying the rules given above and summing the two contributions gives:

$$\begin{aligned}\mathcal{A}_4(1^-, 2^-, 3^-, 4^+) &= \frac{\langle 12\rangle^3}{\langle 2|P_{12}|\xi]\langle 1|P_{12}|\xi]} \frac{1}{P_{12}^2} \frac{\langle 3|P_{12}|\xi]^3}{\langle 34\rangle\langle 4|P_{12}|\xi]} \\ &+ \frac{\langle 23\rangle^3}{\langle 2|P_{23}|\xi]\langle 3|P_{23}|\xi]} \frac{1}{P_{23}^2} \frac{\langle 1|P_{23}|\xi]^3}{\langle 41\rangle\langle 4|P_{23}|\xi]} \\ &= -\frac{[4\xi]^3}{[1\xi][2\xi][3\xi]} \frac{\langle 4|1+3|2]}{[12][23]}. \end{aligned} \tag{2.66}$$

This result can be seen to vanish as expected by applying momentum conservation to the factor $\langle 4|1+3|2]$.

The MHV rules have been very successful at tree-level and have been applied to many processes in QCD. n point amplitudes with gluons and fermions have been computed [47–51], and a recursive formulation [52] has been useful to provide expressions for Higgs amplitudes [53, 54], Electro-weak vector boson currents [55] and QED processes [56]. The MHV rules have also provided an efficient method for deriving IR factorisation properties of QCD amplitudes [57, 58]. The application of MHV rules to Higgs processes is the subject of chapter 3.

Note on off-shell continuation

The reference to off-shell continuation of the MHV amplitudes is slightly misleading. In hindsight it is better to interpret the off-shell continuation as in fact evaluation of the amplitude for a complex momentum $\widehat{P}$ which is just the propagator momentum P shifted by a complex variable z which puts $\widehat{P}$ on-shell,

$$\widehat{P} = P - z\xi \tag{2.67}$$

where $z = \frac{P^2}{2P\cdot\xi}$. From here it is obvious that $|\widehat{P}\rangle = |P|\xi]/[\widehat{P}\xi]$. When computing the MHV diagrams it is easy to see that all the anti-holomorphic spinor products involving $\widehat{P}$ will cancel. This interpretation is discussed in reference [59].

2.4.2. On-shell recursion relations

Recursion relations based on Feynman diagrams [60] have been utilised extensively in tree level matrix element calculations for many years. The main principle is to re-use calculations for lower multiplicity amplitudes to make up higher multiplicity amplitudes. In the past this has been done by building off-shell currents which could be linked together using the standard Feynman interaction vertices [61, 62].

Through studying IR properties of 1-loop amplitudes in $\mathcal{N} = 4$ a new type of recursion relation was discovered where all the propagating particles were on-shell [63, 64]. More remarkably it turned that there was a very simple proof for these relations which only relied on Cauchy's Theorem for complex analysis and multi-particle factorisation properties [65].

The on-shell recursion formula for tree amplitudes of gluons was originally presented in the following form,

$$\mathcal{A}^{(0)}(p_1,\ldots,p_n)=\sum_{i=2}^{n-2}\sum_{h=\pm}\mathcal{A}^{(0)}(\widehat{p}_1,\ldots,p_i,-\widehat{P}^h_{1,i})\frac{1}{P^2_{1,i}}\mathcal{A}^{(0)}(-\widehat{P}^h_{1,i},p_{i+1},\ldots,\widehat{p}_n) \quad (2.68)$$

where,

$$\widehat{p}_1=p_1+z_{1,i}\eta, \qquad \widehat{p}_n=p_n-z_{1,i}\eta. \quad (2.69)$$

Notably two of the momenta, p_1 and p_n in this case, are chosen to be shifted by a complex parameter, z, which is chosen for each term such that $\widehat{P}^2_{1,i}=0$. The shift momentum η is chosen to ensure that p_1 and p_n also remain on-shell after the shift has been performed. This results in two possible solutions for η:

$$\eta=|1]|n\rangle \text{ or } \eta=|1\rangle|n]. \quad (2.70)$$

Using this relation it has been possible to derive extremely compact analytic formulae for QCD amplitudes at tree level [64, 66, 67]

A remarkably simple proof of the relation was presented by Britto, Cachazo, Feng and Witten [65]. The proof proceeds as follows: Consider a colour ordered (cyclic) scattering amplitude $\mathcal{A}(p_1,\ldots,p_n)$. We then choose two momenta to be singled out and shifted into the region of complex momenta, because $\mathcal{A}$ is cyclically ordered we may choose these to be p_1 and p_j without loss of generality. The shift is parameterised by a complex variable z,

$$p_1\to p_1+z\eta, \qquad p_j\to p_j-z\eta, \quad (2.71)$$

where η is chosen to keep p_1,p_j on-shell as described above. Let us choose $\eta=|1\rangle|j]$ for simplicity. We will see later how this choice can affect the validity of the recursion relation depending on the helicity of the particles 1 and j, for all gluon amplitudes at least this choice is valid for $(h_1,h_j)=(+,+),(-,-),(-,+)$.

We now have a complex amplitude $\mathcal{A}(z)$ which is rational in z and has only simple poles, hence by Cauchy's theorem we can write:

$$0=\frac{1}{2\pi i}\int_\gamma dz\frac{\mathcal{A}(z)}{z}=\mathcal{A}(0)+\sum_{\text{poles},\alpha}\text{Res}\left(\frac{\mathcal{A}(z)}{z},z=z_\alpha\right). \quad (2.72)$$

$\mathcal{A}(0)$ is simply the amplitude we wish to calculate and we have managed to write it as a sum of residues of simple poles. We now recall that tree level amplitudes have the following multi-particle factorisation:

$$\mathcal{A}^{(0)}(p_1,\ldots,p_n) \underset{P^2_{i,j}\to 0}{\longrightarrow} \sum_{h=\pm} \mathcal{A}_L(p_i,\ldots,p_j,-P^h_{i,j})\frac{1}{P^2_{i,j}}\mathcal{A}_R(P^{-h}_{i,j},p_{j+1},\ldots,p_{i-1}). \quad (2.73)$$

Poles in $\mathcal{A}(z)$ occur whenever a propagator goes on-shell, $P^2(z) = P^2 - zP\cdot\eta \overset{z\to z_\alpha}{\to} 0$. So the residue at $z = z_\alpha$ can be computed using the tree level factorisation formula (2.73). Given this choice of shift a propagator can only be a function of z if the momentum flowing across it contains at most one of $\{1, j\}$, therefore the sum of residues is given by the total number of partitions of the remaining particles while keeping 1 and j on separate sides of the factorisation (2.73). Using this fact and equation (2.72) we arrive at the recursion relation (2.68) in a slightly more general form,

$$\begin{aligned}\mathcal{A}^{(0)}(p_1,\ldots,p_n) = \sum_{k=j}^{n}\sum_{l=2}^{j-1}\sum_{h=\pm} &\mathcal{A}^{(0)}(p_{k+1},\ldots,\widehat{p}_1,\ldots,p_l,-\widehat{P}^h_{k+1,l}) \\ &\times \frac{1}{P^2_{k+1,l}}\mathcal{A}^{(0)}(-\widehat{P}^h_{k+1,l},p_{l+1},\ldots,\widehat{p}_j,\ldots,p_k). \quad (2.74)\end{aligned}$$

The recursion relations have been shown to apply to a wide range of gauge theory amplitudes at tree level including massless QCD [64, 66, 67], $\mathcal{N} = 8$ supergravity [68, 69] and have been generalised for amplitudes with massive particles [70–74], which will be the subject of chapter 4.

There is one important assumption made in the proof of the recursion relation which is central in finding phenomenological applications of this method. We assumed that as $z \to \infty$ the amplitude $\mathcal{A}(z)$ vanished, hence the integral of (2.72) vanished also. We must study the act of the shift (2.71) on the amplitude more carefully in order to check that the recursion relation will indeed reproduce the full amplitude.

Behaviour of $\mathcal{A}(z)$ at large z

To be more precise the action of Cauchy's theorem on the function $\mathcal{A}(z)/z$ results in

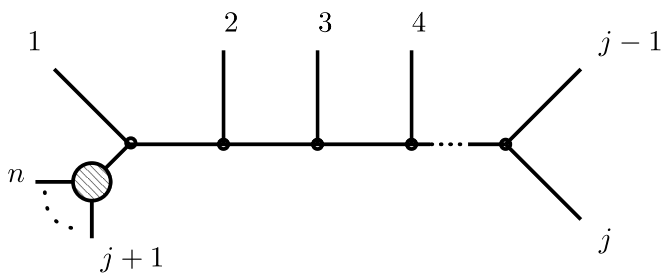

Figure 2.9: The Feynman diagram contributing to the worst z dependence in the large z limit.

the following,

$$\mathcal{A}(0) = -\sum_{\text{poles},\alpha} \text{Res}\left(\frac{\mathcal{A}(z)}{z}, z = z_\alpha\right) - \mathcal{A}_\infty. \tag{2.75}$$

By studying general properties of Feynman graphs contributing to a particular amplitude it is possible to deduce some information about the behaviour of $\mathcal{A}(z)$ at large z and hence choose a momentum shift that avoids boundary conditions. We could also consider an MHV construction as a way to look at large z behaviour [65].

First consider the helicities of the two marked particles to be $(h_1, h_j) = (-, +)$ and choose $\eta = |1\rangle|j]$. The only polarisation vectors to depend on z are ϵ_1 and ϵ_j and from (2.45) we find that $\epsilon_1 \sim 1/z$ and $\epsilon_j \sim 1/z$ as $z \to \infty$. The amplitude $\mathcal{A}(z)$ is made from a sum of colour ordered Feynman diagrams hence the momentum flow in each diagram must be cyclic. The most dangerous (most z dependent) diagram will occur when the z-dependence flow from 1 to j has the maximum number of propagators, i.e. when all vertices are three vertices as shown in figure 2.9. As $z \to \infty$ each vertex contributes a factor of z while each propagator contributes $1/z$. Hence the total z dependence will be z^{v-p-2} where v is the number of vertices and p is the number of propagators. This contribution will always have $v - p = 1$ and so worst diagram goes as $1/z$ and there will be no boundary term. We can see that if we changed to $\eta = |1]|j\rangle$ then the polarisation vectors would contribute z^2 in the and so the diagram would go like z^3 in the limit and there would be a boundary term. In this way we see that the choice of solution for η is extremely important when applying the recursion relations.

For other choices of helicities $(h_1, h_j) = (\pm, \pm)$ it is also possible to show that there will be no boundary term, as shown in [69, 70] from a Feynman diagram argument, or using the MHV construction in [65].

In general, the only part of the proof that is dependent on the type of particle is the vanishing of any boundary term. Amplitudes including one and two pairs of quarks have been considered in references [66, 67] and rules for avoiding boundary conditions have been found. In particular it turns out that one may not choose two adjacent fermions to be shifted. To see this it is useful to compare the MHV vertices for gluons and quarks,

$$\mathcal{A}_n(m_1^-, m_2^-) = \frac{\langle m_1 m_2 \rangle^4}{\prod_{\alpha=1}^{n} \langle \alpha \alpha+1 \rangle} \tag{2.76}$$

$$\mathcal{A}_n(1_q^-, m^-, n_{\bar{q}}^+) = \frac{\langle 1m \rangle^3 \langle nm \rangle}{\prod_{\alpha=1}^{n} \langle \alpha \alpha+1 \rangle}, \tag{2.77}$$

where we have chosen to drop the positive helicity gluons in the right hand expression. It is also useful to define $\eta_+ = |a]|b\rangle$ and $\eta_- = |a\rangle|b]$ to be the two solutions for η when the two shifted particles are (a, b).

The reason that our Feynman argument breaks down is that the counting of z dependence did not include the fact that given two shifted particles (a, b), the spinor products of these two particles will be unshifted:

$$\langle \widehat{ab} \rangle = \langle ab \rangle, \qquad [\widehat{ab}] = [ab]. \tag{2.78}$$

The denominator is the same for both amplitudes and cyclically symmetric hence we have the following cases:

(a) The shifted particles are non-adjacent - here the shifted holomorphic spinor appears twice so the denominator goes as z^2 as z becomes large.

(b) The shifted particles are adjacent - again the shifted holomorphic spinor appears twice but in one instance it appears in combination with the spinor whose anti-holomorphic component is shifted hence, by (2.78), the denominator goes as z as z becomes large.

$(a,b)\backslash(h_a,h_b)$	$(-,+)$	$(-,-)$	$(+,-)$	$(+,+)$
(g,g)	η_-	η_-,η_+	η_+	η_-,η_+
$(q,g)/(\bar{q},g)$	η_-	η_+	η_+	η_-
$(q,\bar{q})$	∞	N/A	∞	N/A
$(q,\bar{Q})$	η_-	η_-,η_+	η_+	η_-,η_+

Table 2.2: Table showing the correct choice of η when shifting particles (a,b) in QCD scattering amplitudes. $\eta_+ = |a]|b\rangle$ and $\eta_- = |a\rangle|b]$ are the two possible solutions for η.

For the gluon amplitude we see that there will only be any z dependence in the numerator if we mark either, or both, of the negative helicity gluons. If both are shifted then the numerator will be z independent by (2.78). When shifting a single negative helicity gluon the numerator will be z independent as long as its anti-holomorphic component is shifted. Hence we have shown explicitly that the boundary contribution vanishes for the cases discussed in general above.

Now we examine the quark amplitude. The numerator in this case has dependence on the positive helicity quark, hence if we mark the two quarks, $(q,\bar{q})$, then the numerator goes as z using η_- and goes like z^3 using η_+. As the amplitude is colour ordered the momentum of the quark and anti-quark will always be adjacent so the denominator is proportional to z and it is not possible to avoid boundary conditions in this case. However, it is possible to avoid boundary conditions when marking a quark/gluon pair as long as we choose the right solution for η.

By using the MHV rule construction we can upgrade these arguments to apply to all quark amplitudes with any number of negative helicity gluons. Table 2.2 summarises the rules to avoid boundary contributions when calculating QCD amplitudes with up to two quark pairs.

2.4.3. Generalised Unitarity

Generalised unitarity is not really a twistor inspired method since it has been considered long before Witten's twistor string duality in early studies of the analytic properties of the S-matrix [75]. However, following studies of twistor space interpretations of 1-loop amplitudes, it became apparent that one could use complex spinors to solve for the on-shell conditions required in the generalised unitarity cuts and thereby solve for the box coefficients of $\mathcal{N}=4$ SYM amplitudes purely algebraically [76].

As mentioned briefly in section 2.1.3, 1-loop amplitudes in $\mathcal{N}=4$ SYM can be written as a linear combination of scalar box integrals. These box integrals come in 5 different types, depending on the number of massive legs at the vertices as shown in figure 2.10. The full decomposition reads,

$$\mathcal{A}_n^{\mathcal{N}=4,(1)} = \sum_i c_i^{1m} I_4^{1m} + c_i^{2me} I_4^{2me} + c_i^{2mh} I_4^{2mh} + c_i^{3m} I_4^{3m} + c_i^{4m} I_4^{4m}. \tag{2.79}$$

where the index i is symbolic of a particular distribution of the n legs around the box integral in question. The 2-mass boxes come in two types, the so-called easy and hard boxes. This is a reference to the difficulty of evaluating each integral. Each of these integrals has the form:

$$I_4 = -i \int \frac{d^D l}{(2\pi)^D} \frac{1}{l^2 (l-K_1)^2 (l-K_1-K_2)^2 (l-K_1-K_2-K_3)^2}, \tag{2.80}$$

where K_i are the momenta flowing into each of the four vertices, which may be either massless or massive. $D = 4-2\epsilon$ where ϵ is the dimensional regularisation parameter.

The principle of generalised unitarity is to extend the idea of unitarity cuts where two propagators are cut to the case where more propagators are cut. If one evaluated an amplitude using two particle cuts we would find that more than one integral would appear in each channel. However when generalising to quadruple cuts we find that each box integral has a unique singularity. This is illustrated by applying unitarity cuts, (2.30), to both the full amplitude and the expansion in terms of box integrals (2.79). Let each integral have a discontinuity ΔI_4 in a given channel then the two particle cut

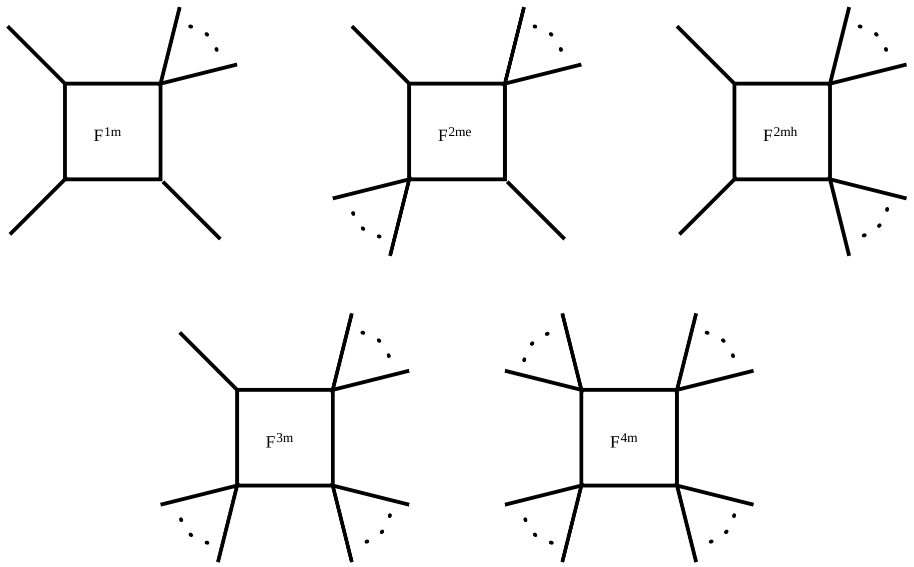

Figure 2.10: The five types of scalar box integrals which form a basis for 1-loop amplitudes in $\mathcal{N} = 4$ SYM.

is given by:

$$\int \mathrm{d}^D\mathrm{LIPS}(l_1, -l_2)\mathcal{A}^{(0)}(l_1, P_1, -l_2)\mathcal{A}^{(0)}(l_2, P_2, -l_1) = \\ \sum c_i^{1m}\Delta I^{1m} + c_i^{2me}\Delta I^{2me} + c_i^{2mh}\Delta I^{2mh} + c_i^{3m}\Delta I^{3m} + c_i^{4m}\Delta I^{4m}, \qquad (2.81)$$

where

$$\mathrm{d}^\mathrm{D}\mathrm{LIPS}(l_1, -l_2) = d^D l_1 d^D l_2 \delta(l_1 + P_1 - l_2)\delta^{(+)}(l_1^2)\delta^{(+)}(l_2^2). \qquad (2.82)$$

Hence in order to determine each of the coefficients we must disentangle the information given by all the possible branch cuts.

We now consider replacing more of the propagators in the integral (2.80) with their imaginary parts, $\delta^{(+)}$. For the 4-mass box it is possible to put all of the propagators on shell and it turns out that the leading singularity is unique to this integral and hence completely determines the coefficient of this integral:

$$\Delta_{LS} I_4^{4m} = \int d^D l \delta^{(+)}(l^2)\delta^{(+)}((l - K_1)^2)\delta^{(+)}((l - K_1 - K_2)^2)\delta^{(+)}((l - K_1 - K_2 - K_3)^2) \qquad (2.83)$$

and on the amplitude side we find that the quadruple cut is now made from a product of four tree amplitudes integrated over the four delta functions given above:

$$\begin{aligned}\mathcal{A}^{(1)}|_{4-\mathrm{cut}} &= \int d^D l \delta^{(+)}(l^2)\delta^{(+)}((l-K_1)^2)\delta^{(+)}((l-K_1-K_2)^2)\delta^{(+)}((l-K_1-K_2-K_3)^2) \\ &\quad \times \mathcal{A}_1^{(0)}\mathcal{A}_2^{(0)}\mathcal{A}_3^{(0)}\mathcal{A}_4^{(0)} \\ &\equiv c_i^{4m}\Delta_{LS} I_4^{4m}. \end{aligned} \tag{2.84}$$

The next step is to notice that these integrals are in fact finite so we can set ϵ to zero and the 4 delta functions fix both integrals and we find:

$$c_i^{4m} = \frac{1}{|S|}\sum_{p=q,g,s} n_p \mathcal{A}(l_1,K_1,-l_2)\mathcal{A}(l_2,K_2,-l_3)\mathcal{A}(l_3,K_3,-l_4)\mathcal{A}(l_4,K_4,-l_1), \tag{2.85}$$

where the sum runs over all particles in the $\mathcal{N}=4$ multiplet and all possible helicity assignments around the loops. n_p is the number of of each species, i.e. $n_p = 1,4,6$ for gluons, quarks and scalars respectively. $|S|$ is the number of solutions to the on-shell conditions specified by the four delta functions. So we can determine all 4-mass box coefficients from quadruple cuts which reduce integrals to an algebraic problem of solving the constraints.

The next obvious step is to attempt to find the coefficients of the other box integrals. However the situation here is more difficult as if we have one or more massless leg then one of the delta functions is trivially satisfied and the quadruple cut results in a delta function singularity. This delta function forces the coefficient to be evaluated at a point where it vanishes. This is consistent with the contribution from the product of four tree amplitudes as one of these must be an on-shell 3-vertex which must vanish for real momenta.

It is at this point in which the twistor inspired methods come to our aid. In both the MHV rules and the on-shell recursion relations we used on-shell 3-point amplitudes as the primitive building blocks. These on-shell amplitudes were non-zero because the momenta were taken to be complex. This allowed us to relax the condition that $\tilde{\lambda} = -\lambda^*$ which is satisfied for real momenta so that the holomorphic and anti-holomorphic spinors are independent. The condition that ensures the 3-point amplitude, $\mathcal{A}(p_1^-, p_2^-, p_3^+)$ vanishes is that of momentum conservation:

$$p_3^2 = s_{12} = -\langle 12\rangle[12] = 0. \tag{2.86}$$

For real momenta both angle and square bracket spinor products will vanish but if we allow the spinors to be independent then we can choose one of these spinor products to vanish and the other to be non-zero. If we choose $[12] = 0$ then the 3-point amplitude,

$$\mathcal{A}_3^{(0)}(1^-, 2^-, 3^+) = \frac{\langle 12\rangle^3}{\langle 23\rangle\langle 31\rangle} \tag{2.87}$$

is non-zero. This fact is also true for real momenta in a $(--++)$ signature [42, 76].

Therefore we can use complex momenta to make sure that the quadruple cut of any box with more than one massless leg does not vanish. Each coefficient can now be computed using the same formula as for the four mass box:

$$c_i = \frac{1}{|S|}\sum_{p=q,g,s} n_p \mathcal{A}(l_1, K_1, -l_2)\mathcal{A}(l_2, K_2, -l_3)\mathcal{A}(l_3, K_3, -l_4)\mathcal{A}(l_4, K_4, -l_1), \tag{2.88}$$

with the on shell conditions given by,

$$S = \left\{l_1^2 = 0, (l_1 - K_1)^2 = 0, (l_1 - K_1 - K_2)^2 = 0, (l_1 - K_1 - K_2 - K_3)^2 = 0\right\}. \tag{2.89}$$

In order to keep all 3-point vertices from vanishing when solving these constraints we choose the spinors of the loop momenta to be proportional to the massless spinor in the following way:

$$\begin{aligned}
\mathcal{A}_3^{\mathrm{MHV}}(l_1, p, -l_2): &\quad \tilde{\lambda}_{l_1} \propto \tilde{\lambda}_p \quad , \quad \tilde{\lambda}_{l_2} \propto \tilde{\lambda}_p, \\
\mathcal{A}_3^{\overline{\mathrm{MHV}}}(l_1, p, -l_2): &\quad \lambda_{l_1} \propto \lambda_p \quad , \quad \lambda_{l_2} \propto \lambda_p.
\end{aligned} \tag{2.90}$$

Using these methods it has been possible to calculate 1-loop amplitudes in $\mathcal{N} = 4$ SYM with up to 8 legs [20, 21, 63, 76]. The methods can also apply well to calculations in $\mathcal{N} = 1$ SYM although here some integrals are left as the bubble and triangle integrals are not completely saturated by delta functions [77–80]. Indeed the cut-constructible (4d) parts of the $\mathcal{N} = 0$ amplitudes with a scalar propagating in the loop have also been computed [81] and generalised unitarity in $d = 4 - 2\epsilon$ has been applied to find the full QCD amplitudes for simple processes involving gluons [82].

2.5. On-shell methods at one loop

We have already discussed unitarity (section 2.1.3) and generalised unitarity (section 2.4.3 as on-shell methods to compute loop integrals but we have not addressed the applications of MHV rules and on-shell recursion as methods for higher order corrections.

Firstly let us consider the MHV rules discussed in section 2.4.1. The twistor-string/$\mathcal{N} = 4$ SYM duality breaks down at 1-loop due to conformal supergravity states propagating in the string theory side [83, 84] but this doesn't mean that the MHV rules at 1-loop are definitely out of the question. Witten has considered the twistor space structure of MHV 1-loop amplitudes [85–88] and has shown that they fit the conjectured formula (2.65), $d = m - 1 + l$. This means that the MHV amplitudes lie on degree 2 curves in twistor space, though not necessarily intersecting straight lines as for NMHV tree level amplitudes [89]. More explicit calculations [90] showed that applying MHV rules to 1-loop MHV amplitudes of gluons reproduced the known results [17] and followed a proof similar to that of previous unitarity based calculations. Indeed these methods applied well to the cut-constructible parts of MHV amplitudes in $\mathcal{N} = 1, 0$ SYM [91, 92]. It remains to be seen whether MHV methods can be successfully applied to non-MHV amplitudes although by looking at generalised unitarity cuts information about the twistor space structure of integral coefficients has been found [93–95].

The main problem with extending MHV methods to loop calculations seems to be the fact that they will only ever be able to find the cut-constructable parts of the amplitude. Therefore we are still left with the problem of finding the remaining rational functions in QCD amplitudes. It is in this area that it much work has been done using the on-shell recursion relations. Bern, Dixon and Kosower have devised a bootstrap method [96–98] for using recursion relations to find the rational functions in non-supersymmetric theories. This program has been very successful and it has been possible to derive new results for "finite" one loop amplitudes (helicity configurations that vanish at tree level) and for the MHV amplitudes [99], both valid for any number of external particles. More

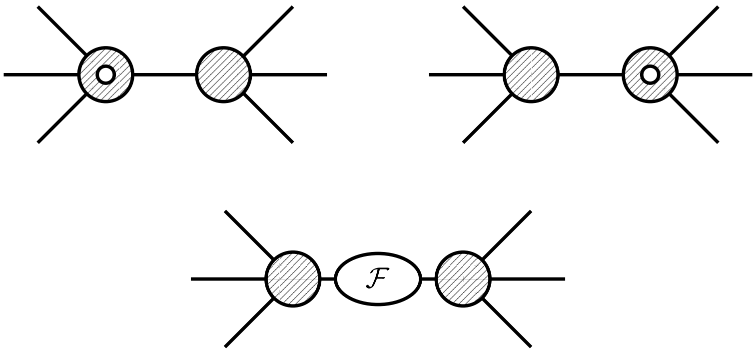

Figure 2.11: Schematic representation of terms contributing to the recursion relation for rational functions in QCD amplitudes.

recently the remaining helicities for QCD amplitudes with 6 and 7 external gluons have been computed [31–33, 100, 101].

The methods at 1-loop are much more complicated as amplitudes contain branch cuts as well as poles after continuation to complex momenta. The multi-particle factorisation for complex momenta for 1-loop amplitudes is not the same as that for real momenta as it was in the tree-level case. Specifically it isn't fully understood how to treat the three point 1-loop amplitudes which occur. However it seems that, for pure QCD amplitudes at least, these problems can be avoided and by using a recursion relation based on the 1-loop multi-particle factorisation [102], this is shown schematically in figure 2.11.

To be more specific let us again consider the integral in (2.72),

$$0 = \frac{1}{2\pi i}\int_\gamma \frac{\mathcal{A}(z)}{z} = \mathcal{A}(0) + \sum_\alpha \mathrm{Res}_{z=z_\alpha}\left(\frac{\mathcal{A}(z)}{z}\right) + \int_{\beta_0}^\infty \frac{dz}{z}\mathrm{Disc}_\beta\left(\mathcal{A}(z)\right) + \mathcal{A}_\infty. \quad (2.91)$$

The amplitude is now a sum over poles and discontinuities across branch cuts plus some possible boundary contribution, figure 2.12 shows how these elements can occur in the complex plane. By splitting the amplitude into cut-constructible and rational pieces it is possible to write the rational piece as a recursion relation. There are however further subtleties associated with unphysical poles occurring in the cut-constructed integral functions, in removing these one introduces extra rational functions whose residues must

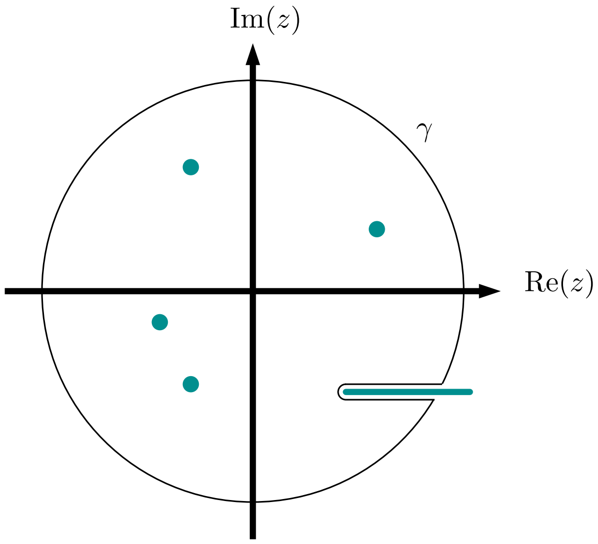

Figure 2.12: Branch cuts and poles of a generic amplitude $\mathcal{A}(z)$ in the complex plane.

be added to the final recursion:

$$\mathcal{A}_n^{(1)}(0) = \widehat{C}_n + \sum_\alpha \mathrm{Res}_{z=z_\alpha}\left(\frac{\widehat{CR}_n(z)}{z}\right) + \sum_{\text{partitions}} \sum_{h=\pm} \left(\mathcal{R}_L^{(1)}(\widehat{P}(z_{ij})^h)\frac{1}{P^2}\mathcal{A}_R^{(0)}(-\widehat{P}(z_{ij})^{-h})\right.$$
$$\left. + \mathcal{A}_L^{(0)}(\widehat{P}(z_{ij})^h)\frac{1}{P^2}\mathcal{R}_R^{(1)}(-\widehat{P}(z_{ij})^{-h}) + \mathcal{A}_L^{(0)}(\widehat{P}(z_{ij})^h)\frac{\mathcal{F}(P)}{P^2}\mathcal{A}_R^{(0)}(-\widehat{P}(z_{ij})^{-h})\right). \tag{2.92}$$

The rational function $\widehat{CR}$ is added to the cut-constructible part C in order to explicitly remove the unphysical singularities,

$$\mathcal{A}_n^{(1)} = C_n + \mathcal{R}_n^{(1)} = (C_n + \widehat{CR}_n) + (\mathcal{R}_n^{(1)} - \widehat{CR}_n) = \widehat{C}_n + \widehat{\mathcal{R}}_n^{(1)}. \tag{2.93}$$

where $\mathcal{R}^{(1)} = \mathcal{A}^{(1)}|_{\text{rational}}$ and z_{ij} are the values of z which put each partition, P, on-shell. This split ensures that we do not have to evaluate residues of the unphysical poles. $\mathcal{F}$ is the one loop factorisation function appearing in the multi-particle factorisation [102] as indicated in figure 2.11. The cut-constructible piece can be calculated using the unitarity based techniques described previously.

Knowledge about boundary conditions is much more difficult to come by. It has been proposed [100] that terms determining the behaviour of $\mathcal{A}(z)$ at large z can also be found recursively, so it appears that a complete program for 1-loop amplitudes is almost complete, allowing simple Feynman calculations for low multiplicity final states to be dressed with QCD corrections to form more complex amplitudes. With on-shell recursion also finding uses in computing integral coefficients [103] it appears that on-shell methods will provide a valuable tool for future amplitude and cross-section calculations required by new collider experiments.

3. MHV rules for Higgs plus multi-parton amplitudes

In this chapter we derive MHV rules for scattering amplitudes of a Higgs boson with many external gluons and quarks. This is achieved by splitting an effective Higgs-gluon coupling into self-dual and anti-self-dual pieces and then applying the MHV rules to both pieces. We begin by discussing the effective vertex before discussing the MHV model and applying it to various amplitudes with consistency checks.

3.1. Higgs-gluon coupling in the large m_t limit

The production of a Higgs boson at a hadron collider will be dominated by gluon radiation so it is useful to define an effective Higgs-gluon interaction. This coupling will be dominated by interaction via a heavy top quark loop, we therefore approximate the interaction in the region where $m_t \gg m_H$. This approximation has been used with great success to calculate a wide variety of processes. We can study the validity of this approximation by examining the decay of the Higgs boson into two gluons. The full decay width can be written [104],

$$\Gamma(H \to gg) = \frac{\alpha_s^2 g^2 m_H^3}{128\pi^3 m_W^2} \sum_{quarks} |\tau_q(1 + (1 - \tau_q)f(\tau_q)|^2 \tag{3.1}$$

where

$$f(\tau_q) = \begin{cases} [\arcsin\sqrt{1/\tau_q}]^2 & \text{if } \tau_q \geq 1, \\ -\frac{1}{4}[\ln(\frac{1+\sqrt{1-\tau_q}}{1-\sqrt{1-\tau_q}}]^2 & \text{if } \tau_q < 1, \end{cases} \tag{3.2}$$

$$\tau_q = \frac{4m_q^2}{m_H^2}. \tag{3.3}$$

We notice that as m_t becomes much larger than the Higgs mass then the decay width goes to a constant. This is best seen in figure 3.1. Here we plot the ratio of the full decay, (3.1), to the constant value in the $m_t \to \infty$ limit against the Higgs mass. Initially we assume that there is one heavy quark i.e. the top quark and we see that the ratio goes to one as the Higgs mass tends to zero. A second curve shows the effect of including bottom quarks in the full decay. Here the approximation is less reliable as the quantity τ_b becomes nearer 1, however for a Higgs mass greater than 100 Gev the effect of the bottom quark is negligible. The third curve in figure 3.1 shows the effect of including a first order correction to the $m_t \to \infty$ limit, i.e. a term $\mathcal{O}(\frac{m_H^2}{m_t^2})$. This significantly reduces the error in the approximation. The error in the $H \to gg$ effective vertex is around $5-6\%$ for a Higgs mass around 120 GeV. Precision fits to electro-weak data indicate that a standard model Higgs has a mass considerably less than $2m_t \approx 340$GeV, currently $m_H < 160$GeV at 95% confidence level [105]. The effective operator has shown to be an excellent approximation by many comparisons to the full NLO QCD calculations [106–109].

The effective Lagrangian can be derived by integrating out the top quark field from the QCD Lagrangian. We can construct an effective Lagrangian by considering gauge invariant operators of the gluon field strength and the Higgs field:

$$\mathcal{L}_{eff} = C\frac{1}{2}\,\mathrm{tr}(G^{\mu\nu}G_{\mu\nu})H + C'\,\mathrm{tr}(G^{\mu}_{\nu}G^{\nu}_{\rho}G^{\rho}_{\mu})H + \dots. \tag{3.4}$$

Here the mass dimension of C' will be two lower than that of C, i.e. it will be suppressed by $\frac{1}{m_t^2}$. Hence we can compute C to $\mathcal{O}(\alpha_s)$ by matching to the matrix elements of the 1-loop $H \to gg$ via a top quark loop in the $m_t \to \infty$ limit.

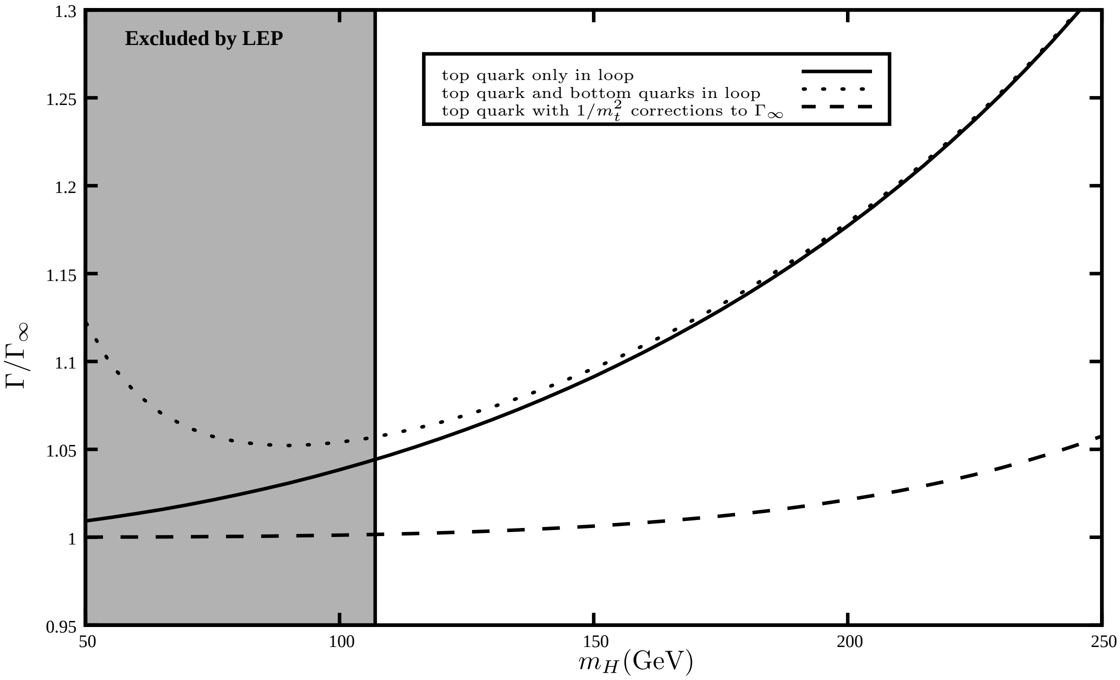

Figure 3.1: A graph showing the validity of the effective Hgg coupling in the large m_t limit.

The lowest order, colour stripped, matrix element for $H \to gg$ from this effective Lagrangian will be

$$\mathcal{M}(H \to gg) = -iC g_{\mu\nu} p_1 \cdot p_2 \epsilon^{*\mu}(p_1)\epsilon^{*\nu}(p_2), \tag{3.5}$$

when working in a light-like axial gauge. The QCD Lagrangian including Higgs interaction for the top quark reads,

$$\mathcal{L} = -\frac{1}{2}\,\mathrm{tr}(G^{\mu\nu}G_{\mu\nu}) + \bar{t}(i\not{D} - m_t)t - \frac{m_t}{v}\bar{t}tH \tag{3.6}$$

We use this to calculate the single triangle contribution shown in figure 3.2 which results in,

$$\mathcal{M}(H \to gg) = -i\frac{\alpha_s}{6\pi v} g_{\mu\nu} p_1 \cdot p_2 \epsilon^{*\mu}(p_1)\epsilon^{*\nu}(p_2) + \mathcal{O}(m_H^2/m_t^2) \tag{3.7}$$

thus the leading order effective Lagrangian is,

$$\mathcal{L}_H = \frac{C}{2} H\,\mathrm{tr}(G^{\mu\nu}G_{\mu\nu}) \tag{3.8}$$

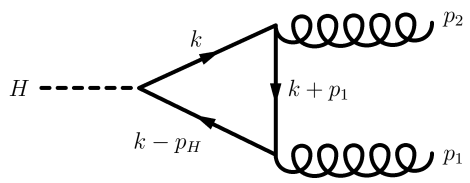

Figure 3.2: Higgs decay to two gluons via a quark loop. This is the only diagram that contributes in the $m_t \to \infty$ limit.

with the strength of the interaction is given by $C = \alpha_s/(6\pi v)$ and $v = 246$ GeV. By considering higher order corrections to the $H \to gg$ matrix element it is also possible to compute the coupling, C, to higher order in α_s. This has been performed to $\mathcal{O}(\alpha_s^2)$ in references [106, 110] and more recently to $\mathcal{O}(\alpha_s^3)$ in [111].

For the rest of this chapter we will concentrate on calculating multi-parton amplitudes for Higgs bosons and up to two quark pairs. Amplitudes of this form have been calculated using the effective Hgg interaction for $Hgggg$ [112], $Hq\bar{q}gg$ [113] and for all 5 parton processes in reference [114]. Amplitudes for higher multiplicities have been available only through numerical programs such as ALPHA[115, 116] and MADGRAPH [117, 118].

3.2. The Higgs MHV Model

The MHV or twistor-space structure of the Higgs-plus-gluons amplitudes is best elucidated by dividing the Higgs coupling to gluons, (3.8), into two terms, containing purely self-dual (SD) and purely anti-self-dual (ASD) gluon field strengths,

$$G_{SD}^{\mu\nu} = \tfrac{1}{2}(G^{\mu\nu} + {}^*G^{\mu\nu}) \ , \quad G_{ASD}^{\mu\nu} = \tfrac{1}{2}(G^{\mu\nu} - {}^*G^{\mu\nu}) \ , \quad {}^*G^{\mu\nu} \equiv \tfrac{i}{2}\epsilon^{\mu\nu\rho\sigma}G_{\rho\sigma} \ . \tag{3.9}$$

This division can be accomplished by considering H to be the real part of a complex field $\phi = \frac{1}{2}(H + iA)$, so that

$$\mathcal{L}_{H,A}^{\text{int}} = \frac{C}{2}\Big[H \, \text{tr}\, G_{\mu\nu}G^{\mu\nu} + iA \, \text{tr}\, G_{\mu\nu}\, {}^*G^{\mu\nu}\Big] \tag{3.10}$$

$$= C\Big[\phi \, \text{tr}\, G_{SD\,\mu\nu}G_{SD}^{\mu\nu} + \phi^\dagger \, \text{tr}\, G_{ASD\,\mu\nu}G_{ASD}^{\mu\nu}\Big] \ . \tag{3.11}$$

The key idea is that, due to self duality, the amplitudes for ϕ plus n gluons, and those for $\phi^\dagger$ plus n gluons, separately have a simpler structure than the amplitudes for H plus n gluons. But because $H = \phi + \phi^\dagger$, the Higgs amplitudes can be recovered as the sum of the ϕ and $\phi^\dagger$ amplitudes.

As another motivation for the split (3.11), note that this interaction can be embedded into an $\mathcal{N} = 1$ supersymmetric effective Lagrangian,

$$\mathcal{L}^{\rm int}_{\rm SUSY} = -C \int d^2\theta \; \Phi \, {\rm tr}\, W^\alpha W_\alpha \; - C \int d^2\bar\theta \; \Phi^\dagger \, {\rm tr}\, \overline{W}_{\dot\alpha} \overline{W}^{\dot\alpha} \, . \tag{3.12}$$

Here $G^{\mu\nu}_{SD}$ is the bosonic component of the chiral superfield W_α, and ϕ is the lowest component of the chiral superfield Φ. We can identify the following helicity assignments:

$$W_\alpha = \{g^-, \Lambda^-\} \, , \qquad \Phi = \{\phi, \psi^-\} \, , \tag{3.13}$$

$$\overline{W}^{\dot\alpha} = \{g^+, \Lambda^+\} \, , \qquad \Phi^\dagger = \{\phi^\dagger, \psi^+\} \, , \tag{3.14}$$

where $g^\pm$ correspond to gluons with $h = \pm 1$ helicities, $\Lambda^\pm$ are gluinos with $h = \pm 1/2$, ϕ and $\phi^\dagger$ are complex scalar fields, and $\psi^\pm$ are their fermionic superpartners. In Appendix B we give the full supersymmetric effective Lagrangian. (This Lagrangian can be generated from a renormalisable, supersymmetric microscopic theory containing a massive top quark/squark chiral multiplet T, coupled to Φ by a Yukawa coupling $\int d^2\theta \Phi T \overline{T}$. Integrating out T produces the interaction (3.12) with a coefficient proportional to the chiral multiplet's contribution to the SYM beta function.)

As in the case of QCD, the fermionic superpartners of the boson ϕ and of the gluons will never enter tree-level processes for ϕ plus n gluons. Thus these bosonic amplitudes must obey supersymmetry Ward identities (SWI) [43, 119, 120] which help to control their structure.

3.3. MHV amplitudes including Higgs bosons and the "two towers"

We start with the (anti)-MHV amplitudes for the Higgs and gluons [53, 54]. First, the decomposition of the HGG vertex into the self-dual and the anti-self-dual terms (3.11), guarantees that the whole class of helicity amplitudes with less than two negative helicities vanish,

$$\mathcal{A}_n(\phi, g_1^{\pm}, g_2^{+}, g_3^{+}, \ldots, g_n^{+}) = 0\,, \quad \mathcal{A}_n(\phi^{\dagger}, g_1^{\pm}, g_2^{-}, g_3^{-}, \ldots, g_n^{-}) = 0\,, \tag{3.15}$$

for all n. This can be shown using Berends-Giele off shell currents, see appendix B.2.

The amplitudes, with precisely two negative helicities, $\phi\, g^- g^+ \ldots g^+ g^- g^+ \ldots g^+$, are the first non-vanishing ϕ amplitudes. These amplitudes will be referred to as the ϕ-MHV amplitudes. General factorisation properties now imply that they have to be extremely simple [53], they read

$$\mathcal{A}_n(\phi, g_1^{+}, g_2^{+}, \ldots, g_p^{-}, \ldots, g_q^{-}, \ldots, g_n^{+}) = \frac{\langle p\, q\rangle^4}{\langle 1\, 2\rangle\, \langle 2\, 3\rangle \cdots \langle n-1,\, n\rangle\, \langle n\, 1\rangle}\,, \tag{3.16}$$

Here only legs p and q have negative helicity. This expression is valid for all n. Besides the correct collinear and multi-particle factorisation behaviour, these amplitudes also correctly reduce to pure QCD MHV amplitudes as the ϕ momentum approaches zero. In fact, the expressions (3.16) for ϕ-MHV n-gluon amplitudes are exactly the same as the MHV n-gluon amplitudes in pure QCD. The only difference of (3.16) with pure QCD is that the total momentum carried by gluons, $p_1 + p_2 + \ldots + p_n = -p_\phi$ is the momentum carried by the ϕ-field and is non-zero. This momentum makes the Higgs case well-defined on-shell for fewer legs than in the pure QCD case. The first few ϕ amplitudes have the form,

$$\mathcal{A}_2(\phi, g_1^{-}, g_2^{-}) = \frac{\langle 1\, 2\rangle^4}{\langle 1\, 2\rangle\, \langle 2\, 1\rangle} = -\langle 1\, 2\rangle^2, \tag{3.17}$$

$$\mathcal{A}_3(\phi, g_1^{-}, g_2^{-}, g_3^{+}) = \frac{\langle 1\, 2\rangle^4}{\langle 1\, 2\rangle\, \langle 2\, 3\rangle\, \langle 3\, 1\rangle} = \frac{\langle 1\, 2\rangle^3}{\langle 2\, 3\rangle\, \langle 3\, 1\rangle}\,, \tag{3.18}$$

$$\mathcal{A}_4(\phi, g_1^{-}, g_2^{-}, g_3^{+}, g_4^{+}) = \frac{\langle 1\, 2\rangle^4}{\langle 1\, 2\rangle\, \langle 2\, 3\rangle\, \langle 3\, 4\rangle\, \langle 4\, 1\rangle}\,. \tag{3.19}$$

Since the MHV amplitudes (3.16) have an identical form to the corresponding amplitudes of pure Yang-Mills theory, their off-shell continuation should also be identical to that proposed in the pure-glue context in [45]. Everywhere the off-shell leg i carrying momentum P_i appears in (3.16), we let the corresponding holomorphic spinor be $\lambda_{i,\alpha} = (P_i)_{\alpha\dot{\alpha}}\xi^{\dot{\alpha}}$. Here $\xi^{\dot{\alpha}}$ is an arbitrary reference spinor, chosen to be the same for all MHV diagrams contributing to the amplitude.

We can now study the helicity structure of the (anti)-self-dual Higgs plus gluon amplitudes. The left (red) tower in figure 3.3 lays out the MHV structure of the ϕ plus multi-gluon amplitudes. All non-vanishing amplitudes are labelled with circles. The fundamental ϕ-MHV vertices, which coincide with the $\phi g^- g^- g^+ \ldots g^+$ amplitudes, are the basic building blocks and are labelled by red dots. The result of combining ϕ-MHV vertices with pure-gauge-theory MHV vertices is to produce amplitudes with more than two negative helicities. These amplitudes are represented as red open circles. Each MHV diagram contains exactly one ϕ-MHV vertex; the rest are pure-gauge-theory MHV vertices. The vertices are combined with scalar propagators. The MHV-drift is always to the left and upwards. Collectively, these amplitudes form the holomorphic (or MHV) tower of accessible amplitudes.

The corresponding amplitudes for $\phi^\dagger$ are shown in the right (green) tower in figure 3.3. They can be obtained by applying parity to the ϕ amplitudes. For practical purposes this means that we compute with ϕ, and reverse the helicities of every gluon. Then we let $\langle i\, j\rangle \leftrightarrow [j\, i]$ to get the desired $\phi^\dagger$ amplitude. The set of building-block amplitudes are therefore anti-MHV. Furthermore, the amplitudes with additional positive-helicity gluons are obtained by combining with anti-MHV gauge theory vertices. The anti-MHV-drift is always to the right and upwards. Collectively, these amplitudes form the anti-holomorphic (or anti-MHV) tower of accessible amplitudes.

The allowed helicity states for H are shown in figure 3.3 and are composed of both holomorphic and anti-holomorphic structures. Where the two towers do not overlap, the amplitudes for the real Higgs boson with gluons coincide with the ϕ ($\phi^\dagger$) amplitudes.

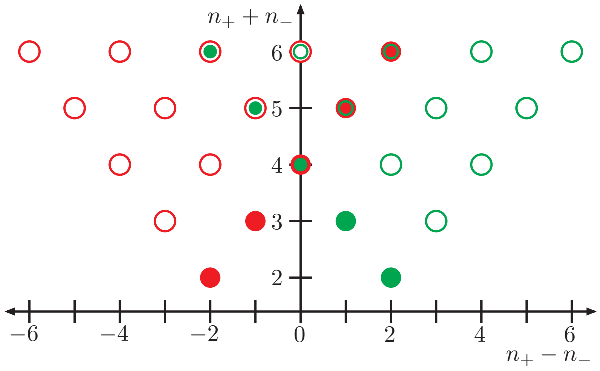

Figure 3.3: The structure of Higgs plus multi-gluon amplitudes obtained by combining the MHV tower for $\phi + n$ gluons and the anti-MHV tower of $\phi^\dagger + n$ gluon amplitudes.

On the other hand, where the towers overlap, we add the ϕ and $\phi^\dagger$ amplitudes.

3.4. MHV amplitude towers including fermions

Quarks do not enter the HGG effective vertex (3.8) or (3.11) directly, they couple to it only through gluons. The division of (3.8) into self-dual and anti-self-dual terms, dictated by (3.11) will continue to be the guiding principle for constructing MHV rules for the Higgs plus quarks and gluons amplitudes. In fact, in this section we will *derive* the MHV rules for the Higgs with gluons and quarks from the simpler MHV rules for amplitudes with the Higgs and gluons only.

Throughout this chapter we will use the standard colour decomposition as described in 2.3. Hence without loss of generality from now on we will concentrate on the colour-ordered partial amplitudes $\mathcal{A}_n$ involving partons (gluons, quark-antiquark pairs, gluinos) plus the single colourless scalar field which can be H, ϕ or $\phi^\dagger$.

The kinematic amplitudes $\mathcal{A}_n$ have the colour information stripped off and hence do not distinguish between fundamental quarks and adjoint gluinos. Hence, if we know kinematic amplitudes involving gluinos in a supersymmetric theory, we automatically know kinematic amplitudes with quarks,

$$\mathcal{A}_n(H, q^+, \ldots, \bar{q}^-, \ldots, g^+, \ldots, g^-) = \mathcal{A}_n(H, \Lambda^+, \ldots, \Lambda^-, \ldots, g^+, \ldots, g^-) \tag{3.20}$$

Here $q^\pm$, $\bar{q}^\pm$, $g^\pm$, $\Lambda^\pm$ denote quarks, antiquarks, gluons and gluinos of $\pm$ helicity, and H represents the colourless scalar H, ϕ, $\phi^\dagger$ or simply nothing. By this we mean that (3.20) is valid with or without the scalar field, this is because the colourless scalar does not modify the colour decomposition. We conclude from (3.20) that knowing kinematic amplitudes in a supersymmetric theory with gluinos allows us to deduce immediately non-supersymmetric amplitudes with quarks and antiquarks.

In the following section we will show that the MHV rules for Higgs and gluon amplitudes uniquely determine the MHV rules for the Higgs plus all partons (i.e. gluons and quarks). More precisely, the MHV amplitudes with the Higgs and gluons determine the MHV amplitudes with the Higgs, gluinos and gluons via supersymmetric Ward identities. Then (3.20) turns gluinos into quarks in a non-supersymmetric theory.

3.4.1. Amplitudes with quarks from SUSY Ward identities

We are now ready to discuss MHV amplitudes with gluons and fermions. To this end we first consider a pure $\mathcal{N}=1$ supersymmetric Yang-Mills (without the Higgs or quarks). An MHV amplitude $\mathcal{A}_n = A_{l+2m}$ with l gluons, g, and $2m$ gluinos, Λ, in the $\mathcal{N}=1$ pure gauge theory exists only for $m = 0, 1, 2$. This is because it must have precisely $n-2$ particles with positive helicity and 2 with negative helicity, and gluinos always come in pairs with helicities $\pm\frac{1}{2}$. Hence, there are three types of MHV tree amplitudes in the $\mathcal{N}=1$ pure gauge theory:

$$\mathcal{A}_n(g_p^-, g_q^-)\ , \quad \mathcal{A}_n(g_t^-, \Lambda_r^-, \Lambda_s^+)\ , \quad \mathcal{A}_n(\Lambda_t^-, \Lambda_s^+, \Lambda_r^-, \Lambda_q^+)\ . \tag{3.21}$$

The MHV purely gluonic amplitude is [60, 121]:

$$\mathcal{A}_n(g_p^-, g_q^-) = \frac{\langle p\ q\rangle^4}{\prod_{i=1}^n \langle i\ i+1\rangle}\ , \tag{3.22}$$

where $\lambda_{n+1} \equiv \lambda_1$. For notational simplicity in this and the following expressions for MHV amplitudes we do not show explicitly the positive helicity gluons g^+. The MHV amplitude with two external fermions and $n-2$ gluons is

$$\mathcal{A}_n(g_t^-, \Lambda_r^-, \Lambda_s^+) = \frac{\langle t\ r\rangle^3\ \langle t\ s\rangle}{\prod_{i=1}^n \langle i\ i+1\rangle}\ , \quad \mathcal{A}_n(g_t^-, \Lambda_s^+, \Lambda_r^-) = -\frac{\langle t\ r\rangle^3\ \langle t\ s\rangle}{\prod_{i=1}^n \langle i\ i+1\rangle}\ , \tag{3.23}$$

where the first expression corresponds to $r < s$ and the second to $s < r$ (and t is arbitrary). The MHV amplitudes with four fermions and $n-4$ gluons on external lines are

$$\mathcal{A}_n(\Lambda_t^-, \Lambda_s^+, \Lambda_r^-, \Lambda_q^+) = \frac{\langle t\ r\rangle^3\ \langle s\ q\rangle}{\prod_{i=1}^n \langle i\ i+1\rangle}\ , \quad \mathcal{A}_n(\Lambda_t^-, \Lambda_r^-, \Lambda_s^+, \Lambda_q^+) = -\frac{\langle t\ r\rangle^3\ \langle s\ q\rangle}{\prod_{i=1}^n \langle i\ i+1\rangle} \tag{3.24}$$

The first expression in (3.24) corresponds to $t < s < r < q$, the second to $t < r < s < q$, and there are other similar expressions, obtained by further permutations of fermions, with the overall sign determined by the ordering.

We now recall that expressions (3.23), (3.24) are not independent inputs into the MHV programme, they follow from the amplitudes (3.22) via supersymmetric Ward identities [41, 43, 119, 120, 122].

Supersymmetric Ward identities [43, 119, 120] follow from the fact that, supercharges Q annihilate the vacuum, and hence we have an equation,

$$\langle [Q\, ,\, \Lambda_k^+ \ldots g_{r_1}^- \ldots g_{r_2}^- \ldots] \rangle \ = \ 0\ , \tag{3.25}$$

where dots indicate positive helicity gluons. In order to make anticommuting spinor Q to be a singlet entering a commutative (rather than anticommutative) algebra with all the fields we contract it with a commuting spinor η and multiply it by a Grassmann number θ. This defines a commuting singlet operator $Q(\eta)$. Following [122] we can write down the following susy algebra relations,

$$\begin{aligned} [Q(\eta)\, ,\, \Lambda^+(k)] \ &= \ -\theta\langle \eta\ k\rangle\, g^+(k)\ , \quad [Q(\eta)\, ,\, \Lambda^-(k)] \ = \ +\theta[\eta\ k]\, g^-(k)\ , \\ [Q(\eta)\, ,\, g^-(k)] \ &= \ +\theta\langle \eta\ k\rangle\, \Lambda^-(k)\ , \quad [Q(\eta)\, ,\, g^+(k)] \ = \ -\theta[\eta\ k]\, \Lambda^+(k)\ . \end{aligned} \tag{3.26}$$

In what follows, the anticommuting parameter θ will cancel from the relevant expressions for the amplitudes. The arbitrary spinors η_a, $\eta_{\dot a}$, will be fixed below. It then follows from (3.26) that

$$\theta\langle\eta\ k\rangle\,\mathcal{A}_n(g^-_{r_1},g^-_{r_2}) = \ -\theta\langle\eta\ r_1\rangle\,\mathcal{A}_n(\Lambda^+_k,\Lambda^-_{r_1},g^-_{r_2}) -\ \theta\langle\eta\ r_2\rangle\,\mathcal{A}_n(\Lambda^+_k,g^-_{r_1},\Lambda^-_{r_2})\ . \qquad (3.27)$$

The minus signs on the right hand side arise from anticommuting θ with gluino fields. After cancelling θ and choosing η to be one of the two r_j we find from (3.27) that the purely gluonic amplitude is proportional to the amplitude with two gluinos,

$$\mathcal{A}_n(g^-_{r_1},g^-_{r_2}) \ = \ -\frac{\langle r_2\ r_1\rangle}{\langle r_2\ k\rangle}\,\mathcal{A}_n(\Lambda^+_k,\Lambda^-_{r_1},g^-_{r_2}) \ = \ -\frac{\langle r_1\ r_2\rangle}{\langle r_1\ k\rangle}\,\mathcal{A}_n(\Lambda^+_k,g^-_{r_1},\Lambda^-_{r_2})\ . \qquad (3.28)$$

This gives the MHV amplitudes (3.23). Equations (3.24) follow from a similar construction.

We can now add the Higgs scalars ϕ and $\phi^\dagger$ to the construction of MHV amplitudes above. To achieve this we can use the SUSY Lagrangian with the effective bosonic interaction (3.11) embedded given in (3.12),

$$\mathcal{L}^{\rm int} = -C\int d^2\theta\ \phi\ {\rm tr}\, W^\alpha W_\alpha\ - C\int d^2\bar\theta\ \phi^\dagger\ {\rm tr}\,\overline{W}_{\dot\alpha}\overline{W}^{\dot\alpha}\,. \qquad (3.29)$$

Here $G^{\mu\nu}_{SD}$ is the bosonic component of the $\mathcal{N}=1$ chiral superfield $W_\alpha(x,\theta)$, but ϕ is not a superfield, it is still a (single component) scalar field $\phi(x)$ which has no superpartners. So, the theory described by (3.12) is not a supersymmetric theory. However, there is a continuous symmetry group which leaves this action invariant. It is generated by the 'supercharges' Q which act non-trivially on gluons and gluinos – precisely as in (3.26) – and at the same time annihilate the scalar field,

$$[Q(\eta)\,,\,\phi(p)] \ = \ 0\ , \qquad [Q(\eta)\,,\,\phi^\dagger(p)] \ = \ 0\ . \qquad (3.30)$$

Applying the commutation relations, (3.12), (3.30) to equation

$$\langle[Q\,,\,\phi\,\Lambda^+_k\ldots g^-_{r_1}\ldots g^-_{r_2}\ldots]\rangle \ = \ 0\ , \qquad (3.31)$$

we find the same relation as in (3.28), but now for the MHV amplitudes with the Higgs field ϕ.

We conclude that from the fact that the purely gluonic MHV amplitudes, (3.16) and (3.22) take the same form, the pseudo-supersymmetry Ward identities guarantee that the tree-level ϕ-MHV amplitudes with fermions and gluons have exactly the same algebraic form as the corresponding MHV amplitudes in pure $\mathcal{N} = 1$ gauge theory, (3.23) and (3.24). Hence we now can insert the ϕ field on the left hand sides of (3.23) and (3.24), and, furthermore, replace gluinos with quarks as in (3.20).

We need to be slightly more careful in order to deduce the ϕ-MHV amplitudes with two quark-antiquark pairs of different flavours, i.e. $A_n(\phi, q^+, \bar{q}^-, Q^+, \bar{Q}^-)$ where q and Q denote the two different quarks. Such amplitudes are obtained from the $\mathcal{N} = 2$ supersymmetric amplitudes $A_n(\phi, \Lambda^+_{(1)}, \Lambda^-_{(1)}, \Lambda^+_{(2)}, \Lambda^-_{(2)})$ where $\Lambda_{(1)}$ and $\Lambda_{(2)}$ are gluinos from two different $\mathcal{N} = 1$ supermultiplets. All such amplitudes can be read off from the general expression for the MHV $\mathcal{N} = 4$ supervertex of Nair [123] using the algorithm described in [47, 124]. The supervertex and the corresponding component vertices comply with the supersymmetric Ward identities in pure $\mathcal{N} = 4$ theory. The Higgs field ϕ can always be added to these amplitudes in precisely the same way as above, without changing the expression for the vertex. This follows from promoting the $\mathcal{N} = 4$ or $\mathcal{N} = 2$ supersymmetry to a 'pseudo' supersymmetry by augmenting the algebra with the condition (3.30).

3.5. MHV rules

We have argued that the complete set of MHV amplitudes in QCD coupled to the Higgs field consists of n-parton amplitudes made out of one or less scalar field ϕ, an arbitrary number of gluons and $m = 0, 1, 2$ quark-antiquark pairs. All these amplitudes have precisely two negative helicities. Schematically, they are

$$\mathcal{A}_n(\phi, g_p^-, g_q^-) \ , \quad \mathcal{A}_n(\phi, q_1^{-\lambda}, g_r^-, \bar{q}_n^{\lambda}) \ , \quad \mathcal{A}_n(\phi, q_1^{-\lambda_1}, \bar{Q}_s^{\lambda_2}, Q_{s+1}^{-\lambda_2}, \bar{q}_n^{\lambda_1}) \ , \tag{3.32}$$

$$\mathcal{A}_n(g_p^-, g_q^-) \ , \quad \mathcal{A}_n(q_1^{-\lambda}, g_r^-, \bar{q}_n^{\lambda}) \ , \quad \mathcal{A}_n(q_1^{-\lambda_1}, \bar{Q}_s^{\lambda_2}, Q_{s+1}^{-\lambda_2}, \bar{q}_n^{\lambda_1}) \ . \tag{3.33}$$

Here we have not shown the positive helicity gluons and did not exhibit all different orderings for amplitudes with two quark-antiquark pairs. As before, $Q^{-\lambda_2}$ and $\bar{Q}^{\lambda_2}$ denote the second flavour of (anti)quarks with helicities $\pm\lambda_2$.

The first line, (3.32), gives the ϕ-MHV amplitudes, and the second line, (3.33) corresponds to standard QCD MHV amplitudes. The $\overline{\text{MHV}}$ amplitudes are obtained from ((3.32)) and ((3.33)) by parity. They are

$$\mathcal{A}_n(\phi^\dagger, g_p^+, g_q^+)\ , \quad \mathcal{A}_n(\phi^\dagger, q_1^\lambda, g_r^+, \bar{q}_n^{-\lambda})\ , \quad \mathcal{A}_n(\phi^\dagger, q_1^{\lambda_1}, \bar{Q}_s^{-\lambda_2}, Q_{s+1}^{\lambda_2}, \bar{q}_n^{-\lambda_1})\ , \tag{3.34}$$

$$\mathcal{A}_n(g_p^+, g_q^+)\ , \quad \mathcal{A}_n(q_1^\lambda, g_r^+, \bar{q}_n^{-\lambda})\ , \quad \mathcal{A}_n(q_1^{\lambda_1}, \bar{Q}_s^{-\lambda_2}, Q_{s+1}^{\lambda_2}, \bar{q}_n^{-\lambda_1})\ , \tag{3.35}$$

where we have not shown the negative helicity gluons.

Figure 3.3 showed how the picture of two overlapping towers of amplitudes emerged from the self-dual and anti-self-dual Higgs fields interacting with gluons. We observe similar properties for amplitudes with one quark-antiquark pair. Helicity must be conserved along the quark line so the all plus configuration is trivially zero. The case where antiquark has opposite helicity to the quark and all gluons have positive helicity is also zero, see Appendix B.3 for a proof which does not appeal to supersymmetry. So the first non-vanishing amplitude is again with two negative helicities and one of them lying on a gluon: $\mathcal{A}_n(\phi, q_1^\lambda, \ldots, g_s^-, \ldots, \bar{q}_n^{-\lambda})$. This is precisely the second ϕ-MHV amplitude in (3.34).

The structure of the two MHV towers for amplitudes with the Higgs and one quark-antiquark pair is set out in figure 3.4. Here the ϕ-MHV amplitudes are represented by filled red dots and the ϕ-$\overline{\text{MHV}}$ by filled green dots. The open red(green) dots are amplitudes which can be found by combining two or more MHV($\overline{\text{MHV}}$) vertices. The $\overline{\text{MHV}}$ amplitudes can be obtained directly from the MHV amplitudes via parity transformation. Once again, Higgs amplitudes are given directly by ϕ or $\phi^\dagger$ amplitudes, or by adding them when the towers overlap.

The case of two quark-antiquark pairs proceeds in an almost identical way. Helicity conservation along both quark lines immediately leads us to the fact that the first non-

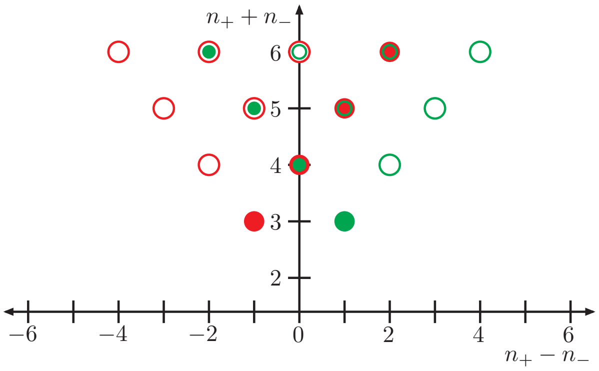

Figure 3.4: The structure of Higgs plus multi-gluon plus quark-antiquark pair amplitudes obtained by combining the MHV tower for $\phi + q\bar{q} + n$ gluons and the anti-MHV tower of $\phi^\dagger + q\bar{q} + n$ gluon amplitudes.

zero ϕ-amplitude contains two negative helicities, $A(q^{\lambda_1}, \bar{q}^{-\lambda_1}, Q^{\lambda_2}, \bar{Q}^{-\lambda_2})$, and this is precisely the third ϕ-MHV amplitude in (3.34). Figure 3.5 shows the structure of the MHV and $\overline{\text{MHV}}$ towers. In the same way as before we add together the MHV(red) and $\overline{\text{MHV}}$(green) amplitudes to get the Higgs amplitudes.

In all three figures we combine the MHV amplitudes at tree level by first continuing appropriate lines off-shell in the same way as in [45], and then connecting them by scalar propagators. The propagators connecting gluon or fermion lines are always of the scalar type, $1/q^2$, as explained in [47, 48].

3.6. Applications to gluon amplitudes

The use of the MHV rules as described in the previous sections to compute scattering amplitudes with a Higgs boson coupling to gluons has been performed in reference [53]. Here I will consider two simple examples of gluons amplitudes to show how the method can be applied. The colour ordering of these amplitudes is given by equation (2.58) from section 2.3.

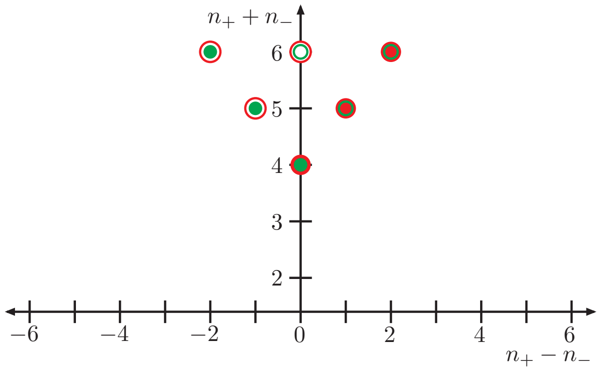

Figure 3.5: The structure of Higgs plus multi-gluon plus two quark-antiquark pair amplitudes obtained by combining the MHV tower for $\phi + q\bar{q} + Q\bar{Q} + n$ gluons and the anti-MHV tower of $\phi^\dagger + q\bar{q} + Q\bar{Q} + n$ gluon amplitudes.

3.6.1. $H \to - - -$

This amplitude is the simplest NMHV amplitude from the ϕ-MHV tower. It is a sum of three MHV diagrams:

$$\begin{aligned}\mathcal{A}(H;1^-,2^-,3^-) &= \sum_{\text{perms}} -\langle 1P_{23}\rangle^2 \frac{1}{P_{23}^2} \frac{\langle 23\rangle^3}{\langle 3P_{23}\rangle\langle P_{23}2\rangle} \\ &= \sum_{\text{perms}} \frac{\langle 1|P_{23}|\xi]^2}{[23][2\xi][3\xi]} \\ &= \frac{\langle 1|P_{23}|\xi]^2}{[23][2\xi][3\xi]} + \frac{\langle 2|P_{31}|\xi]^2}{[31][3\xi][1\xi]} + \frac{\langle 3|P_{12}|\xi]^2}{[12][1\xi][2\xi]} \end{aligned} \tag{3.36}$$

We can check numerically that (3.36) is independent of ξ and agrees with the known result however in this case it is also relatively easy to choose a value for ξ and check the relation analytically. We can set $\xi^\mu = 1^\mu + 2^\mu \epsilon$, with ϵ small. Eventually we will want to set ϵ to zero but first we need to cancel singularities that come from the $1/[1\xi]$ factors. The first term in (3.36) becomes,

$$\frac{(\langle 1|P_{23}|1] + \epsilon\langle 13\rangle[32])^2}{[23][21]([31]+\epsilon[32])} = -\frac{\langle 1|P_{23}|1]^2}{[12][23][31]} + \mathcal{O}(\epsilon). \tag{3.37}$$

whereas the second and third terms both contain singularities.

$$\text{term 2}: \frac{\langle 23\rangle^2}{\epsilon[12]} + 2\frac{\langle 23\rangle\langle 2|P_{31}|2]}{[12][31]} + \frac{\langle 23\rangle^2[23]}{[12][31]} + \mathcal{O}(\epsilon).$$
$$\text{term 3}: -\frac{\langle 23\rangle^2}{\epsilon[12]} + 2\frac{\langle 23\rangle\langle 13\rangle}{[12]} + \mathcal{O}(\epsilon). \tag{3.38}$$

Summing all three terms leaves us with an expression free of $1/\epsilon$ poles which can be re-written in the form:

$$\mathcal{A}(H;1^-,2^-,3^-) = -\frac{m_H^4}{[12][23][31]}, \tag{3.39}$$

which matches previous results.

3.6.2. $H \to ++--$

This amplitude is the simplest case to receive contributions from both the ϕ-MHV and the $\phi^\dagger$-$\overline{\text{MHV}}$ towers. It is simply a sum of the MHV and $\overline{\text{MHV}}$ amplitudes from each tower:

$$\begin{aligned}\mathcal{A}(H;1^+,2^+,3^-,4^-) &= \mathcal{A}(\phi;1^+,2^+,3^-,4^-) + \mathcal{A}(\phi^\dagger;1^+,2^+,3^-,4^-) \\ &= \frac{\langle 34\rangle^3}{\langle 41\rangle\langle 12\rangle\langle 23\rangle} + \frac{[12]^3}{[23][34][41]}\end{aligned} \tag{3.40}$$

which agrees with previous Feynman calculations [114].

3.7. Amplitudes with one quark-antiquark pair

When there is a single quark-antiquark pair, the tree-level amplitude can be decomposed into colour-ordered amplitudes as follows,

$$\begin{aligned}&\mathcal{A}_n(\phi,\{p_i,\lambda_i,a_i\},\{p_j,\lambda_j,i_j\}) \\ &\quad= iCg^{n-2}\sum_{\sigma\in S_{n-2}}(T^{a_{\sigma(2)}}\cdots T^{a_{\sigma(n-1)}})_{i_1 i_n}\,\mathcal{A}_n(\phi,1^\lambda,\sigma(2^{\lambda_2},\ldots,(n-1)^{\lambda_{n-1}}),n^{-\lambda}).\end{aligned} \tag{3.41}$$

where S_{n-2} is the set of permutations of $(n-2)$ gluons. Gluons are characterised with adjoint colour label a_i, momentum p_i and helicity λ_i for $i = 1,\ldots,n-1$, while the

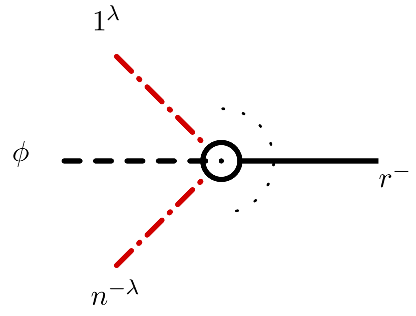

Figure 3.6: MHV vertices for ϕ and one quark pair. The quark line is represented by the red dot-dashed line where $\pm\lambda_1$ are the helicities of the quark and anti-quark. The negative helicity gluon is represented as a solid black line.

fermions carry fundamental colour label i_j, momentum p_j and helicity λ_j for $j = 1, n$. By current conservation, the quark and antiquark helicities are related such that $\lambda_1 = -\lambda_n \equiv \lambda$ where $\lambda = \pm\frac{1}{2}$.

3.7.1. MHV Amplitudes

There are two MHV vertices for a scalar, ϕ, and a quark pair indicated in figure 3.6. Together with the usual MHV vertices (3.33) and a scalar with gluons (3.16) we can begin to construct tree-level Higgs amplitudes with one quark pair. The expressions for the new vertices are:

$$\mathcal{A}_n(\phi, q_1^-, \ldots, g_r^-, \ldots, \bar{q}_n^+) = \frac{\langle r\,1\rangle^3 \langle r\,n\rangle}{\prod_{l=1}^n \langle l\,l+1\rangle}, \qquad (3.42)$$

$$\mathcal{A}_n(\phi, q_1^+, \ldots, g_r^-, \ldots, \bar{q}_n^-) = \frac{\langle r\,1\rangle \langle r\,n\rangle^3}{\prod_{l=1}^n \langle l\,l+1\rangle}. \qquad (3.43)$$

The $\overline{\text{MHV}}$ amplitudes can be obtained by the following parity transformation:

$$\mathcal{A}_n(\phi^\dagger, q_1^\lambda, \ldots, g_r^+, \ldots, \bar{q}_n^{-\lambda}) = (-1)^n \left(\mathcal{A}_n(\phi, q_1^{-\lambda}, \ldots, g_r^-, \ldots, \bar{q}_n^\lambda)\right)^* \qquad (3.44)$$

Besides having the correct collinear and multi-particle factorisation behaviour, these amplitudes also correctly reduce to pure QCD amplitudes as the ϕ momentum approaches zero. As discussed in Sec. 2, eqs. (3.42) and (3.43) follow from the analogous MHV amplitudes for $\phi-$gluon interactions (3.16) by supersymmetry. Alternatively, eqs. (3.42) and (3.43) can be proved recursively, along the lines of the proof in the QCD case [60], or using the light-cone recursive currents of ref. [125].

3.7.2. $H \to q^- g^- g^+ \bar{q}^+$

This amplitude corresponds to $n_+ + n_- = 4$, $n_+ - n_- = 0$. As we see from figure 3.4, the amplitude receives contributions from both the MHV and $\overline{\text{MHV}}$ towers, so that

$$\begin{aligned} \mathcal{A}_n(H, q_1^-, g_2^-, g_3^+, \bar{q}_4^+) &= \mathcal{A}_n(\phi, q_1^-, g_2^-, g_3^+, \bar{q}_4^+) + \mathcal{A}_n(\phi^\dagger, q_1^-, g_2^-, g_3^+, \bar{q}_4^+) \\ &= -\frac{[34]^2[13]}{[12][23][41]} - \frac{\langle 1\,2\rangle^2 \langle 2\,4\rangle}{\langle 2\,3\rangle \langle 3\,4\rangle \langle 4\,1\rangle}. \end{aligned} \tag{3.45}$$

This expression agrees with the known analytic formulae of Ref. [113].

3.7.3. NMHV Amplitudes

We continue by deriving the Next-to-MHV (NMHV) amplitude

$$\mathcal{A}_n(\phi, q_1^\lambda, \ldots, m_2^-, \ldots, m_3^-, \ldots, \bar{q}_n^{-\lambda}), \tag{3.46}$$

with three negative helicity particles – one negative helicity quark(antiquark) and two negative helicity gluons labelled as m_2^- and m_3^-. From now on we will suppress the dots for positive helicity gluons in the MHV tower of amplitudes. When labelling the partons in each NMHV diagram we systematically choose to put the ϕ-MHV vertex on the left. Figure 3.7 shows a skeleton diagram of a generic NMHV amplitude and shows how the partons are labelled cyclically. The dotted semicircles denote the emission of positive helicity gluons from the vertex. We use this convention in all of the NMHV diagrams with one or two quark pairs. All possible diagrams contributing to (3.46) are shown in figure 3.8. Each of these diagrams is drawn for the fixed arrangement of negative helicity gluons, such that q_1^λ is followed by m_2^-, followed by m_3^- followed by $\bar{q}_n^{-\lambda}$. The full NMHV amplitude is given by,

$$\mathcal{A}_n(\phi, 1^\lambda, m_2^-, m_3^-, n^{-\lambda}) = \frac{1}{\prod_{l=1}^n \langle l\, l+1\rangle} \sum_{i=1}^{8} \mathcal{A}_n^{(i),\lambda}(m_2, m_3)\ , \tag{3.47}$$

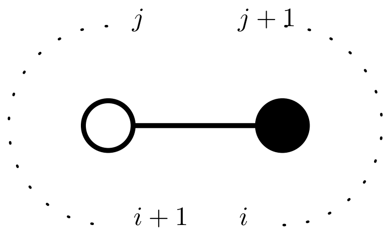

Figure 3.7: Skeleton diagram showing the labelling of the positive helicity gluons in NMHV amplitudes. The gluons are shown as dotted lines with labels showing the bounding g^+ lines in each MHV vertex.

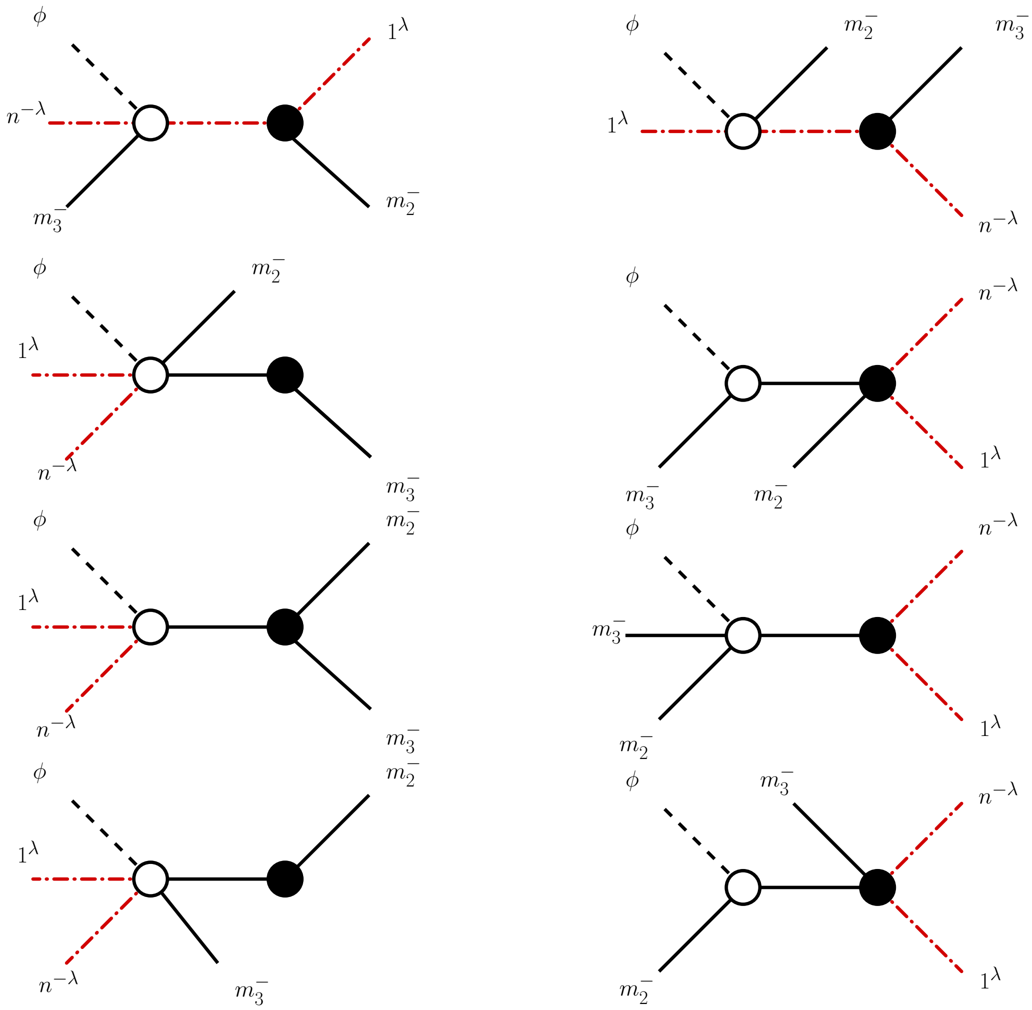

Figure 3.8: Tree diagrams with MHV vertices contributing to the amplitude $\mathcal{A}_n(\phi, q_1^{\lambda}, \ldots, m_2^-, \ldots, m_3^-, \ldots, \bar{q}_n^{-\lambda})$. The scalar ϕ is represented by a dashed line and negative helicity gluons, g^-, by solid lines. The quark-antiquark line is represented by the red dot-dashed line.

where the common standard denominator of cyclic products of $\langle l\, l+1\rangle$ is factored out for convenience. We label the parton momenta as p_i (where i is defined modulo n) and introduce the composite (off-shell) momentum,

$$q_{i+1,j} = p_{i+1} + \ldots + \ldots + p_j. \tag{3.48}$$

Note that the momentum of ϕ, p_ϕ, does not enter the sum. In particular, $q_{i+1,i} = -p_\phi$. As usual, the off-shell continuation of the helicity spinor is defined as [45],

$$\lambda_{i+1,j\ \alpha} = q_{i+1,j\alpha\dot\alpha}\, \xi^{\dot\alpha}, \tag{3.49}$$

where $\xi^{\dot\alpha}$ is a reference spinor that can be arbitrarily chosen. Following the organisational structure of [48, 53], the contributions of the individual diagrams in figure 3.8 are given by

$$\begin{aligned}
\mathcal{A}_n^{(1),\lambda}(m_2,m_3) &= \sum_{i=m_2}^{m_3-1}\sum_{j=n}^{n} \frac{\mathcal{A}_n^{(1),\lambda}(q_{j+1,i},m_2,m_3)}{D(j,i,q_{j+1,i})}, \\
\mathcal{A}_n^{(3),\lambda}(m_2,m_3) &= \sum_{i=m_3}^{n-1}\sum_{j=m_2}^{m_3-1} \frac{\mathcal{A}_n^{(3),\lambda}(q_{j+1,i},m_2,m_3)}{D(j,i,q_{j+1,i})}, \\
\mathcal{A}_n^{(5),\lambda}(m_2,m_3) &= \sum_{i=m_3}^{n-1}\sum_{j=1}^{m_2-1} \frac{\mathcal{A}_n^{(5),\lambda}(q_{j+1,i},m_2,m_3)}{D(j,i,q_{j+1,i})}, \\
\mathcal{A}_n^{(7),\lambda}(m_2,m_3) &= \sum_{i=m_2}^{m_3-1}\sum_{j=1}^{m_2-1} \frac{\mathcal{A}_n^{(7),\lambda}(q_{j+1,i},m_2,m_3)}{D(j,i,q_{j+1,i})}, \\
\mathcal{A}_n^{(2k),\lambda}(q_{j+1,i},m_2,m_3) &= \frac{\mathcal{A}_n^{(2k-1),\lambda}(q_{i+1,j},m_2,m_3)}{D(i,j,q_{i+1,j})} \qquad \text{for} \qquad k=1,\ldots,4
\end{aligned} \tag{3.50}$$

and where

$$D(i,j,q) = \langle i^-|\not{q}|\xi^-\rangle\langle j+1^-|\not{q}|\xi^-\rangle\langle i+1^-|\not{q}|\xi^-\rangle\langle j^-|\not{q}|\xi^-\rangle \frac{q^2}{\langle i\, i+1\rangle\,\langle j\, j+1\rangle}. \tag{3.51}$$

The amplitudes where the quark carries negative helicity are given by:

$$\begin{aligned}
\mathcal{A}_n^{(1),-}(q,m_2,m_3) &= \langle m_2\,1\rangle^3 \left\langle m_2^-\right| \not{q}\left|\xi^-\right\rangle \left\langle m_3^-\right| \not{q}\left|\xi^-\right\rangle^3 \langle m_3\,n\rangle\,, \\
\mathcal{A}_n^{(3),-}(q,m_2,m_3) &= \langle m_2\,1\rangle^3 \langle m_2\,n\rangle \left\langle m_3^-\right| \not{q}\left|\xi^-\right\rangle^4\,, \\
\mathcal{A}_n^{(5),-}(q,m_2,m_3) &= \left\langle 1^-\right| \not{q}\left|\xi^-\right\rangle^3 \left\langle n^-\right| \not{q}\left|\xi^-\right\rangle \langle m_2\,m_3\rangle^4\,, \\
\mathcal{A}_n^{(7),-}(q,m_2,m_3) &= \langle m_3\,1\rangle^3 \langle m_3\,n\rangle \left\langle m_2^-\right| \not{q}\left|\xi^-\right\rangle^4\,,
\end{aligned} \tag{3.52}$$

while the amplitudes where the quark carries positive helicity are given by,

$$\begin{aligned}
\mathcal{A}_n^{(1),+}(q,m_2,m_3) &= \langle m_2\,1\rangle \left\langle m_2^-\right| \not{q}\left|\xi^-\right\rangle^3 \left\langle m_3^-\right| \not{q}\left|\xi^-\right\rangle \langle m_3\,n\rangle^3\,, \\
\mathcal{A}_n^{(3),+}(q,m_2,m_3) &= \langle m_2\,1\rangle \langle m_2\,n\rangle^3 \left\langle m_3^-\right| \not{q}\left|\xi^-\right\rangle^4\,, \\
\mathcal{A}_n^{(5),+}(q,m_2,m_3) &= \left\langle 1^-\right| \not{q}\left|\xi^-\right\rangle \left\langle n^-\right| \not{q}\left|\xi^-\right\rangle^3 \langle m_2\,m_3\rangle^4\,, \\
\mathcal{A}_n^{(7),+}(q,m_2,m_3) &= \langle m_3\,1\rangle \langle m_3\,n\rangle^3 \left\langle m_2^-\right| \not{q}\left|\xi^-\right\rangle^4\,.
\end{aligned} \tag{3.53}$$

As in Ref. [53] we leave the reference spinor ξ arbitrary and specifically do not set it to be equal to one of the momenta in the problem. This has two advantages. First, we do not introduce unphysical singularities in diagrams containing a three gluon vertex. Second, it allows a powerful numerical check of gauge invariance i.e. all colour ordered amplitudes must be independent of the specific choice of ξ.

Equation 3.47 describes all amplitudes coupling ϕ to a quark-antiquark pair, 2 negative helicity gluons and any number of positive helicity gluons. In particular, it describes $\phi \to q^- g^- g^- \bar{q}^+$. This final state only receives contributions from the MHV tower of amplitudes and the amplitude for $\phi \to q^- g^- g^- \bar{q}^+$ is therefore equivalent to the amplitude for $H \to q^- g^- g^- \bar{q}^+$.

From the amplitudes (3.52) and (3.53) we can observe that in the limit $p_\phi \to 0$ each even numbered diagram collapses on to the corresponding odd numbered diagram. The momentum conservation law $q_{1,n} = p_\phi \to 0$ implies that $q_{i+1,j} = -q_{j+1,i}$ i.e. the transformation $i \leftrightarrow j$ leaves the amplitude unchanged as there are even numbers of q's in the expressions. This means that we recover the 4 NMHV quark-gluon diagrams twice.

3.7.4. $H \to q^- g^- g^- \bar{q}^+$

In this case, we can take $\lambda = -$, $m_2 = 2$ and $m_3 = 3$. The third and seventh classes of diagrams in figure 3.8 collapse since there are not enough gluons to prevent the right hand vertex vanishing.

We have checked, with a help of a symbolic manipulator, that our results are ξ-independent (gauge invariant) and numerically agree with the known analytic formulae [113],

$$\begin{aligned}\mathcal{A}_4(H, 1_q^-, 2^-, 3^-, 4_{\bar{q}}^+) &= \frac{\langle 3^-|\not{p}_H|4^-\rangle^2 \langle 1\,2\rangle}{[4\,2]\, s_{124}} \left(\frac{1}{s_{12}} + \frac{1}{s_{14}}\right) - \frac{\langle 2^-|\not{p}_H|4^-\rangle^2 \langle 1\,3\rangle}{[4\,3]\, s_{134} s_{14}} \\ &\quad - \frac{\langle 1^-|\not{p}_H|4^-\rangle^2}{\langle 1\,4\rangle\, [4\,2]\, [4\,3]\, [2\,3]} \end{aligned} \tag{3.54}$$

where $p_H = p_\phi$.

3.7.5. $H \to q^\lambda g^- g^- g^+ \bar{q}^{-\lambda}$

As discussed in Ref. [114], there are three independent amplitudes, corresponding to having any of the three gluons with positive helicity. Each amplitude receives contributions from both the MHV and anti-MHV towers so that setting (m_2, m_3) to be $(2, 3)$, for example,

$$\begin{aligned}\mathcal{A}_5(H, 1_q^\lambda, 2^-, 3^-, 4^+, 5_{\bar{q}}^{-\lambda}) &= \mathcal{A}_5(\phi, 1_q^\lambda, 2^-, 3^-, 4^+, 5_{\bar{q}}^{-\lambda}) \\ &+ \mathcal{A}_5(\phi^\dagger, 1_q^\lambda, 2^-, 3^-, 4^+, 5_{\bar{q}}^{-\lambda}). \end{aligned} \tag{3.55}$$

We can obtain the negative helicities in other positions by taking (m_2, m_3) to be either $(2, 4)$ or $(3, 4)$. We have checked numerically that eq. (3.55) is gauge invariant and gives the same result as an independent Feynman diagram calculation. The same holds for the other assignments of negative helicity gluons.

3.8. Amplitudes with two quark-antiquark pairs

When there are two quark-antiquark pairs the tree-level amplitude can be decomposed into colour ordered amplitudes as,

$$\begin{aligned} & A_n(\phi,\{p_i,\lambda_i,a_i\},\{p_j,\lambda_j,i_j\}) = iC'g^{n-2}\sum_{k}^{n-4}\sum_{\sigma\in S_k}\sum_{\rho\in S_l}\Bigg\{ \\ & (T^{a_{\sigma(1)}}\cdots T^{a_{\sigma(k)}})_{i_1 i_4}(T^{a_{\rho(1)}}\cdots T^{a_{\rho(l)}})_{i_3 i_2} \\ & \times\mathcal{A}_n(\phi,q_1^{\lambda_1},\sigma(1),\ldots,\sigma(k)),\bar{Q}_s^{-\lambda_2};Q_{s+1}^{\lambda_2},\rho(1),\ldots,\rho(l),\bar{q}_n^{-\lambda_1}) \\ - \; & \frac{1}{N}(T^{a_{\sigma(1)}}\cdots T^{a_{\sigma(k)}})_{i_1 i_2}(T^{a_{\rho(1)}}\cdots T^{a_{\rho(l)}})_{i_3 i_4} \\ & \times\tilde{\mathcal{A}}_n(\phi,q_1^{\lambda_1},\sigma(1),\ldots,\sigma(k),\bar{q}_s^{-\lambda_1};Q_{s+1}^{\lambda_2},\rho(1),\ldots,\rho(l),\bar{Q}_n^{-\lambda_1})\Bigg\} \end{aligned} \tag{3.56}$$

where S_k and S_l are permutation groups such that $k+l=n-4$ and represent the possible ways of distributing the gluons in a colour ordered way between the quarks. For $i=j=0$, $(T^{a_i}\ldots T^{a_j})_{kl}$ reduces to δ_{kl}. The first quark-antiquark pair has fundamental colour indices i_1 and i_2 respectively with helicities λ_1,$-\lambda_1$ whereas the second quark-antiquark pair has fundamental colour indices i_3 and i_4 with helicities λ_2,$-\lambda_2$. We see that the two amplitudes $\mathcal{A}_n$ and $\tilde{\mathcal{A}}_n$ correspond to different ways of connecting the fundamental colour charges. For the $\mathcal{A}$ amplitudes, there is a colour line connecting q and $\bar{Q}$ and a second line connecting Q and $\bar{q}$, while for the QED-like $\tilde{A}$ amplitudes the colour lines connect q to $\bar{q}$ and Q to $\bar{Q}$. Any number of gluons may be radiated from each colour line.

3.8.1. MHV Amplitudes

For each colour structure there are four MHV amplitudes where two of the fermions have negative helicity and two have positive helicity as shown in figure 3.9. Any number of positive helicity gluons can be radiated from each of the quark colour lines. Figure 3.9 explicitly shows the two ways of connecting up the colours. For each helicity

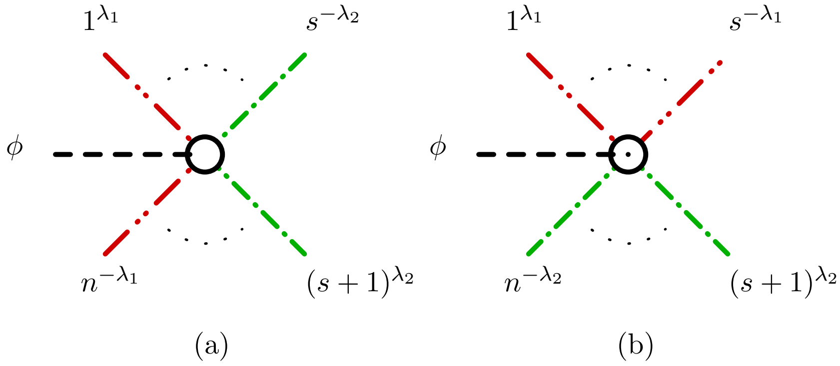

Figure 3.9: MHV vertices for ϕ and two quark pairs. Quarks of the same flavour are represented by lines of the same type - i.e. red or green dot-dashed lines. The colour connection is organised cyclically and each colour connected quark-antiquark pair may have any number of positive helicity gluons radiated from it, represented by the dots. λ_1,λ_2 are the helicities of the quarks. Figure (a) represents the colour ordering for the 'A' amplitudes while (b) represents the colour ordering for the '$\tilde{A}$' amplitudes.

configuration we can write,

$$\mathcal{A}_n(\phi, q_1^+, \ldots, \bar{Q}_s^-, Q_{s+1}^+, \ldots, \bar{q}_n^-) = \frac{\langle 1\, s\rangle \langle s\, n\rangle^2 \langle n\, s+1\rangle}{\prod_{l=1}^n \langle l\, l+1\rangle}, \tag{3.57}$$

$$\mathcal{A}_n(\phi, q_1^+, \ldots, \bar{Q}_s^+, Q_{s+1}^-, \ldots, \bar{q}_n^-) = \frac{\langle 1\, s\rangle \langle n\, s+1\rangle^3}{\prod_{l=1}^n \langle l\, l+1\rangle}, \tag{3.58}$$

$$\mathcal{A}_n(\phi, q_1^-, \ldots, \bar{Q}_s^+, Q_{s+1}^-, \ldots, \bar{q}_n^+) = \frac{\langle s\, 1\rangle \langle 1\, s+1\rangle^2 \langle s+1\, n\rangle}{\prod_{l=1}^n \langle l\, l+1\rangle}, \tag{3.59}$$

$$\mathcal{A}_n(\phi, q_1^-, \ldots, \bar{Q}_s^-, Q_{s+1}^+, \ldots, \bar{q}_n^+) = \frac{\langle 1\, s\rangle^3 \langle n\, s+1\rangle}{\prod_{l=1}^n \langle l\, l+1\rangle}, \tag{3.60}$$

with the other colour ordering given by,

$$\tilde{\mathcal{A}}_n(\phi, q_1^+, \ldots, \bar{q}_s^-, Q_{s+1}^+, \ldots, \bar{Q}_n^-) = \frac{\langle 1\, n\rangle \langle n\, s\rangle^2 \langle s\, s+1\rangle}{\prod_{l=1}^n \langle l\, l+1\rangle}, \tag{3.61}$$

$$\tilde{\mathcal{A}}_n(\phi, q_1^+, \ldots, \bar{q}_s^-, Q_{s+1}^-, \ldots, \bar{Q}_n^+) = \frac{\langle 1\, n\rangle \langle s\, s+1\rangle^3}{\prod_{l=1}^n \langle l\, l+1\rangle}, \tag{3.62}$$

$$\tilde{\mathcal{A}}_n(\phi, q_1^-, \ldots, \bar{q}_s^+, Q_{s+1}^-, \ldots, \bar{Q}_n^+) = \frac{\langle n\, 1\rangle \langle 1\, s+1\rangle^2 \langle s+1\, s\rangle}{\prod_{l=1}^n \langle l\, l+1\rangle}, \tag{3.63}$$

$$\tilde{\mathcal{A}}_n(\phi, q_1^-, \ldots, \bar{q}_s^+, Q_{s+1}^+, \ldots, \bar{Q}_n^-) = \frac{\langle 1\, n\rangle^3 \langle s\, s+1\rangle}{\prod_{l=1}^n \langle l\, l+1\rangle}. \tag{3.64}$$

These MHV vertices are derived from the ϕ-gluon vertices using a (pseudo) $\mathcal{N} = 2$ supersymmetric Ward identity as discussed in section 2. The amplitudes involving $\phi^\dagger$

are related by parity and can be obtained by conjugating the MHV expressions,

$$\mathcal{A}_n(\phi^\dagger, q_1^{\lambda_1}, \bar{Q}_s^{-\lambda_2}; Q_{s+1}^{\lambda_2}, \bar{q}_n^{-\lambda_1}) = (-1)^n \left(\mathcal{A}_n(\phi, q_1^{-\lambda_1}, \bar{Q}_s^{\lambda_2}; Q_{s+1}^{-\lambda_2}, \bar{q}_n^{\lambda_1})\right)^*, \tag{3.65}$$

and similarly for the $\tilde{\mathcal{A}}_n$ amplitudes.

Equations (3.57)–(3.64) have an identical form to the pure QCD amplitudes. As such, they have the correct collinear and multi-particle factorisation behaviour and a correct limit as the ϕ momentum approaches zero.

3.8.2. $H \to q^- \bar{Q}^+ Q^- \bar{q}^+$

When $n = 4$, there is only one possibility, $n_+ = n_- = 2$. As can be seen from figure 3.5, this lies in the intersection of the MHV and $\overline{\text{MHV}}$ towers so that, setting $s = 2$,

$$\begin{aligned} \mathcal{A}_4(H, q_1^-, \bar{Q}_2^+, Q_3^-, \bar{q}_4^+) &= \mathcal{A}_4(\phi, q_1^-, \bar{Q}_2^+, Q_3^-, \bar{q}_4^+) + \mathcal{A}_4(\phi^\dagger, q_1^-, \bar{Q}_2^+, Q_3^-, \bar{q}_4^+) \\ &= -\frac{\langle 1\,3\rangle^2}{\langle 2\,3\rangle\,\langle 4\,1\rangle} - \frac{[24]^2}{[23][41]} \end{aligned} \tag{3.66}$$

which agrees with the known analytic formulae of ref. [113].

3.8.3. NMHV Amplitudes

There are four different helicity configurations for amplitudes with two quark pairs and a single negative helicity gluon. We choose the first quark pair to have helicities $\pm\lambda_1$ and the second pair to carry helicities $\pm\lambda_2$. Again suppressing the positive helicity gluons, we can write the NMHV amplitude as,

$$\mathcal{A}_n(\phi, q_1^{\lambda_1}, g_{m_2}^-, \bar{Q}_{m_3}^{-\lambda_2}; Q_{m_3+1}^{\lambda_2}, \bar{q}_n^{-\lambda_1}) = \frac{1}{\prod_{l=1}^n \langle l\, l+1\rangle} \sum_{i=1}^{10} \mathcal{A}_{1:n}^{(i),\lambda_1\lambda_2}(m_2, m_3), \tag{3.67}$$

$$\tilde{\mathcal{A}}_n(\phi, q_1^{\lambda_1}, g_{m_2}^-, \bar{q}_{m_3}^{-\lambda_1}; Q_{m_3+1}^{\lambda_2}, \bar{Q}_n^{-\lambda_2}) = \frac{1}{\prod_{l=1}^n \langle l\, l+1\rangle} \sum_{i=1}^{8} \tilde{\mathcal{A}}_{1:n}^{(i),\lambda_1\lambda_2}(m_2, m_3). \tag{3.68}$$

There are two other amplitudes where the negative helicity gluon appears on the other quark line, for example,

$$\mathcal{A}_n(\phi, q_1^{\lambda_1}, \bar{Q}_{m_3}^{-\lambda_2}; Q_{m_3+1}^{\lambda_2}, g_{m_2}^-, \bar{q}_n^{-\lambda_1}),$$

however these amplitudes can be obtained by using the property that the amplitudes are cyclic in the quark lines, we can move the gluon from one quark colour line to the other by exchanging the two lines and relabelling, $q_1 \leftrightarrow Q^{\lambda_2}_{m_3+1}$, $\bar{Q}^{-\lambda_2}_{m_3} \leftrightarrow \bar{q}^{-\lambda_1}_n$. A similar relabelling applies to $\tilde{\mathcal{A}}_n$

The 10 diagrams describing the $\mathcal{A}_n$ colour ordering are shown in figure 3.10. The resulting amplitudes are given by,

$$
\begin{aligned}
\mathcal{A}^{(1),\lambda_1\lambda_2}_n(m_2,m_3) &= \sum_{i=1}^{m_2-1}\sum_{j=m_3}^{m_3}\frac{\mathcal{A}^{(1),\lambda_1\lambda_2}_n(q_{j+1,i};m_2,m_3)}{D(j,i,q_{j+1,i})},\\
\mathcal{A}^{(3),\lambda_1\lambda_2}_n(m_2,m_3) &= \sum_{i=m_2}^{m_3-1}\sum_{j=n}^{n}\frac{\mathcal{A}^{(3),\lambda_1\lambda_2}_n(q_{j+1,i};m_2,m_3)}{D(j,i,q_{j+1,i})},\\
\mathcal{A}^{(5),\lambda_1\lambda_2}_n(m_2,m_3) &= \sum_{i=m_2}^{m_3-1}\sum_{j=1}^{m_2-1}\frac{\mathcal{A}^{(5),\lambda_1\lambda_2}_n(q_{j+1,i};m_2,m_3)}{D(j,i,q_{j+1,i})},\\
\mathcal{A}^{(7),\lambda_1\lambda_2}_n(m_2,m_3) &= \sum_{i=m_3+1}^{n-1}\sum_{j=1}^{m_2-1}\frac{\mathcal{A}^{(7),\lambda_1\lambda_2}_n(q_{j+1,i};m_2,m_3)}{D(j,i,q_{j+1,i})},\\
\mathcal{A}^{(9),\lambda_1\lambda_2}_n(m_2,m_3) &= \sum_{i=m_2}^{m_3-1}\sum_{j=m_3+1}^{n-1}\frac{\mathcal{A}^{(9),\lambda_1\lambda_2}_n(q_{j+1,i};m_2,m_3)}{D(j,i,q_{j+1,i})},
\end{aligned}
\tag{3.69}
$$

and

$$
\mathcal{A}^{(2k),\lambda_1\lambda_2}_n(q_{j+1,i};m_2,m_3) = \frac{\mathcal{A}^{(2k-1),\lambda_1\lambda_2}_n(q_{i+1,j};m_2,m_3)}{D(i,j,q_{i+1,j})} \qquad \text{for} \qquad k=1,\ldots,5.
\tag{3.70}
$$

The quantity $D(i,j,q)$ is defined as in equation (3.51). The amplitudes for each helicity

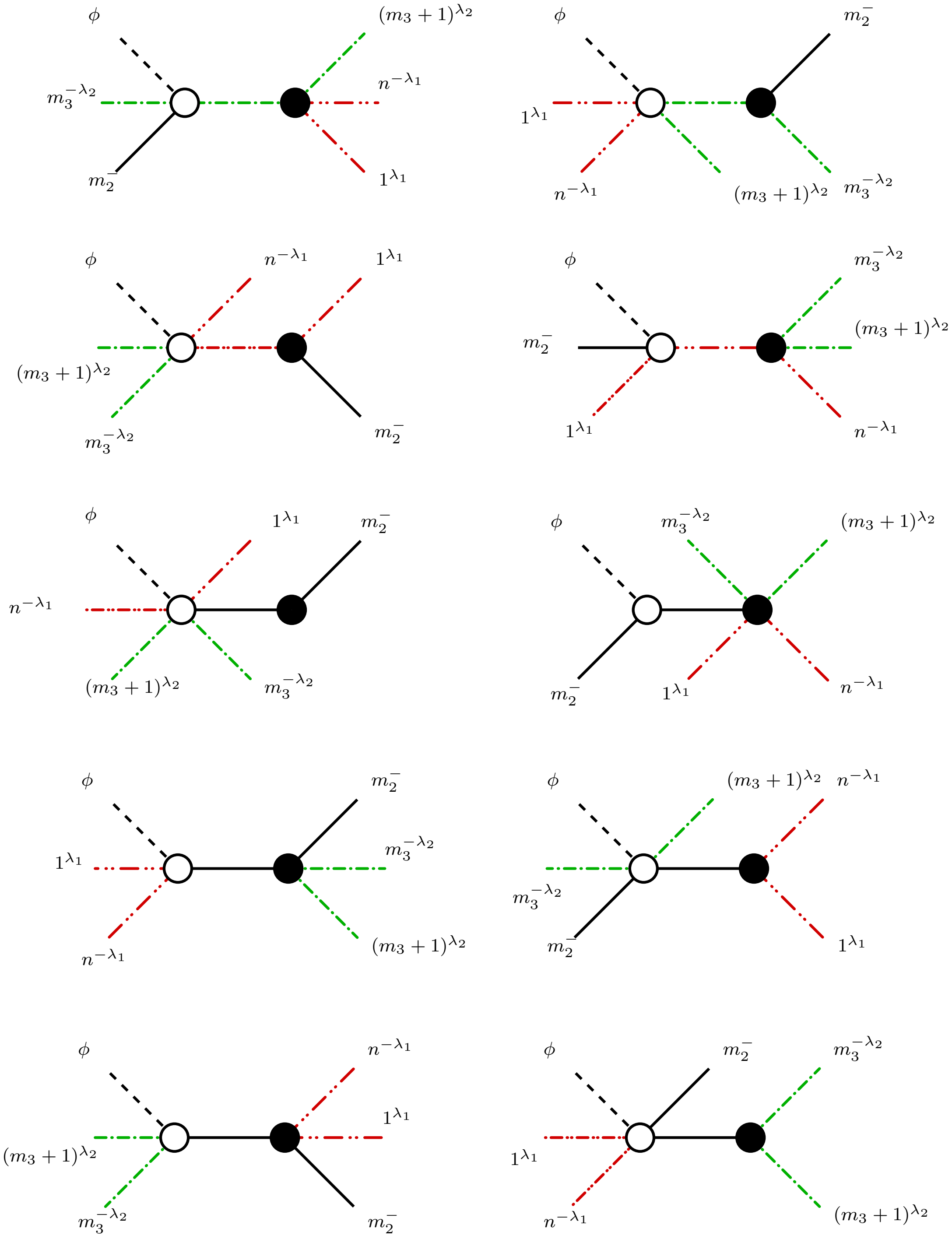

Figure 3.10: Tree diagrams with MHV vertices contributing to the amplitude $\mathcal{A}_n(\phi, q_1^{\lambda_1}, g_{m_2}^-, \bar{Q}_{m_3}^{-\lambda_2}; Q_{m_3+1}^{\lambda_2}, \bar{q}_n^{-\lambda_1})$. The scalar ϕ is represented by a dashed line whereas the two quark lines a represented by coloured dot-dashed lines. The negative helicity gluons are the solid black lines.

configuration are given by:

$$\begin{aligned}
\mathcal{A}_n^{(1),--}(q;m_2,m_3) &= \left\langle m_2^-\right|\not{q}\left|\xi^-\right\rangle^3 \langle m_2\,m_3\rangle\,\langle n\,m_3+1\rangle\,\langle m_3+1\,1\rangle^2 \left\langle 1^-\right|\not{q}\left|\xi^-\right\rangle, \\
\mathcal{A}_n^{(3),--}(q;m_2,m_3) &= \langle m_2\,1\rangle^3 \left\langle m_2^-\right|\not{q}\left|\xi^-\right\rangle \langle m_3+1\,n\rangle \left\langle m_3+1^-\right|\not{q}\left|\xi^-\right\rangle^2 \left\langle m_3^-\right|\not{q}\left|\xi^-\right\rangle, \\
\mathcal{A}_n^{(5),--}(q;m_2,m_3) &= \langle m_3\,1\rangle\,\langle 1\,m_3+1\rangle^2\,\langle m_3+1\,n\rangle \left\langle m_2^-\right|\not{q}\left|\xi^-\right\rangle^4, \\
\mathcal{A}_n^{(7),--}(q;m_2,m_3) &= \left\langle 1^-\right|\not{q}\left|\xi^-\right\rangle^3 \left\langle n^-\right|\not{q}\left|\xi^-\right\rangle \langle m_2\,m_3+1\rangle^3\,\langle m_2\,m_3\rangle, \\
\mathcal{A}_n^{(9),--}(q;m_2,m_3) &= \left\langle m_3+1^-\right|\not{q}\left|\xi^-\right\rangle^3 \left\langle m_3^-\right|\not{q}\left|\xi^-\right\rangle \langle m_2\,1\rangle^3\,\langle m_2\,n\rangle, \qquad (3.71) \\
\mathcal{A}_n^{(1),-+}(q;m_2,m_3) &= \left\langle m_2^-\right|\not{q}\left|\xi^-\right\rangle \langle m_2\,m_3\rangle^3\,\langle n\,m_3+1\rangle \left\langle 1^-\right|\not{q}\left|\xi^-\right\rangle^3, \\
\mathcal{A}_n^{(3),-+}(q;m_2,m_3) &= \langle m_2\,1\rangle^3 \left\langle m_2^-\right|\not{q}\left|\xi^-\right\rangle \left\langle m_3^-\right|\not{q}\left|\xi^-\right\rangle^3 \langle m_3+1\,n\rangle, \\
\mathcal{A}_n^{(5),-+}(q;m_2,m_3) &= \langle m_3\,1\rangle^3\,\langle m_3+1\,n\rangle \left\langle m_2^-\right|\not{q}\left|\xi^-\right\rangle^4, \\
\mathcal{A}_n^{(7),-+}(q;m_2,m_3) &= \left\langle 1^-\right|\not{q}\left|\xi^-\right\rangle^3 \left\langle n^-\right|\not{q}\left|\xi^-\right\rangle \langle m_2\,m_3+1\rangle\,\langle m_2\,m_3\rangle^3, \\
\mathcal{A}_n^{(9),-+}(q;m_2,m_3) &= \left\langle m_3+1^-\right|\not{q}\left|\xi^-\right\rangle \left\langle m_3^-\right|\not{q}\left|\xi^-\right\rangle^3 \langle m_2\,1\rangle^3\,\langle m_2\,n\rangle, \qquad (3.72) \\
\mathcal{A}_n^{(1),+-}(q;m_2,m_3) &= \left\langle m_2^-\right|\not{q}\left|\xi^-\right\rangle^3 \langle m_2\,m_3\rangle\,\langle n\,m_3+1\rangle^3 \left\langle 1^-\right|\not{q}\left|\xi^-\right\rangle, \\
\mathcal{A}_n^{(3),+-}(q;m_2,m_3) &= \langle m_2\,1\rangle \left\langle m_2^-\right|\not{q}\left|\xi^-\right\rangle^3 \left\langle m_3^-\right|\not{q}\left|\xi^-\right\rangle \langle m_3+1\,n\rangle^3, \\
\mathcal{A}_n^{(5),+-}(q;m_2,m_3) &= \langle m_3\,1\rangle\,\langle m_3+1\,n\rangle^3 \left\langle m_2^-\right|\not{q}\left|\xi^-\right\rangle^4, \\
\mathcal{A}_n^{(7),+-}(q;m_2,m_3) &= \left\langle 1^-\right|\not{q}\left|\xi^-\right\rangle \left\langle n^-\right|\not{q}\left|\xi^-\right\rangle^3 \langle m_2\,m_3+1\rangle^3\,\langle m_2\,m_3\rangle, \\
\mathcal{A}_n^{(9),+-}(q;m_2,m_3) &= \left\langle m_3+1^-\right|\not{q}\left|\xi^-\right\rangle^3 \left\langle m_3^-\right|\not{q}\left|\xi^-\right\rangle \langle m_2\,1\rangle\,\langle m_2\,n\rangle^3, \qquad (3.73) \\
\mathcal{A}_n^{(1),++}(q;m_2,m_3) &= \left\langle m_2^-\right|\not{q}\left|\xi^-\right\rangle \langle m_2\,m_3\rangle^3\,\langle n\,m_3+1\rangle \left\langle n^-\right|\not{q}\left|\xi^-\right\rangle^2 \left\langle 1^-\right|\not{q}\left|\xi^-\right\rangle, \\
\mathcal{A}_n^{(3),++}(q;m_2,m_3) &= \langle m_2\,1\rangle \left\langle m_2^-\right|\not{q}\left|\xi^-\right\rangle^3 \left\langle m_3^-\right|\not{q}\left|\xi^-\right\rangle \langle m_3\,n\rangle^2\,\langle m_3+1\,n\rangle, \\
\mathcal{A}_n^{(5),++}(q;m_2,m_3) &= \langle 1\,m_3\rangle\,\langle m_3\,n\rangle^2\,\langle n\,m_3+1\rangle \left\langle m_2^-\right|\not{q}\left|\xi^-\right\rangle^4, \\
\mathcal{A}_n^{(7),++}(q;m_2,m_3) &= \left\langle 1^-\right|\not{q}\left|\xi^-\right\rangle \left\langle n^-\right|\not{q}\left|\xi^-\right\rangle^3 \langle m_2\,m_3+1\rangle\,\langle m_2\,m_3\rangle^3, \\
\mathcal{A}_n^{(9),++}(q;m_2,m_3) &= \left\langle m_3+1^-\right|\not{q}\left|\xi^-\right\rangle \left\langle m_3^-\right|\not{q}\left|\xi^-\right\rangle^3 \langle m_2\,1\rangle\,\langle m_2\,n\rangle^3. \qquad (3.74)
\end{aligned}$$

For the $\tilde{A}$ colour ordering there are only 8 diagrams shown in figure 3.11. The corre-

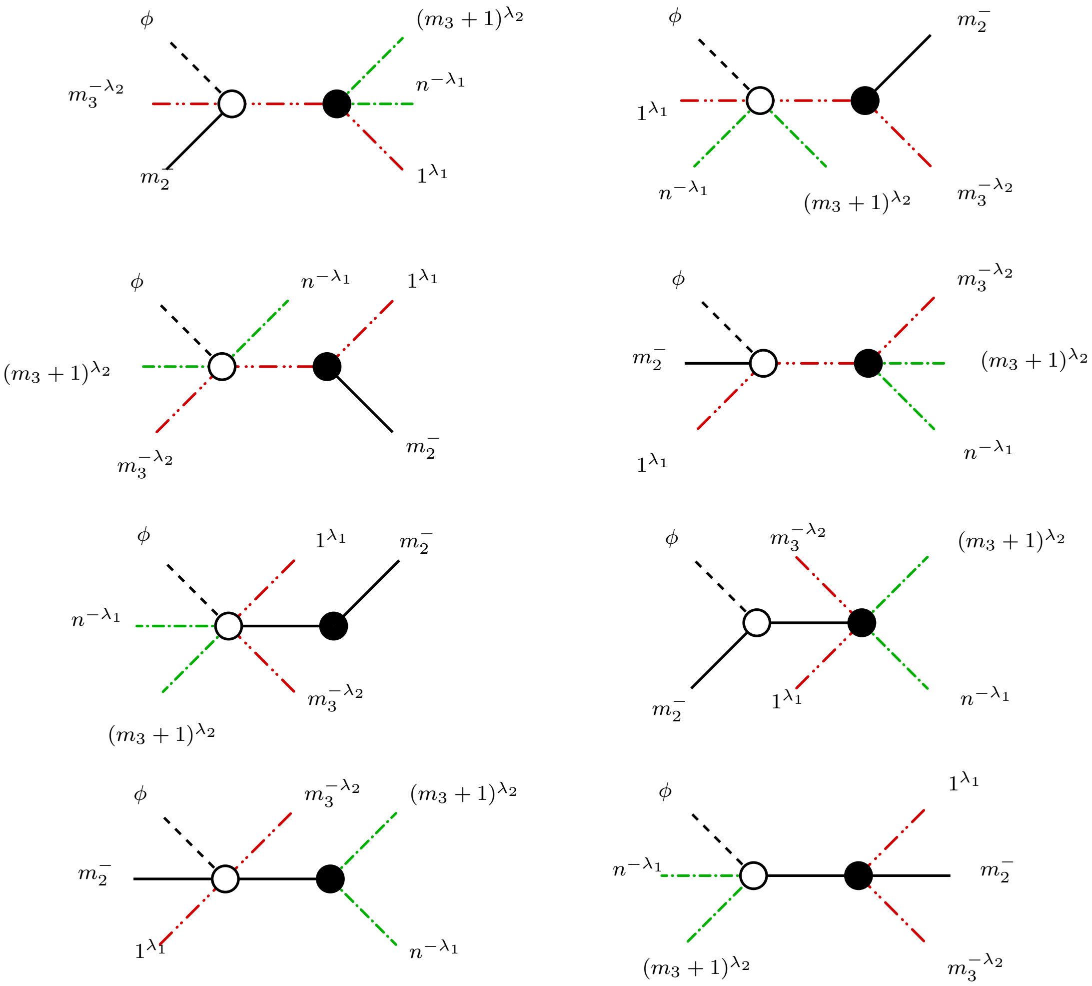

Figure 3.11: Tree diagrams with MHV vertices contributing to the amplitude $\tilde{A}_n(\phi, q_1^{\lambda_1}, g_{m_2}^-, \bar{q}_{m_3}^{-\lambda_1}; Q_{m_3+1}^{\lambda_2}, \bar{Q}_n^{-\lambda_2})$. The scalar ϕ is represented by a dashed line whereas the two quark lines a represented by coloured dot-dashed lines. The negative helicity gluons are the solid black lines.

sponding amplitudes are given by,

$$\begin{aligned}
\tilde{\mathcal{A}}_n^{(1),\lambda_1\lambda_2}(m_2,m_3) &= \sum_{i=1}^{m_2-1}\sum_{j=m_3}^{m_3}\frac{\tilde{\mathcal{A}}_n^{(1),\lambda_1\lambda_2}(q_{j+1,i};m_2,m_3)}{D(j,i,q_{j+1,i})},\\
\tilde{\mathcal{A}}_n^{(3),\lambda_1\lambda_2}(m_2,m_3) &= \sum_{i=m_2}^{m_3-1}\sum_{j=n}^{n}\frac{\tilde{\mathcal{A}}_n^{(3),\lambda_1\lambda_2}(q_{j+1,i};m_2,m_3)}{D(j,i,q_{j+1,i})},\\
\tilde{\mathcal{A}}_n^{(5),\lambda_1\lambda_2}(m_2,m_3) &= \sum_{i=m_2}^{m_3-1}\sum_{j=1}^{m_2-1}\frac{\tilde{\mathcal{A}}_n^{(5),\lambda_1\lambda_2}(q_{j+1,i};m_2,m_3)}{D(j,i,q_{j+1,i})},\\
\tilde{\mathcal{A}}_n^{(7),\lambda_1\lambda_2}(m_2,m_3) &= \sum_{i=n}^{n}\sum_{j=m_3}^{m_3}\frac{\tilde{\mathcal{A}}_n^{(7),\lambda_1\lambda_2}(q_{j+1,i};m_2,m_3)}{D(j,i,q_{j+1,i})},
\end{aligned}\qquad(3.75)$$

with

$$\tilde{\mathcal{A}}_n^{(2k),\lambda_1\lambda_2}(q_{j+1,i};m_2,m_3) = \frac{\tilde{\mathcal{A}}_n^{(2k-1),\lambda_1\lambda_2}(q_{i+1,j};m_2,m_3)}{D(i,j,q_{i+1,j})}\qquad \text{for}\qquad k=1,\ldots,4 \qquad(3.76)$$

The amplitudes for each helicity combination are,

$$\begin{aligned}
\tilde{\mathcal{A}}_n^{(1),--}(q;m_2,m_3) &= \langle m_2\,m_3\rangle\left\langle m_2^-\right|\not{q}\left|\xi^-\right\rangle^3\langle n\,1\rangle\langle 1\,m_3+1\rangle^2\left\langle m_3+1^-\right|\not{q}\left|\xi^-\right\rangle,\\
\tilde{\mathcal{A}}_n^{(3),--}(q;m_2,m_3) &= \left\langle m_2^-\right|\not{q}\left|\xi^-\right\rangle\langle m_2\,1\rangle^3\left\langle n^-\right|\not{q}\left|\xi^-\right\rangle\left\langle m_3+1^-\right|\not{q}\left|\xi^-\right\rangle^2\langle m_3+1\,m_3\rangle,\\
\tilde{\mathcal{A}}_n^{(5),--}(q;m_2,m_3) &= \langle n\,1\rangle\langle 1\,m_3+1\rangle^2\langle m_3+1\,m_3\rangle\left\langle m_2^-\right|\not{q}\left|\xi^-\right\rangle^4,\\
\tilde{\mathcal{A}}_n^{(7),--}(q;m_2,m_3) &= \langle m_2\,1\rangle^3\langle m_2\,m_3\rangle\left\langle m_3+1^-\right|\not{q}\left|\xi^-\right\rangle^3\left\langle n^-\right|\not{q}\left|\xi^-\right\rangle,
\end{aligned}\qquad(3.77)$$

$$
\begin{aligned}
\tilde{\mathcal{A}}_n^{(1),-+}(q;m_2,m_3) &= \langle m_2\, m_3\rangle \left\langle m_2^-\right| \not{q} \left|\xi^-\right\rangle^3 \langle n\, 1\rangle^3 \left\langle m_3+1^-\right| \not{q} \left|\xi^-\right\rangle, \\
\tilde{\mathcal{A}}_n^{(3),-+}(q;m_2,m_3) &= \left\langle m_2^-\right| \not{q} \left|\xi^-\right\rangle \langle m_2\, 1\rangle^3 \left\langle n^-\right| \not{q} \left|\xi^-\right\rangle^3 \langle m_3+1\, m_3\rangle, \\
\tilde{\mathcal{A}}_n^{(5),-+}(q;m_2,m_3) &= \langle 1\, n\rangle^3 \langle m_3\, m_3+1\rangle \left\langle m_2^-\right| \not{q} \left|\xi^-\right\rangle^4, \\
\tilde{\mathcal{A}}_n^{(7),-+}(q;m_2,m_3) &= \langle m_2\, 1\rangle^3 \langle m_2\, m_3\rangle \left\langle m_3+1^-\right| \not{q} \left|\xi^-\right\rangle \left\langle n^-\right| \not{q} \left|\xi^-\right\rangle^3, \qquad (3.78) \\
\tilde{\mathcal{A}}_n^{(1),+-}(q;m_2,m_3) &= \langle m_2\, m_3\rangle^3 \left\langle m_2^-\right| \not{q} \left|\xi^-\right\rangle \langle n\, 1\rangle \left\langle m_3+1^-\right| \not{q} \left|n^-\right\rangle^3, \\
\tilde{\mathcal{A}}_n^{(3),+-}(q;m_2,m_3) &= \left\langle m_2^-\right| \not{q} \left|\xi^-\right\rangle^3 \langle m_2\, 1\rangle \left\langle n^-\right| \not{q} \left|\xi^-\right\rangle \langle m_3+1\, m_3\rangle^3, \\
\tilde{\mathcal{A}}_n^{(5),+-}(q;m_2,m_3) &= \langle 1\, n\rangle \langle m_3\, m_3+1\rangle^3 \left\langle m_2^-\right| \not{q} \left|\xi^-\right\rangle^4, \\
\tilde{\mathcal{A}}_n^{(7),+-}(q;m_2,m_3) &= \langle m_2\, 1\rangle \langle m_2\, m_3\rangle^3 \left\langle m_3+1^-\right| \not{q} \left|\xi^-\right\rangle^3 \left\langle n^-\right| \not{q} \left|\xi^-\right\rangle, \qquad (3.79) \\
\tilde{\mathcal{A}}_n^{(1),++}(q;m_2,m_3) &= \langle m_2\, m_3\rangle^3 \left\langle m_2^-\right| \not{q} \left|\xi^-\right\rangle \langle n\, 1\rangle \left\langle n^-\right| \not{q} \left|\xi^-\right\rangle^2 \left\langle m_3+1^-\right| \not{q} \left|\xi^-\right\rangle, \\
\tilde{\mathcal{A}}_n^{(3),++}(q;m_2,m_3) &= \langle m_2\, 1\rangle \left\langle m_2^-\right| \not{q} \left|\xi^-\right\rangle^3 \left\langle n^-\right| \not{q} \left|\xi^-\right\rangle \langle n\, m_3\rangle^2 \langle m_3+1\, m_3\rangle, \\
\tilde{\mathcal{A}}_n^{(5),++}(q;m_2,m_3) &= \langle 1\, n\rangle \langle n\, m_3\rangle^2 \langle m_3\, m_3+1\rangle \left\langle m_2^-\right| \not{q} \left|\xi^-\right\rangle^4, \\
\tilde{\mathcal{A}}_n^{(7),++}(q;m_2,m_3) &= \langle m_2\, 1\rangle \langle m_2\, m_3\rangle^3 \left\langle m_3+1^-\right| \not{q} \left|\xi^-\right\rangle \left\langle n^-\right| \not{q} \left|\xi^-\right\rangle^3. \qquad (3.80)
\end{aligned}
$$

Eqs. (3.67) and (3.68) are sufficient to describe all amplitudes involving ϕ, two pairs of quarks and a single negative helicity gluon. Amplitudes involving $\phi^\dagger$ are obtained by parity. Note that all NMHV amplitudes lie in the overlap of the MHV and $\overline{\text{MHV}}$ towers.

The only NMHV amplitudes previously available were those involving for four quarks and a single gluon [114].

3.8.4. $H \to q^{\lambda_1} g^- \bar{Q}^{-\lambda_2} Q^{\lambda_2} \bar{q}^{-\lambda_1}$

In this case quarks of opposite flavour are colour connected corresponding to the leading colour $\mathcal{A}_n^{\lambda_1\lambda_2}$ NMHV with $m_2 = 2$ and $m_3 = 3$. To recover the amplitude for Higgs we add the $\overline{\text{MHV}}$ amplitude with the same colour and helicity configuration,

$$
\begin{aligned}
\mathcal{A}_5(H, 1_q^{\lambda_1}, 2^-, 3_{\bar{Q}}^{-\lambda_2}, 4_Q^{\lambda_2}, 5_{\bar{q}}^{-\lambda_1}) &= \mathcal{A}_5(\phi, 1_q^{\lambda_1}, 2^-, 3_{\bar{Q}}^{-\lambda_2}, 4_Q^{\lambda_2}, 5_{\bar{q}}^{-\lambda_1}) \\
&+ \mathcal{A}_5(\phi^\dagger, 1_q^{\lambda_1}, 2^-, 3_{\bar{Q}}^{-\lambda_2}, 4_Q^{\lambda_2}, 5_{\bar{q}}^{-\lambda_1}). \qquad (3.81)
\end{aligned}
$$

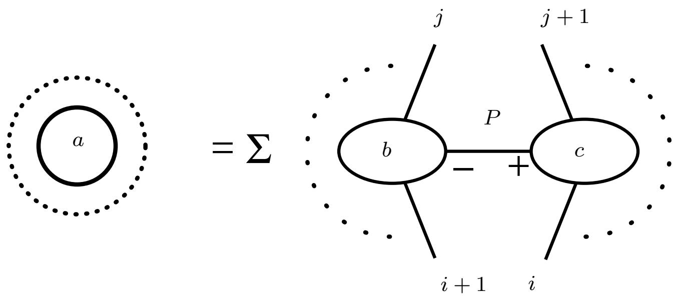

Figure 3.12: The recursion relation for amplitudes involving a negative helicity particles. The dots indicate the emission of particles of any helicity. a, b and c count the number of negative helicity external particles connected to each vertex, such that $a = b + c$. The summation runs over all possible distributions of external particles. P denotes the off-shell momentum linking the two vertices.

By substituting in specific phase space points with various choices of the gauge vector ξ, we find numerically that the amplitude is gauge invariant. We also find agreement with the results of an independent calculation of the twelve Feynman diagrams.

3.8.5. $H \to q^{\lambda_1} g^- \bar{q}^{-\lambda_1} Q^{\lambda_2} \bar{Q}^{-\lambda_2}$

In this case, each quark is colour connected to the antiquark of the same flavour. We therefore take the subleading colour $\tilde{A}_n^{\lambda_1\lambda_2}$ NMHV with $m_2 = 2$ and $m_3 = 3$ and add the $\overline{\text{MHV}}$ with the same configuration

$$\begin{aligned} \mathcal{A}_5(H, 1_q^{\lambda_1}, 2^-, 3_{\bar{q}}^{-\lambda_1}, 4_Q^{\lambda_2}, 5_{\bar{Q}}^{-\lambda_2}) &= \tilde{\mathcal{A}}_5(\phi, 1_q^{\lambda_1}, 2^-, 3_{\bar{q}}^{-\lambda_1}, 4_Q^{\lambda_2}, 5_{\bar{Q}}^{-\lambda_2}) \\ &+ \tilde{\mathcal{A}}_5(\phi^\dagger, 1_q^{\lambda_1}, 2^-, 3_{\bar{q}}^{-\lambda_1}, 4_Q^{\lambda_2}, 5_{\bar{Q}}^{-\lambda_2}). \end{aligned} \tag{3.82}$$

Once again, we find that the amplitude is gauge invariant and reproduces the numerical result found using an independent Feynman diagram calculation.

3.9. Recursive formulation of non-MHV amplitudes

The NMHV amplitudes of the previous sections were obtained by connecting two MHV vertices by a scalar propagator in all possible ways. Typically there are of order 10 such diagrams. NNMHV amplitudes can be constructed either by connecting three MHV vertices, or by connecting an MHV vertex to an on-shell NMHV amplitude. The first approach involves around 50 scalar graphs, while the second method recursively makes use of previously computed results. Recursion relations were first used in the context of QCD amplitudes by Berends and Giele [60] and subsequently by Kosower [125]. More recently, they have been employed to obtain helicity amplitudes for gluon scattering using MHV rules [52].

Following [52], an n-gluon amplitude with a negative helicities, $\mathcal{A}^g_{n;a}$, can be written in terms of amplitudes involving fewer external particles with b and c negative helicities as,

$$\mathcal{A}^g_{n;a}(1,\ldots,n) = \frac{1}{(a-2)}\sum_{i=1}^{n}\sum_{j=i+2}^{i-2}$$
$$\mathcal{A}^g_{j-i+1;b+1}(i+1,\ldots,j,-q^-_{i+1,j})\,\frac{1}{s_{i+1,j}}\,\mathcal{A}^g_{i-j+1;c}(j+1,\ldots,i,-q^+_{j+1,i}), \qquad (3.83)$$

where $a = b + c$. This relation is schematically shown in figure 3.12. The helicities of individual particles have been suppressed, however, it is understood that out of the n particles, a have negative helicity. Furthermore, b (c) particles in the range $i+1,\ldots,j$ ($j+1,\ldots,i$) have negative helicities. All momenta are outgoing, and the off-shell line linking the two amplitudes carries momentum $q_{i+1,j} = -q_{j+1,i}$, such that $s_{i+1,j} = q^2_{i+1,j}$, and we choose to connect it to the left-(right-) hand amplitude with negative (positive) helicity. Note that the range $[i+1,j]$ must contain at least 1 negative helicity and the range $[j+1,i-1]$ must contain at least 2 negative helicities. Vertices generated which do not satisfy these properties will be zero. It is also understood that all sums and ranges are defined modulo n. The factor $\frac{1}{(a-2)}$ makes sure that there is no over counting of diagrams.

For our present purposes, we wish to use eq. (3.83) algebraically to reduce the amplitude to a combination of MHV vertices $\mathcal{A}^g_{n;2}$ with some number of off-shell legs. The off-shell continuation is then performed in the usual manner [45], $\langle i\,P\rangle \to \langle i|\not{P}|\xi\rangle$. In this case, it is convenient to treat all external particles as on-shell and treat the off-shell legs analytically. For purely numerical evaluation, it may be simpler to deal with vertices with all legs off-shell at the beginning and take them on-shell afterwards [52]. The off-shell continuation of Kosower [59] is particularly well suited to the numerical approach.

We must now extend the recursive formula of ref. [52] to include both fermions and scalars. The relevant building blocks for amplitudes with up to one quark pair and/or one ϕ are thus the four MHV vertices, $\mathcal{A}^g_{n;2}$, $\mathcal{A}^q_{n;2}$, $\mathcal{A}^{\phi g}_{n;2}$ and $\mathcal{A}^{\phi q}_{n;2}$. We do not indicate whether the quark or antiquark has negative helicity, and so the quark MHV vertices are represented by a single $\mathcal{A}$.

We first write down the recursion relation for amplitudes involving ϕ and gluons,

$$
\begin{aligned}
\mathcal{A}^{\phi g}_{n;a}(1,\ldots,n) = \frac{1}{(a-2)}\Bigg\{ & \\
& \sum_{i=1}^{n}\sum_{j=i+2}^{i-1} \mathcal{A}^{g}_{j-i+1;b+1}(i+1,\ldots,j,-q^-_{i+1,j})\,\frac{1}{s_{i+1,j}}\,\mathcal{A}^{\phi g}_{i-j+1;c}(j+1,\ldots,i,q^+_{i+1,j}) \\
& +\sum_{i=1}^{n}\sum_{j=i+1}^{i-2} \mathcal{A}^{\phi g}_{j-i+1;b+1}(i+1,\ldots,j,q^-_{j+1,i})\,\frac{1}{s_{j+1,i}}\,\mathcal{A}^{g}_{i-j+1;c}(j+1,\ldots,i,-q^+_{j+1,i}),\Bigg\}.
\end{aligned}
\tag{3.84}
$$

Note that for amplitudes involving ϕ, the outgoing gluon momenta no longer sum to zero. We therefore choose to use the momentum constructed solely from gluon momenta, $q_{i+1,j}$ $(q_{j+1,i})$ in the $\phi-$gluon vertex appearing on first (second) terms on the rhs of eq. (3.84). This expression is sufficient to rederive the NMHV and Next-to-NMHV (NNMHV) amplitudes given explicitly in Ref. [53]. We have checked that it correctly gives NMHV and NNMHV amplitudes with up to six gluons.

The recursion relation involving only quarks and gluons is given by,

$$
\begin{aligned}
\mathcal{A}^q_{n;a}(1_q^{\lambda},\ldots,n_{\bar{q}}^{-\lambda}) = \frac{1}{(a-2)}\Bigg(&\\
&\sum_{i=1}^{n-3}\sum_{j=i+2}^{n-1}\Bigg\{\\
&\mathcal{A}^g_{j-i+1;b+1}(i+1,\ldots,j,-q^-_{i+1,j})\,\frac{1}{s_{i+1,j}}\,\mathcal{A}^q_{i-j+n+1;c}(1_q^{\lambda},2,\ldots,i,-q^+_{j+1,i},j+1,\ldots,n_{\bar{q}}^{-\lambda})\\
&+\mathcal{A}^g_{j-i+1;b}(i+1,\ldots,j,-q^+_{i+1,j})\,\frac{1}{s_{i+1,j}}\,\mathcal{A}^q_{i-j+n+1;c+1}(1_q^{\lambda},2,\ldots,i,-q^-_{j+1,i},j+1,\ldots,n_{\bar{q}}^{-\lambda})\Bigg\}\\
&+\sum_{i=2}^{n-2}\mathcal{A}^q_{i+1;b'+1}(1_q^{\lambda},2,\ldots,i,-q^{-\lambda}_{1,i})\frac{1}{s_{1,i}}\mathcal{A}^q_{n-i+1;c'+1}(q^{\lambda}_{1,i},i+1,\ldots,n_{\bar{q}}^{-\lambda})\Bigg),
\end{aligned}
\tag{3.85}
$$

where b' (c') is the number of negative helicities in the range $2,\ldots,i$ ($i+1,\ldots,n-1$) and $a = b'+c'-1$. Eq. (3.85) is sufficient to describe amplitudes involving any number of gluons and a single quark pair.

Finally, the recursion relation for quarks, gluons and a ϕ is,

$$
\begin{aligned}
&\mathcal{A}^{\phi q}_{n;a}(1^{\lambda}_q,\ldots,n^{-\lambda}_{\bar{q}}) = \frac{1}{(a-2)}\Bigg(\\
&\quad\sum_{i=1}^{n-2}\sum_{j=i+1}^{n-1}\Bigg\{\\
&\quad\mathcal{A}^{\phi g}_{j-i+1;b+1}(i+1,\ldots,j,q^{-}_{j+1,i})\,\frac{1}{s_{j+1,i}}\,\mathcal{A}^{q}_{i-j+n+1;c}(1^{\lambda}_q,2,\ldots,i,-q^{+}_{j+1,i},j+1,\ldots,n^{-\lambda}_{\bar{q}})\\
&\quad+\mathcal{A}^{\phi g}_{j-i+1;b}(i+1,\ldots,j,q^{+}_{j+1,i})\,\frac{1}{s_{j+1,i}}\,\mathcal{A}^{q}_{i-j+n+1;c+1}(1^{\lambda}_q,2,\ldots,i,-q^{-}_{j+1,i},j+1,\ldots,n^{-\lambda}_{\bar{q}})\Bigg\}\\
&\quad+\sum_{i=1}^{n-3}\sum_{j=i+2}^{n-1}\Bigg\{\\
&\quad\mathcal{A}^{g}_{j-i+1;b+1}(i+1,\ldots,j,-q^{-}_{i+1,j})\,\frac{1}{s_{i+1,j}}\,\mathcal{A}^{\phi q}_{i-j+n+1;c}(1^{\lambda}_q,2,\ldots,i,q^{+}_{i+1,j},j+1,\ldots,n^{-\lambda}_{\bar{q}})\\
&\quad+\mathcal{A}^{g}_{j-i+1;b}(i+1,\ldots,j,-q^{+}_{i+1,j})\,\frac{1}{s_{i+1,j}}\,\mathcal{A}^{\phi q}_{i-j+n+1;c+1}(1^{\lambda}_q,2,\ldots,i,q^{-}_{i+1,j},j+1,\ldots,n^{-\lambda}_{\bar{q}})\Bigg\}\\
&\quad+\sum_{i=2}^{n-2}\Bigg\{\\
&\quad\mathcal{A}^{\phi q}_{i+1;b'+1}(1^{\lambda}_q,2,\ldots,i,q^{-\lambda}_{i+1,n})\,\frac{1}{s_{i+1,n}}\,\mathcal{A}^{q}_{n-i+1;c'+1}(-q^{\lambda}_{i+1,n},i+1,\ldots,n^{-\lambda}_{\bar{q}})\\
&\quad+\mathcal{A}^{q}_{i+1;b'+1}(1^{\lambda}_q,2,\ldots,i,-q^{-\lambda}_{1,i})\,\frac{1}{s_{1,i}}\,\mathcal{A}^{\phi q}_{n-i+1;c'+1}(q^{\lambda}_{1,i},i+1,\ldots,n^{-\lambda}_{\bar{q}})\Bigg\}\Bigg). \qquad (3.86)
\end{aligned}
$$

We have checked that eq. (3.86) correctly reproduces the NMHV amplitudes given in section 3 for up to 6 gluons. Note that in order for the recursion relation to be effective, and unlike the case for the explicit formulae for NMHV amplitudes in eq. (3.47) that is valid for all n, the number of particles must be specified. The recursion relation and the explicit all n results are therefore complementary.

Equations (3.83)–(3.86) provide a way to generate expressions for all non-MHV amplitudes with fermions, gluons and a single massive scalar, ϕ. As usual, amplitudes involving $\phi^{\dagger}$ are obtained by parity.

3.9.1. $H \to q^- g^- g^- g^- \bar{q}^+$

The only NNMHV amplitude previously available in the literature is for $H \to q^- g^- g^- g^- \bar{q}^+$ [114]. This corresponds to the point with $n_+ + n_- = 5$ and $n_+ - n_- = -3$ in figure 3.4. There is no $\overline{\text{MHV}}$ contribution with this helicity configuration. The full amplitude is thus,

$$\mathcal{A}_5(H, q_1^-, g_2^-, g_3^-, g_4^-, \bar{q}_5^+) = \mathcal{A}_5(\phi, q_1^-, g_2^-, g_3^-, g_4^-, \bar{q}_5^+). \tag{3.87}$$

We have checked numerically that the amplitude obtained using the recursion relation (3.86) is gauge invariant and that it agrees with the results obtained by computing the 74 Feynman diagrams directly.

3.10. Conclusions

In this chapter we have shown how to use MHV rules to calculate scattering amplitudes for a single scalar Higgs boson and many gluons and quarks. This was done using an effective Higgs/gluon coupling valid in the large top mass limit. The essential part of the MHV construction for such amplitudes was the ability to split the Higgs field into self-dual and anti-self-dual fields, the Higgs amplitudes can then be computed by using both the MHV and $\overline{\text{MHV}}$ rules for each tower and subsequently adding up the two pieces. This was done for amplitudes with gluons and up to two pairs of quarks. Explicit expressions were given for MHV and NMHV amplitudes with one and two quarks pairs while recursion relations were formed to calculate amplitudes with arbitrary helicity amplitudes.

All explicit results have been numerically checked against Feynman diagram calculations. Although the MHV technique is guaranteed to provide correct results at tree level using on-shell recursion relations to prove gluonic MHV rules [46] and supersymmetric ward identities to relate these to amplitudes with fermions.

We have also shown that the approximation of an infinitely massive top quark is a reasonable approximation for a Higgs boson mass around 100-150 GeV, with an approximate error of 5-10%. However, it should also be possible to model the $\frac{1}{m_t^2}$ corrections to this approximation with higher dimensional operators such as,

$$\frac{1}{m_t^2}\,\mathrm{tr}(G_\mu^\nu G_\nu^\rho G_\rho^\mu). \tag{3.88}$$

Indeed operators of this kind have already been shown to fit into the MHV construction [53]. Finding these corrections would require computing the effective couplings for all the effective operators to $\mathcal{O}(\frac{1}{m_t^2})$ including all triple and quartic gluon self couplings. Hopefully these corrections would reduce the errors in the amplitudes significantly.

4. Recursion relations for gauge theory scattering amplitudes with massive particles

Amplitudes with massive particles are obviously extremely important phenomenologically. Within the Standard Model the masses of the electro-weak vector bosons $W^{\pm}, Z$, and the top quark mass are the most significant. The Higgs mass also plays a large role in scattering processes as has been discussed in the previous chapter, 3. The on-shell techniques described in chapter 2 were only concerned with massless particles. The aim of this chapter is to extend the on-shell recursion relations of section 2.4.2 to include massive particles and then apply the new relations to amplitudes with massive scalars [70, 72], vector bosons and fermions [71, 73, 74, 126, 127]. Throughout we use the spinor helicity formalism outlined in section 2.2 and all amplitudes will be colour ordered as described in section 2.3.

As well as motivation from the Standard Model there is another strong motivation for considering amplitudes involving a pair of massive scalars. One loop amplitudes in supersymmetric theories have been successfully calculated using both MHV rules and generalised unitarity. However, as discussed in section 2.1.3, on-shell methods which rely on the particles being in 4-dimensions will not be able to fully re-construct amplitudes in non-supersymmetric theories. The missing pieces are rational functions and have been the subject of much research into recursion relations for QCD amplitudes at 1-loop [31–33, 96–101].

Alternatively one can avoid the problem of missing rational functions by applying the unitarity methods in D-dimensions in which case the full amplitude would be reconstructed from the start. A further simplification comes from decomposing 1-loop QCD amplitudes of n gluons in terms of supersymmetric multiplets circulating inside the loop:

$$\mathcal{A}^{(1)}_{QCD} = \mathcal{A}^{(1)}_{\mathcal{N}=4} - 4\mathcal{A}^{(1)}_{\mathcal{N}=1,\text{chiral}} + \mathcal{A}^{(1)}_{\text{scalar}}. \tag{4.1}$$

As supersymmetric amplitudes are cut constructible in 4 dimensions the only contribution that needs to be computed with D-dimensional cuts is the scalar contribution, $\mathcal{A}^{(1)}_{\text{scalar}}$. The next important observation is that one can view a D-dimensional scalar particle as a massive 4-dimensional scalar [22, 23] where the extra degrees of freedom act like a mass μ,

$$p_D^2 = p_4^2 - \mu^2. \tag{4.2}$$

Therefore the vital ingredients needed to calculate higher point amplitudes at 1-loop in QCD using D-dimensional unitarity are tree amplitudes involving two adjacent massive scalar particles. This method has been successfully applied to gluon amplitudes with all positive helicities, which are finite at 1-loop [23] and to some specific helicity configurations with up to 5 gluons using generalised unitarity [82].

4.1. On-shell recursion with massive particles

Consider a colour ordered tree level scattering amplitude of n incoming particles, some of which might be massive

$$\mathcal{A}(p_1, p_2, \ldots, p_n)\ , \qquad p_i^2 = m_i^2\ . \tag{4.3}$$

Single out two particles, i, j, for special treatment. These particles can be either massive or massless. For given p_i, p_j pick a null vector $\eta = \lambda_\eta \tilde{\lambda}_\eta$ that is orthogonal to both p_i and p_j

$$\eta \cdot p_i = \eta \cdot p_j = \eta^2 = 0\ . \tag{4.4}$$

For generic p_i and p_j, there are exactly two such η up to scaling. To see this, consider the plane spanned by p_i and p_j. Geometrically, the first two conditions in (4.4) mean that η lies in the plane orthogonal to the plane spanned by p_i, p_j. The last condition sets η to be in the intersection of this plane with the light cone. A generic plane going through the origin intersects the complex light cone at two complex rays. These rays define the two solutions for η up to a scaling by a complex number. We now will construct these solutions.

Solution for the shift momentum

Let us find now explicit solutions of eqs. (4.4) for complex momenta. We will discuss in turn the case when both i, j are massless, when one of i, j is massive and at last the case when both i, j are massive.

If the marked momenta are null, $p_i = \lambda_i\tilde{\lambda}_i$, $p_j = \lambda_j\tilde{\lambda}_j$, then the condition that η is orthogonal to p_i gives $2\eta \cdot p_i = -\langle \eta, i\rangle[\eta, i] = 0$, so either $\lambda_\eta = \lambda_i$ or $\tilde{\lambda}_\eta = \tilde{\lambda}_i$,. Similarly, vanishing of the Lorentz invariant product of η and p_j implies $\lambda_\eta = \lambda_j$ or $\tilde{\lambda}_\eta = \tilde{\lambda}_j$. Combining these two conditions, we find two solutions

$$\eta = \lambda_j\tilde{\lambda}_i \ , \qquad \eta' = \lambda_i\tilde{\lambda}_j \ . \tag{4.5}$$

Now consider the case where the particle i is massless and the particle j is massive. The condition that momentum η is orthogonal to p_i gives $\lambda_\eta = \lambda_i$ or $\tilde{\lambda}_\eta = \tilde{\lambda}_i$. If $\lambda_\eta = \lambda_i$, the orthogonality to p_j reads

$$2\eta \cdot p_j = \lambda_i^a \, p_{ja\dot{a}} \, \tilde{\lambda}_\eta^{\dot{a}} = 0 \ , \tag{4.6}$$

hence $\tilde{\lambda}_\eta^{\dot{a}} = \lambda_{ia} \, p_j^{a\dot{a}} = (\lambda_i p_j)^{\dot{a}}$. So the two possible null vectors orthogonal to both p_i and p_j are

$$\eta^{a\dot{a}} = \lambda_i^a(\lambda_i p_j)^{\dot{a}} \ , \qquad \eta'^{a\dot{a}} = (p_j\tilde{\lambda}_i)^a\tilde{\lambda}_i^{\dot{a}} \ . \tag{4.7}$$

The case when i is massive and j is massless is treated analogously.

The last case to consider is when both particles i and j are massive. Here, neither p_i nor p_j is a product of two spinors so the expression for η is not as simple. We use the condition $2\eta \cdot p_i = \lambda_\eta^a \tilde{\lambda}_\eta^{\dot{a}} p_{ia\dot{a}} = 0$ to express $\lambda_{\eta a} = p_{ia\dot{a}} \tilde{\lambda}_\eta^{\dot{a}}$. Putting this into the second orthogonality condition gives a quadratic equation for λ_η

$$\lambda_\eta^a \lambda_\eta^b p_{ia\dot{a}} p_{jb\dot{b}} \epsilon^{\dot{a}\dot{b}} = \langle \eta | p_i \cdot p_j | \eta \rangle = 0 \ . \tag{4.8}$$

This equation has two solutions, $\lambda_\eta^\pm$, which we can find, for example, by setting $\lambda_\eta^a = (1, x)$ and solving the quadratic equation for x. The analogous condition for the positive helicity spinor $\tilde{\lambda}_\eta^{\dot{a}}$

$$\tilde{\lambda}_\eta^{\dot{a}} \tilde{\lambda}_\eta^{\dot{b}} p_{ia\dot{a}} p_{jb\dot{b}} \epsilon^{ab} = -[\eta | p_i \cdot p_j | \eta] = 0 \tag{4.9}$$

has also two solutions. Altogether, up to scaling, there are two null vectors $\eta = \lambda_\eta \tilde{\lambda}_\eta$ that are orthogonal to p_i, p_j. We do not know of a convenient Lorentz invariant solution to (4.8) and (4.9). This makes the case where both marked particles are massive less tractable than the two simpler cases where at least one of the marked particles is light-like.

4.1.1. Derivation of the recursion relations

To construct massive recursion relation for a tree-level n-particle amplitude $\mathcal{A}(p_1, p_2, \ldots, p_n)$, we first mark particles i and j for special treatment and pick one of the two null vectors η satisfying the conditions in eqs. (4.4). Following [65], consider the auxiliary function of one complex variable

$$\mathcal{A}(z) = \mathcal{A}(p_1(z), \ldots, p_i(z), \ldots, p_j(z), \ldots, p_n(z)) \ , \tag{4.10}$$

where $p_k(z) = p_k$ for $k \neq i, j$, and

$$p_i(z) = p_i + z\eta \ , \qquad p_j(z) = p_j - z\eta \ . \tag{4.11}$$

Since η is null and orthogonal to p_i, p_j, the shifted momenta are on-shell

$$p_i^2(z) = p_i^2 \ , \qquad p_j^2(z) = p_j^2 \ . \tag{4.12}$$

Equations (4.11) imply that $p_i(z) + p_j(z) = p_i + p_j$, so $\mathcal{A}(z)$ obeys momentum conservation. Hence, it is an on-shell scattering amplitude of particles with complex momenta and can be computed from the usual Feynman rules.

Clearly, the momenta of the external particles are linear functions of z. Notice that the spinors of massless external particles are linear functions of z as well. In the case where both marked particles are massless, there are two possible η's given by eq. (4.5). For $\eta = \lambda_j\tilde{\lambda}_i$, the shift (4.11) is accomplished by

$$\lambda_i(z) = \lambda_i + z\lambda_j \ , \qquad \tilde{\lambda}_j(z) = \tilde{\lambda}_j - z\tilde{\lambda}_i \ . \tag{4.13}$$

The second solution for the shift vector, $\eta' = \lambda_i\tilde{\lambda}_j$, gives

$$\tilde{\lambda}_i(z) = \tilde{\lambda}_i + z\tilde{\lambda}_j \qquad \lambda_j(z) = \lambda_j - z\lambda_i. \tag{4.14}$$

Consider now the case when one of the particles, say particle i, is massless and the other particle j is massive. Then (4.7) gives $\eta^{a\dot{a}} = \lambda_i^a(\lambda_i p_j)^{\dot{a}}$. The shift of marked momenta (4.11) is accomplished by

$$\tilde{\lambda}_i^{\dot{a}}(z) = \tilde{\lambda}_i^{\dot{a}} + z(\lambda_i p_j)^{\dot{a}} \ , \qquad p_j^{a\dot{a}}(z) = p_j^{a\dot{a}} - z\lambda_i^a(\lambda_i p_j)^{\dot{a}} \ . \tag{4.15}$$

For $\eta^{a\dot{a}} = (p_j\tilde{\lambda}_i)^a\tilde{\lambda}_i^{\dot{a}}$ there are analogous expressions

$$\lambda_i^a(z) = \lambda_i^a + z(p_j\tilde{\lambda}_i)^a \ , \qquad p_j^{a\dot{a}}(z) = p_j^{a\dot{a}} - z(p_j\tilde{\lambda}_i)^a\tilde{\lambda}_i^{\dot{a}} \ . \tag{4.16}$$

It follows that $\mathcal{A}(z)$ is a rational function of z because at tree level, the scattering amplitude is a rational function of the spinors of massless external particles and of the momenta of massive external particles.

At tree-level the rational function $\mathcal{A}(z)$ can only have simple poles in z coming from internal propagators $1/P(z)^2$. Each propagator divides the external particles into two groups, the particles to the 'left' and to the 'right' of the propagator as illustrated in figure 4.1. Hence, the momentum $P(z)$ of a propagator is the sum of the momenta of the external particles to the left of the propagator

$$P = p_r + \ldots + p_i + \ldots + p_s \ . \tag{4.17}$$

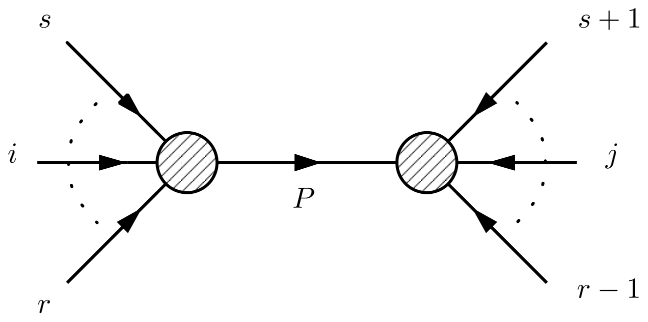

Figure 4.1: Diagrammatic representation of the recursion relation. Arrows label the momentum flow.

The momentum $P(z)$ depends on z only if the particles i and j are on opposite sides of the propagator. We choose the particle i to be on the left of the propagator and the particle j to be on the right, as in figure 4.1. Then

$$P(z) = P + z\eta \ , \tag{4.18}$$

and the propagator is,

$$\frac{1}{P(z)^2 - m^2} = \frac{1}{P^2 - m^2 + 2zP \cdot \eta} \ , \tag{4.19}$$

where m is the mass of the internal particle. The propagator (4.19) has a simple pole at

$$z = -\frac{P^2 - m^2}{2P \cdot \eta} \ . \tag{4.20}$$

For generic external momenta, all internal momenta are different, hence, the locations of all poles are different. It follows that the tree-level amplitude $\mathcal{A}(z)$ has only simple poles as a function of z.

To find the recursion relations, we use the familiar theorem from complex analysis that the sum of residues of a rational function on a Riemann sphere is zero. Applying this to $\mathcal{A}(z)/z$ we express $\mathcal{A}(0)$ as a sum over residues

$$\mathcal{A}(0) = \text{Res}\left(\frac{\mathcal{A}(z)}{z}\right)_{z=0} = -\sum_{\alpha}\text{Res}\left(\frac{\mathcal{A}(z)}{z}\right)_{z=z_\alpha} - \text{Res}\left(\frac{\mathcal{A}(z)}{z}\right)_{z=\infty} \ , \tag{4.21}$$

where the sum is over all finite poles z_α of the amplitude $\mathcal{A}(z)$. These come from the propagators $1/P^2(z)$ that separate the particles i and j. The residues at finite z are determined by the factorisation of the scattering amplitude when the Feynman propagator

(4.19) goes on-shell

$$\operatorname{Res}\left(\frac{\mathcal{A}(z)}{z}\right)_{z=z_\alpha} = -\frac{\mathcal{A}_L(z_\alpha)\mathcal{A}_R(z_\alpha)}{P^2 - m^2} . \tag{4.22}$$

Here, $\mathcal{A}_L$ and $\mathcal{A}_R$ are the tree-level amplitudes of the particles to the left and to the right of the propagator and z_α is given by (4.20).

Hence, any tree-level scattering scattering amplitude $\mathcal{A} = \mathcal{A}(0)$ can be written in the form

$$\mathcal{A} = +\sum_\alpha \frac{\mathcal{A}_L(z_\alpha)\mathcal{A}_R(z_\alpha)}{P_\alpha^2 - m_\alpha^2} - \operatorname{Res}\left(\frac{\mathcal{A}(z)}{z}\right)_\infty , \tag{4.23}$$

where the sum is over all channels α such that the particles i and j are on different sides of the channel, and z_α is given by (4.20). The relation (4.23) is useful for computing scattering amplitudes only if there is an efficient way to determine the boundary contribution $\operatorname{Res}(\mathcal{A}(z)/z)_\infty$. The most favourable scenario is when this contribution vanishes. This happens if and only if $\mathcal{A}(z)$ vanishes at infinity,

$$\operatorname{Res}\left(\frac{\mathcal{A}(z)}{z}\right)_\infty = 0 \quad \Leftrightarrow \quad \mathcal{A}(z) \to 0, \text{ for } z \to \infty , \tag{4.24}$$

in which case, there is a simple recursion relation:

$$\mathcal{A} = \sum_\alpha \mathcal{A}_L(z_\alpha)\frac{1}{P_\alpha^2 - m_\alpha^2}\mathcal{A}_R(z_\alpha) \tag{4.25}$$

that expresses $\mathcal{A}$ in terms of lower-point on-shell scattering amplitudes $\mathcal{A}_L(z_\alpha)$ and $\mathcal{A}_R(z_\alpha)$. The summation in (4.25) runs over all partitions of particles between $\mathcal{A}_L(z_\alpha)$ and $\mathcal{A}_R(z_\alpha)$, such that p_i is on the left, and p_j is on the right of P_α, and also over all helicities h of the intermediate state P_α.

The above considerations apply to the case with massive or massless marked particles. However, for calculations carried out in this paper it will be sufficient to take both marked particles to be massless. In this case, the necessary conditions for the vanishing of the boundary contribution (4.24) put constraints on the possible helicities of the marked particles i and j. These conditions have been discussed in section 2.4.2.

4.1.2. Recursion relations: summary

We will use the recursion relations to calculate tree-level scattering amplitudes in Yang-Mills theory coupled to matter fields. The matter fields may be massive or massless and transform in a generic representation of the gauge group. We consider the colour-ordered partial amplitudes $\mathcal{A} = \mathcal{A}(p_1, \ldots, p_n)$, in which the coloured particles come in a definite cyclic order $1, 2, \ldots, n$. These amplitudes are obtained by stripping away the colour factors from the full amplitude. hence, they depend on the kinematic variables, momenta and helicities, p_k and h_k only.

In the remainder of the paper we will take both marked particles to be massless. We shift two massless momenta $p_i = |i\rangle|i]$ and $p_j = |j\rangle|j]$ of the marked particles by $\eta = |j\rangle|i]$, so the shifted momenta are

$$\widehat{p}_i = p_i + z|j\rangle|i] \ , \tag{4.26}$$

$$\widehat{p}_j = p_j - z|j\rangle|i] \ , \tag{4.27}$$

$$\widehat{P} = P + z|j\rangle|i] \ , \tag{4.28}$$

where $P = p_r + \ldots + p_i + \ldots + p_s$ is the momentum of the intermediate particle. For the particles i, j this is equivalent to shifting the spinors

$$|\widehat{i}] = |i] \ , \qquad |\widehat{i}\rangle = |i\rangle + z|j\rangle \ , \tag{4.29}$$

$$|\widehat{j}\rangle = |j\rangle \ , \qquad |\widehat{j}] = |j] - z|i] \ . \tag{4.30}$$

The recursion relation (4.25) written more explicitly is (c.f. figure 4.1)

$$\mathcal{A}(p_1, \ldots, p_n) = \sum_{\text{partitions}} \sum_{h=\pm} \mathcal{A}_L(p_r, \ldots, \widehat{p}_i, \ldots, p_s, -\widehat{P}^h_{r,s}) \frac{1}{P^2_{r,s} - m^2} \times \mathcal{A}_R(\widehat{P}^{-h}_{r,s}, p_{s+1} \ldots, \widehat{p}_j, \ldots, p_{r-1}) \tag{4.31}$$

where summation is over all partitions of n external particles between $\mathcal{A}_L$ and $\mathcal{A}_R$, such that p_i is on the left, and p_j is on the right, and also over the helicities, h, of the intermediate state. z can be found from the on-shell condition $\widehat{P}^2 = m_p^2$,

$$z = -\frac{P^2 - m_p^2}{2P \cdot \eta} = -\frac{P^2 - m_p^2}{\langle j|P|i]} \ . \tag{4.32}$$

When the intermediate state P is a massless particle (e.g. a gluon), we can simplify the spinor products involving $|\widehat{P}\rangle$ and $|\widehat{P}]$ as in Ref. [64]:

$$\begin{aligned} \langle k\ \widehat{P}\rangle &= \frac{\langle k|\widehat{P}|i]}{[\widehat{P}\ i]} \equiv \frac{\langle k|P|i]}{\omega}\ , & (4.33) \\ [\widehat{P}\ k] &= \frac{\langle j|\widehat{P}|k]}{\langle j\ \widehat{P}\rangle} \equiv \frac{\langle j|P|k]}{\overline{\omega}}\ , & (4.34) \end{aligned}$$

where ω and $\overline{\omega}$ enter the amplitude always in the combination $\omega\overline{\omega} = -\langle j|P|i]$.

For practical computations it is essential that $\mathcal{A}(z)$ vanishes for large z, so that the recursion relations do not have a boundary contribution at infinity. As discussed in section 2.4.2, this puts a constraint on the helicities of the particles i and j. For our choice of the shift momentum, $\eta = |j\rangle|i]$, the helicities of the marked particles can take the values,

$$\eta = |j\rangle|i]\ : \qquad (h_i, h_j)\ =\ (+,-)\ ,\ (+,+)\ ,\ (-,-) \tag{4.35}$$

but not $(h_i, h_j) = (-,+)$. Conditions (4.35) are the same for massive and for massless amplitudes.

4.2. Amplitudes with gluons and massive scalars

In this section we consider scattering amplitudes of gluons with massive complex scalars. These amplitudes are related to amplitudes with *massless* scalars that have D-dimensional momenta. The scalars with D-dimensional momenta P_D can be thought of as massive scalars in 4 dimensions. The D-dimensional on-shell condition, ${P_D}^2 = 0$, gives the 4-dimensional mass-shell equation, ${P_4}^2 = \mu^2$, where the mass term, μ^2, arises from the extra $D-4$ dimensions of momenta.

We will derive amplitudes with 2 scalars and up to 4 gluons with arbitrary helicity configurations. The amplitudes with the same-helicity gluons have been previously derived in [23].

4.2.1. Primitive vertices

The recursion relations construct n-point amplitudes from on-shell m-point amplitudes with $m < n$. The m-point amplitudes are connected to each other with scalar propagators. Using the recursion relation $n-3$ times gives a representation of the n-point amplitude entirely in terms of the 3-point vertices. Hence, 3-point vertices are the building blocks of the amplitudes in the recursive approach*, they will be called the primitive vertices.

The recursion relation reduce the task of computing general amplitudes to the computation of all 3-point primitive vertices. In this paper we consider amplitudes with massless gluons g and massive scalars ϕ. These can be built from the ggg and $\phi g \phi^\dagger$ vertices.

The three-gluon primitive amplitudes can have $--+$ or $++-$ helicity configurations. These are the standard MHV and $\overline{\text{MHV}}$ 3-point on-shell amplitudes

$$\mathcal{A}_3(g_1^-, g_2^-, g_3^+) = \frac{\langle 12\rangle^3}{\langle 23\rangle\langle 31\rangle} \ , \qquad \mathcal{A}_3(g_1^+, g_2^+, g_3^-) = -\frac{[12]^3}{[23][31]} \ . \tag{4.36}$$

The gluon momenta k_i are assumed to be complex which ensures that these amplitudes do not vanish on-shell [42, 64].

In order to compute scattering amplitudes of gluons and massive scalars, we need to determine the $\phi g \phi^\dagger$ vertices. To obtain these, we start with the off-shell Feynman vertex of two scalars of mass μ and momenta l_1, l_2, and a single gluon with momentum k,

$$V_3(l_1^+, k^\mu, l_2^-) = \frac{1}{\sqrt{2}}\,(l_2^\mu - l_1^\mu) \ . \tag{4.37}$$

The $\sqrt{2}$ comes from the normalisation conventions used in colour-ordered Feynman rules [122], and the $+$ and $-$ indices are labels for a scalar and an anti-scalar. To derive the desired on-shell amplitudes, $\mathcal{A}_3(l_1^+, k^\pm, l_2^-)$, we contract $V_3(l_1^+, k^\mu, l_2^-)$ with the gluon

*In particular, this implies that the 4-point vertices in the microscopic Lagrangian are not used in the recursive construction of gauge-invariant amplitudes [64].

polarisation vector, $\epsilon^{\pm}_{\mu}(k,q)$

$$\epsilon^{+}(k,q)_{a\dot{a}} = \sqrt{2}\,\frac{q_a\,k_{\dot{a}}}{\langle q\ k\rangle}\ , \qquad \epsilon^{-}_{\mu}(k,q) = \sqrt{2}\,\frac{k_a\,q_{\dot{a}}}{[k\ q]}\ , \tag{4.38}$$

where $q = |q\rangle|q]$ is an arbitrary reference vector that is not proportional to k. The two independent on-shell vertices immediately follow

$$\mathcal{A}_3(l_1^+, k^+, l_2^-) \ = \ \mathcal{A}_3(l_1^-, k^+, l_2^+) = -\frac{\langle q_1|l_1|k]}{\langle q_1 k\rangle}\ , \tag{4.39}$$

$$\mathcal{A}_3(l_1^+, k^-, l_2^-) \ = \ \mathcal{A}_3(l_1^-, k^-, l_2^+) = \frac{\langle k|l_1|q_2]}{[q_2 k]}\ . \tag{4.40}$$

We have already noted that the primitive vertices vanish for on-shell real momenta in Minkowski space, but are nonzero for on-shell complex momenta. Indeed, the on-shell conditions, $l_1^2 = l_2^2 = \mu^2$ and $k^2 = 0$, together with the momentum conservation imply that the momentum of the gluon is orthogonal to the momenta of the scalars $k \cdot l_1 = k \cdot l_2 = 0$. For real massless momentum k in Minkowski space, the spinors $k^a, \tilde{k}_{\dot{a}}$ are complex conjugates $k_a^* = \pm\tilde{k}^{\dot{a}}$. Similarly a real massive momentum forms a Hermitian matrix $(l_{a\dot{b}})^\dagger = l_{b\dot{a}}$. Hence for real momenta, the conditions $l_i^{a\dot{a}} k_a \tilde{k}_{\dot{a}} = 0, i = 1, 2$ imply $l_i^{a\dot{a}} k_a = l_i^{a\dot{a}}\tilde{k}_{\dot{a}} = 0$ for $i = 1, 2$. It follows that the 3-point vertices (4.40-4.39) vanish. For example we have $\mathcal{A}(l_1^+, k^+, l_2^-) \propto q_a l_1^{a\dot{a}}\tilde{k}_{\dot{a}} = 0$.

For complex momenta the spinors $k^a, \tilde{k}^{\dot{a}}$ become independent variables. This additional freedom allows us to take the momenta of the scalars on-shell while keeping the three-valent amplitudes nonzero.

Finally, we note that the primitive amplitudes are gauge-invariant, even though eqs. (4.39)-(4.40) contain explicit q-dependence. Different choice of the reference vector q amounts to a gauge transformation, hence the on-shell amplitudes should not depend on the choice of q by virtue of gauge symmetry. It is easy to see this explicitly e.g. for the $(\phi^+ g^+ \phi^-)$ amplitude. The reference spinor $q^a, a = 1, 2$ lives in a two dimensional complex vector space. The spinors q^a and k^a are independent due to the condition $\langle qk\rangle \neq 0$, so we take them as a basis of the vector space. Hence a change in the reference spinor can be parameterised as

$$q'^a = \alpha q^a + \beta k^a\ . \tag{4.41}$$

Changing q, the amplitude becomes

$$\mathcal{A}'(l_1^+, k^+, l_2^-) = -\frac{\alpha\langle q|l_1|k] + \beta\langle k|l_1|k]}{\alpha\langle qk\rangle} \ . \tag{4.42}$$

Here, $\langle k|l_1|k] = 2k\cdot l_1 = \mu^2 - l_2^2 = 0$ is zero by momentum conservation. The remaining α dependence gets cancelled between the numerator and the denominator leaving us with the original amplitude.

It follows that the choice of the reference momenta q_i of the gluons does not affect the amplitude so in principle we could set them to arbitrary values. In the following sections, when using recursion relations to calculate amplitudes with scalars, we will find it convenient to set the reference momentum of a marked gluon in a primitive vertex (4.39) or (4.40) to be the momentum of the other marked gluon.

In the following sections we will calculate tree-level amplitudes of the form

$$\mathcal{A}(\phi_{l_1}^\dagger, g_1, g_2, \ldots, g_m, \phi_{l_2}) \ . \tag{4.43}$$

These are the colour-ordered subamplitudes with two massive scalars and m gluons ($2 \leq m \leq 4$) of arbitrary helicities.

When scalars transform in the fundamental representation of the gauge group, the 'string' of fields in the amplitudes must always start and end with the scalar, precisely as in (4.43). Using cyclic symmetry of colour-ordered amplitudes, the scalars in (4.43) can be thought of as adjacent. Scalars in the adjoint representation can appear anywhere in the string, i.e. they do not have to be adjacent. Such amplitudes can also be calculated straightforwardly with our methods.

We will determine all the independent helicity configurations in (4.43), all the remaining configurations can be obtained from those via the following identities:

$$\begin{aligned}
\mathcal{A}_{m+2}(\phi_{l_1}^+, g_1^{h_1}, g_2^{h_2}, \ldots, g_m^{h_m}, \phi_{l_2}^-) &= \mathcal{A}_{m+2}(\phi_{l_1}^-, g_1^{h_1}, g_2^{h_2}, \ldots, g_m^{h_m}, \phi_{l_2}^+) && (4.44)\\
&= (-1)^m \, \mathcal{A}_{m+2}(\phi_{l_2}^-, g_m^{h_m}, \ldots, g_2^{h_2}, g_1^{h_1}, \phi_{l_1}^+) && (4.45)\\
&= \mathcal{A}_{m+2}^*(\phi_{l_1}^-, g_1^{-h_1}, g_2^{-h_2}, \ldots, g_m^{-h_m}, \phi_{l_2}^+) && (4.46)
\end{aligned}$$

where ... indicate gluon fields and h_i is the helicity of the i^{th} gluon. Equations (4.45) and (4.46) follow from reflection and parity symmetry of the colour-ordered amplitudes, and (4.44) follows from eqs. (4.39)-(4.40).

4.2.2. 4-point amplitudes

There are two independent helicity amplitudes in this case, the recursion relation (4.31) gives only one term for each of the amplitudes, as illustrated in figure 4.2.

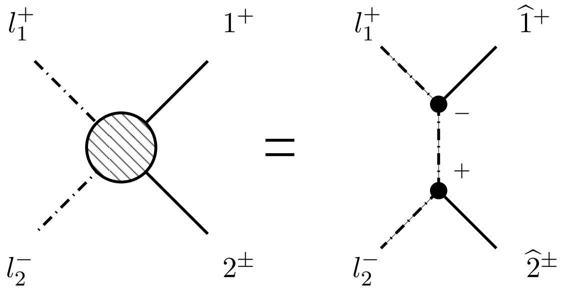

Figure 4.2: Representation of the 4-point amplitude using the recursion relation with 1 and 2 as the shifted momenta.

In the case of two positive helicity gluons, we have:

$$\mathcal{A}_4(l_1^+, 1^+, 2^+, l_2^-) = \mathcal{A}_3(l_1^+, \widehat{1}^+, -\widehat{P}^-) \frac{1}{P^2 - \mu^2} \mathcal{A}_3(\widehat{P}^+, \widehat{2}^+, l_2^-) , \tag{4.47}$$

where we took the marked particles to be the gluons with momenta k_1 and k_2. We set the reference vectors q_1 and q_2 of the two gluons equal to the marked momenta gluon on the opposite side of the diagram

$$q_2 = \widehat{k}_1 = |\widehat{k}_1\rangle|\widehat{k}_1] , \qquad q_1 = \widehat{k}_2 = |\widehat{k}_2\rangle|\widehat{k}_2] . \tag{4.48}$$

We shift the momenta along the vector $\eta = |2\rangle|1]$, so that $|\widehat{1}] = |1]$, $|\widehat{2}\rangle = |2\rangle$. The amplitude then becomes

$$-\frac{\langle 2|l_1|1]\langle\widehat{1}|l_2|\widehat{2}]}{\langle 12\rangle^2((l_1+k_1)^2-\mu^2)} .$$

Using $l_1 + l_2 + \widehat{k}_1 + \widehat{k}_2 = 0 = l_1 + l_2 + k_1 + k_2$, this can be written as

$$-\frac{\mathrm{tr}(\widehat{\not{k}}_1 \not{l}_1 \widehat{\not{k}}_2 \not{l}_1)}{2\langle 12\rangle^2((l_1+k_1)^2-\mu^2)} = \frac{\langle 12\rangle[12](l_1\cdot l_1) - 2(\widehat{k}_1\cdot l_1)(\widehat{k}_2\cdot l_1)}{\langle 12\rangle^2((l_1+k_1)^2-\mu^2)} .$$

To get the second expression we used a Fierz identity. The second term in the numerator vanishes, $\widehat{k}_1 \cdot l_1 = 0$. The easiest way to see this is to use momentum conservation in the 3-point vertex, $l_1 + \widehat{k}_1 = \widehat{P}$, and the on-shell conditions $l_1^2 = \widehat{P}^2 = \mu^2$, $\widehat{k}_1^{\,2} = 0$. Alternatively this can be shown with the use of the definition (4.27) of $\widehat{k}$

$$\widehat{k}_1 \cdot l_1 = k_1 \cdot l_1 - \frac{(l_1 + k_1)^2 - \mu^2}{2\langle 2|l_1|1]}\langle 2|l_1|1] = 0 \ .$$

This leaves us with the final answer

$$\mathcal{A}_4(l_1^+, 1^+, 2^+, l_2^-) = -\frac{\mu^2[12]}{\langle 12\rangle((l_1 + k_1)^2 - \mu^2)} \ . \tag{4.49}$$

This agrees with the previously known result computed by Bern, Dixon and Kosower [23].

For the amplitude with one positive helicity gluon and one negative helicity gluon the recursion relation in figure 4.2 yields,

$$\mathcal{A}_4(l_1^+, 1^+, 2^-, l_2^-) = \mathcal{A}_3(l_1^+, \widehat{1}^+, -\widehat{P}^-)\,\frac{1}{\widehat{P}^2 - \mu^2}\,\mathcal{A}_3(P^+, \widehat{2}^-, l_2^-) \ . \tag{4.50}$$

Using the same choice for the marked gluons and the reference vectors (4.48) as before gives the result

$$\mathcal{A}_4(l_1^+, 1^+, 2^-, l_2^-) = \frac{\langle 2|l_1|1]^2}{\langle 12\rangle[12]((l_1 + k_1)^2 - \mu^2)} \ , \tag{4.51}$$

which we checked against a Feynman diagram calculation.

4.2.3. 5-point amplitudes

The amplitudes with three gluons and a pair of scalars have three independent helicity configurations. As before, we mark the gluons with momenta k_1 and k_2, and pick their reference momenta to be $q_1 = \hat{k}_2$, $q_2 = \hat{k}_1$. The recursion relation is depicted in figure 4.3. For the amplitude with all gluons of positive helicities, the recursion relations have single non-zero diagram. The diagram with gluon exchange vanishes as the choice of

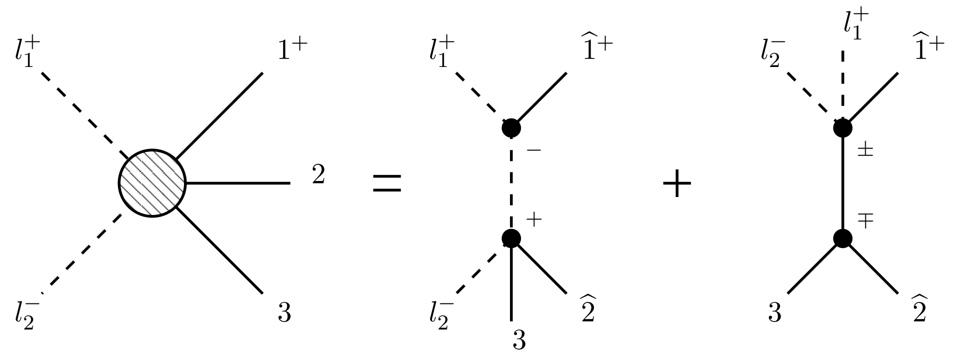

Figure 4.3: The decomposition of the 5-point amplitude using the recursion relation with 1 and 2 as the shifted momenta.

shift vector η implies vanishing of the $\mathcal{A}(\hat{2}^+, 3^+, \hat{p}^\pm)$ $\overline{\text{MHV}}$ amplitude. The amplitude follows immediately:

$$\mathcal{A}_5(l_1^+, 1^+, 2^+, 3^+, l_2^-) = \frac{\mu^2[3|(1+2)l_1|1]}{((l_1+k_1)^2-\mu^2)\langle 12\rangle\langle 23\rangle((l_2+k_3)^2-\mu^2)} \,. \tag{4.52}$$

This is in agreement with the result in [23].

For the case where one of the gluons has negative helicity we have two independent helicity configurations, each of which has two non-zero contributions:

$$\begin{aligned}\mathcal{A}_5(l_1^+, 1^+, 2^+, 3^-, l_2^-) &= -\frac{\langle 3|l_2(1+2)l_1|1]^2}{((l_1+k_1)^2-\mu^2)\langle 12\rangle\langle 23\rangle((l_2+k_3)^2-\mu^2)[3|(1+2)l_1|1]} \\ &\quad - \frac{\mu^2[12]^3}{s_{123}[23][3|(1+2)l_1|1]} \,, \end{aligned} \tag{4.53}$$

$$\begin{aligned}\mathcal{A}_5(l_1^+, 1^+, 2^-, 3^+, l_2^-) &= -\frac{\langle 2|l_1|1]^2\langle 2|l_2|3]^2}{((l_1+k_1)^2-\mu^2)\langle 12\rangle\langle 23\rangle((l_2+k_3)^2-\mu^2)[3|(1+2)l_1|1]} \\ &\quad + \frac{\mu^2[13]^4}{s_{123}[12][23][3|(1+2)l_1|1]} \,. \end{aligned} \tag{4.54}$$

These results are new. Our results (4.52)-(4.54) numerically agree with the much lengthier expressions which we obtained by a direct calculation of the 25 Feynman diagrams.

4.2.4. 6-point amplitudes

We mark gluon momenta 1 and 2, and write down the recursion relation for the 6-point amplitudes with 4 gluons in figure 4.4.

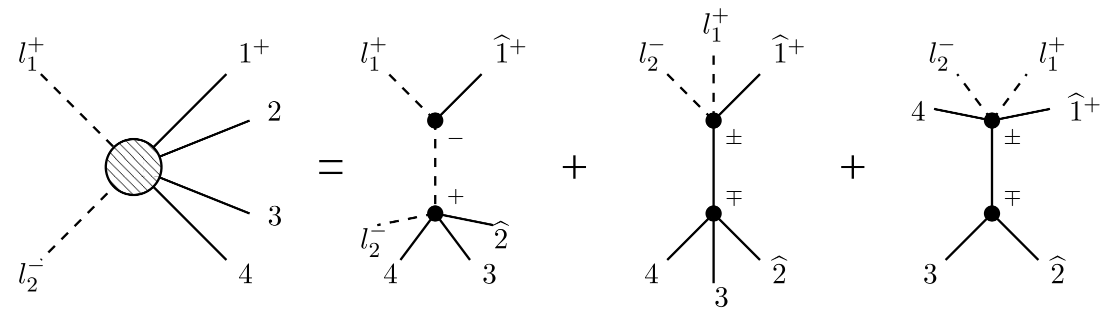

Figure 4.4: The decomposition of the 6 point amplitude using the recursion relation with 1 and 2 as the shifted momenta.

In the case of all gluons of the same helicity, only the first diagram contributes. We find,

$$\mathcal{A}_6(l_1^+, 1^+, 2^+, 3^+, 4^+, l_2^-) = \frac{\mu^2[4|l_2(3+4)(1+2)l_1|1]}{Q_1Q_2Q_3\langle 12\rangle\langle 23\rangle\langle 34\rangle},$$

where $Q_1 = ((l_1+k_1)^2 - \mu^2)$, $Q_2 = ((l_1+k_1+k_2)^2 - \mu^2)$ and $Q_3 = ((l_2+k_4)^2 - \mu^2)$. Eq.4.55 is a slightly shorter form of the result given in [23].

Now we compute the remaining independent 6-point amplitudes. There are two amplitudes with one negative helicity gluon:

$$\begin{aligned}
&\mathcal{A}_6(l_1^+, 1^+, 2^+, 3^+, 4^-, l_2^-) = \\
&-\frac{\left(Q_2\langle 4|l_2(1+2+3)l_1|1] - \mu^2(\langle 4|l_2 32|1])\right)^2}{Q_1Q_2Q_3\langle 12\rangle\langle 23\rangle\langle 34\rangle[4|l_2(3+4)(1+2)l_1|1]} \\
&+\frac{\mu^2[3|(1+2)l_1|1]^3}{Q_1\langle 12\rangle[34]\langle 2|(3+4)(l_1+l_2)l_1|1][4|l_2(3+4)(1+2)l_1|1]} \\
&+\frac{\mu^2\langle 4|2+3|1]^3}{s_{1234}s_{234}\langle 23\rangle\langle 34\rangle\langle 2|(3+4)(l_1+l_2)l_1|1]}
\end{aligned} \tag{4.55}$$

.

$$\begin{aligned}
&\mathcal{A}_6(l_1^+,1^+,2^+,3^-,4^+,l_2^-) = \\
&+\frac{(Q_2\langle 3|l_1|1]-\mu^2\langle 32\rangle[21])^2\langle 3|l_2|4]^2}{Q_1Q_2Q_3\langle 12\rangle\langle 23\rangle\langle 34\rangle[4|l_2(3+4)(1+2)l_1|1]} \\
&+\frac{\mu^2[4|(1+2)l_1|1]^4}{Q_1\langle 12\rangle[34][3|(1+2)l_1|1]\langle 2|(3+4)(l_1+l_2)l_1|1][4|l_2(3+4)(1+2)l_1|1]} \\
&+\frac{\mu^2\langle 3|2+4|1]^4}{s_{1234}s_{234}\langle 4|2+3|1]\langle 23\rangle\langle 34\rangle\langle 2|(3+4)(l_1+l_2)l_1|1]} \\
&-\frac{\mu^2[4|(1+2+3)l_1|1][12]^3}{s_{123}\langle 4|2+3|1]Q_3[23][3|(1+2)l_1|1]}
\end{aligned} \tag{4.56}$$

These amplitudes agree with the massless MHV-type amplitudes as $\mu^2 \to 0$. There are three independent helicity amplitudes with two negative helicity gluons:

$$\begin{aligned}
&\mathcal{A}_6(l_1^+,1^+,2^+,3^-,4^-,l_2^-) = \\
&+\frac{\big(Q_2\langle 4|l_2(3+4)l_1|1]-\mu^2\langle 4|l_2(3+4)2|1]\big)^2}{Q_1Q_2Q_3\langle 12\rangle[34]\langle 4|l_2(3+4)|2\rangle[3|(1+2)l_1|1]} \\
&-\frac{\mu^2\langle 2|l_1|1]^2\langle 34\rangle^3}{Q_1\langle 12\rangle\langle 23\rangle\langle 2|(3+4)(l_1+l_2)l_1|1]\langle 4|l_2(3+4)|2\rangle} \\
&-\frac{[1|l_2l_1|1]^2\langle 34\rangle^3}{s_{1234}s_{234}\langle 4|2+3|1]\langle 23\rangle\langle 2|(3+4)(l_1+l_2)l_1|1]} \\
&+\frac{\langle 4|l_2(1+2+3)l_1|1]^2[12]^3}{Q_3s_{123}\langle 4|2+3|1][4|(1+2+3)l_1|1][23][3|(1+2)l_1|1]} \\
&-\frac{\mu^2[12]^3}{s_{1234}[23][34][4|(1+2+3)l_1|1]}
\end{aligned} \tag{4.57}$$

$$\mathcal{A}_6(l_1^+,1^+,2^-,3^+,4^-,l_2^-) =$$
$$- \frac{\langle 2|l_1|1]^2\langle 2|l_1+1|3]^2\langle 4|l_2|3]^2}{Q_1Q_2Q_3\langle 12\rangle[34]\langle 4|l_2(3+4)|2\rangle[3|(1+2)l_1|1]}$$
$$+ \frac{\mu^2\langle 24\rangle^4\langle 2|l_1|1]^2}{Q_1\langle 12\rangle\langle 23\rangle\langle 34\rangle\langle 2|(3+4)(l_1+l_2)l_1|1]\langle 4|l_2(3+4)|2\rangle}$$
$$- \frac{[1|l_2l_1|1]^2\langle 24\rangle^4}{s_{1234}s_{234}\langle 4|2+3|1]\langle 23\rangle\langle 34\rangle\langle 2|(3+4)(l_1+l_2)l_1|1]}$$
$$+ \frac{\langle 4|l_2(1+2+3)l_1|1]^2[13]^4}{Q_3s_{123}[12][23][4|(1+2+3)l_1|1][3|(1+2)l_1|1]\langle 4|2+3|1]}$$
$$- \frac{\mu^2[13]^4}{s_{1234}[12][23][34][4|(1+2+3)l_1|1]} \tag{4.58}$$

$$\mathcal{A}_6(l_1^+,1^+,2^-,3^-,4^+,l_2^-) =$$
$$- \frac{\langle 2|l_1|1]^2(Q_3[4|l_1+1|2\rangle - \mu^2[43]\langle 32\rangle)^2}{Q_1Q_2Q_3\langle 12\rangle[34][3|(1+2)l_1|1]\langle 4|l_2(3+4)|2\rangle}$$
$$- \frac{\mu^2\langle 23\rangle^3\langle 2|l_1|1]^2}{Q_1\langle 12\rangle\langle 34\rangle\langle 4|l_2(3+4)|2\rangle\langle 2|(3+4)(l_1+l_2)l_1|1]}$$
$$- \frac{[1|l_2l_1|1]^2\langle 23\rangle^3}{s_{1234}s_{234}\langle 34\rangle\langle 2|(3+4)(l_1+l_2)l_1|1]\langle 4|2+3|1]}$$
$$+ \frac{[1|(2+3)l_1|1]^2[1|(2+3)l_2|4]^2}{s_{123}Q_3[12][23][3|(1+2)l_1|1][4|(1+2+3)l_1|1]\langle 4|2+3|1]}$$
$$- \frac{\mu^2[14]^4}{s_{1234}[12][23][34][4|(1+2+3)l_1|1]} \tag{4.59}$$

All of the above six-point amplitudes have been checked numerically against an independent calculation of the 220 Feynman diagrams.

4.3. Massive Vector Bosons

In the next two sections we will apply the on-shell recursion relations to tree-level amplitudes involving massive or off-shell particles with spin coupled to massless particles. To begin with we will consider massive vector bosons coupled to massless gauge fields and fermions. Essentially we consider a generic theory with a non-Abelian gauge group being a product $G_1 \times G_2$, where G_1 is unbroken, and G_2 is broken by the Higgs mechanism. Gauge fields of the G_1 group are massless and the gauge fields of broken group G_2 are massive or off-shell vector bosons V. Two gauge groups are coupled to each other via fermions which are charged under both groups. We will use the 'colour decomposition' representation for scattering amplitudes with respect to both groups, and hence the colour-stripped amplitudes will be purely kinematic quantities which will not depend on the choice of G_1 and G_2 nor on the representations for the matter fermions.

This set-up is rather general, and in particular it incorporates the elements of the Standard Model. In this case G_1 is $SU(3)$ and the corresponding gauge fields are gluons g; the gauge fields of the (partially) broken group, $G_2 = SU(2) \times U(1)$, are massive or off-shell vector bosons $W^{\pm}$, Z^0 and γ^*. The fermions can be taken to be (anti)-quarks, $\bar{q}$, q, transforming in the (anti)-fundamental representations of both groups. Even in the general case, we will continue denoting massless gauge fields as gluons, and fermions as quarks. Massive vector bosons will be denoted as V's.

The quantities we want to consider are the G_1- and G_2-colour-stripped purely kinematic tree-level amplitudes

$$S_{\mu_1 \ldots \mu_m}(1_q, 2, 3, \ldots, n-1, n_{\bar{q}}). \tag{4.60}$$

These are the $(m+n)$-point amplitudes with m massive vector bosons $V_{\mu_1}, \ldots V_{\mu_m}$ coupled to n massless partons. More specifically, we consider the case of a single quark-antiquark pair[†] denoted in (4.60) as $1_q, n_{\bar{q}}$ and $n-2$ gluons labelled $2, 3, \ldots, n-2$.

The group-theoretical dependence in the amplitudes can be easily restored in the usual way, see for example [128]. For the case of fundamental fermions the amplitude (4.60) is multiplied by $(T^{a_2} \ldots T^{a_{n-1}})_{i_1 i_n}$ and by $(T^{b_1} \ldots T^{b_m})_{k_q k_{\bar{q}}}$. Then it is summed over all permutations of $a_2, \ldots, a_{n-1}$ and over all permutations of $b_1, \ldots, b_m$. Here T^a and T^b

[†]One cannot have less than one $q\bar{q}$-pair in amplitudes coupling V's to g's at tree level. Amplitudes with more than one $q\bar{q}$-pair will not be considered in this paper, but they can be calculated in a similar way.

are the generators of the G_1 and the G_2 groups respectively.

The physical states corresponding to all massless particles in amplitudes (4.60) will always be represented in the helicity basis, e.g. $1_q^-, 2^+, 3^- \ldots, (n-1)^+, n_{\bar{q}^-}$. At the same time, for the massive (off-shell) vectors $V_{\mu_1}, \ldots V_{\mu_m}$ we will always choose to not multiply them by external wave functions, and instead of helicities or polarisations they will be characterised by their Lorentz indices $\mu_1, \ldots, \mu_m$. Thus, the amplitudes $S_{\mu_1 \ldots \mu_m}$ are the multi-vector boson currents.

Working with multi-currents (4.60) will first of all facilitate our calculation: single vector currents will be used in calculations of double currents and so on, as will be seen in section 4.5. Furthermore, multi-currents can be easily used to calculate full physical amplitudes which include the decay of the massive (off-shell) vector bosons into light stable states. This is achieved by contracting each Lorentz index μ in (4.60) with the current L^μ describing the relevant decay mode of each vector boson V_μ.

In the Standard Model, for example, one can consider decays of unstable vector bosons into a fermion-antifermion (lepton or quark) pair, so that for virtual photon γ^* or for $V = W^\pm, Z$ boson decay we have:

$$
\begin{aligned}
L^\mu_{\gamma^*} &= -e^2 Q_f Q_q \frac{\bar{u}(p_f)\gamma_\mu u(p_{\bar{f}})}{P^2_{\gamma^*}} \\
L^\mu_V &= -e^2 \frac{v^{f\bar{f}}_{V;H} v^{q\bar{q}}_{V;H} \bar{u}(p_f)\gamma_\mu u(p_{\bar{f}})}{(P_V^2 - M_V^2 + i\Gamma_V M_V)}.
\end{aligned}
\tag{4.61}
$$

Here the couplings $v_{V;H}$ for V either W or Z bosons with either left (L) or right (R) handed polarisations are given by

$$
\begin{aligned}
&v^{f\bar{f}}_{Z;R} = -Q_f \tfrac{\sin\theta_w}{\cos\theta_w}\ , \qquad v^{f\bar{f}}_{Z;L} = -Q_f \tfrac{I^3_{w,f} - \sin^2\theta_w}{\sin\theta_w \cos\theta_w}\ , \qquad v^{\nu_i \bar{l}_j}_{W;L} = \tfrac{1}{\sqrt{2}\sin\theta_w}\delta_{ij}\ , \\
&v^{l_i \bar{\nu}_j}_{W;L} = \tfrac{1}{\sqrt{2}\sin\theta_w}\delta_{ij}\ , \qquad v^{u_i \bar{d}_j}_{W;L} = \tfrac{1}{\sqrt{2}\sin\theta_w} U^\dagger_{ji}\ , \qquad v^{d_i \bar{u}_j}_{W;L} = \tfrac{1}{\sqrt{2}\sin\theta_w} U_{ji}\ .
\end{aligned}
\tag{4.62}
$$

and all others zero. U_{ij} is the CKM mixing matrix and the rest of notation is standard.

4.4. Single Vector Boson Currents

The single vector boson currents were previously calculated by Berends, Giele and Kuijf [61] using the recursive technique based on iterations of classical equations of motion [60]. More recently these single vector currents were also discussed and derived in [55] using a combination of Berends-Giele recursion relations and the MHV rules of [45]. Here we will employ the BCFW on-shell recursion relations of section 4.1 to derive slightly more compact expressions as well as new results for n-parton single currents for some specific helicity arrangements of partons. As mentioned earlier, single off-shell currents S_μ are not only interesting on their own right, more significantly, they play an important part in a recursive construction of currents with two and more vector bosons as will be explained in the next section. We note that a similar observation has also been made in [55].

We now proceed to construct the single vector boson currents,

$$S_\mu(1_q^\lambda, 2^{h_2}, \ldots, (n-1)^{h_{n-1}}, n_{\bar{q}}^{-\lambda}). \tag{4.63}$$

The on-shell recursion relations construct amplitudes from on-shell amplitudes with fewer particles. Assuming that one can always avoid contributions at $z \to \infty$ and using the recursion relation $n-3$ times gives a representation of the n-point amplitude entirely in terms of the 3-point vertices. Hence, 3-point vertices are the building blocks of all larger amplitudes and hence the on-shell recursion relations reduce the task of computing general amplitudes to the computation of all 3-point vertices. This is indeed the case in theories with massless vectors coupled to fermions and also to massless and massive scalars‡ [64, 65, 71].

The three-gluon and the quark-gluon-antiquark primitive amplitudes are given by the

‡This is however not always the case in theories involving scalar self-interactions. The 4-point vertex corresponding to a ϕ^4 interaction clearly cannot be reduced to 3-point vertices. Recursion relation cannot be applied to this vertex since it is a constant. Hence the corresponding amplitude $A_4(z)$ does not depend on z, and this necessarily leads to a non-vanishing contribution at $z \to \infty$. We thank George Georgiou for pointing this out to us.

standard MHV and $\overline{\text{MHV}}$ expressions:

$$\begin{aligned}
\mathcal{A}_3(1^-,2^-,3^+) &= \tfrac{\langle 12\rangle^3}{\langle 23\rangle\langle 31\rangle} \,, & \mathcal{A}_3(1^+,2^+,3^-) &= -\frac{[12]^3}{[23][31]} \,, & (4.64)\\
\mathcal{A}_3(1_q^-,2^-,3_{\bar q}^+) &= \tfrac{\langle 12\rangle^2}{\langle 13\rangle} \,, & \mathcal{A}_3(1_q^-,2^+,3_{\bar q}^+) &= -\frac{[23]^2}{[13]} \,, & (4.65)\\
\mathcal{A}_3(1_q^+,2^-,3_{\bar q}^-) &= \tfrac{\langle 23\rangle^2}{\langle 13\rangle} \,, & \mathcal{A}_3(1_q^+,2^+,3_{\bar q}^-) &= -\frac{[12]^2}{[13]} \,. & (4.66)
\end{aligned}$$

Here as always, all momenta k_i are assumed to be complex which ensures that these 3-point amplitudes do not vanish on-shell [64, 65].

In addition we need to introduce two new primitive vertices for an off-shell vector boson coupled to a $q\bar q$ pair. They are derived directly from the Feynman rules:

$$\begin{aligned}
S_\mu(1_q^-,2_{\bar q}^+) &= \langle 1|\sigma_\mu|2] \equiv [2|\bar\sigma_\mu|1\rangle \,,\\
S_\mu(1_q^+,2_{\bar q}^-) &= [1|\bar\sigma_\mu|2\rangle \equiv \langle 2|\sigma_\mu|1] \,. \qquad (4.67)
\end{aligned}$$

Here, $\sigma_{\mu\,\alpha\dot\alpha}$ and $\bar\sigma_\mu^{\dot\alpha\alpha}$ are the standard four Pauli matrices. Our conventions for spinor contractions are summarised in the Appendix.

Action of parity symmetry reduces the number of independent currents. Parity transformation is simply the complex conjugation in terms of $S_{\alpha\dot\beta} := S_\mu\sigma^\mu_{\alpha\dot\beta}$,

$$S_{\alpha\dot\beta}(1_q^\lambda,2^{h_2},\ldots,(n-1)^{h_{n-1}},n_{\bar q}^{-\lambda}) = \Big(S_{\beta\dot\alpha}(1_q^{-\lambda},2^{-h_2},\ldots,(n-1)^{-h_{n-1}},n_{\bar q}^{\lambda})\Big)^* . \qquad (4.68)$$

This formula is generalised to multi-vector boson currents in an obvious way:

$$S_{\alpha_1\dot\beta_1\ldots\alpha_m\dot\beta_m} = (S_{\beta_1\dot\alpha_1\ldots\beta_m\dot\alpha_m})^*. \qquad (4.69)$$

4.4.1. Single Currents with $n = 4, 5, 6$ partons

In the four-parton case the recursion relation for S_μ reduces to,

$$S_\mu(1_q^-,2^\pm,3_{\bar q}^+) = S_\mu(\widehat{1}_q^-,-\widehat{P}_{\bar q}^+)\frac{1}{s_{23}}\mathcal{A}(\widehat{P}_q^-,\widehat{2}^\pm,3_{\bar q}^+). \qquad (4.70)$$

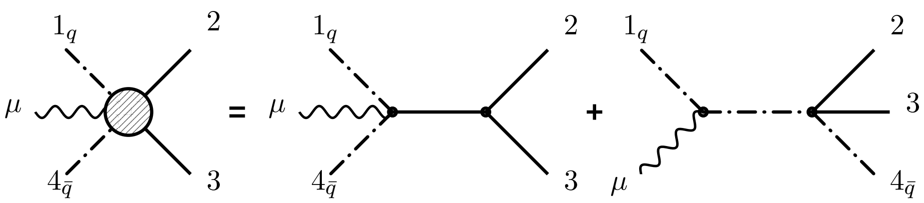

Figure 4.5: Decomposition of the five-point current after applying the recursion relation.

We now have to choose which of the marked particles, $\widehat{1}$, $\widehat{2}$, is $\hat{\imath}$ and which is $\hat{\jmath}$. In order to avoid boundary contributions according to (4.35) we must choose $i = 2$ for the 2^+ helicity and $j = 2$ for 2^- helicity. This results in,

$$S_\mu(1_q^-, 2^+, 3_{\bar{q}}^+) = -\frac{\langle 1|\sigma_\mu P_V|1\rangle}{\langle 12\rangle\langle 23\rangle}\,, \tag{4.71}$$

$$S_\mu(1_q^-, 2^-, 3_{\bar{q}}^+) = \frac{[3|P_V\sigma_\mu|3]}{[12][23]}\,, \tag{4.72}$$

where P_V is the momentum of the vector boson. Momentum conservation implies $P_V = -p_1 - p_2 - p_3$. The two remaining helicity configurations can be obtained by parity transformations.

Figure 4.5 shows the decomposition of the five-parton current. Just as in the four-parton case here we mark the quark $\widehat{1}$ and adjacent gluon $\widehat{2}$,

$$S_\mu(1_q^-, 2^+, 3^+, 4_{\bar{q}}^+) = \frac{\langle 1|\sigma_\mu P_V|1\rangle}{\langle 12\rangle\langle 23\rangle\langle 34\rangle}\,, \tag{4.73}$$

$$\begin{aligned} S_\mu(1_q^-, 2^-, 3^+, 4_{\bar{q}}^+) = &\ \frac{[13][3|(1+2)P_V\bar{\sigma}_\mu(1+2)|3]}{s_{123}[12][23]\langle 4|2+3|1]} \\ &+ \frac{\langle 24\rangle\langle 2|(3+4)\bar{\sigma}_\mu P_V(3+4)|2\rangle}{s_{234}\langle 23\rangle\langle 34\rangle\langle 4|2+3|1]}\,, \end{aligned} \tag{4.74}$$

$$\begin{aligned} S_\mu(1_q^-, 2^+, 3^-, 4_{\bar{q}}^+) = &\ \frac{[24]^3\langle 1|\sigma_\mu P_V|1\rangle}{s_{234}[23][34]\langle 1|2+3|4]} \\ &+ \frac{\langle 13\rangle^3[4|P_V\sigma_\mu|4]}{s_{123}\langle 12\rangle\langle 23\rangle\langle 1|2+3|4]}\,. \end{aligned} \tag{4.75}$$

The $S_\mu(+;++;-)$ configuration can be obtained from eq. (4.73) by using the "line reversal" symmetry,

$$S_\mu(1_q^\lambda, 2^{h_2}, \ldots, n-1^{h_{n-1}}, n_{\bar{q}}^{-\lambda}) = (-1)^{n+1} S_\mu(n_q^{-\lambda}, n-1^{h_{n-1}}, \ldots, 2^{h_2}, 1_{\bar{q}}^\lambda)\,. \tag{4.76}$$

The other 4 helicity amplitudes can then by obtained via parity transformations. Notice that if we use both (4.68) and (4.76) we can also relate (4.72) and (4.71).

The 6-point amplitudes can be computed in much the same way. We choose to mark massless particles in such a way as to generate the most compact analytic expression. The following amplitude was computed using $i = 2$ and $j = 1$:

$$S_\mu(1_q^-, 2^+, 3^+, 4^+, 5_{\bar q}^+) = -\frac{\langle 1|\sigma_\mu P_V|1\rangle}{\langle 12\rangle\langle 23\rangle\langle 34\rangle\langle 45\rangle}\,. \tag{4.77}$$

The following expressions was derived using $i = 3$ and $j = 4$:

$$\begin{aligned}S_\mu(1_q^-, 2^-, 3^+, 4^+, 5_{\bar q}^+) = &-\frac{\langle 25\rangle\langle 2|(3+4+5)P_V\sigma_\mu(3+4+5)|2\rangle}{s_{2345}\langle 23\rangle\langle 34\rangle\langle 45\rangle\langle 5|P_V|1]}\\ &+\frac{[13][3|(1+2)\sigma_\mu P_V(1+2)|3]}{s_{123}\langle 45\rangle[12][23]\langle 4|2+3|1]}\\ &+\frac{\langle 2|3+4|1]\langle 2|(3+4)(1+2+3+4)\sigma_\mu P_V(1+2+3+4)(3+4)|2\rangle}{s_{1234}s_{234}\langle 23\rangle\langle 34\rangle\langle 5|P_V|1]\langle 4|2+3|1]}\,.\end{aligned} \tag{4.78}$$

For the choice $i = 2$ and $j = 1$ we find:

$$\begin{aligned}S_\mu(1_q^-, 2^+, 3^-, 4^+, 5_{\bar q}^+) = &-\frac{\langle 13\rangle^3\langle 35\rangle\langle 3|(4+5)P_V\sigma_\mu(4+5)|3\rangle}{\langle 12\rangle\langle 23\rangle\langle 34\rangle\langle 45\rangle\langle 5|P_V(1+2)|3\rangle\langle 3|(4+5)P_V|1\rangle}\\ &+\frac{\langle 35\rangle\langle 3|4+5|2]^3\langle 1|\sigma_\mu P_V|1\rangle}{s_{2345}s_{345}\langle 34\rangle\langle 45\rangle\langle 3|(4+5)P_V|1\rangle\langle 5|3+4|2]}\\ &-\frac{\langle 13\rangle^3\langle 3|1+2|4][4|(1+2+3)\sigma_\mu P_V(1+2+3)|4]}{s_{1234}s_{123}\langle 12\rangle\langle 23\rangle\langle 5|P_V(1+2)|3\rangle\langle 1|2+3|4]}\\ &-\frac{[24]^4\langle 1|\sigma_\mu P_V|1\rangle}{s_{234}\langle 5|3+4|2]\langle 1|2+3|4][23][34]}\,.\end{aligned} \tag{4.79}$$

Finally using $i = 3$ and $j = 2$ we find,

$$\begin{aligned}S_\mu(1_q^-, 2^+, 3^+, 4^-, 5_{\bar q}^+) = &\frac{\langle 14\rangle^3[5|P_V\sigma_\mu|5]}{s_{1234}\langle 12\rangle\langle 23\rangle\langle 34\rangle\langle 1|P_V|5]}\\ &-\frac{[35]^3\langle 1|\sigma_\mu P_V|1\rangle}{s_{345}\langle 12\rangle\langle 2|3+4|5][34][45]}\\ &+\frac{\langle 4|2+3|5]^3\langle 1|\sigma_\mu P_V|1\rangle}{s_{234}s_{2345}\langle 23\rangle\langle 34\rangle\langle 2|3+4|5]\langle 1|P_V|5]}\,.\end{aligned} \tag{4.80}$$

Using the parity and line reversal symmetries of eqs. (4.68) and (4.76) we can easily obtain expressions for the other 12 helicity configurations.

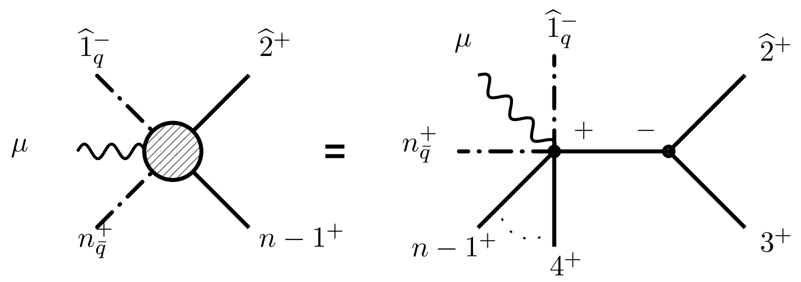

Figure 4.6: Decomposition of the n-point vector boson current with $n-2$ positive helicity gluons.

All the amplitudes presented in this section have been numerically checked against Feynman-diagram based calculations.

4.4.2. n-point Currents

It is also possible to construct single vector boson currents with n partons in the helicity configurations with maximal helicity violation, next-to-maximal helicity violation and beyond. The current for vector boson decaying to a quark pair and any number of positive helicity gluons has been known for some time [61],

$$S_\mu(1_q^-, 2^+, \ldots, (n-1)^+, n_{\bar{q}}^+) = (-1)^n \frac{\langle 1|\sigma_\mu P_V|1\rangle}{\prod_{\alpha=1}^{n-1}\langle \alpha\, \alpha+1\rangle}\,. \tag{4.81}$$

As usual P_V is the momentum of the vector boson and $P_V = -p_1 - \ldots - p_n$. This can be easily proved by induction using on-shell recursion relations. The fact that any pure QCD amplitude with less than two negative helicities is zero guarantees that the only contribution to the n-point current involves an $(n-1)$-point current and an on-shell (complex) 3-gluon vertex, as shown in figure 4.6. This is the first non-vanishing helicity amplitude and hence it is the MHV current. For completeness, the other MHV-type

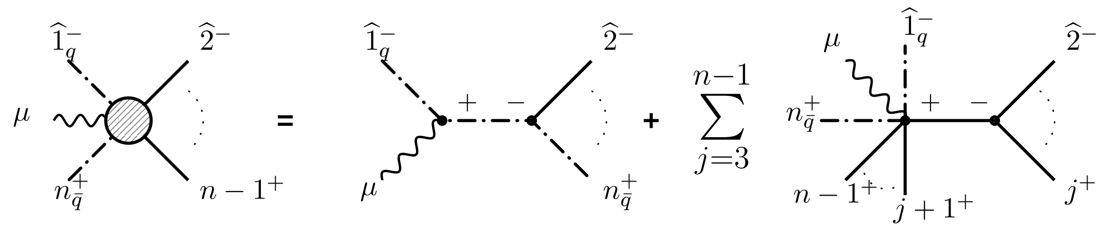

Figure 4.7: Decomposition of the n-point vector boson current with $n-3$ positive helicity gluons and two adjacent negative helicities.

currents are given by,

$$\begin{aligned} S_\mu(1_q^+, 2^+, \ldots, (n-1)^+, n_{\bar{q}}^-) &= -(-1)^n \frac{\langle n|\sigma_\mu P_V|n\rangle}{\prod_{\alpha=1}^{n-1}\langle \alpha\, \alpha+1\rangle}, \\ S_\mu(1_q^+, 2^-, \ldots, (n-1)^-, n_{\bar{q}}^-) &= -\frac{[1|P_V\bar{\sigma}_\mu|1]}{\prod_{\alpha=1}^{n-1}[\alpha\, \alpha+1]}, \\ S_\mu(1_q^-, 2^-, \ldots, (n-1)^-, n_{\bar{q}}^+) &= \frac{[n|P_V\bar{\sigma}_\mu|n]}{\prod_{\alpha=1}^{n-1}[\alpha\, \alpha+1]}. \end{aligned} \tag{4.82}$$

It is interesting to note that eq. (4.81) allows us to immediately write down compact expressions for the NMHV currents with both adjacent and non-adjacent minuses. If we mark the two negative helicity particles then each sub-amplitude in the recursion relation will contain at most 2 negative helicities. Figure 4.7 shows the decomposition into a sum of sub-diagrams. We draw a pure QCD amplitude on the right of each diagram which must contain at least two negative helicity particles, this fixes the helicity on the right of each propagator to be negative. Helicity conservation then ensures that the vector currents have only one negative helicity, the marked quark, and so are MHV currents. We can therefore use (4.81) to write down the NMHV current, marking $i=1$ and $j=2$:

$$\begin{aligned} S_\mu(1_q^-, 2^-, 3^+, \ldots, (n-1)^+, n_{\bar{q}}^+) = \frac{-(-1)^n}{\prod_{\alpha=2}^{n-1}\langle \alpha\, \alpha+1\rangle} \Bigg(\frac{\langle 2|K_{3,n}P_V\sigma_\mu K_{3,n}|2\rangle\langle 2n\rangle}{s_{2,n}\langle n|K_{2,n-1}|1]} \\ + \sum_{j=3}^{n-1} \frac{\langle 2|K_{3,j}K_{1,j}P_V\bar{\sigma}_\mu K_{1,j}K_{3,j}|2\rangle\langle 2|K_{3,j}|1]\langle j\, j+1\rangle}{s_{2,j}s_{1,j}\langle j|K_{2,j-1}|1]\langle j+1|K_{2,j}|1]} \Bigg), \end{aligned} \tag{4.83}$$

This expression is the n-parton generalisation of equations (4.74) and (4.78).

We can also consider the case where the helicity along the quark line is flipped. This is a special case as we can still eliminate all contributions from NMHV vertices. The result is,

$$S_\mu(1_q^-,2^+,\ldots,(n-2)^+,(n-1)^-,n_{\bar q}^+) = \frac{(-1)^n}{\prod_{\alpha=1}^{n-2}\langle \alpha\,\alpha+1\rangle}\Bigg(\frac{\langle 1 n-1\rangle^3[n|\bar\sigma_\mu P_V|n]}{s_{1,n-1}\langle 1|P_V|n]}$$
$$+\sum_{j=1}^{n-3}\frac{\langle n-1|K_{j+1,n-2}|n]^3\langle 1|\sigma_\mu P_V|1\rangle\langle j\,j+1\rangle}{s_{j+1,n}s_{j+1,n-1}\langle j+1|K_{j+1,n-1}|n]\langle j|K_{j+1,n-1}|n]}\Bigg), \tag{4.84}$$

matching equations (4.75) and (4.80) when $n=4$ and 5 respectively.

For NMHV currents with non-adjacent negative helicities we can re-use the above result to find the amplitude where the negative helicities are separated by one positive helicity. The corresponding diagrams are shown in Fig. 4.8 where we mark $i=2$ and $j=1$,

$$S_\mu(1_q^-,2^+,3^-,4^+,\ldots,n-1^+,n_{\bar q}^+) = \frac{\langle 1|P_V\bar\sigma_\mu|1\rangle\langle 3|K_{4,n}|2]^3\langle 3n\rangle}{s_{2,n}s_{3,n}\langle 1|K_{2,n}K_{4,n}|3\rangle\langle n|K_{3,n-1}|2]\prod_{\alpha=3}^{n-1}\langle\alpha\,\alpha+1\rangle}$$
$$+\sum_{j=4}^{n-1}\frac{\langle 1|\sigma_\mu P_V|1\rangle\langle 3|K_{4,j}|2]^4\langle j\,j+1\rangle}{s_{2,j}s_{3,j}\langle 1|K_{2,j}K_{4,j}|3\rangle\langle j|K_{3,j-1}|2]\langle j+1|K_{3,j}|2]\prod_{\alpha=3}^{n-1}\langle\alpha\,\alpha+1\rangle}$$
$$+S_\mu(\widehat{1}_q^-,\widehat{P}^-,4^+,\ldots,n-1^+,n_{\bar q}^+)\frac{\langle 31\rangle^3}{\langle 12\rangle\langle 23\rangle\bar w^2} \tag{4.85}$$

Substituting eq. (4.83) and simplifying the shifts results in the following expression:

$$S_\mu(1_q^-,2^+,3^-,4^+,\ldots,n-1^+,n_{\bar q}^+) = \frac{1}{\prod_{\alpha=3}^{n-1}\langle\alpha\,\alpha+1\rangle}\Bigg(\frac{\langle 1|P_V\bar\sigma_\mu|1\rangle\langle 3|K_{4,n}|2]^3\langle 3n\rangle}{s_{2,n}s_{3,n}\langle 1|K_{2,n}K_{4,n}|3\rangle\langle n|K_{3,n-1}|2]}$$
$$+\sum_{j=4}^{n-1}\frac{\langle 1|\sigma_\mu P_V|1\rangle\langle 3|K_{4,j}|2]^4\langle j\,j+1\rangle}{s_{2,j}s_{3,j}\langle 1|K_{2,j}K_{4,j}|3\rangle\langle j|K_{3,j-1}|2]\langle j+1|K_{3,j}|2]}$$
$$+\frac{\langle 13\rangle^3\langle n3\rangle\langle 3|K_{4,n}P_V\sigma_\mu K_{4,n}|3\rangle}{\langle 1|K_{2,n}K_{4,n}|3\rangle\langle n|K_{1,n-1}K_{12}|3\rangle\langle 12\rangle\langle 23\rangle}$$
$$+\sum_{j=4}^{n-1}\frac{\langle 13\rangle^3\langle 3|K_{4,j}K_{1,j}P_V\bar\sigma_\mu K_{1,j}K_{4,j}|3\rangle\langle 3|K_{12}K_{4,j}|3\rangle\langle j\,j+1\rangle}{s_{1,j}\langle 1|K_{2,j}K_{4,j}|3\rangle\langle j|K_{1,j-1}K_{12}|3\rangle\langle j+1|K_{1,j}K_{12}|3\rangle\langle 12\rangle\langle 23\rangle}\Bigg). \tag{4.86}$$

Remaining NMHV currents can be constructed in a similar way. We can keep adding an extra positive helicity separating the negative helicities. We have checked that the n-parton result in eq. (4.86) agrees with eqs. (4.75) and (4.79) for $n=4$ and $n=5$ respectively.

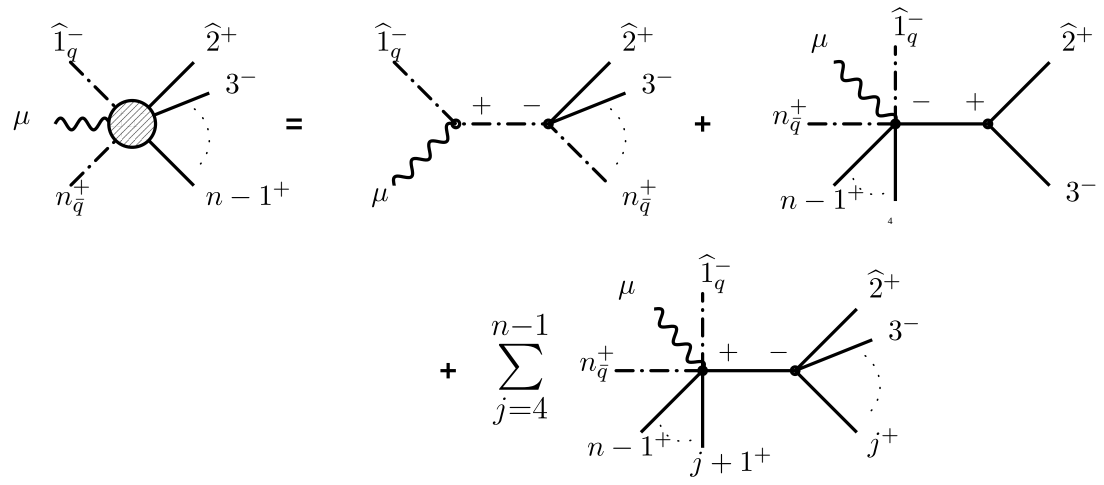

Figure 4.8: Decomposition of the n-point vector boson current with $n-3$ positive helicity gluons and two negative helicities, separated by a single gluon with positive helicity. The second contribution involves the NMHV current with adjacent negative helicities given in (4.83)

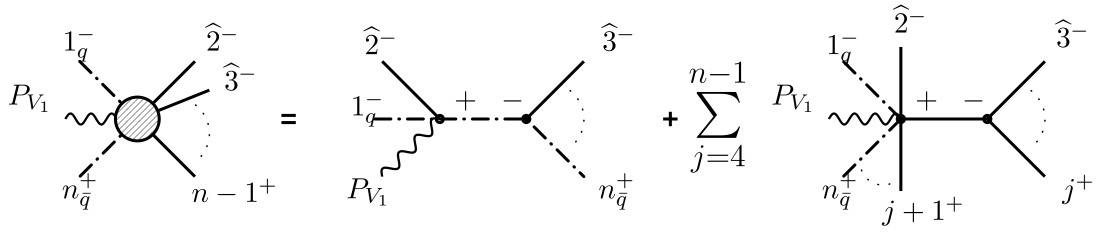

Figure 4.9: Decomposition of the single vector boson current with three consecutive negative helicities. The recursion re-uses the current with two consecutive negative helicities.

As a final example we consider the NNMHV current with three adjacent negative helicities.

By marking particles $i = 2$ and $j = 3$ we ensure that only the NMHV current (4.83)

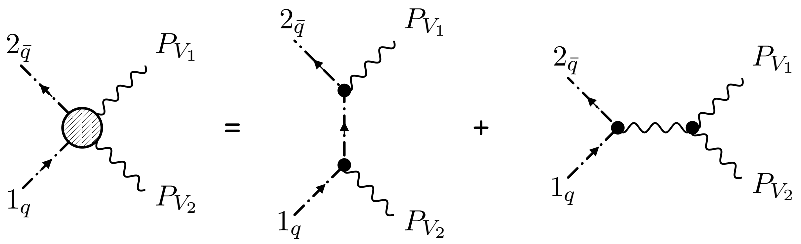

Figure 4.10: The two Feynman diagrams contributing to the amplitude with two massive vector bosons and a quark pair.

is needed. Explicit calculation yields,

$$\begin{aligned}
S_\mu(1_q^-, 2^-, 3^-, 4^+, \ldots, n-1^+, n_{\bar{q}}^+) &= \frac{(-1)^n}{\prod_{\alpha=3}^{n-1}\langle \alpha\, \alpha+1\rangle}\Bigg(\frac{\langle 3n\rangle\langle 3|K_{4,n}P_V\sigma_\mu K_{4,n}|3\rangle}{s_{3,n}[12]\langle n|K_{3,n-1}|2]} \\
&+\sum_{j=4}^{n-1}\frac{\langle 3|K_{4,j}|1]\langle 3|K_{4,j}K_{1,j}P_V\sigma_\mu K_{1,j}K_{4,j}|3\rangle\langle j\, j+1\rangle}{s_{3,j}s_{1,j}[12]\langle j+1|K_{2,j}|1]\langle j|K_{3,j-1}|2]} \\
&-\sum_{j=4}^{n-1}\sum_{l=j+1}^{n-1}\frac{\langle 3|K_{4,j}K_{2,j}K_{2,l}|1]\langle 3|K_{4,j}K_{2,j}K_{2,l}K_{1,l}P_V\bar{\sigma}_\mu K_{1,l}K_{2,l}K_{2,j}K_{4,j}|3\rangle\langle j\, j+1\rangle\langle l\, l+1\rangle}{s_{1,l}s_{2,l}s_{2,j}s_{3,j}\langle l|K_{2,l-1}|1]\langle l+1|K_{2,l}|1]\langle j+1|K_{3,j}|2]\langle j|K_{3,j-1}|2]} \\
&-\sum_{j=4}^{n-1}\frac{\langle 3|K_{4,j}K_{2,j}|n\rangle\langle 3|K_{4,j}K_{2,j}K_{2,n}P_V\bar{\sigma}_\mu K_{2,n}K_{2,j}K_{4,j}|3\rangle\langle j\, j+1\rangle}{s_{3,j}s_{2,n}s_{2,j}\langle n|K_{2,n-1}|1]\langle j+1|K_{3,j}|2]\langle j|K_{3,j-1}|2]}\Bigg).
\end{aligned} \tag{4.87}$$

We have explicitly checked eq. (4.87) for up to six partons.

By repeated use of the recursion formulae, further n-point currents may be obtained.

4.5. Double Vector Boson Currents

We now turn to double vector boson currents $S_{\mu\nu}$. We start by considering the smallest amplitude of this type, the one with only two partons, $S_{\mu\nu}(q,\bar{q})$. One might expect that on-shell recursion relations can be used to derive $S_{\mu\nu}(q,\bar{q})$ from two single vector boson amplitudes $S_\mu(q,\bar{q})$. However there is a difficulty in writing down such a recursion relation. We cannot mark the two massless particles in $S_{\mu\nu}(q,\bar{q})$ since it is known that marking adjacent massless quarks results in a non-vanishing boundary contribution [66] to the amplitude. Choosing to mark massive particles also leads to (unnecessary) technical complications. It is actually much simpler to derive the four-point amplitude $S_{\mu\nu}(q,\bar{q})$ from Feynman diagrams and use this four-point amplitude as a new primitive vertex in further recursive calculations of $S_{\mu\nu}(1_q,\ldots,n_{\bar{q}})$.

In fact, we will use a more elegant approach. In general, there are two Feynman diagrams contributing to $S_{\mu\nu}(q,\bar{q})$, as shown in figure 4.10. We could evaluate both diagrams and use the whole amplitude as a building block for larger amplitudes, however, it is much more efficient to split the calculation into two parts, as considered in [128], in order to re-use the single vector boson currents computed in section **4.4**.

The first part corresponds to the second diagram in figure 4.10, it contains the non-Abelian three-vertex of massive vector bosons. We can compute such contributions to a generic $S_{\mu\nu}(1_q,\ldots,n_{\bar{q}})$ by contracting a single vector boson current $S_{\mu}(1_q,\ldots,n'_{\bar{q}})$ of the previous section with the colour ordered Feynman three-point vertex. This approach was used to calculate the non-Abelian contribution to $S_{\mu\nu}(q,g,\bar{q})$ in reference [55]. Note that if one is dealing with uncharged gauge bosons which have no self-coupling, for example Z bosons, this term is trivially zero.

The second part does not contain a non-Abelian three-vertex of vector bosons, it corresponds to the first diagram in figure 4.10. This second Abelian contribution to a generic $S_{\mu\nu}(1_q,\ldots,n_{\bar{q}})$ can then be evaluated using on-shell recursion relations.

Thus, guided by figure 4.10 we represent the colour ordered double current with n partons in the form [128]:

$$\begin{aligned} S_{\mu\nu}(1_q,\ldots,n_{\bar{q}}) = {} & T^{(3)}_{\mu\nu\rho}(P_{V_1},P_{V_2},-P)\,\frac{1}{(P^2-M_P^2)}\,S^{\rho}(1_q,\ldots,n_{\bar{q}}) \\ & + S^{Abelian}_{\mu\nu}(1_q,\ldots,n_{\bar{q}}). \end{aligned} \tag{4.88}$$

Here

$$T^{(3)}_{\mu_1\mu_2\mu_3}(p_1,p_2,p_3) = g_{\mu_1\mu_2}(p_1-p_2)_{\mu_3} + g_{\mu_2\mu_3}(p_2-p_3)_{\mu_1} + g_{\mu_3\mu_1}(p_3-p_1)_{\mu_2} \tag{4.89}$$

is the colour-ordered three-vertex of massive vector bosons, with all momenta defined to be in-going.

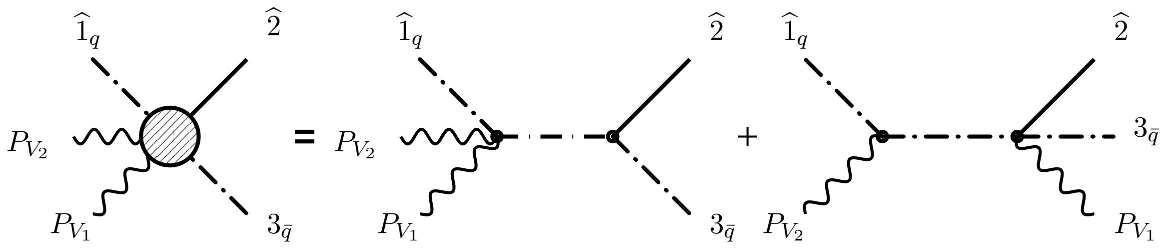

Figure 4.11: Recursive decomposition of the five-point Abelian amplitude for two vector bosons, a quark pair and a gluon using the recursion relation.

The *primitive vertex* for the Abelian contribution is given by the first Feynman diagram in figure 4.10 which evaluates to:

$$S_{\mu\nu}^{Abelian}(1_q^-, 2_{\bar{q}}^+) = \frac{1}{s_{1P_{V_2}}} \langle 1|\sigma_\nu(1 + P_{V_2})\sigma_\mu|2]. \tag{4.90}$$

The remaining non-Abelian part of this four-point amplitude is determined by the first line of (4.88)

$$S_{\mu\nu}^{non-Abelian}(1_q, 2_{\bar{q}}) = T_{\mu\nu\rho}^{(3)}(P_{V_1}, P_{V_2}, -P)\, \frac{1}{(P^2 - M_P^2)}\, S^\rho(1_q, 2_{\bar{q}}) \tag{4.91}$$

where $S^\rho(1_q, 2_{\bar{q}})$ is given in (4.67).

In general one needs to determine only the Abelian components of the n-parton double currents $S_{\mu\nu}(1_q, \ldots, n_{\bar{q}})$, the non-Abelian components are fully determined by the first line of (4.88) in terms of the known single currents.

Abelian components are characterised by having massive vector bosons only on external lines, and they can always be calculated recursively. In general, in order to calculate the Abelian part of any double current, $S_{\mu\nu}^{Abelian}(1_q, 2, \ldots, n_{\bar{q}}^+)$, one needs to draw all recursive decompositions of this current such that the internal line is a quark or a gluon and not a massive vector boson.

First we calculate the two five-point amplitudes by marking the quark and adjacent gluon. The recursion relation for $S_{\mu\nu}^{Abelian}(1_q, 2, 3_{\bar{q}})$ is depicted in figure 4.11. It yields,

$$
\begin{aligned}
S_{\mu\nu}^{Abelian}(1_q^-, 2^-, 3_{\bar{q}}^+) = &+\frac{[13][3|\bar{\sigma}_\mu(1+P_{V_2})\bar{\sigma}_\nu(1+2)|3]}{[12][23][3|P_{V_1}P_{V_2}|1]} \\
&+\frac{\langle 2|\sigma_\mu|3][1|\bar{\sigma}_\nu(1+2)|3]}{[12][3|P_{V_1}P_{V_2}|1]} \\
&-\frac{\langle 2|(1+P_{V_2})\bar{\sigma}_\nu P_{V_2}(1+P_{V_2})|2\rangle[3|P_{V_1}\sigma_\mu|3]}{s_{1P_{V_2}}s_{3P_{V_1}}[3|P_{V_1}P_{V_2}|1]}, \qquad (4.92)\\
S_{\mu\nu}^{Abelian}(1_q^-, 2^+, 3_{\bar{q}}^+) = &\frac{\langle 13\rangle\langle 1|(2+3)\bar{\sigma}_\mu(1+P_{V_2})\bar{\sigma}_\nu|1\rangle}{\langle 12\rangle\langle 23\rangle\langle 1|P_{V_2}P_{V_1}|3\rangle} \\
&+\frac{\langle 1|\sigma_\nu|2]\langle 1|(2+3)\bar{\sigma}_\mu|1\rangle}{\langle 12\rangle\langle 1|P_{V_2}P_{V_1}|3\rangle} \\
&-\frac{\langle 1|P_{V_2}\bar{\sigma}_\nu|1\rangle[2|(1+P_{V_2})P_{V_1}\bar{\sigma}_\mu(1+P_{V_2})|2]}{s_{1P_{V_2}}s_{3P_{V_1}}\langle 1|P_{V_2}P_{V_1}|3\rangle}. \qquad (4.93)
\end{aligned}
$$

These formulae agree with the results of [128] after appropriate permutations of the labels and correcting for propagator conventions. The $S_{\mu\nu}(+;\pm;-)$ configurations can be obtained from eqs. (4.73) by using either parity (4.69) or the "line reversal" symmetry,

$$
S_{\mu\nu}(1_q^\lambda, 2^{h_2}, \ldots, n-1^{h_{n-1}}, n_{\bar{q}}^{-\lambda}) = (-1)^{n+1} S_{\nu\mu}(n_q^{-\lambda}, n-1^{h_{n-1}}, \ldots, 2^{h_2}, 1_{\bar{q}}^\lambda). \qquad (4.94)
$$

Finally we give results for the six point amplitudes $S_{\mu\nu}^{Abelian}(1_q, 2, 3, 4_{\bar{q}})$. Taking the generalised parity relation (4.69) and the line-reversal identity (4.94), there are three independent helicity configurations. Again we use on-shell recursion relations and mark the quark and adjacent gluon. Choosing $i = 2$ and $j = 1$ we find,

$$
\begin{aligned}
S_{\mu\nu}^{Abelian}(1_q^-, 2^+, 3^+, 4_{\bar{q}}^+) = &-\frac{\langle 14\rangle\langle 1|\sigma_\nu|2]\langle 1|(2+3+4)\bar{\sigma}_\mu|1\rangle}{\langle 12\rangle\langle 13\rangle\langle 34\rangle\langle 1|P_{V_2}P_{V_1}|4\rangle} \\
&-\frac{\langle 14\rangle\langle 1|(2+3+4)\bar{\sigma}_\mu(1+P_{V_2})\bar{\sigma}_\nu|1\rangle}{\langle 12\rangle\langle 23\rangle\langle 34\rangle\langle 1|P_{V_2}P_{V_1}|4\rangle} \\
&+\frac{\langle 1|(2+3)\bar{\sigma}_\nu|1\rangle\langle 1|(P_{V_1}+P_{V_2})\bar{\sigma}_\mu|1\rangle}{\langle 12\rangle\langle 13\rangle\langle 23\rangle\langle 1|P_{V_2}P_{V_1}|4\rangle} \\
&+\frac{\langle 1|P_{V_2}\bar{\sigma}_\nu|1\rangle\langle 1|(2+3)(4+P_{V_1})P_{V_1}\bar{\sigma}_\mu(4+P_{V_1})(2+3)|1\rangle}{s_{4P_{V_1}}\langle 12\rangle\langle 23\rangle\langle 1|P_{V_2}P_{V_1}|4\rangle\langle 1|P_{V_2}(4+P_{V_1})|3\rangle} \\
&+\frac{\langle 1|P_{V_2}\bar{\sigma}_\nu|1\rangle[2|(1+P_{V_2})P_{V_1}\bar{\sigma}_\mu(1+P_{V_2})|2]}{s_{1P_{V_2}}s_{12P_{V_2}}\langle 34\rangle\langle 1|P_{V_2}(4+P_{V_1})|3\rangle}, \qquad (4.95)
\end{aligned}
$$

and

$$S^{Abelian}_{\mu\nu}(1^-_q, 2^+, 3^-, 4^+_{\bar{q}}) = -\frac{\langle 13\rangle^3\langle 3|1+2|4][4|\bar{\sigma}_\mu(1+P_{V_2})\bar{\sigma}_\nu(1+2+3)|4]}{s_{123}\langle 12\rangle\langle 23\rangle\langle 1|2+3|4]\langle 3|(1+2)P_{V_2}P_{V_1}|4]}$$
$$-\frac{\langle 13\rangle^3\langle 3|(4+P_{V_1})\bar{\sigma}_\nu P_{V_2}(4+P_{V_1})|3\rangle[4|P_{V_1}\sigma_\mu|4]}{s_{4P_{V_1}}\langle 12\rangle\langle 23\rangle\langle 1|P_{V_2}(4+P_{V_1})|3\rangle\langle 3|(1+2)P_{V_2}P_{V_1}|4]}$$
$$-\frac{\langle 13\rangle^2\langle 1|\sigma_\mu|4]\langle 3|1+2|4][2|\bar{\sigma}_\nu(1+2+3)|4]}{s_{123}\langle 12\rangle\langle 1|2+3|4]\langle 3|(1+2)P_{V_2}P_{V_1}|4]}$$
$$+\frac{\langle 13\rangle^2\langle 3|\sigma_\mu|4]\langle 3|(1+2)\bar{\sigma}_\nu(1+2+3)|4]}{s_{123}\langle 12\rangle\langle 23\rangle\langle 3|(1+2)P_{V_2}P_{V_1}|4]}$$
$$-\frac{[24]^3\langle 1|3+4|2]\langle 1|(2+3+4)\bar{\sigma}_\mu(1+P_{V_2})\bar{\sigma}_\nu|1\rangle}{s_{234}\langle 1|P_{V_2}P_{V_1}(3+4)|2]\langle 1|2+3|4][23][34]}$$
$$-\frac{[24]^3\langle 1|\sigma_\nu|2]\langle 1|(2+3+4)\bar{\sigma}_\mu|1\rangle}{\langle 1|P_{V_2}P_{V_1}(3+4)|2]\langle 1|2+3|4][23][34]}$$
$$-\frac{[24]^3\langle 1|P_{V_2}\bar{\sigma}_\nu|1\rangle[2|(1+P_{V_2})P_{V_1}\bar{\sigma}_\mu(1+P_{V_2})|2]}{s_{1P_{V_2}}\langle 1|P_{V_2}P_{V_1}(3+4)|2][23][34][2|(1+P_{V_2})P_{V_1}|4]}$$
$$-\frac{\langle 3|1+P_{V_2}|2]^3\langle 1|P_{V_2}\bar{\sigma}_\nu|1\rangle[4|P_{V_1}\sigma_\mu|4]}{s_{4P_{V_1}}s_{1P_{V_2}}s_{12P_{V_2}}\langle 1|P_{V_2}(4+P_{V_1})|3\rangle[2|(1+P_{V_2})P_{V_1}|4]}. \quad (4.96)$$

For the last amplitude we choose $i = 1$ and $j = 2$ which yields the following expression,

$$S^{Abelian}_{\mu\nu}(1^-_q, 2^-, 3^+, 4^+_{\bar{q}}) = -\frac{\langle 24\rangle[1|\bar{\sigma}_\nu(P_{V_1}+P_{V_2})(3+4)|2\rangle\langle 2|(3+4)\bar{\sigma}_\mu|2\rangle}{\langle 23\rangle\langle 34\rangle\langle 2|(3+4)P_{V_1}P_{V_2}|1]\langle 4|2+3|1]}$$
$$-\frac{\langle 24\rangle\langle 2|3+4|1]\langle 2|(3+4)\bar{\sigma}_\mu(1+P_{V_2})\bar{\sigma}_\nu(P_{V_1}+P_{V_2})(3+4)|2\rangle}{s_{234}\langle 23\rangle\langle 34\rangle\langle 2|(3+4)P_{V_1}P_{V_2}|1]\langle 4|2+3|1]}$$
$$+\frac{\langle 24\rangle\langle 2|(1+P_{V_2})\bar{\sigma}_\nu P_{V_2}(1+P_{V_2})|2\rangle\langle 2|(3+4)P_{V_1}\sigma_\mu(3+4)|2\rangle}{s_{1P_{V_2}}\langle 23\rangle\langle 34\rangle\langle 2|(1+P_{V_2})P_{V_1}|4\rangle\langle 2|(3+4)P_{V_1}P_{V_2}|1]}$$
$$-\frac{[13][3|1+2|4\rangle[3|(1+2)(P_{V_1}+P_{V_2})\bar{\sigma}_\mu(1+P_{V_2})\bar{\sigma}_\nu(1+2)|3]}{s_{123}\langle 4|2+3|1][12][23][3|(1+2)P_{V_2}P_{V_1}|4\rangle}$$
$$-\frac{[13][3|(1+2)P_{V_2}\bar{\sigma}_\nu(1+2)|3][3|(4+P_{V_1})P_{V_1}\bar{\sigma}_\mu(4+P_{V_1})|3]}{s_{4P_{V_1}}[12][23][3|(4+P_{V_1})P_{V_2}|1][3|(1+2)P_{V_2}P_{V_1}|4\rangle}$$
$$-\frac{\langle 2|1+P_{V_2}|3]\langle 2|(1+P_{V_2})\bar{\sigma}_\nu P_{V_2}(1+P_{V_2})|2\rangle[3|(4+P_{V_1})P_{V_1}\bar{\sigma}_\mu(4+P_{V_1})|3]}{s_{4P_{V_1}}s_{1P_{V_2}}s_{12P_{V_2}}\langle 2|(1+P_{V_2})P_{V_1}|4\rangle[1|P_{V_2}(4+P_{V_1})|3]}$$
$$-\frac{[3|(1+2)(P_{V_1}+P_{V_2})\bar{\sigma}_\mu|2\rangle[3|1+2|4\rangle[1|\bar{\sigma}_\nu(1+2)|3]}{s_{123}\langle 4|2+3|1][12][3|(1+2)P_{V_2}P_{V_1}|4\rangle}$$
$$+\frac{[3|\bar{\sigma}_\nu(1+2)|3][3|(1+2)(P_{V_1}+P_{V_2})\bar{\sigma}_\mu(1+2)|3]}{s_{123}[12][23][3|(1+2)P_{V_2}P_{V_1}|4\rangle}. \quad (4.97)$$

The procedure described here can straightforwardly be generalised to processes involving three or more vector bosons. In each case, there will be a mixture of terms that either involve a triple or quartic gauge boson vertex (non-Abelian) or a new multi-gauge boson current (Abelian). The non-Abelian contribution is straightforward and involves currents with coupling that couples currents involving fewer gauge bosons. These are in principle known. For each additional vector boson, the Abelian contribution must be recomputed. There will be a new primitive vertex which can be obtained directly from the single (colour-ordered) Feynman diagram.

This is illustrated in Fig. 4.12 for three vector bosons. The first diagram yields a new primitive vertex $S_{\mu_1\mu_2\mu_3}(1_q, 2_{\bar{q}})$ which forms the seed for recursively calculating the Abelian contribution to the amplitude. The other three (Non-Abelian) graphs can be straightforwardly obtained by reusing the single and double vector boson currents. The colour ordered triple current with n partons is thus,

$$
\begin{aligned}
S_{\mu_1\mu_2\mu_3}(1_q,\ldots,n_{\bar{q}}) = \; & S^{Abelian}_{\mu_1\mu_2\mu_3}(1_q,\ldots,n_{\bar{q}}) \\
& + T^{(3)}_{\mu_1\mu_2\rho}(P_{V_1}, P_{V_2}, -P_{12})\,\frac{1}{(P_{12}^2 - M_{P_{12}}^2)}\,S^{\rho\mu_3}(1_q,\ldots,n_{\bar{q}}) \\
& + T^{(3)}_{\mu_2\mu_3\rho}(P_{V_2}, P_{V_3}, -P_{23})\,\frac{1}{(P_{23}^2 - M_{P_{23}}^2)}\,S^{\mu_1\rho}(1_q,\ldots,n_{\bar{q}}) \\
& + T^{(4)}_{\mu_1\mu_2\mu_3\rho}(P_{V_1}, P_{V_2}, P_{V_3}, -P_{123})\,\frac{1}{(P_{123}^2 - M_{P_{123}}^2)}\,S^{\rho}(1_q,\ldots,n_{\bar{q}}).
\end{aligned}
\tag{4.98}
$$

The colour ordered quartic gauge boson vertex is given by,

$$
T^{(4)}_{\mu_1\mu_2\mu_3\mu_4}(p_1, p_2, p_3, p_4) = 2g_{\mu_1\mu_3}g_{\mu_2\mu_4} - g_{\mu_1\mu_3}g_{\mu_2\mu_4} - g_{\mu_1\mu_2}g_{\mu_3\mu_4}. \tag{4.99}
$$

4.6. Recursion Relations for Massive Particles with Spin on Internal Lines

So far we have been considering application of recursion relations where massive particles with spin were absent from the internal lines. In other words, we have been able to set up the recursive calculations of double vector boson currents in such a way that the

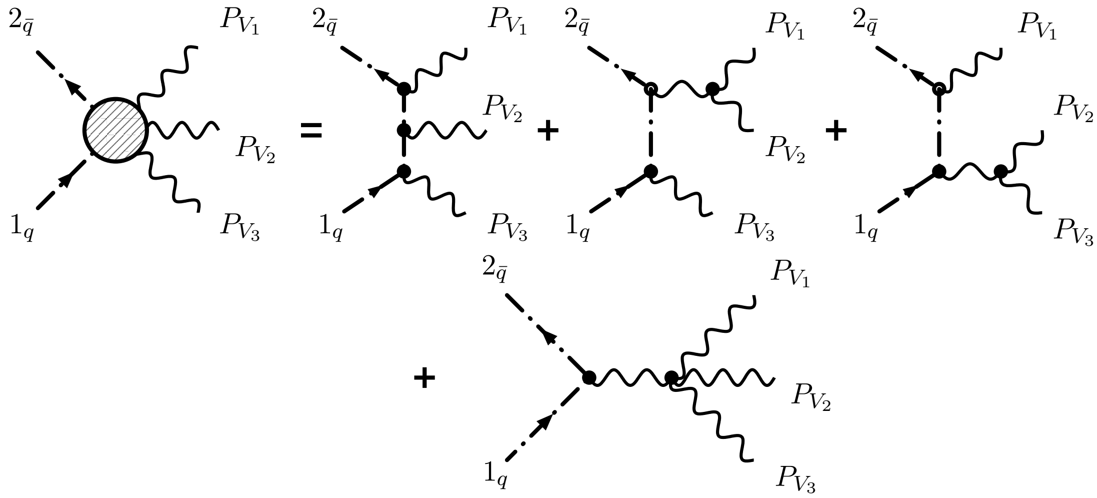

Figure 4.12: Contributions to the amplitude with three massive vector bosons and a quark anti-quark pair.

massive vector bosons were playing the role of 'external sources' in the left and in the right hand vertices, but were not propagating through the recursive diagram. We now would like to show how to use recursion relations also for propagating massive particles. In our earlier work [71] we have accomplished this for massive scalars, and now we want to generalise this approach to massive particles with spin.

The main difference between internal massive scalars of Ref. [71] and internal massive fermions or vector bosons is that the latter have more than one polarisation or spin state. In the standard recursion relation (4.31) all particles are assumed to be in a state with fixed helicity, and there is a summation over all these states. We want to avoid using helicity states for internal massive particles and instead to use a more natural basis of states

In this section we will describe a new way to implement the recursion relation in this case and will illustrate its use by calculating a simple amplitude of two heavy quarks scattering into two gluons.

The main point here is that the sum over helicities h of the internal particle in the standard recursion relation,

$$\mathcal{A}_n(p_1,\ldots,p_n) = \sum_{\text{partitions}}\sum_h \mathcal{A}_L(p_r,\ldots,\widehat{p}_i,\ldots,p_s,-\widehat{P}^h)\,\frac{1}{P^2-m_P^2}$$
$$\times\,\mathcal{A}_R(\widehat{P}^{-h},p_{s+1},\ldots,\widehat{p}_j,\ldots,p_{r-1})\ , \tag{4.100}$$

can be replaced by the sum over all of the spin states, rather than helicity quantum numbers which are not well suited for massive particles. So, we first replace the sum over helicities by the sum over appropriately defined spin states. For massive fermions this is the conventional spin sum:

$$\sum_{s=1,2} u_s(p)\bar{u}_s(p) = \not{p} + m_p \tag{4.101}$$
$$\sum_{s=1,2} v_s(p)\bar{v}_s(p) = \not{p} - m_p \tag{4.102}$$

The remaining spinors and polarisation vectors of the external massive particles can be left unfixed and simplified after squaring the amplitude with the spin sums in the conventional way.

Using this in the recursion relation in which a massive quark propagates between the two diagrams we have

$$\sum_s \mathcal{A}_L(p_{r;\bar{q}},\ldots,\widehat{p}_i,\ldots,p_s,-\widehat{P}_q^s)\frac{1}{P^2-m_P^2}\mathcal{A}_R(\widehat{P}_{\bar{q}}^{-s},p_{s+1},\ldots,\widehat{p}_j,\ldots,p_{r-1;q})$$
$$=\mathcal{A}_L(p_{r;\bar{q}},\ldots,\widehat{p}_i,\ldots,p_s,-\widehat{P}^*)\frac{\widehat{\not{P}}+m_P}{P^2-m_P^2}\mathcal{A}_R(\widehat{P}^*,p_{s+1},\ldots,\widehat{p}_j,\ldots,p_{r-1;q}) \tag{4.103}$$

where P^* indicates the external spinor wave-function has been stripped off this amplitude. In this way we can use the benefits of using the recursion relations to provide reasonably compact formulae for amplitudes with massive particles.

4.6.1. Example: Calculation of $\mathcal{A}_4(1_t,2,3,4_{\bar{t}})$

We now compute the four point amplitude of a top quark pair scattering to two gluons as an example of the method described above. We use on-shell recursion relations and mark

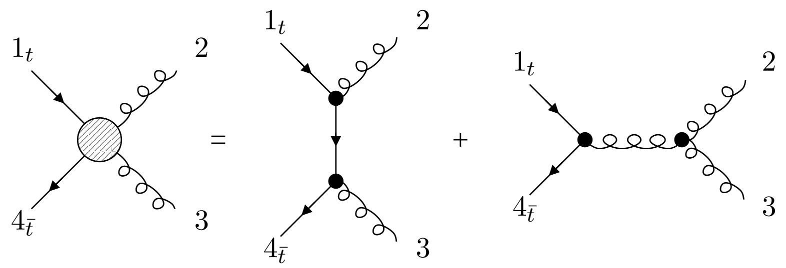

Figure 4.13: The two Feynman diagrams contributing to the amplitude $\mathcal{A}_4(1_t, 2, 3, 4_{\bar{t}})$.

two massless gluons. This leads to a single recursive diagram with a massive fermion propagator. We will show that the contribution of this single diagram precisely matches the two Feynman diagrams for this process shown in figure 4.13. With all particles outgoing the recursion relation result is,

$$\mathcal{A}(1_t, 2, 3, 4_{\bar{t}}) = \frac{1}{(P^2 - m_t^2)} \bar{u}(p_1) \not{\epsilon}(p_2, \xi_2) \left(\sum_s u_s(\widehat{P}) \bar{u}_s(\widehat{P}) \right) \not{\epsilon}(p_3, \xi_3) v(p_4). \tag{4.104}$$

Here $P = p_1 + p_2$ is the momentum on the internal line and ξ_2, ξ_3 are reference spinors necessary to specify gluon polarisation vectors $\epsilon^\pm$. We will use the Weyl representation of the Dirac γ-matrices and polarisation vectors,

$$\gamma_\mu = \begin{pmatrix} 0 & \sigma_\mu \\ \bar{\sigma}_\mu & 0 \end{pmatrix}, \quad \not{\epsilon}^+(p, \xi) = \frac{1}{\langle \xi p \rangle} \begin{pmatrix} 0 & |\xi\rangle[p| \\ |p]\langle \xi| & 0 \end{pmatrix}, \quad \not{\epsilon}^-(p, \xi) = \frac{1}{[\xi p]} \begin{pmatrix} 0 & |p\rangle[\xi| \\ |\xi]\langle p| & 0 \end{pmatrix}. \tag{4.105}$$

First we consider the case where the gluons have opposite helicity, $\mathcal{A}(1_t, 2^-, 3^+, 4_{\bar{t}})$. It is convenient to choose $\xi_2 = p_3$ and $\xi_3 = p_2$ so that,

$$\mathcal{A}(1_t, 2^-, 3^+, 4_{\bar{t}}) = \frac{1}{(P^2 - m_t^2) s_{23}} \bar{u}(p_1) \begin{pmatrix} 0 & |\widehat{2}\rangle[3| \\ |3]\langle \widehat{2}| & 0 \end{pmatrix} \begin{pmatrix} m_t & \widehat{\not{P}} \\ \widehat{\not{P}} & m_t \end{pmatrix} \begin{pmatrix} 0 & |2\rangle[\widehat{3}| \\ |\widehat{3}]\langle 2| & 0 \end{pmatrix} v(p_4). \tag{4.106}$$

We choose the marking prescription $i = 3$ and $j = 2$ and this ensures that the shifts on the polarisation vectors disappear. It can also be seen that the shift in $\widehat{P}$ is also killed by either of the two polarisation vectors and hence we can erase all the hats in equation (4.106). This is then exactly equivalent to the first diagram of figure 4.13. It can be easily shown using $\epsilon^-(2, 3) \cdot \epsilon^+(3, 2) = 0$ that, with this particular choice of reference momenta, that the remaining second Feynman diagram gives a vanishing contribution and so our recursion relation result is in agreement with the Feynman diagrams answer.

The amplitude with both gluons of negative helicity $\mathcal{A}(1_t, 2^+, 3^+, 4_{\bar{t}})$ is of a non-MHV type and it provides another interesting test of the recursion relation, which this time requires a little algebra. The recursion relation reads:

$$\mathcal{A}(1_t, 2^+, 3^+, 4_{\bar{t}}) = \frac{1}{(P^2 - m_t^2)\langle 23\rangle^2}\bar{u}(p_1)\begin{pmatrix} 0 & |3\rangle[\widehat{2}| \\ |\widehat{2}]\langle 3| & 0 \end{pmatrix}\begin{pmatrix} m_t & \widehat{\not{P}} \\ \widehat{\not{P}} & m_t \end{pmatrix}\begin{pmatrix} 0 & |2\rangle[\widehat{3}| \\ |\widehat{3}]\langle 2| & 0 \end{pmatrix} v(p_4). \tag{4.107}$$

Again, choosing $i = 3$ and $j = 2$ removes the shifts on the propagator and the polarisation vector of gluon p_3. However in this case all the shifts do not vanish as $|\widehat{2}] = |2] - z|3]$ hence we are left with the exact expression for the first Feynman diagram *plus* an extra term coming from the surviving shifts:

$$-\frac{z}{(P^2 - m_t^2)\langle 23\rangle^2}\bar{u}(p_1)\begin{pmatrix} 0 & |3\rangle[3| \\ |3]\langle 3| & 0 \end{pmatrix}\begin{pmatrix} m_t & \not{P} \\ \not{P} & m_t \end{pmatrix}\begin{pmatrix} 0 & |2\rangle[3| \\ |3]\langle 2| & 0 \end{pmatrix} v(p_4), \tag{4.108}$$

which simplifies to,

$$-\frac{1}{\langle 2|p_4|3]\langle 23\rangle^2}\bar{u}(p_1)\begin{pmatrix} 0 & |3\rangle\langle 2|p_4|3][3| \\ |3]\langle 3|p_4|3]\langle 2| & m_t|3]\langle 32\rangle[3| \end{pmatrix} v(p_4). \tag{4.109}$$

If the result from the recursion relation is to match the result of the Feynman calculation this expression should be equivalent to the second diagram in figure 4.13. Making use of the Dirac equation one can simplify the Feynman calculation to

$$-\frac{1}{\langle 23\rangle^2}\bar{u}(p_1)\begin{pmatrix} 0 & p_3 \\ p_3 & 0 \end{pmatrix} v(p_4). \tag{4.110}$$

It may not be immediately obvious that the expressions (4.109) and (4.110) are equivalent, but they are. Firstly we note that the four component spinor can be written in terms of two component spinors,

$$u(p) = \begin{pmatrix} |u_p\rangle \\ |u_p] \end{pmatrix}. \tag{4.111}$$

This allows us to expand out (4.109) and immediately identify that the top row is in the correct form. The bottom row can be simplified by using $m_t|v_4] = \not{p}_4|v_4\rangle$ and by decomposing $|v_4\rangle = \alpha|3\rangle + \beta|2\rangle$ we can re-form the bottom row into the correct form and reconstruct (4.110).

This shows that recursion relations can be used to successfully calculate amplitudes with massive particles with spin on internal lines, as expected.

4.7. Conclusions

In this chapter we have generalised the on-shell recursion relations introduced in section 2.4.2 to accommodate massive particles which are allowed to propagate through the on-shell diagrams. We have shown how to apply these relations to amplitudes involving massive scalars and vector bosons as well as a brief demonstration of how to apply the relations to massive fermions.

In all cases it was possible to calculate the amplitudes by selecting massless particles to be shifted. Although it is in theory possible to choose a maximum of one massive particle to be shifted it turns out that this often results in non-zero terms at large z which invalidate the recursion relation. The method has also been applied to calculate D-dimensional amplitudes with fermions and scalars considered as D-dimensional objects [73]. Techniques combining off-shell and on-shell methods for dealing with massive fermions and scalars have also been developed and provide extremely compact forms of the amplitudes in both cases [126, 127].

Using the formulae presented in section 4.2 it has been possible to find full 1-loop amplitudes with up to 5 gluons by using D-dimensional generalised unitarity techniques [82].

5. Higgs plus multi-gluon amplitudes at 1-loop

In this chapter we will use a combination of the MHV rules and the standard unitarity method to derive the cut-constructible part of Higgs plus multi-gluon amplitudes [129]. We will use the same split into self-dual and anti-self-dual components as described in chapter 3 and we will make use of the compact expressions for n-point amplitudes derived in reference [53]. The rational parts of the amplitudes must be fixed by other methods and it has recently been shown that on-shell recursive methods apply well to the finite one-loop amplitudes which vanish at tree level [130]. There have also been developments in computing one-loop amplitudes using semi-numerical methods [131–134] which have been applied to amplitudes for Higgs with up to 4 partons [135].

5.1. Colour ordering

The colour orderings for one-loop amplitudes with a Higgs boson and many gluons are the same as for pure gluonic amplitudes discussed in section 2.3, specifically equation (2.59). In this chapter we will compute the leading colour contribution which is defined by [129, 130],

$$A_n^{(1)}(\phi,\{k_i,\lambda_i,a_i\}) = iCg^n \sum_{c=1}^{[n/2]+1} \sum_{\sigma\in S_n/S_{n;c}} G_{n;c}(\sigma)\mathcal{A}_n^{(1)}(\phi,\sigma(1^{\lambda_1},\dots,n^{\lambda_n})) \tag{5.1}$$

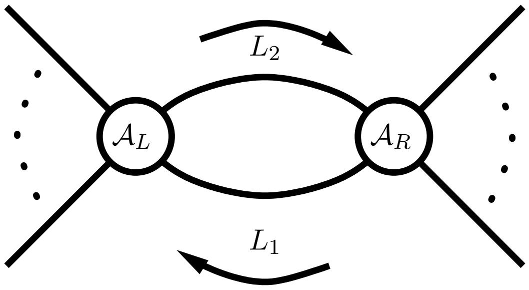

Figure 5.1: A generic one loop MHV diagram or unitarity cut.

where

$$G_{n;1}(1) = N\,\mathrm{tr}(T^{a_1} \cdots T^{a_n}) \tag{5.2}$$

$$G_{n;c}(1) = \mathrm{tr}(T^{a_1} \cdots T^{a_{c-1}})\,\mathrm{tr}(T^{a_c} \cdots T^{a_n}) \ , \ c > 2. \tag{5.3}$$

The sub-leading terms can be computed by summing over various permutations of the leading colour amplitudes [17]. We will split the calculation into two parts, evaluating the cut-constructible and non-cut-constructible components separately:

$$\mathcal{A}_n^{(1)} = \mathcal{A}_n^{(1),CC} + \mathcal{A}_n^{(1),NCC}, \tag{5.4}$$

where we have dropped the leading colour subscript, $\mathcal{A}_{n;1}^{(1)} \equiv \mathcal{A}_n^{(1)}$.

5.2. MHV diagrams and unitarity cuts

In a landmark paper, Brandhuber, Spence and Travaglini [90] showed that it is possible to calculate one-loop MHV amplitudes in $\mathcal{N} = 4$ using MHV rules. The calculation has many similarities to the unitarity based approach of Refs. [17, 18], the main difference being that the MHV rules reproduce the cut-constructible parts of the amplitude directly, without having to worry about double counting. This is the method that we wish to employ here.

The four-dimensional cut-constructible part of one-loop amplitudes can be constructed by joining two on-shell vertices by two scalar propagators, both of which need to be continued off-shell. A generic diagram is shown in figure 5.1 and the full amplitude will be a sum over all possible permutations and helicity configurations. One must integrate over the loop momenta in much the same way as one would evaluate a unitarity cut, however in this case the loop momenta are continued off-shell as for the tree level MHV rules and can be written [90],

$$L_i = l_i + z_i\eta. \tag{5.5}$$

A generic diagram can be written:

$$\mathcal{D} = \frac{1}{(2\pi)^4}\int \frac{d^4L_1}{L_1^2}\frac{d^4L_2}{L_2^2}\delta^{(4)}(L_1 - L_2 - P)\mathcal{A}_L(l_1, -P, -l_2)\mathcal{A}_R(l_2, P, -l_1) \tag{5.6}$$

where $\mathcal{A}_{L(R)}$ are the amplitudes for the left(right) vertices and P is the sum of momenta incoming to the right hand amplitude. The important step is the evaluation of this expression is to re-write the integration measure as an integral over the on-shell degrees of freedom and a separate integral over the complex variable z [90]:

$$\begin{aligned}\frac{d^4L_1}{L_1^2}\frac{d^4L_2}{L_2^2} &= (4i)^2\frac{dz_1}{z_1}\frac{dz_2}{z_2}d^4l_1d^4l_2\delta^{(+)}(l_1^2)\delta^{(+)}(l_2^2)\\ &= (4i)^2\frac{2dzdz'}{(z-z')(z+z')}d^4l_1d^4l_2\delta^{(+)}(l_1^2)\delta^{(+)}(l_2^2),\end{aligned} \tag{5.7}$$

where $z = z_1 - z_2$ and $z' = z_1 + z_2$. The integrand can only depend on z, z' through the momentum conserving delta function,

$$\delta^{(4)}(L_1 - L_2 - P) = \delta^{(4)}(l_1 - l_2 - P + z\eta) = \delta^{(4)}(l_1 - l_2 - \widehat{P}), \tag{5.8}$$

where $\widehat{P} = P - z\eta$. This means that the integral over z' can be performed so that,

$$\begin{aligned}\mathcal{D} &= \frac{(4i)^2 2\pi i}{(2\pi)^4}\int\frac{dz}{z}\int d^4l_1d^4l_2\delta^{(+)}(l_1^2)\delta^{(+)}(l_2^2)\delta^{(4)}(l_1 - l_2 - \widehat{P})\mathcal{A}_L(l_1, -P, -l_2)\mathcal{A}_R(l_2, P, -l_1)\\ &= (4i)^2 2\pi i\int\frac{dz}{z}\int d\mathrm{LIPS}^{(4)}(-l_1, l_2, \widehat{P})\mathcal{A}_L(l_1, -P, -l_2)\mathcal{A}_R(l_2, P, -l_1),\end{aligned} \tag{5.9}$$

where,

$$d\mathrm{LIPS}^{(4)}(-l_1, l_2, \widehat{P}) = \frac{1}{(2\pi)^4}d^4l_1d^4l_2\delta^{(+)}(l_1^2)\delta^{(+)}(l_2^2)\delta^{(4)}(l_1 - l_2 - \widehat{P}) \tag{5.10}$$

The phase space integral is regulated using dimensional regularisation. It is then necessary to reduce the tensor integral arising from the product of tree amplitudes down to scalar integrals either by using spinor algebra or standard Passarino-Veltman reduction. The remaining scalar integrals have been evaluated previously by Van-Neerven [136].

5.3. Higgs to multi-gluon amplitudes

In order to calculate the cut-constructible parts of the Higgs amplitudes we are able to use the all multiplicity tree level results calculated using the MHV rules as presented in chapter 3. The decomposition of the HGG vertex into the self-dual and the anti-self-dual terms eq. (3.11), guarantees that the whole class of (colour ordered) tree-level helicity amplitudes must vanish [53];

$$A_n^{(0)}(\phi, g_1^\pm, g_2^+, g_3^+, \ldots, g_n^+) = 0\,, \tag{5.11}$$

$$A_n^{(0)}(\phi^\dagger, g_1^\pm, g_2^-, g_3^-, \ldots, g_n^-) = 0\,, \tag{5.12}$$

for all n.

The tree amplitudes, with precisely two negative helicities are the first non-vanishing ϕ amplitudes. These amplitudes are the ϕ-MHV amplitudes. General factorisation properties now imply that they have to be extremely simple [53], and when legs q and p have negative helicity, are given by

$$\begin{aligned} &A_n^{(0)}(\phi, g_1^+, g_2^+, \ldots, g_p^-, \ldots, g_q^-, \ldots, g_n^+) \\ &= \frac{\langle p\, q\rangle^4}{\langle 1\, 2\rangle\, \langle 2\, 3\rangle \cdots \langle n-1,\, n\rangle\, \langle n\, 1\rangle}\,. \end{aligned} \tag{5.13}$$

In fact, the expressions eq. (5.13) for ϕ-MHV n-gluon amplitudes have the same form as the MHV n-gluon amplitudes in pure QCD. The only difference is that the total momentum carried by gluons, $p_1 + p_2 + \ldots + p_n = -p_\phi$ is the momentum carried by the ϕ-field and is non-zero. The $\overline{\mathrm{MHV}}$ amplitudes are also present in the calculations so are listed here for completeness:

$$\begin{aligned} &A_n^{(0)}(g_1^-, g_2^-, \ldots, g_p^+, \ldots, g_q^+, \ldots, g_n^-) \\ &= (-1)^n \frac{[p\, q]^4}{[1\, 2]\, [2\, 3] \cdots [n-1,\, n]\, [n\, 1]}\,. \end{aligned} \tag{5.14}$$

The tree amplitude with all negative helicity gluons, the ϕ-all-minus amplitude, also

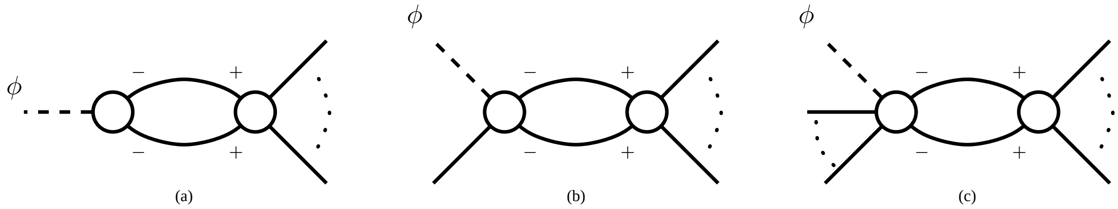

Figure 5.2: The MHV loop diagrams contributing to the $\phi \to g_1^- g_2^- \ldots g_n^-$ amplitude.

has a simple structure,

$$
\begin{aligned}
& A_n^{(0)}(\phi; 1^-, \ldots, n^-) \\
& = (-1)^n \frac{m_H^4}{[1\,2]\,[2\,3] \cdots [n-1,\, n]\,[n\,1]} \,.
\end{aligned}
\tag{5.15}
$$

Amplitudes with fewer (but more than two) negative helicities have been computed with Feynman diagrams (up to 4 partons) in Ref. [114] and using MHV rules and recursion relations in Refs. [53, 54].

5.3.1. $\phi \to g_1^- g_2^- \ldots g_n^-$

The amplitude for Higgs to any number of negative helicity gluons is the simplest since it only receives a cut constructible contribution from the ϕ component of the Higgs field. There are three types of diagram contributing to the cut-constructible part as shown in figure 5.2. For each diagram we find that the allowed helicity assignments around the loop only permits gluons to circulate so the cut constructible part will have no fermionic component.

Let us consider diagram 5.2(a) to begin with. We can take the momenta to be labelled from 1 to n around the right hand amplitude so that we consider a $s_{1,n}$ cut. Other diagrams which take the same form are accessible by permuting the arguments of the

$s_{1,n}$ channel. The product of the two vertices can be written:

$$\begin{aligned}\mathcal{A}_L\mathcal{A}_R &= -\frac{m_H^4}{[l_1l_2]^2}\frac{(-1)^{n+2}[l_1l_2]^3}{[l_21][12]\cdots[n-1n][nl_1]}\\ &= \mathcal{A}^{(0)}(\phi;1^-,\ldots,n^-)\frac{[l_1l_2][n1]}{[l_21][nl_1]}.\end{aligned} \tag{5.16}$$

By applying a Schouten identity to the numerator and using momentum conservation in the form $l_1 = l_2 + \widehat{P}_{1,n}$ we find,

$$\mathcal{A}_L\mathcal{A}_R = \mathcal{A}^{(0)}(\phi;1^-,\ldots,n^-)\left(-\frac{N(\widehat{P}_{1,n},1,n)}{(l_1-n)^2(l_2+1)^2} - \frac{\widehat{P}_{1,n}\cdot n}{(l_1-n)^2} + \frac{\widehat{P}_{1,n}\cdot 1}{(l_2+1)^2}\right), \tag{5.17}$$

where $N(P,p_1,p_2) = P^2(p_1\cdot p_2) - 2(P\cdot p_1)(P\cdot p_2)$. This is now written in terms of scalar integrals so we can directly use the results of van-Neerven[136] to perform the phase space integration:

$$\begin{aligned}&\int d^D\text{LIPS}(-l_1,l_2,P)\frac{N(P,p1,p2)}{(l_1+p_1)^2(l_2+p_2)^2} =\\ &\qquad \frac{c_\Gamma}{(4\pi)^2\epsilon^2}2i\sin(\pi\epsilon)\mu^{2\epsilon}|P^2|^{-\epsilon}\,{}_2F_1\left(1,-\epsilon;1-\epsilon;\frac{p_1\cdot p_2P^2}{N(P,p_1,p_2)}\right)\end{aligned} \tag{5.18}$$

$$\begin{aligned}&\int d^D\text{LIPS}(-l_1,l_2,P)\frac{2(P\cdot p_1)}{(l_1+p_1)^2} =\\ &\qquad \frac{c_\Gamma}{(4\pi)^2\epsilon^2}2i\sin(\pi\epsilon)\mu^{2\epsilon}|P^2|^{-\epsilon}\end{aligned} \tag{5.19}$$

$$\int d^D\text{LIPS}(-l_1,l_2,P) = -\frac{c_\Gamma}{(4\pi)^2\epsilon(1-2\epsilon)}2i\sin(\pi\epsilon)\mu^{2\epsilon}|P^2|^{-\epsilon}. \tag{5.20}$$

where the factor c_Γ is given by,

$$c_\Gamma = (4\pi)^{\epsilon-2}\frac{\Gamma(1+\epsilon)\Gamma^2(1-\epsilon)}{\Gamma(1-2\epsilon)}. \tag{5.21}$$

The final integration is over the z variable. The only dependence on z appears through the quantity $\widehat{P}_{1,n}$ so it is convenient to make a change of variables,

$$\frac{dz}{z} = \frac{d(\widehat{P})^2}{P^2-\widehat{P}^2}. \tag{5.22}$$

The final integration is therefore just a dispersion integral that will re-construct the parts of the cut-constructible amplitude proportional to $(s_{1,n})^{-\epsilon}$,

$$\int \frac{d(\widehat{P})^2}{P^2-\widehat{P}^2}2i\sin(\pi\epsilon)|\widehat{P}^2|^{-\epsilon} = 2\pi i(-P^2)^{\epsilon}. \tag{5.23}$$

The final result for this diagram then reads:

$$\mathcal{D}_a(1,n) = \frac{c_\Gamma}{\epsilon^2}\mathcal{A}^{(0)}\left(\frac{\mu^2}{-s_{1,n}}\right)^{\epsilon}\left({}_2F_1\left(1,-\epsilon;1-\epsilon;\frac{p_1\cdot p_n s_{1,n}}{N(P_{1,n},p_1,p_n)}\right)+1\right). \tag{5.24}$$

Diagrams 5.2(b) and 5.2(c) are calculated in exactly the same way. By applying Schouten identities and momentum conservation we can reduce both of these to scalar box and triangle integrals. The results are:

$$\begin{aligned}
\mathcal{D}_b(2,n) = \frac{c_\Gamma}{\epsilon^2}\mathcal{A}^{(0)}\left(\frac{\mu^2}{-s_{2,n}}\right)^{\epsilon}\Bigg(&{}_2F_1\left(1,-\epsilon;1-\epsilon;\frac{p_2\cdot p_n s_{2,n}}{N(P_{2,n},p_2,p_n)}\right)\\
&+{}_2F_1\left(1,-\epsilon;1-\epsilon;\frac{p_1\cdot p_n s_{2,n}}{N(P_{2,n},p_1,p_n)}\right)\\
&-{}_2F_1\left(1,-\epsilon;1-\epsilon;\frac{p_1\cdot p_2 s_{2,n}}{N(P_{2,n},p_1,p_2)}\right)+1\Bigg) && (5.25)\\
\mathcal{D}_c(i,n) = \frac{c_\Gamma}{\epsilon^2}\mathcal{A}^{(0)}\left(\frac{\mu^2}{-s_{i,n}}\right)^{\epsilon}\Bigg(&{}_2F_1\left(1,-\epsilon;1-\epsilon;\frac{p_i\cdot p_n s_{i,n}}{N(P_{i,n},p_i,p_n)}\right)\\
&+{}_2F_1\left(1,-\epsilon;1-\epsilon;\frac{p_{i+1}\cdot p_1 s_{i,n}}{N(P_{i,n},p_{i+1},p_1)}\right)\\
&-{}_2F_1\left(1,-\epsilon;1-\epsilon;\frac{p_i\cdot p_1 s_{i,n}}{N(P_{i,n},p_i,p_1)}\right)\\
&-{}_2F_1\left(1,-\epsilon;1-\epsilon;\frac{p_{i+1}\cdot p_n s_{i,n}}{N(P_{i,n},p_{i+1},p_n)}\right)\Bigg). && (5.26)
\end{aligned}$$

These results do not hold for the two particle channels, i.e. s_{12}, where we must be careful to eliminate terms proportional to $N(\widehat{P}_{12},1,2)$ etc. before integration since such terms will vanish for the particular choices of $\eta = 1,2$. These two particle channels will make up contributions from the single mass boxes.

To complete the calculation of this part of the amplitude we must sum over the permutations of the various diagrams and identify the full integrals from the individual cuts. The scalar integrals are given by:

$$
\begin{aligned}
F_4^{0m}(s,t) &= \frac{2c_\Gamma}{\epsilon^2}\Bigg[\left(\frac{\mu^2}{-s}\right)^\epsilon {}_2F_1\left(1,-\epsilon;1-\epsilon;-\frac{u}{t}\right) \\
&\quad + \left(\frac{\mu^2}{-t}\right)^\epsilon {}_2F_1\left(1,-\epsilon;1-\epsilon;-\frac{u}{s}\right)\Bigg] && (5.27)\\
F_4^{1m}(P^2;s,t) &= \frac{2c_\Gamma}{\epsilon^2}\Bigg[\left(\frac{\mu^2}{-s}\right)^\epsilon {}_2F_1\left(1,-\epsilon;1-\epsilon;-\frac{u}{t}\right) \\
&\quad + \left(\frac{\mu^2}{-t}\right)^\epsilon {}_2F_1\left(1,-\epsilon;1-\epsilon;-\frac{u}{s}\right) \\
&\quad - \left(\frac{\mu^2}{-P^2}\right)^\epsilon {}_2F_1\left(1,-\epsilon;1-\epsilon;-\frac{uP^2}{st}\right)\Bigg] && (5.28)\\
F_4^{2me}(P^2,Q^2;s,t) &= \frac{2c_\Gamma}{\epsilon^2}\Bigg[\left(\frac{\mu^2}{-s}\right)^\epsilon {}_2F_1\left(1,-\epsilon;1-\epsilon;\frac{us}{P^2Q^2-st}\right) \\
&\quad + \left(\frac{\mu^2}{-t}\right)^\epsilon {}_2F_1\left(1,-\epsilon;1-\epsilon;\frac{ut}{P^2Q^2-st}\right) \\
&\quad - \left(\frac{\mu^2}{-P^2}\right)^\epsilon {}_2F_1\left(1,-\epsilon;1-\epsilon;\frac{uP^2}{P^2Q^2-st}\right) \\
&\quad - \left(\frac{\mu^2}{-Q^2}\right)^\epsilon {}_2F_1\left(1,-\epsilon;1-\epsilon;\frac{uQ^2}{P^2Q^2-st}\right)\Bigg] && (5.29)\\
F_3^{1m}(s) &= \frac{c_\Gamma}{\epsilon^2}\left(\frac{\mu^2}{-s}\right)^\epsilon && (5.30)\\
\mathrm{Bub}(s) &= \frac{c_\Gamma}{\epsilon(1-2\epsilon)}\left(\frac{\mu^2}{-s}\right)^\epsilon && (5.31)
\end{aligned}
$$

and the unrenormalised, cut-constructible contribution for the all-minus configuration can be written:

$$
\begin{aligned}
&\mathcal{A}_n^{(1),CC}(\phi,1^-,\ldots,n^-) = \mathcal{A}_n^{(0)}(\phi,1^-,\ldots,n^-)\Bigg[\sum_{i=1}^{n}\left(F_3^{1m}(s_{i,n+i-2}) - F_3^{1m}(s_{i,n+i-1})\right) \\
&-\frac{1}{2}\sum_{i=1}^{n}\sum_{j=i+2}^{n+i-2} F_4^{2me}(s_{i,j},s_{i+1,j-1};s_{i,j+1},s_{i+1,j}) - \frac{1}{2}\sum_{i=1}^{n} F_4^{1m}(s_{i,i+2};s_{i,i+1},s_{i+1,i+2})\Bigg]
\end{aligned}
\tag{5.32}
$$

Since the cut-constructible part of the corresponding $\phi^\dagger$ amplitude is trivially zero,

$$
\mathcal{A}_n^{(1),CC}(\phi^\dagger,1^-,2^-,\ldots,n^-) = 0, \tag{5.33}
$$

the full cut-constructible part of the full Higgs amplitude is also given by equation (5.32).

For the specific cases of $n = 3, 4$ the amplitudes simplify considerably;

$$\mathcal{A}_3^{(1),CC}(\phi, 1^-, 2^-, 3^-) = \mathcal{A}_n^{(0)}(\phi, 1^-, 2^-, 3^-)\Bigg[F_3^{1m}(s_{12}) + F_3^{1m}(s_{23}) + F_3^{1m}(s_{31})$$
$$- 3F_3^{1m}(s_{123}) - \frac{1}{2}F_4^{1m}(s_{123}; s_{12}, s_{23}) - \frac{1}{2}F_4^{1m}(s_{123}; s_{13}, s_{23}) - \frac{1}{2}F_4^{1m}(s_{123}; s_{12}, s_{13})\Bigg] \tag{5.34}$$

and

$$\mathcal{A}_4^{(1),CC}(\phi, 1^-, 2^-, 3^-, 4^-) = \mathcal{A}_n^{(0)}(\phi, 1^-, 2^-, 3^-, 4^-)\Bigg[F_3^{1m}(s_{123}) + F_3^{1m}(s_{234}) + F_3^{1m}(s_{341})$$
$$+ F_3^{1m}(s_{412}) - 4F_3^{1m}(s_{1234})$$
$$- \frac{1}{2}F_4^{1m}(s_{123}; s_{12}, s_{23}) - \frac{1}{2}F_4^{1m}(s_{234}; s_{23}, s_{34}) - \frac{1}{2}F_4^{1m}(s_{341}; s_{34}, s_{41})$$
$$- \frac{1}{2}F_4^{1m}(s_{412}; s_{41}, s_{12}) - \frac{1}{2}F_4^{2me}(s_{1234}, s_{12}; s_{412}, s_{123}) - \frac{1}{2}F_4^{2me}(s_{1234}, s_{23}; s_{123}, s_{234})$$
$$- \frac{1}{2}F_4^{2me}(s_{1234}, s_{34}; s_{234}, s_{341}) - \frac{1}{2}F_4^{2me}(s_{1234}, s_{41}; s_{341}, s_{412})\Bigg]. \tag{5.35}$$

5.3.2. $\phi \to g_1^- g_2^- g_3^+ \ldots g_n^+$

For this amplitude the contributing MHV diagrams are slightly more complicated since there are helicity configurations which allow fermions to circulate around the loop. There are 7 independent diagrams required for the full cut-constructible component as shown in figure 5.3. The last four diagrams have both fermionic and gluonic contributions. Note also that all fermion loops always appear in association with a factor of N_F, the number of fermion species, and a factor of -1 as associated with all fermion loops.

For these more complicated configurations it is more suitable to apply a more general reduction technique for each diagram. One can use a 4-dimensional Passarino-Veltman reduction since the cut is always in 4-dimensions. Schouten identities reduce all of the gluon-only channels, diagrams 5.3(a),(b) and (c), to scalar integrals as before. However when considering the channels with alternating helicity configurations around the loop we find that even after the Schouten identities have been applied, we are still left with

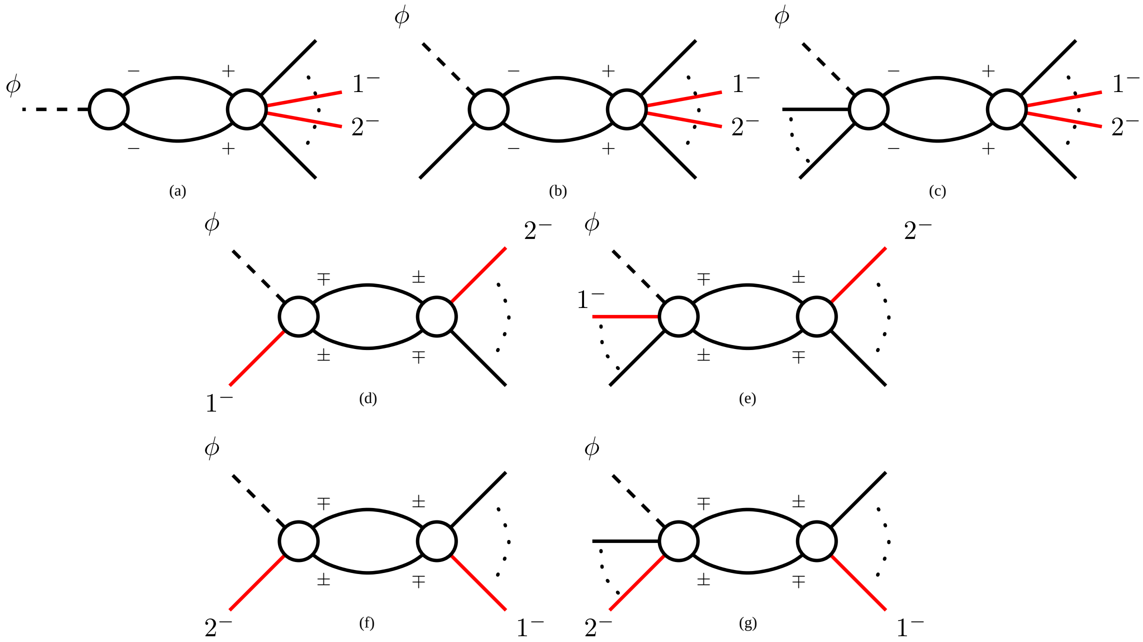

Figure 5.3: The MHV loop diagrams contributing to the $\phi \to g_1^- g_2^- g_3^+ \dots g_n^+$ amplitude.

tensor integrals which must be further reduced to scalar integrals by expanding in terms of all possible tensor structures. This feature has also been seen in the context of finding the cut-constructible part of pure QCD amplitudes and was also addressed applying Passarino-Veltman reduction [92].

Diagrams 5.3(a),(b) and (c) reduce in the same way to the corresponding diagrams for the all-minus configuration, indeed with the exception of the tree factor the calculation is exactly the same. For diagram 5.3(d), the $s_{2,n}$ channel, the presence of tensor integrals and fermion loops results in new structures of order $1/\epsilon$. The result for this diagram is:

$$\begin{aligned}\mathcal{D}_d(2,n) = \frac{c_\Gamma}{\epsilon^2}\mathcal{A}^{(0)}\left(\frac{\mu^2}{-s_{2,n}}\right)^\epsilon \Bigg[& 1 + {}_2F_1\left(1,-\epsilon;1-\epsilon;\frac{p_2\cdot p_n s_{2,n}}{N(P_{2,n},p_2,p_n)}\right)\\ & + {}_2F_1\left(1,-\epsilon;1-\epsilon;\frac{p_1\cdot p_n s_{2,n}}{N(P_{2,n},p_1,p_n)}\right)\\ & - {}_2F_1\left(1,-\epsilon;1-\epsilon;\frac{p_1\cdot p_2 s_{2,n}}{N(P_{2,n},p_1,p_2)}\right)\\ & - \left(1-\frac{N_F}{N}\right)\left(\frac{2\,\mathrm{tr}_-(2P_{3,n-1}n1)^3}{3s_{12}^3(2P\cdot n)^3} + \frac{\mathrm{tr}_-(P_{3,n-1}n1)^2}{s_{12}^2(2P\cdot n)^2}\right)\frac{\epsilon}{1-2\epsilon}\\ & - 4\left(1-\frac{N_F}{4N}\right)\left(\frac{\mathrm{tr}_-(P_{3,n-1}n1)}{s_{12}(2P\cdot n)}\right)\frac{\epsilon}{1-2\epsilon}\Bigg]. \end{aligned} \tag{5.36}$$

This is better illustrated in figure 5.4 which shows the cuts of each integral function that appear. Figure 5.5 shows the decomposition of the $s_{2,i}$ channels (figure 5.3(e)) which follows exactly the same steps as the previous case. Diagrams 5.3(f) and 5.3(g) are analogous to diagrams 5.3(d) and 5.3(e) and can be found be permuting the arguments: $1,2,\ldots,n \to 2,1,n,\ldots,3$.

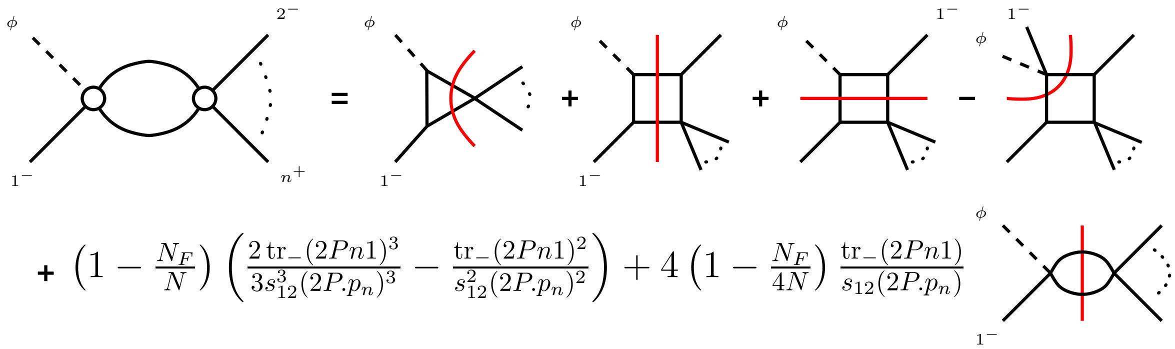

Figure 5.4: Decomposition of the MHV diagram of fig. 5.3(d) contributing to the $P_{2,n}$ channel

When summing over all the possible diagrams we find that the bubble integrals always appear in the combination,

$$\mathrm{Bub}(s) - \mathrm{Bub}(t) = \mathcal{O}(\epsilon^0), \tag{5.37}$$

and hence the pole structure is formed by exactly the same combination of box and triangle integrals as in the all-minus case but now is proportional to a different tree

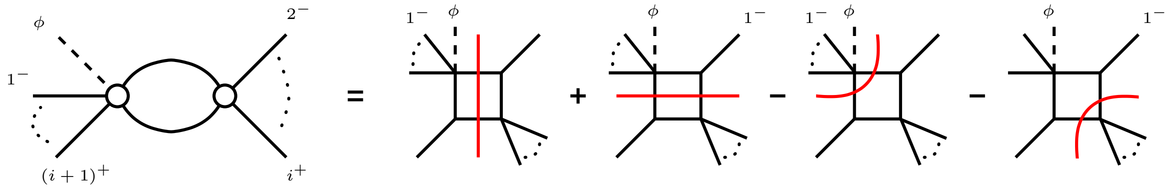

$$- \left[\left(1 - \frac{N_F}{N}\right) \left(\frac{2\,\mathrm{tr}_-(2P(i+1)1)^3}{3s_{12}^3(2P.p_{i+1})^3} - \frac{\mathrm{tr}_-(2P(i+1)1)^2}{s_{12}^2(2P.p_{i+1})^2} \right) + 4\left(1 - \frac{N_F}{4N}\right) \frac{\mathrm{tr}_-(2P(i+1)1)}{s_{12}(2P.p_{i+1})} \right.$$

$$\left. - \left(1 - \frac{N_F}{N}\right) \left(\frac{2\,\mathrm{tr}_-(2Pi1)^3}{3s_{12}^3(2P.p_i)^3} - \frac{\mathrm{tr}_-(2Pi1)^2}{s_{12}^2(2P.p_i)^2} \right) + 4\left(1 - \frac{N_F}{4N}\right) \frac{\mathrm{tr}_-(2Pi1)}{s_{12}(2P.p_i)} \right]$$

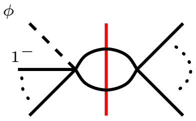

Figure 5.5: Decomposition of the MHV diagram of fig. 5.3(e) contributing to the $P_{2,i}$ channel

amplitude. The combination of bubble integrals can be written in terms of a basis of pure logarithms,

$$L_k(s,t) = \frac{\log(s/t)}{(s-t)^k}. \tag{5.38}$$

These logarithm functions are not proportional to the tree amplitude, but are multiplied by new spinor structures written in terms of traces (defined in section 2.2). The full, unrenormalised result for this helicity configuration is thus:

$$\begin{aligned}
&\mathcal{A}_n^{(1),CC}(\phi,1^-,2^-,3^+\ldots,n^+) = \mathcal{A}_n^{(0)}(\phi,1^-,2^-,3^+,\ldots,n^+)\Bigg[\sum_{i=1}^{n}\left(\mathrm{F}_3^{1\mathrm{m}}(s_{i,n+i-2}) - \mathrm{F}_3^{1\mathrm{m}}(s_{i,n+i-1})\right) \\
&- \frac{1}{2}\sum_{i=1}^{n}\sum_{j=i+2}^{n+i-2}\mathrm{F}_4^{2\mathrm{me}}(s_{i,j},s_{i+1,j-1};s_{i,j+1},s_{i+1,j}) - \frac{1}{2}\sum_{i=1}^{n}\mathrm{F}_4^{1\mathrm{m}}(si,i+2;s_{i,i+1},s_{i+1,i+2}) \\
&+ \sum_{i=4}^{n}\Bigg(\frac{2}{3}\left(1-\frac{N_F}{N}\right)\frac{\mathrm{tr}_-(1P_{i,n}(i-1)2)^3}{s_{12}^3}L_3(s_{i-1,1},s_{i,1}) - \left(1-\frac{N_F}{N}\right)\frac{\mathrm{tr}_-(1P_{i,n}(i-1)2)^2}{s_{12}^2}L_2(s_{i-1,1},s_{i,1}) \\
&\quad + 4\left(1-\frac{N_F}{4N}\right)\frac{\mathrm{tr}_-(1P_{i,n}(i-1)2)}{s_{12}}L_1(s_{i-1,1},s_{i,1}) + \frac{2}{3}\left(1-\frac{N_F}{N}\right)\frac{\mathrm{tr}_-(2P_{3,i-1}i1)^3}{s_{12}^3}L_3(s_{2,i},s_{2,i-1}) \\
&\quad - \left(1-\frac{N_F}{N}\right)\frac{\mathrm{tr}_-(2P_{3,i-1}i1)^2}{s_{12}^2}L_2(s_{2,i},s_{2,i-1}) + 4\left(1-\frac{N_F}{4N}\right)\frac{\mathrm{tr}_-(2P_{3,i-1}i1)}{s_{12}}L_1(s_{2,i},s_{2,i-1})\Bigg)\Bigg].
\end{aligned} \tag{5.39}$$

The functions $L_k(s,t)$ contain unphysical singularities as $s \to t$ so it is useful to redefine the cut-containing contribution in terms of a new basis which have good behaviour in the various limits. This is done at the cost of adding some rational terms,

$$L_1(s,t) = \widehat{L}_1(s,t) \tag{5.40}$$

$$L_2(s,t) = \frac{\widehat{L}_2(s,t)}{t} + \frac{1}{t(s-t)} \tag{5.41}$$

$$L_3(s,t) = \frac{\widehat{L}_3(s,t)}{t^2} + \frac{1}{t(s-t)^2} - \frac{1}{2t^2(s-t)}. \tag{5.42}$$

The new $\widehat{L}_k$ functions are now free from spurious singularities. Replacing the L_k functions in (5.39) with the corresponding $\widehat{L}$ functions we are left with the following "completed cut term":

$$\begin{aligned}
&\mathcal{A}^{(1),\widehat{CR}}(\phi,1^-,2^-,3^+,\ldots,n^+) = \frac{N_p}{96\pi^2}\mathcal{A}_n^{(0)}(\phi,1^-,2^-,3^+,\ldots,n^+)\sum_{i=4}^{n}\Bigg[\\
&2\frac{\mathrm{tr}_-(1P_{i,n}(i-1)2)^3}{s_{12}^3}\left(\frac{1}{s_{i,1}(s_{i-1,1}-s_{i,1})^2} - \frac{1}{2s_{i,1}^2(s_{i-1,1}-s_{i,1})}\right)\\
&-3\frac{\mathrm{tr}_-(1P_{i,n}(i-1)2)^2}{s_{12}^2}\frac{1}{s_{i,1}(s_{i-1,1}-s_{i,1})}\\
&2\frac{\mathrm{tr}_-(2P_{3,i-1}i1)^3}{s_{12}^3}\left(\frac{1}{s_{2,i-1}(s_{2,i}-s_{2,i-1})^2} - \frac{1}{2s_{2,i-1}^2(s_{2,i}-s_{2,i-1})}\right)\\
&-3\frac{\mathrm{tr}_-(2P_{3,i-1}i1)^2}{s_{12}^2}\frac{1}{s_{2,i-1}(s_{2,i}-s_{2,i-1})}\Bigg],
\end{aligned} \tag{5.43}$$

where $N_p = 2(1 - N_F/N)$.

In order to find the full Higgs amplitudes this helicity configuration is actually only sufficient for 3 and 4 partons. The 3 parton ϕ-amplitude simplifies to:

$$\begin{aligned}
&\mathcal{A}_3^{(1),CC}(\phi,1^-,2^-,3^+) = \mathcal{A}_n^{(0)}(\phi,1^-,2^-,3^+)\Bigg[F_3^{1m}(s_{12}) + F_3^{1m}(s_{23}) + F_3^{1m}(s_{31})\\
&-3F_3^{1m}(s_{123}) - \frac{1}{2}F_4^{1m}(s_{123};s_{12},s_{23}) - \frac{1}{2}F_4^{1m}(s_{123};s_{13},s_{23}) - \frac{1}{2}F_4^{1m}(s_{123};s_{12},s_{13})\Bigg]
\end{aligned} \tag{5.44}$$

while $\mathcal{A}_3^{(1),CC}(\phi^\dagger,1^-,2^-,3^+)$ is zero so that $\mathcal{A}_3^{(1),CC}(H,1^-,2^-,3^+) = \mathcal{A}_3^{(1),CC}(\phi,1^-,2^-,3^+)$.

The case of 4 partons has the following contribution from the ϕ-amplitude,

$$\begin{aligned}
\mathcal{A}_n^{(1),CC}(\phi,1^-,2^-,3^+,4^+) &= \mathcal{A}_n^{(0)}(\phi,1^-,2^-,3^+,4^+)\Bigg[F_3^{1m}(s_{123})+F_3^{1m}(s_{234})+F_3^{1m}(s_{341})\\
&+F_3^{1m}(s_{412})-4F_3^{1m}(s_{1234})\\
&-\frac{1}{2}F_4^{1m}(s_{123};s_{12},s_{23})-\frac{1}{2}F_4^{1m}(s_{234};s_{23},s_{34})-\frac{1}{2}F_4^{1m}(s_{341};s_{34},s_{41})\\
&-\frac{1}{2}F_4^{1m}(s_{412};s_{41},s_{12})-\frac{1}{2}F_4^{2me}(s_{1234},s_{12};s_{412},s_{123})-\frac{1}{2}F_4^{2me}(s_{1234},s_{23};s_{123},s_{234})\\
&-\frac{1}{2}F_4^{2me}(s_{1234},s_{34};s_{234},s_{341})-\frac{1}{2}F_4^{2me}(s_{1234},s_{41};s_{341},s_{412})\\
&\frac{2}{3}\left(1-\frac{N_F}{N}\right)\frac{\mathrm{tr}_-(1432)^3}{s_{12}^3}L_3(s_{341},s_{41})-\left(1-\frac{N_F}{N}\right)\frac{\mathrm{tr}_-(1432)^2}{s_{12}^2}L_2(s_{341},s_{41})\\
&+4\left(1-\frac{N_F}{4N}\right)\frac{\mathrm{tr}_-(1432)}{s_{12}}L_1(s_{341},s_{41})+\frac{2}{3}\left(1-\frac{N_F}{N}\right)\frac{\mathrm{tr}_-(2341)^3}{s_{12}^3}L_3(s_{234},s_{23})\\
&-\left(1-\frac{N_F}{N}\right)\frac{\mathrm{tr}_-(2341)^2}{s_{12}^2}L_2(s_{234},s_{23})+4\left(1-\frac{N_F}{4N}\right)\frac{\mathrm{tr}_-(2341)}{s_{12}}L_1(s_{234},s_{23})\Bigg)\Bigg].
\end{aligned} \tag{5.45}$$

The corresponding $\phi^\dagger$ amplitude can be found by complex conjugation and re-labelling the ϕ amplitude,

$$\mathcal{A}_n^{(1),CC}(\phi^\dagger,1^-,2^-,3^+,4^+) = \left(\mathcal{A}_n^{(1),CC}(\phi,3^-,4^-,1^+,2^+)\right)^\dagger, \tag{5.46}$$

with the Higgs amplitude being the sum of both contributions:

$$\mathcal{A}_n^{(1),CC}(H,1^-,2^-,3^+,4^+) = \mathcal{A}_n^{(1),CC}(\phi,1^-,2^-,3^+,4^+)+\mathcal{A}_n^{(1),CC}(\phi^\dagger,1^-,2^-,3^+,4^+). \tag{5.47}$$

5.3.3. The non cut-constructible contributions

The rational part of the amplitudes cannot be reconstructed from unitarity cuts however it is often possible to fix these terms using the collinear limits [17, 18]. We also note in passing that there has been recent progress in using recursion relations to determine these contributions [31–33, 96–98, 100, 101, 130]. Here, we use Feynman diagrams and observe that the quark loop contribution fixes the rational part. Note that in the supersymmetric case, where the number of bosons and fermions are equal, the entire amplitude is cut-constructible and the rational parts are therefore proportional to $N - N_F$. For the amplitudes considered here, this reduces the number of external legs in the relevant Feynman diagrams by one.

The amplitude for three negative gluons is given in [137],

$$\mathcal{A}^{(1),NCC}(H;1^-,2^-,3^-) = \frac{N_P}{96\pi^2}\frac{s_{12}s_{23}+s_{23}s_{31}+s_{12}s_{31}}{[12][23][31]} \tag{5.48}$$

For four negative helicity gluons, we find that the unrenormalised amplitude is [129],

$$\begin{aligned}&\mathcal{A}_4^{(1),NCC}(H;1^-,2^-,3^-,4^-)\\ &= \frac{N_p}{96\pi^2}\left[-\frac{s_{13}\langle 4|1+3|2]^2}{s_{123}\,[1\,2]^2\,[2\,3]^2} + \frac{\langle 3\,4\rangle^2}{[1\,2]^2} + 2\frac{\langle 3\,4\rangle\,\langle 4\,1\rangle}{[1\,2]\,[2\,3]} + \frac{s_{12}s_{34}+s_{123}s_{234}-s_{12}^2}{2\,[1\,2]\,[2\,3]\,[3\,4]\,[4\,1]}\right] + 3 \text{ cyclic perms}\end{aligned} \tag{5.49}$$

where $N_p = 2(1 - N_F/N)$.

The result for the two negative helicity gluon and one positive helicity gluons has also been derived in reference [137],

$$\mathcal{A}^{(1),NCC}(H;1^-,2^-,3^+) = \frac{N_p}{96\pi^2}\frac{\langle 12\rangle[23][31]}{[12]^2}. \tag{5.50}$$

For two negative helicity gluons and two positive helicity gluons the tree-level amplitude is given by

$$\begin{aligned}\mathcal{A}^{(0)}(H;1^-,2^-,3^+,4^+) &= \mathcal{A}^{(0)}(\phi;1^-,2^-,3^+,4^+) + \mathcal{A}^{(0)}(\phi^\dagger;1^-,2^-,3^+,4^+)\\ &= \frac{\langle 12\rangle^4}{\langle 12\rangle\langle 23\rangle\langle 34\rangle\langle 41\rangle} + \frac{[34]^4}{[12][23][34][41]}.\end{aligned} \tag{5.51}$$

Note that both $\mathcal{A}^{(0)}(\phi;1^-,2^-,3^+,4^+)$ and $\mathcal{A}^{(0)}(\phi^\dagger;1^-,2^-,3^+,4^+)$ are symmetric under the interchange $(1 \leftrightarrow 2, 3 \leftrightarrow 4)$, while the $\phi^\dagger$ amplitude can be obtained from the ϕ amplitude by the interchange $(1 \leftrightarrow 3, 2 \leftrightarrow 4, \langle\ \rangle \leftrightarrow [\ ])$. We can therefore make use of this symmetry to write the non-cut constructible contribution to the one-loop amplitude in a compact way,

$$\begin{aligned}\mathcal{A}^{(1),NCC}(H;1^-,2^-,3^+,4^+) &= F(1,2,3,4,\langle\ \rangle,[\ ]) + F(3,4,1,2,[\ ],\langle\ \rangle)\\ &\quad +(1 \leftrightarrow 2, 3 \leftrightarrow 4),\end{aligned} \tag{5.52}$$

where

$$F(1,2,3,4,\langle\ \ \rangle,[\ \ ]) = \times\frac{N_p}{96\pi^2}\left[\frac{(s_{12}+s_{23})\langle 2|1+3|4]^2}{s_{123}\langle 23\rangle^2[12]^2} - \frac{s_{234}\langle 12\rangle[41]}{\langle 23\rangle\langle 34\rangle[12]^2} - \frac{\langle 2|1+3|4][34]}{\langle 23\rangle[12]^2} + \frac{1}{4}\left(\frac{\langle 12\rangle}{\langle 34\rangle} - \frac{[34]}{[12]}\right)^2\right] \tag{5.53}$$

5.4. Cross Checks and Limits

5.4.1. Infra-red pole structure

As discussed in chapter 2 the infra-red poles are constrained to have a certain form proportional to the tree level amplitude [13, 15],

$$\mathcal{A}_n^{(1)} = -\frac{c_\Gamma}{\epsilon^2}\mathcal{A}_n^{(0)}\sum_{i=1}^{n}\left(\frac{\mu^2}{-s_{ii+1}}\right)^\epsilon + \mathcal{O}(\epsilon^0). \tag{5.54}$$

Expanding the hypergeometric functions as a series in ϵ quickly leads to a proof of this fact, and it can be seen that all logarithms vanish at order $1/\epsilon$. Clearly this works in the same way for both helicity configurations, eq. (5.32) and eq. (5.39), since the pole structures are identical.

5.4.2. Collinear Limits

Collinear factorisation at one-loop is a little more complicated than the tree-level case considered in section 2.1.2. In general the collinear behaviour of one-loop amplitudes can be written[17, 138]:

$$\begin{aligned}\mathcal{A}_n^{(1)}(\ldots,i^{\lambda_i},i+1^{\lambda_{i+1}},\ldots) &\overset{i||i+1}{\longrightarrow} \\ &\sum_{h=\pm}\mathcal{A}_{n-1}^{(1)}(\ldots,i-1^{\lambda_{i-1}},P^h,i+2^{\lambda_{i+2}},\ldots)\,\mathrm{Split}^{(0)}(-P^{-h};i^{\lambda_i},i+1^{\lambda_{i+1}}) \\ &+\mathcal{A}_{n-1}^{(0)}(\ldots,i-1^{\lambda_{i-1}},P^h,i+2^{\lambda_{i+2}},\ldots)\,\mathrm{Split}^{(1)}(-P^{-h};i^{\lambda_i},i+1^{\lambda_{i+1}})\end{aligned} \tag{5.55}$$

where the collinear limit is defined through $p_i \to zP$ and $p_{i+1} \to (1-z)P$. The universal splitting functions for QCD have been calculated in reference [17, 18, 139]. The functions relevant for our amplitudes are:

$$\text{Split}^{(0)}(-P^+, 1^-, 2^+) = \frac{z^2}{\sqrt{z(1-z)}\langle 12\rangle} \tag{5.56}$$

$$\text{Split}^{(0)}(-P^+, 1^+, 2^-) = \frac{(1-z)^2}{\sqrt{z(1-z)}\langle 12\rangle} \tag{5.57}$$

$$\text{Split}^{(0)}(-P^-, 1^+, 2^+) = \frac{1}{\sqrt{z(1-z)}\langle 12\rangle} \tag{5.58}$$

$$\text{Split}^{(0)}(-P^-, 1^-, 2^-) = 0. \tag{5.59}$$

For the one-loop splitting functions it is useful to quote them in terms of cut-constructible and non-cut-constructible components since this is consistent with the formulae given for the Higgs amplitudes,

$$\text{Split}^{(1)}(-P^{-h}, 1^{\lambda_1}, 2^{\lambda_2}) = \text{Split}^{(1),CC}(-P^{-h}, 1^{\lambda_1}, 2^{\lambda_2}) + \text{Split}^{(1),NCC}(-P^{-h}, 1^{\lambda_1}, 2^{\lambda_2}) \tag{5.60}$$

where

$$\text{Split}^{(1),CC}(-P^{\pm}, 1^-, 2^+) = \text{Split}^{(0)}(-P^{\pm}, 1^-, 2^+)\frac{c_\Gamma}{\epsilon^2}\times$$
$$\left(\frac{\mu^2}{-s_{12}}\right)^{\epsilon}\left(1 - {}_2F_1\left(1, -\epsilon; 1-\epsilon; \frac{z}{1-z}\right) - {}_2F_1\left(1, -\epsilon; 1-\epsilon; \frac{1-z}{z}\right)\right), \tag{5.61}$$

$$\text{Split}^{(1),CC}(-P^{+}, 1^-, 2^-) = \text{Split}^{(0)}(-P^{+}, 1^-, 2^-)\frac{c_\Gamma}{\epsilon^2}\times$$
$$\left(\frac{\mu^2}{-s_{12}}\right)^{\epsilon}\left(1 - {}_2F_1\left(1, -\epsilon; 1-\epsilon; \frac{z}{1-z}\right) - {}_2F_1\left(1, -\epsilon; 1-\epsilon; \frac{1-z}{z}\right)\right), \tag{5.62}$$

$$\text{Split}^{(1),CC}(-P^{-}, 1^-, 2^-) = 0, \tag{5.63}$$

$$\text{Split}^{(1),NCC}(-P^{\pm}, 1^-, 2^+) = 0, \tag{5.64}$$

$$\text{Split}^{(1),NCC}(-P^{+}, 1^-, 2^-) = \frac{N_p}{96\pi^2}\frac{\sqrt{z(1-z)}}{[12]}, \tag{5.65}$$

$$\text{Split}^{(1),NCC}(-P^{-}, 1^-, 2^-) = \frac{N_p}{96\pi^2}\frac{\sqrt{z(1-z)}\langle 12\rangle}{[12]^2}. \tag{5.66}$$

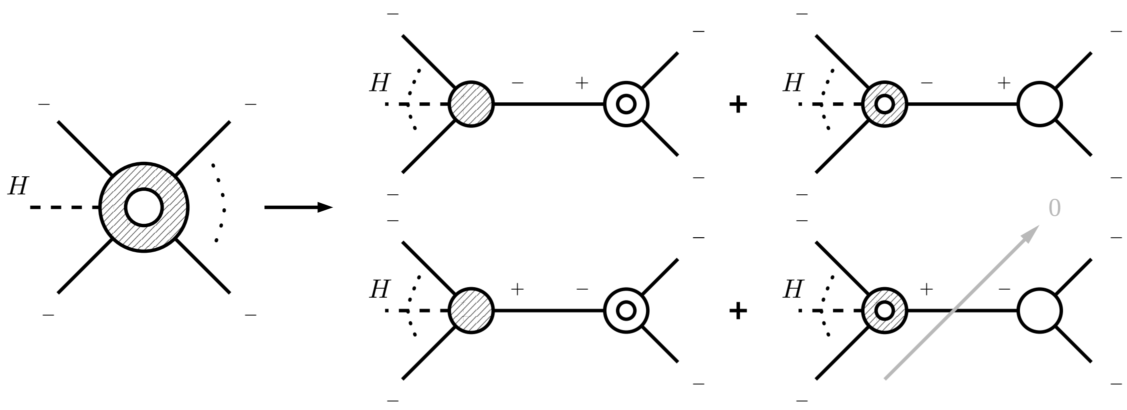

Figure 5.6: Collinear factorisation of the one-loop Higgs to "all-minus" amplitude. The 4^{th} diagram vanishes as the tree splitting $---$ function vanishes, see eq. (5.59)

Collinear factorisation of the all-minus configuration

For the all-minus configuration the factorisation is shown in figure 5.6, we can take p_1 and p_2 to be collinear without loss of generality since the amplitude is cyclic. The contribution from the cut-constructible part is extremely simple since we can quickly apply the method of Brandhuber, Spence and Travaglini [140] to show that the only diagram contributing in the $1||2$ limit is the s_{12} channel which factorises onto the cut-constructible part of the one-loop splitting function $\mathrm{Split}^{(1)}(-P^+, 1^-, 2^-)$ plus the cut-constructible part of the $(n-1)$-point one-loop amplitude times the tree splitting:

$$\begin{aligned}\mathcal{A}^{(1),CC}(\phi; 1^-, \dots, n^-) \xrightarrow{1||2} & \mathcal{A}^{(0)}(\phi; P^-, 3^-, \dots, n^-)\,\mathrm{Split}^{(1),CC}(-P^+, 1^-, 2^-) \\ & + \mathcal{A}^{(1),CC}(\phi; P^-, 3^-, \dots, n^-)\,\mathrm{Split}^{(0)}(-P^+, 1^-, 2^-). \qquad (5.67)\end{aligned}$$

The non-cut-constructible part for the 4-point all-minus configuration factorises onto the remaining terms:

$$\begin{aligned}\mathcal{A}^{(1),NCC}(H; 1^-, 2^-, 3^-, 4^-) \xrightarrow{1||2} & \mathcal{A}^{(1),NCC}(H; P^-, 3^-, 4^-) \times \mathrm{Split}^{(0)}(-P^+, 1^-, 2^-) \\ & + \mathcal{A}^{(0)}(H; P^+, 3^-, 4^-) \times \mathrm{Split}^{(1),NCC}(-P^-, 1^-, 2^-) \\ & + \mathcal{A}^{(0)}(H; P^-, 3^-, 4^-) \times \mathrm{Split}^{(1),NCC}(-P^+, 1^-, 2^-). \qquad (5.68)\end{aligned}$$

Combining this with eq. (5.67) shows that the all-minus amplitude does indeed factorise as expected.

Collinear factorisation of the "two minus" configuration

There are three collinear limits to consider for the "two-minus" amplitude. Let us first consider the case where we take a negative and a positive helicity collinear, e.g. the $2||3$ limit shown in figure 5.7. The third diagram always vanishes since there is no tree ϕ vertex with only one negative helicity gluon.

Here we see that the fourth diagram vanishes as the one-loop ϕ-amplitudes are finite [130] and so have no cut-constructible part. The boxes and triangles contributing in eq. (5.39) are the same as those for the all-minus case and hence will factorise in the same way onto the cut-constructible one-loop splitting function and the boxes and triangles of the $(n-1)$-point amplitude. The finite logarithms also factorise in the expected way when we notice:

$$\frac{\mathrm{tr}_-(1P_{i,n}(i-1)2)}{s_{12}} \xrightarrow{2||3} \frac{\mathrm{tr}_-(1P_{i,n}(i-1)P)}{s_{1P}} \qquad ; i > 4, \tag{5.69}$$

$$\frac{\mathrm{tr}_-(2P_{3,i-1}i1)}{s_{12}} \xrightarrow{2||3} \frac{\mathrm{tr}_-(PP_{4,i-1}i1)}{s_{1P}} \qquad ; i > 4, \tag{5.70}$$

and

$$\frac{\mathrm{tr}_-(1P_{4,n}32))}{s_{12}} \xrightarrow{2||3} 0 \tag{5.71}$$

$$\frac{\mathrm{tr}_-(2341))}{s_{12}} \xrightarrow{2||3} 0 \tag{5.72}$$

the terms with divergent logarithms, i.e. $L_k(s_{23}, s_{234})$, will always be proportional to a trace which vanishes in the limit and hence do not appear in the one-loop splitting

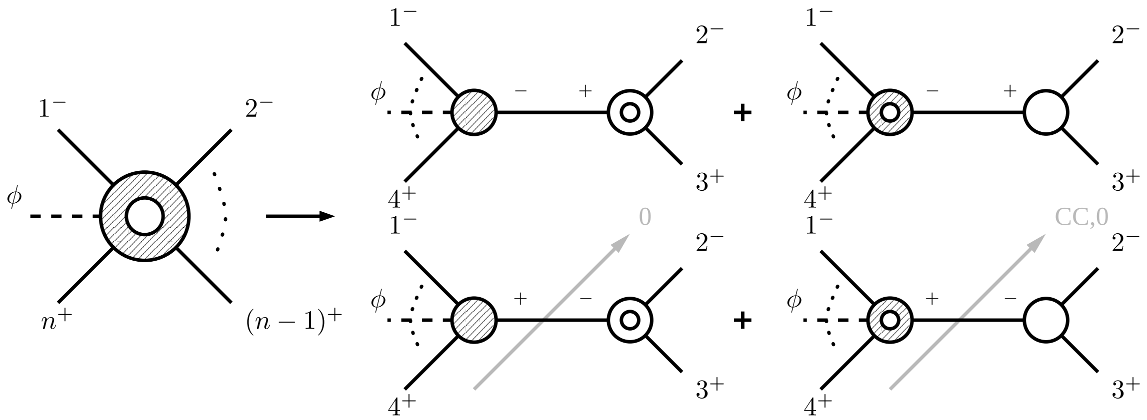

Figure 5.7: Collinear factorisation of $\mathcal{A}^{(1)}(\phi;1^-,2^-,3^+,\ldots,n^+)$ taking p_2 and p_3 parallel. Here the 3rd diagram vanishes since the tree amplitude with a single negative helicity vanishes whereas the 4th diagram vanishes only for the cut-constructible part since the loop amplitude is finite.

function.

$$\begin{aligned}\mathcal{A}^{(1),CC}(\phi;1^-,2^-,3^+,\ldots,n^+) &\stackrel{2||3}{\rightarrow} \\ &\mathcal{A}^{(0)}(\phi;1^-,P^-,4^+,\ldots,n^+)\,\mathrm{Split}^{(1),CC}(-P^+,2^-,3^+) \\ &+\mathcal{A}^{(1),CC}(\phi;1^-,P^-,4^+,\ldots,n^+)\,\mathrm{Split}^{(0)}(-P^+,2^-,3^+).\end{aligned} \tag{5.73}$$

The $1||2$ limit is rather trivial as all cut-constructible parts of the splitting functions or amplitudes vanish in the limit as shown in figure 5.8. The tree amplitude in this case vanishes,

$$\mathcal{A}_n^{(0)}(1^-,2^-,3^+,\ldots,n^+) \stackrel{1||2}{\rightarrow} 0, \tag{5.74}$$

therefore it is obvious that all the box and triangle terms of eq. (5.39) will vanish. The remaining finite logs appear to have a singularity in s_{12}, the worst coming from the traces raised to the 3rd power,

$$\frac{\mathrm{tr}_-(1XY2)^3}{s_{12}^3} = \frac{\langle 1|XY|2\rangle^3}{\langle 12\rangle^3} \quad , \quad \frac{\mathrm{tr}_-(2XY1)^3}{s_{12}^3} = -\frac{\langle 2|XY|1\rangle^3}{\langle 12\rangle^3}. \tag{5.75}$$

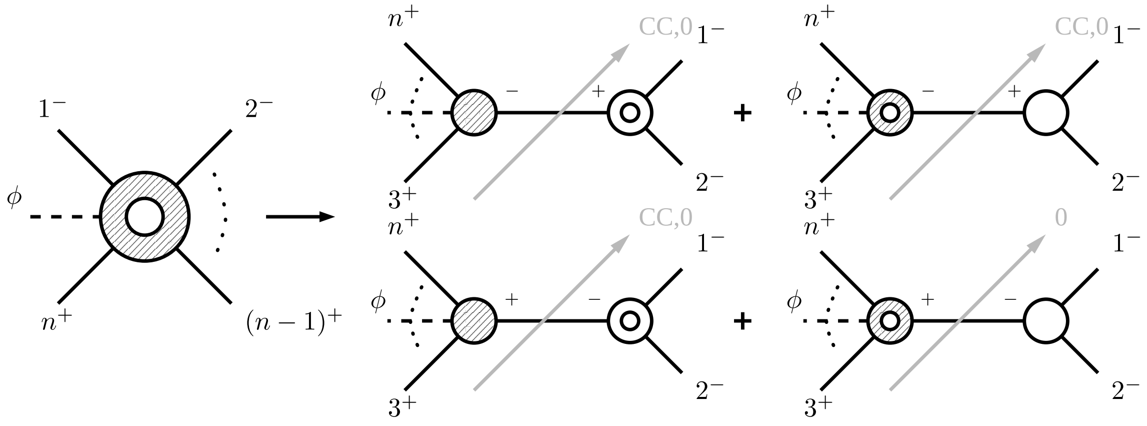

Figure 5.8: Collinear factorisation of $\mathcal{A}^{(1)}(\phi; 1^-, 2^-, 3^+, \ldots, n^+)$ taking p_1 and p_2 parallel. All diagrams vanish for the cut-constructible part since the tree amplitude vanishes, for the rational part only the 4$^{\text{th}}$ diagram vanishes.

However the tree amplitude is proportional to $\langle 12\rangle^3$ so $\mathcal{A}_n^{(1),CC}(1^-, 2^-, 3^+, \ldots, n^+)$ vanishes in the limit as expected.

The final limit which eq. (5.39) must satisfy is that when we take any adjacent pair of positive helicities collinear. The factorisation in this case is shown in figure 5.9. We can drop the top row of contributions here since we are looking at the cut-constructible part of the amplitude and $\text{Split}^{(1),CC}(-P^+, p^+, q^+) = 0$ as well as the finite ϕ amplitude. Just as in the $2||3$ limit here we have the same pole structure as the all minus amplitude and hence we know that we arrive at the correct loop splitting function, boxes and triangles. We must also be able to show that there are no divergent terms coming from the finite logs and that these terms correctly factorise onto the lower point amplitude. This turns out to be slightly more involved than in the $2||3$ case. First let us choose to take two adjacent particles a and b collinear where p_a lies to the left of p_b in the clockwise ordering. Using,

$$s_{b,i} \stackrel{a||b}{\to} (1-z)s_{P,i} + zs_{b+1,i}, \tag{5.76}$$

$$s_{i,a} \stackrel{a||b}{\to} zs_{i,P} + (1-z)s_{i,a-1}, \tag{5.77}$$

it is then possible to show:

$$\frac{\mathrm{tr}_-(2P_{3,a-1}a1)^k}{s_{12}^k}L_k(s_{2,a},s_{2,a-1})+\frac{\mathrm{tr}_-(2P_{3,a}b1)^k}{s_{12}^k}L_k(s_{2,b},s_{2,a})$$
$$\stackrel{a||b}{\to}\frac{\mathrm{tr}_-(2P_{3,a-1}P1)^k}{s_{12}^k}L_k(s_{2,a-1;P},s_{2,a-1}), \tag{5.78}$$

and,

$$\frac{\mathrm{tr}_-(1P_{b+1,i}b2)^k}{s_{12}^k}L_k(s_{b,i},s_{b+1,i})+\frac{\mathrm{tr}_-(1P_{b,i}a2)^k}{s_{12}^k}L_k(s_{a,i},s_{b,i})$$
$$\stackrel{a||b}{\to}\frac{\mathrm{tr}_-(1P_{b+1,i}P2)^k}{s_{12}^k}L_k(s_{P;b+1,i},s_{b+1,i}). \tag{5.79}$$

Using these identities and recognising that $\mathrm{tr}_-(1ab2)\stackrel{a||b}{\to}0$ it is possible to show that eq. (5.39) has the correct factorisation properties,

$$\begin{aligned}&\mathcal{A}^{(1),CC}(\phi;1^-,2^-,3^+,\ldots,a^+,b^+,\ldots,n^+)\stackrel{a||b}{\to}\\&\mathcal{A}^{(1),CC}(\phi;1^-,2^-,3^+,\ldots,a-1^+,P^+,b+1^+,\ldots,n^+)\,\mathrm{Split}^{(0)}(-P^-,a^+,b^+)\\+&\mathcal{A}^{(0)}(\phi;1^-,2^-,3^+,\ldots,a-1^+,P^+,b+1^+,\ldots,n^+)\,\mathrm{Split}^{(1),CC}(-P^-,a^+,b^+).\end{aligned} \tag{5.80}$$

Note that the precise way in which the above identities apply relies on the number of gluons and the choice of limit.

Collinear factorisation of $\mathcal{A}^{(1),NCC}(H;1^-,2^-,3^+,4^+)$

The non-cut-constructible part of the 4 gluon amplitude with two negative and two positive helicities has 3 independent collinear limits, $1||2$, $2||3$ and $3||4$. Let us first consider the case where p_1 and p_2 are parallel.

From figure 5.8 we see that the first three diagrams now have contributions. The final diagram still vanishes since $\mathrm{Split}^{(0)}(-P^-,1^-,2^-)$ is always zero. The factorised amplitudes do not vanish since we are now considering full Higgs amplitudes rather than just the ϕ contribution. We must be careful in taking the limit to extract any singularities which are hidden under double poles e.g. $s_{23}s_{14}/[12]^3$. This is achieved by

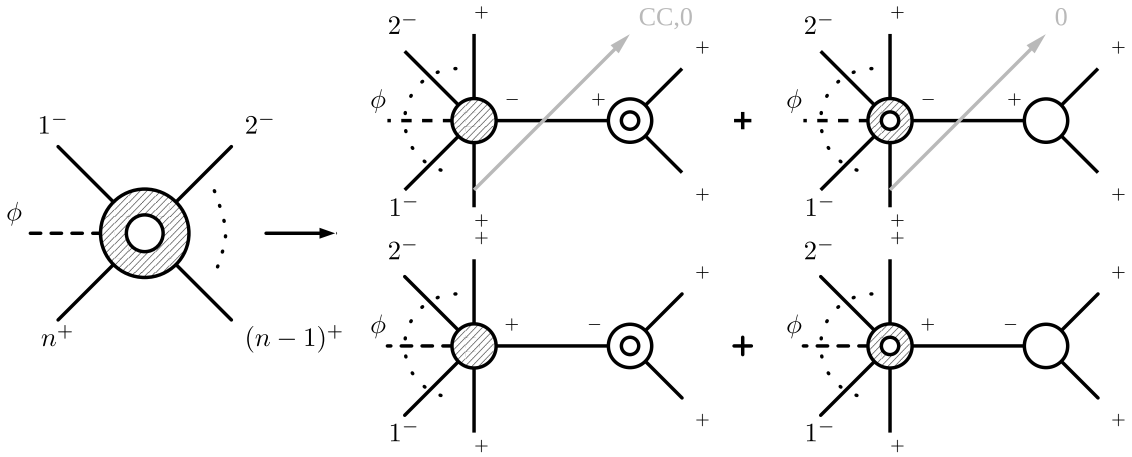

Figure 5.9: Collinear factorisation of $\mathcal{A}^{(1),CC}(\phi;1^-,2^-,3^+,\ldots,n^+)$ taking any two positive helicities parallel. Diagram 2 vanishes by eq. (5.59) and diagram 1 vanishes for the cut-constructible contribution as the one-loop ϕ amplitude is finite.

applying the following identities:

$$\begin{aligned} s_{12}s_{34}-s_{13}s_{24}+s_{14}*s_{23} &= \mathrm{tr}(1234) \\ &= \mathrm{tr}_-(1234)+\mathrm{tr}_+(1234) \\ &= \langle 12\rangle[23]\langle 34\rangle[41]+[12]\langle 23\rangle[34]\langle 41\rangle \end{aligned} \tag{5.81}$$

and

$$\frac{s_{24}}{s_{123}}-\frac{s_{24}}{s_{412}}=\frac{s_{23}s_{14}-s_{24}s_{13}+s_{12}(s_{23}-s_{24})}{s_{123}s_{412}} \tag{5.82}$$

It is then fairly straightforward to show that eq. (5.52) has the expected factorisation,

$$\begin{aligned} &\mathcal{A}^{(1),NCC}(H;1^-,2^-,3^+,4^+) \stackrel{1||2}{\to} \\ &\mathcal{A}^{(1),NCC}(H;P^-,3^+,4^+)\,\mathrm{Split}^{(0)}(-P^+,1^-,2^-) \\ &+\mathcal{A}^{(0)}(H;P^-,3^+,4^+)\,\mathrm{Split}^{(1),NCC}(-P^+,1^-,2^-) \\ &+\mathcal{A}^{(0)}(H;P^+,3^+,4^+)\,\mathrm{Split}^{(1),NCC}(-P^-,1^-,2^-). \end{aligned} \tag{5.83}$$

The 2||3 limit, shown in figure 5.7, has two contributing diagrams for the non-cut-constructible piece. Diagrams 1 and 3 vanish since the one-loop splitting function,

$\text{Split}^{(1),NCC}(-P^{\pm}, 2^-, 3^+)$ vanishes. Here we must also include the limit of the "completed cut" terms from eq. (5.43), which vanishes in both the 1||2 and 3||4 limits. By using the appropriate forms of the identities (5.81) and (5.82) the amplitude (5.52) can then be shown to satisfy,

$$\begin{aligned}
&\mathcal{A}^{(1),NCC}(H;1^-,2^-,3^+,4^+) + \mathcal{A}^{(1),\widehat{CR}}(H;1^-,2^-,3^+,4^+) \stackrel{2||3}{\to} \\
&+\mathcal{A}^{(1),NCC}(H;1^-,P^+,4^+)\,\text{Split}^{(0)}(-P^-,2^-,3^+) \\
&+\mathcal{A}^{(1),NCC}(H;1^-,P^-,4^+)\,\text{Split}^{(0)}(-P^+,2^-,3^+).
\end{aligned} \tag{5.84}$$

The final limit, 3||4, has three contributions in a similar way to the 1||2 limit. These can be seen in figure 5.9 where the ϕ field is replaced with the Higgs field. Since this limit is essentially complex conjugation of the 1||2 limit by using the same method we quickly find the expected behaviour,

$$\begin{aligned}
&\mathcal{A}^{(1),NCC}(H;1^-,2^-,3^+,4^+) \stackrel{3||4}{\to} \\
&\mathcal{A}^{(1),NCC}(H;1^-,2^-,P^+)\,\text{Split}^{(0)}(-P^-,3^+,4^+) \\
&+\mathcal{A}^{(0)}(H;1^-,2^-,P^+)\,\text{Split}^{(1),NCC}(-P^-,3^+,4^+) \\
&+\mathcal{A}^{(0)}(H;1^-,2^-,P^-)\,\text{Split}^{(1),NCC}(-P^+,3^+,4^+).
\end{aligned} \tag{5.85}$$

5.4.3. Soft Higgs Limit

For the case of a massless Higgs boson, we can consider the kinematic limit $p_H \to 0$. In this limit, because of the form of the $HG_{\mu\nu}G^{\mu\nu}$ interaction, the Higgs field behaves like a constant, so the Higgs-plus-n-gluon amplitudes should be related to pure gauge theory amplitudes. Low energy theorems relate the amplitudes with zero Higgs momentum to pure gauge theory amplitudes [104]:

$$A_n^{(l)}(H,\{g_i,\lambda_i\}) \stackrel{p_H\to 0}{\to} Cg\frac{\partial}{\partial g}A_n^{(l)}(\{g_i,\lambda_i\}), \tag{5.86}$$

where $C = \frac{\alpha_s}{6\pi v}$ is the effective coupling of Higgs field to the gluon fields. The n-gluon tree amplitude is proportional to g^{n-2} (see equation (2.55)) therefore,

$$\mathcal{A}_n^{(0)}(H,\{g_i,\lambda_i\}) \stackrel{p_H\to 0}{\to} (\text{const.}) \times (n-2)\mathcal{A}_n^{(0)}(\{g_i,\lambda_i\}). \tag{5.87}$$

The one-loop amplitudes are proportional to g^n hence similarly one can deduce the following behaviour in the soft Higgs limit,

$$\mathcal{A}_n^{(1)}(H, \{g_i, \lambda_i\}) \overset{p_H \to 0}{\longrightarrow} (\text{const.}) \times n\mathcal{A}_n^{(1)}(\{g_i, \lambda_i\}). \tag{5.88}$$

The 4-gluon MHV amplitude at one-loop in QCD has been derived in [141] and is given, unrenormalised, as:

$$\begin{aligned}\mathcal{A}_4^{(1),CC}(1^-, 2^-, 3^+, 4^+) =& -\frac{2c_\Gamma}{\epsilon^2}\left[\left(\frac{\mu^2}{-s_{14}}\right)^\epsilon + \left(\frac{\mu^2}{-s_{12}}\right)^\epsilon\right] + \log^2\left(\frac{s_{12}}{s_{14}}\right) + \pi^2 \\ & -\frac{\beta_0}{N\epsilon}\left(\frac{\mu^2}{-s_{14}}\right)^\epsilon \end{aligned}\tag{5.89}$$

$$\mathcal{A}_4^{(1),NCC}(1^-, 2^-, 3^+, 4^+) = 0 \tag{5.90}$$

The finite one-loop gluon amplitudes have also been computed recently using on-shell recursion relations [96, 97],

$$\mathcal{A}_4^{(1),CC}(1^-, 2^-, 3^-, 4^-) = 0 \tag{5.91}$$

$$\mathcal{A}_4^{(1),NCC}(1^-, 2^-, 3^-, 4^-) = -\frac{N_p}{96\pi^2}\frac{\langle 12\rangle\langle 34\rangle}{[12][34]} \tag{5.92}$$

Soft limit of $\mathcal{A}_4^{(1)}(H, 1^-, 2^-, 3^-, 4^-)$

The soft limit of the cut-constructible part of this amplitude is trivial since the tree amplitude is proportional to m_H^4 and hence this part of the amplitude vanishes. We must find the correct behaviour for the non-cut-constructible part, eq. (5.49). The first and fourth terms in (5.49) both vanish once we take $p_1 + p_2 + p_3 + p_4 = 0$. We can then use the momentum conservation to write:

$$\frac{\langle 34\rangle^2}{[12]^2} \overset{p_\phi \to 0}{\longrightarrow} \frac{\langle 12\rangle\langle 34\rangle}{[12][34]} \tag{5.93}$$

$$\frac{\langle 34\rangle\langle 41\rangle}{[12][23]} \overset{p_\phi \to 0}{\longrightarrow} -\frac{\langle 12\rangle\langle 34\rangle}{[12][34]}. \tag{5.94}$$

Since both of these terms are cyclically symmetric it is clear that each of the 4 permutations will produce the same contribution and the amplitude factorises on to the 4 gluon amplitude (5.92),

$$\mathcal{A}_4^{(1)}(H,1^-,2^-,3^-,4^-) \overset{p_\phi\to 0}{\to} 4\mathcal{A}_4^{(1)}(1^-,2^-,3^-,4^-) \tag{5.95}$$

and we find the factor of $n=4$ as predicted from the low-energy theorem.

Soft limit of $\mathcal{A}_4^{(1)}(H,1^-,2^-,3^+,4^+)$

Firstly let us consider the soft limit of the cut constructible components, eq.(5.45) and eq.(5.46). The 1-mass and 2-mass easy box functions and triangle functions have smooth soft limits where we take:

$$\left(\frac{\mu^2}{-m_\phi^2}\right)^\epsilon \overset{p_\phi\to 0}{\to} 0 \tag{5.96}$$

$$\left(\frac{\mu^2}{-s_{\phi;p}}\right)^\epsilon \overset{p_\phi\to 0}{\to} 0. \tag{5.97}$$

We must apply the same relations to the finite logs coming from the tensor triangle integrals, for instance we find:

$$L_k(s_{23},s_{234}) = \frac{\mathrm{Bub}(s_{23})-\mathrm{Bub}(s_{234})}{(s_{23}-s_{234})^k} \overset{p_\phi\to 0}{\to} \frac{1}{s_{23}^k\epsilon}\left(\frac{\mu^2}{-s_{23}}\right)^\epsilon. \tag{5.98}$$

Applying these relations together with momentum conservation to the cut-constructible part of the 4 gluon amplitude, eq. (5.45) and eq. (5.46), we find that the boxes and triangle functions collapse onto the correct $1/\epsilon^2$ poles while the tensor triangles simplify considerably using:

$$\left(\frac{\mathrm{tr}_-(1432)}{s_{12}}\right)^k \overset{p_\phi\to 0}{\to} (-1)^k s_{14}^k, \tag{5.99}$$

so that the logarithms reduce to,

$$\frac{2}{\epsilon}\left(\frac{\mu^2}{-s_{14}}\right)^\epsilon\left(-\frac{1}{3}\left(1-\frac{N_F}{N}\right)+4\left(1-\frac{N_F}{4N}\right)\right) = \left(\frac{\mu^2}{-s_{14}}\right)^\epsilon\frac{2\beta_0}{N\epsilon}. \tag{5.100}$$

Combining this with the $1/\epsilon^2$ poles we find,

$$\mathcal{A}_4^{(1)}(\phi,1^-,2^-,3^+,4^+) \overset{p_\phi\to 0}{\to} 2\mathcal{A}_4^{(1)}(1^-,2^-,3^+,4^+) \tag{5.101}$$

$$\mathcal{A}_4^{(1)}(\phi^\dagger,1^-,2^-,3^+,4^+) \overset{p_\phi^\dagger\to 0}{\to} 2\mathcal{A}_4^{(1)}(1^-,2^-,3^+,4^+). \tag{5.102}$$

The soft limit of the non-cut-constructible part, eq. (5.52) is fairly simple and can easily be shown to vanish as expected,

$$\mathcal{A}_4^{(1),NCC}(H;1^-,2^-,3^+,4^+) \stackrel{p_H\to 0}{\to} 0. \tag{5.103}$$

Therefore, we find that the Higgs amplitude has the expected soft limit,

$$\mathcal{A}_4^{(1)}(H,1^-,2^-,3^+,4^+) \stackrel{p_H\to 0}{\to} 4\mathcal{A}_4^{(1)}(1^-,2^-,3^+,4^+). \tag{5.104}$$

5.5. Conclusions

In this chapter we have used the MHV rules to evaluate the cut-constructible parts of one-loop amplitudes of gluons coupling to a single Higgs boson, expanding on the results of [129]. We used the MHV construction to organise the unitarity cuts as used in $\mathcal{N}=4,1,0$ SYM in references [90–92]. The results presented are for n-point amplitudes firstly when all the gluons have negative helicity and secondly when two adjacent gluons have negative helicity and the rest have positive helicity (the analogue of the MHV amplitudes in QCD). The remaining rational functions were fixed through a reduced Feynman programme where only fermion loops were evaluated. These amplitudes are sufficient to find compact analytical solutions for the 4-point amplitudes $\mathcal{A}^{(1)}(H,1^-,2^-,3^-,4^-)$ and $\mathcal{A}^{(1)}(H,1^-,2^-,3^+,4^+)$. Using the techniques of on-shell recursion [96–100] it should be possible to find rational functions for higher point amplitudes and Berger et al. have recently computed the finite one-loop amplitudes for ϕ to many gluons where the helicity configurations vanish at tree level [130].

We have made extensive checks of the collinear and soft Higgs factorisation properties and in each case we have found the expected behaviour. In particular we find that in the soft Higgs limit the amplitudes do satisfy the "naive" criterion predicted by the low energy theorem. This is in disagreement with the analysis in reference [130] which suggests that the cut-constructible part of the amplitude may have a soft limit which is inconsistent with the low energy theorem because the order of the $p_H \to 0$ and $\epsilon \to 0$

limits does not commute. It may be that for more complicated helicity configurations the appearance of 2-mass hard boxes would produce a non-uniform soft limit since it is known that these functions do not exhibit the same smooth behaviour as the 1-mass and 2-mass easy boxes. Unfortunately our method does not allow us to test the behaviour of the rational parts of the ϕ and $\phi^\dagger$ amplitude separately since we evaluate the rational part of the full Higgs amplitude only.

Our method should have no problem in extending to other helicity configurations although the tensor reduction procedure would be more complicated. Clearly introducing external fermions would cause no problems in principle and the necessary tree amplitudes for one-loop amplitudes with an external fermion pair are given in reference [54].

6. Conclusions

In this thesis we have discussed the application of new on-shell methods for calculating scattering amplitudes in QCD. The inspiration for these developments came from the remarkable paper by Witten [42] which found a duality between $\mathcal{N} = 4$ SYM and a topological string theory on twistor space. This had an implication for QCD phenomenology as it pointed out the remarkable fact that tree level helicity amplitudes, at which order the two theories are equivalent, had a simple geometric structure in twistor space. In particular, the simplest helicity amplitudes or MHV amplitudes were seen as straight lines in twistor space.

It was then proposed that one could use the simplest helicity amplitudes, the MHV amplitudes, as vertices in a new scalar perturbation series. This procedure became known as the MHV rules [45] and was quickly shown to be an extremely quick and easy way to re-derive tree-level amplitudes even though no proof existed*. The main reasons for these simplifications seem to come firstly from the fact that twistor space is a complex space and hence allows one to exploit the analytic properties of the amplitudes and secondly from the fact that the method uses gauge invariant helicity amplitudes as building blocks where cancellations between Feynman diagrams have already taken place. The method explicitly differentiates between helicity states allowing some extremely compact results for amplitudes with arbitrary multiplicity.

The MHV rules have been shown to apply to a wide variety of tree-level processes

*A proof of the method by Risager [46] followed later based on a variation of the argument used to prove the BCF recursion relations within the standard model. In Chapter 3 we discussed such application to Higgs bosons coupling to QCD via an effective gluon interaction in the limit $m_t \to \infty$. In all cases it has been observed that the MHV rules re-produce the results of the standard off-shell techniques but the analytic form of each amplitude is much more compact.

Another on-shell technique that has been discussed is a recursion relation between on-shell amplitudes known as BCF recursion relations [64]. Here we saw that analytical continuation of any scattering amplitude to the complex plane allowed the exploitation of its simple analytic properties and lead to the derivation of extremely compact forms for the amplitudes. Again this method was especially suited for helicity amplitudes as for complex momenta, the 2-component spinors representing the helicity states are independent allowing the simplicity in the helicity structure to be apparent throughout the calculations.

Throughout this thesis we have been primarily interested in showing that the new on-shell techniques can indeed be applied to a wide variety of SM processes. The most striking feature is that the results of such calculations are extremely compact. One would therefore expect that amplitudes obtained with both the MHV rules and the BCF recursion relations would be quicker to evaluate than those using the off-shell recursive methods of Berends and Giele which currently provide the basis for many MC event generators. However numerical studies [72, 142, 143] have shown that because of the extra cost of evaluating the shift into complex momenta the BCF recursion relations actually perform worse than the Berends and Giele relations for high multiplicity final states. Recursive implementations of the MHV rules have also been shown to perform worse than the off-shell methods but this seems to be mainly because the method of Bena, Bern and Kosower [52] includes an explicit over-counting in the formulae.

However the on-shell methods have lead to a great deal of new understanding of gauge theory, in particular it has provided some new insights into $\mathcal{N} = 8$ supergravity [144–146]. One rapidly developing application for on-shell methods is to NLO processes in the SM. Although the tree-level applications were an interesting playground for the new techniques there were already extremely efficient tools for the computation of tree-amplitudes as has been shown in the numerical studies. At one-loop no such tools exist and currently the on-shell techniques, combining unitarity and on-shell recursion, are a very promising direction for the automation of NLO processes.

We have considered the various approaches to one-loop calculations and have shown that the MHV rules at one-loop [90] can quickly generate all cut-containing pieces of Higgs to gluon amplitudes using the SD/ASD split of the Higgs field which was so successful at tree level [53]. The method is similar to applying standard unitarity cuts although the sum over MHV diagrams results in a complete re-construction of the integral functions without having to worry about double counting. The computation of the remaining rational functions should also be possible through on-shell recursion as it has been shown for QCD [96–101] although a complete understanding of the collinear factorisation with complex momenta would be necessary. For limited multiplicity one can use Feynman techniques to complete the remaining terms, which is much simpler than calculating the full amplitude [31–33].

As we lay out in the introduction, calculations of scattering amplitudes are just one of the ingredients required to make accurate predictions of the SM. In order to successfully remove background QCD signals from observations at hadron colliders and distinguish new physics we will need to perform the phase space integrals together with the IR subtractions. These calculations must then be interfaced with the parton shower and jet algorithms and convoluted with the PDF's.

On the formal side, calculations of all-multiplicity amplitudes at higher and higher orders can provide important information about the nature of the perturbative series. Of particular interest is the ADS/CFT correspondence which conjectures a duality between $\mathcal{N} = 4$ SYM theory and type IIb heterotic string theory on anti-de-sitter space in the limit of the number of colours becoming infinite. Iterative structures within $\mathcal{N} = 4$ SYM have already been conjectured and tested up to 3-loops [147]. Witten's conjecture of a weak-weak duality between $\mathcal{N} = 4$ SYM and a topological string theory on twistor space is also yet to see any progress beyond one-loop. The main problem here has been on the string theory side where it has not been possible to decouple conformal super-gravity states which clearly do not have any meaning in $\mathcal{N} = 4$ SYM [83, 84].

A. Dimensional Regularisation

As mentioned in chapter 2 in order to make explicit cancellation of the UV and IR divergences present in the various components of the scattering amplitudes we must introduce some kind of regularisation to our integrals. In dimensional regularisation [148–151] the number of dimensions of the Lagrangian is changed for 4 to D (the action is still dimensionless). The loop integrals are then evaluated in $D = 4 - 2\epsilon$ dimensions where, for sufficiently small number of dimensions, they will converge. An important consequence of such a regularisation is that in changing the dimension of the Lagrangian we also change the dimensions of the coupling constant. It is useful to make the appearance of a new scale in the theory explicit by redefining the coupling as,

$$g \to g\mu^{\epsilon}. \tag{A.1}$$

Using Feynman parameterisation and reducing to a basis of scalar integrals it is possible to express any loop integral as*:

$$I_n = \int \frac{d^D l}{(2\pi)^D} \frac{1}{[l^2 - M^2]^n}. \tag{A.2}$$

We take the signature of the D dimensional space to have a single time direction and $D - 1$ space directions hence to make the integral easier to evaluate we the integral in Euclidean space by Wick rotating the time-like direction, $l^0 \to i l_E^0$ and $l^i \to l_E^i$. Thus

*In this expression we have omitted the small imaginary part coming from the definition of the Feynman propagator, technically this is necessary to make the integral in Euclidean space well defined for space-like regions where $M^2 < 0$

the integral (A.2) now becomes,

$$I_n = (-1)^n \int \frac{d^D l_E}{(2\pi)^D} \frac{1}{[l_E^2 + M^2]^n}. \tag{A.3}$$

Switching to polar co-ordinates leaves us with,

$$I_n = (-1)^n \int \Omega_D \int \frac{d(l_E^2)}{2(2\pi)^D} \frac{(l_E^2)^{D/2-1}}{[l_E^2 + M^2]^n}. \tag{A.4}$$

This can now be evaluated using the following tricks:

$$\begin{aligned}
(\pi)^{D/2} &= \left(\int dx e^{-x^2} \right)^D = \int d^D x \exp(-\sum_{i=1}^{D} x_i^2) \\
&= \int \Omega_D \int_0^\infty \frac{dy}{2} \, y^{D/2-1} e^{-y} = \frac{1}{2}\Gamma(D/2) \int \Omega_D \\
&\Rightarrow \int \Omega_D = \frac{2(\pi)^{D/2}}{\Gamma(D/2)}
\end{aligned} \tag{A.5}$$

and[†]

$$\begin{aligned}
&\int_0^\infty \frac{d(l_E^2)}{2(2\pi)^D} \frac{(l_E^2)^{D/2-1}}{[l_E^2 + M^2]^n} \\
=&\frac{(M^2)^{D/2-n}}{2(2\pi)^D} \int_0^1 dx x^{n-D/2-1}(1-x)^{D/2-1} \\
=&\frac{(M^2)^{D/2-n}}{2(2\pi)^D} \frac{\Gamma(n-D/2)\Gamma(D/2)}{\Gamma(n)}
\end{aligned} \tag{A.6}$$

Therefore the final result is written just in terms of Gamma functions, M^2 and the dimension D,

$$I_n = (-1)^n \frac{(M^2)^{D/2-n}}{2^D \pi^{D/2}} \frac{\Gamma(n-D/2)}{\Gamma(n)}. \tag{A.7}$$

This formula can be applied to integrals in non-integer dimensions by analytically continuing the Γ function to all complex numbers. Details on the validity of integration in a continuous number of dimensions can be found in reference [152].

Once the loop integrals have been computed using the techniques shown above we can expand them around $D = 4$, i.e. $\epsilon = 0$. For this we use the expansion of the gamma function,

$$\Gamma(\epsilon) = \frac{1}{\epsilon} + \gamma_E + \mathcal{O}(\epsilon), \tag{A.8}$$

[†]Making use of the substitution $x = \frac{M^2}{l_E^2 + M^2}$

where γ_E is the Euler-Mascheroni constant, $\gamma_E \approx 0.5772$. When calculating the counter-terms for renormalisation in this way it becomes useful to define a scheme in which the counter-terms are only made to remove the poles in ϵ. This is an alternative to the renormalisation conditions given in (2.17) and is known as the *minimal subtraction* scheme, MS. The only difference in this scheme is exactly where the finite terms in the expansion about $\epsilon = 0$ are included. Indeed since the divergent integrals contain the factor,

$$(4\pi)^{\epsilon}\Gamma(\epsilon) = \frac{1}{\epsilon} - \gamma_e + \log(4\pi) + \mathcal{O}(\epsilon) \tag{A.9}$$

so it makes sense to include the extra finite terms in the subtraction as well. This defines the modified minimal subtraction scheme denoted $\overline{MS}$.

When using dimensional regularisation we must also worry about the dimensions of the Dirac gamma matrices, γ_μ, which can appear in the numerator of the loop integrals. One can argue that the $4-2\epsilon$ dimensional space is in fact an infinite dimensional vector space and therefore the gamma matrices are in fact an infinite dimensional representation of the Clifford algebra [152],

$$\{\gamma_\mu, \gamma_\nu\} = 2g_{\mu\nu}. \tag{A.10}$$

We can proceed in evaluating traces exactly as before only we must remember the $tr(g^{\mu\nu}) = D$. The problem with the gamma matrices comes when we try to define helicity states through the γ_5 matrix. It is not possible to find a Lorentz invariant definition of γ_5 in D dimensions so the notion of helicity is lost when $D \neq 4$. A way around this is to use a 4-dimensional helicity scheme in which the external particles are treated in 4-dimensions and the internal loop momenta are treated in D-dimensions.

When performing unitarity cuts it is necessary to consider the helicity states circulating within the loop. This is again is consistent as the cuts are always made in four dimensions. Performing unitarity cuts in D dimensions is however also possible and is discussed in reference [22].

Another technical point when using dimensional regularisation to regulate both IR and UV divergences that occur in the same integral is that integrals that are IR divergent in

4 dimensions are well defined in $D > 4$ dimensions where as UV divergent integrals are well defined in $D < 4$ dimensions. This appears to be a problem for loop integrals which contain both types of divergences but in practise the integrals are analytic in ϵ hence it's sign is not important. As long as one calculates the counter-terms from off-shell objects, $\Sigma, \Pi^{\mu\nu}$ etc., where there are no IR divergences, the UV singularities can still be subtracted from the any loop integral leaving the IR singularities as an analytic function of ϵ.

B. Details for (anti-)self-dual Higgs amplitudes

B.1. Full $\mathcal{N} = 1$ SUSY model with embedded effective interaction

$$\begin{aligned}
\mathcal{L} &= \int d^4\theta\ \Phi^\dagger\Phi + \int d^2\theta\ \left[\frac{m_H}{2}\Phi^2 + \frac{1}{4}(1-4C\Phi)\operatorname{tr} W^\alpha W_\alpha\right] \\
&\qquad + \int d^2\bar\theta\ \left[\frac{m_H}{2}\Phi^{\dagger 2} + \frac{1}{4}(1-4C\Phi^\dagger)\operatorname{tr} \overline{W}_{\dot\alpha}\overline{W}^{\dot\alpha}\right] \qquad (B.1) \\
&= F^\dagger F - \partial_\mu\phi^\dagger\partial^\mu\phi - i\bar\psi\bar{\partial\!\!\!/}\psi + \frac{1}{2}\operatorname{tr} D^2 - \frac{1}{4}\operatorname{tr} G_{\mu\nu}G^{\mu\nu} - i\bar\Lambda \bar{D\!\!\!/}\Lambda \\
&\quad + \Bigg\{ m_H\Big(F\phi - \frac{1}{2}\psi^2\Big) - C\Big[-F\operatorname{tr}\Lambda\Lambda - 2\sqrt{2}i\psi^\alpha \operatorname{tr}\Big(\Lambda_\alpha D - (\sigma_{\mu\nu})_\alpha^{\ \beta}\Lambda_\beta\, G^{\mu\nu}_{SD}\Big) \\
&\qquad + \phi\operatorname{tr}\Big(-2i\bar\Lambda\bar{D\!\!\!/}\Lambda - G_{SD\,\mu\nu}G^{\mu\nu}_{SD}\Big)\Big]\ +\ \text{h. c.}\Bigg\}. \qquad (B.2)
\end{aligned}$$

Because the term linear in the auxiliary field D is also linear in the coefficient C, the D-term 'potential' from integrating out D is quadratic in C and may be neglected. On the other hand, the F-term interaction has a linear term,

$$\mathcal{L}_F = -|m_H\phi - C\Lambda\Lambda|^2 = -m_H^2\phi^\dagger\phi + Cm_H(\phi^\dagger\Lambda\Lambda + \phi\bar\Lambda\bar\Lambda) + \mathcal{O}(C^2). \qquad (B.3)$$

B.2. Vanishing of $\mathcal{A}_n(\phi, 1^\pm, 2^+, 3^+, \ldots, n^+)$

We can also show that $A_n(\phi, 1^\pm, 2^+, 3^+, \ldots, n^+)$ vanishes using the Berends-Giele recursion relations and off-shell currents [60]. (For a review, see ref. [122].)

The two-point vertex coupling ϕ to two (off-shell) gluons with outgoing momenta k_1 and k_2 and Lorentz indices μ_1 and μ_2 is

$$V^{\phi}_{\mu_1\mu_2}(k_1, k_2) = \eta_{\mu_1\mu_2} k_1 \cdot k_2 - k_{1\,\mu_2} k_{2\,\mu_1} + i\varepsilon_{\mu_1\mu_2\nu_1\nu_2} k_1^{\nu_1} k_2^{\nu_2} \,. \tag{B.4}$$

For $\phi^\dagger$ the sign of the Levi-Civita term would be reversed.

First let us compute the simplest amplitudes $A_2(\phi, 1^\pm, 2^\pm)$ using this vertex. (The opposite-helicity cases vanish using angular-momentum conservation, $A_2(\phi, 1^\pm, 2^\mp) = 0$.) For gluon polarisation vectors we use (2.45). From identities (2.46) it follows that only the second and third terms in the vertex (B.4) contribute to $A_2(\phi, 1^\pm, 2^\pm)$. Consider the ratio of their contributions in the positive-helicity case,

$$R^{++} \equiv \frac{i\varepsilon_{\mu_1\mu_2\nu_1\nu_2}\varepsilon^{+,\mu_1}\varepsilon^{+,\mu_2} k_1^{\nu_1} k_2^{\nu_2}}{-\varepsilon_1^+ \cdot k_2 \; \varepsilon_2^+ \cdot k_1} = -\frac{1}{4}\frac{\mathrm{tr}[\gamma_5 \not{\varepsilon}_1^+ \not{\varepsilon}_2^+ \not{k}_1 \not{k}_2]}{\varepsilon_1^+ \cdot k_2 \; \varepsilon_2^+ \cdot k_1} \tag{B.5}$$

$$= \frac{\left\{\mathrm{tr}\left[\frac{1}{2}(1-\gamma_5)\gamma_{\mu_1}\gamma_{\mu_2}\not{k}_1\not{k}_2\right] - \mathrm{tr}\left[\frac{1}{2}(1+\gamma_5)\gamma_{\mu_1}\gamma_{\mu_2}\not{k}_1\not{k}_2\right]\right\}\langle\xi^-|\gamma^{\mu_1}|k_1^-\rangle\langle\xi^-|\gamma^{\mu_2}|k_2^-\rangle}{4\,\langle\xi\, 2\rangle\,[2\, 1]\;\langle\xi\, 1\rangle\,[1\, 2]} \,. \tag{B.6}$$

Using the identities:

$$i\epsilon_{\mu_1\mu_2\mu_3\mu_4} = \frac{1}{4}\mathrm{tr}(\gamma_5\gamma^{\mu_1}\gamma^{\mu_2}\gamma^{\mu_3}\gamma^{\mu_4}), \tag{B.7}$$

$$\tfrac{1}{2}(1\pm\gamma_5)\gamma_\mu\langle a\pm|\gamma^\mu|b\pm\rangle = 2|b\pm\rangle\langle a\pm|, \tag{B.8}$$

one can show,

$$R^{++} = \frac{\langle\xi\,\xi\rangle\,[2\,1]\,\langle 1\,2\rangle\,[2\,1] - [1\,2]\,\langle\xi\,1\rangle\,[1\,2]\,\langle 2\,\xi\rangle}{\langle\xi\,2\rangle\,[2\,1]\;\langle\xi\,1\rangle\,[1\,2]} = -1. \tag{B.9}$$

Repeating the analysis for two negative-helicity gluons yields the opposite sign,

$$R^{--} \equiv \frac{i\varepsilon_{\mu_1\mu_2\nu_1\nu_2}\varepsilon^{-,\mu_1}\varepsilon^{-,\mu_2} k_1^{\nu_1} k_2^{\nu_2}}{-\varepsilon_1^- \cdot k_2 \; \varepsilon_2^- \cdot k_1} = +1. \tag{B.10}$$

Thus the second and third terms cancel in the positive-helicity case, so $A_2(\phi, 1^+, 2^+) = 0$; whereas they add in the negative-helicity case, for which one finds eq. (3.17).

To compute $A_n(\phi, 1^\pm, 2^+, 3^+, \ldots, n^+)$ using the Berends-Giele off-shell currents, we merely join each gluon produced by the vertices from $\phi\,\mathrm{tr}(G^{\mu\nu} - \tilde{G}^{\mu\nu})^2$ to an off-shell current. The two currents we need are [60, 122]

$$J_{1,n}^{+,\mu} \equiv J^\mu(1^+, 2^+, \ldots, n^+) = \frac{\langle \xi^- | \gamma^\mu \, \not{P}_{1,n} | \xi^+ \rangle}{\sqrt{2}\, \langle \xi\, 1 \rangle \langle 1\, 2 \rangle \cdots \langle n-1,\, n \rangle \langle n\, \xi \rangle}\,, \tag{B.11}$$

where all reference momenta are taken to be equal to ξ, and

$$J_{1,n}^{-,\mu} \equiv J^\mu(1^-, 2^+, \ldots, n^+) = \frac{\langle 1^- | \gamma^\mu \, \not{P}_{1,n} | 1^+ \rangle}{\sqrt{2}\, \langle 1\, 2 \rangle \cdots \langle n\, 1 \rangle} \sum_{m=3}^{n} \frac{\langle 1^- | \not{k}_m \, \not{P}_{1,m} | 1^+ \rangle}{P_{1,m-1}^2 P_{1,m}^2}\,, \tag{B.12}$$

where the reference momentum choice is $\xi_1 = k_2$, $\xi_2 = \cdots = \xi_n = k_1$. In these formulae, $P_{p,q} = k_p + k_{p+1} + \ldots + k_{q-1} + k_q$.

Actually, the current (B.12) is not quite sufficient for the proof in the one-minus case. We really need the current where the negative-helicity gluon appears at an arbitrary position in the chain of positive-helicity gluons (all with the same reference momentum), $J^\mu(2^+, 3^+, \ldots, 1^-, \ldots, n^+)$. This current has been constructed by Mahlon [153]. The expression is rather complicated, so we do not present it here. It is sufficient for our purposes to note that it is also proportional to $\langle 1^- | \gamma^\mu \, \not{P}_{1,n} | 1^+ \rangle$.

For $A_n(\phi, 1^+, 2^+, 3^+, \ldots, n^+)$, we take all reference momenta equal to ξ, a generic vector. For $A_n(\phi, 1^-, 2^+, 3^+, \ldots, n^+)$, we take $\xi_1 = k_2$, $\xi_2 = \cdots = \xi_n = k_1 \equiv \xi$. Then in both cases all the currents attaching to the Higgs vertex are proportional to $\langle \xi^- | \gamma^\mu \ldots$. In terms of spinor notation, all currents are proportional to ξ_α. This property is all we need to demonstrate (again via Fierz identities) that

$$\begin{aligned} J^+ \cdot J^+ = J^+ \cdot J^- &= 0, & \text{(B.13)} \\ \varepsilon_{\mu_1\mu_2\mu_3\mu_4} J^{+,\mu_1} J^{+,\mu_2} J^{-,\mu_3} &= 0. & \text{(B.14)} \end{aligned}$$

These relations in turn suffice to show that the Feynman vertices coupling ϕ to 3 or 4 gluons, ϕggg and $\phi gggg$, do not contribute to $A_n(\phi, 1^\pm, 2^+, 3^+, \ldots, n^+)$. Terms in these vertices without a Levi-Civita tensor always attach a Minkowski metric $\eta_{\mu_1\mu_2}$ to two currents; their contribution vanishes according to eq. (B.13). (The same is true of the first term in the ϕgg vertex (B.4).) Terms containing the Levi-Civita tensor $\varepsilon_{\mu_1\mu_2\mu_3\mu_4}$ attach it directly to at least three currents; their contribution vanishes according to eq. (B.14). This leaves just the contributions of the second and third terms in the ϕgg vertex (B.4). They cancel against each other, just as in the case of $A_2(\phi, 1^+, 2^+)$ above. Suppose that gluons $p+1$ through m (cyclically) attach to one leg of the ϕgg vertex, and gluons $m+1$ through p (cyclically) attach to the other leg. Then the ratio analogous to eq. (B.5) is

$$R^{*,\pm+}_{p,m} \equiv \frac{i\varepsilon_{\mu_1\mu_2\nu_1\nu_2}\langle\xi^-|\gamma^{\mu_1}\ \not{P}_{p+1,m}|\xi^+\rangle\langle\xi^-|\gamma^{\mu_2}\ \not{P}_{m+1,p}|\xi^+\rangle k_1^{\nu_1}k_2^{\nu_2}}{-\langle\xi^-|\ \not{P}_{m+1,p}\ \not{P}_{p+1,m}|\xi^+\rangle\langle\xi^-|\ \not{P}_{p+1,m}\ \not{P}_{m+1,p}|\xi^+\rangle} \tag{B.15}$$

$$= -1, \tag{B.16}$$

using the same Fierz identities as before. This completes the recursive proof that

$$A_n(\phi, 1^\pm, 2^+, 3^+, \ldots, n^+) = 0. \tag{B.17}$$

B.3. Vanishing of $\mathcal{A}_n(\phi, 1_q^\lambda, 2^+, 3^+, \ldots, n-1^+, n_{\bar{q}}^{-\lambda})$

In an analogous way to the recursive proof given in the previous we will prove the vanishing of $\mathcal{A}_n(\phi, 1_q^\lambda, 2^+, 3^+, \ldots, n-1^+, n_{\bar{q}}^{-\lambda})$ combining Feynman diagrams and off-shell recursive currents.

We form the amplitude by contracting the three vertex (B.4) with two off shell currents as shown in figure B.1. The first of these is the all-plus gluon current, J_+^μ, used in the previous section (B.11). The second consists of an off-shell gluon attached to a quark pair and any number of positive helicity gluons which we denote $S^\mu/+$ It is important to notice that the scalar ϕ can only couple to gluons in our effective model and hence there is no $\phi \to q\bar{q}$ vertex. For simplicity we will set the quark helicity to be negative, $\lambda = -1$. The case where $\lambda = +1$ follows by an identical calculation.

We can compute the case of $A_3(\phi, q_1^-, g_2^\pm, \bar{q}_3^+)$ very simply by contracting the ver-

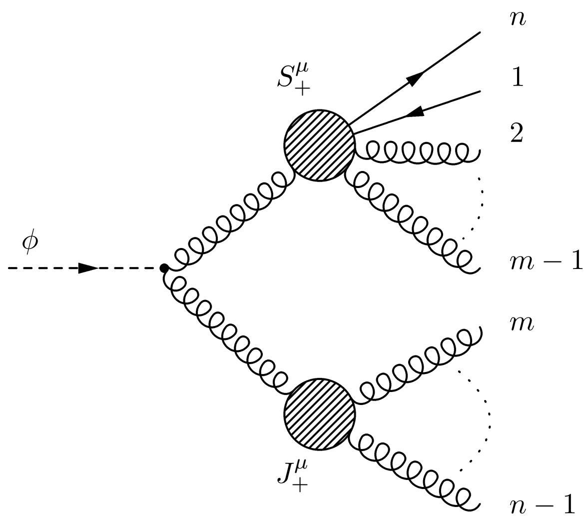

Figure B.1: The contribution to $A_n(\phi, q_1^-, g_2^+, \ldots, g_{n-1}^+, \bar{q}_n^+)$ coming from a quark "all plus" current and a gluon "all plus" current joined by a ϕgg vertex.

tex (B.4) with a polarisation vector $\epsilon_\pm^\mu(p_2)$ and a quark-antiquark current $\epsilon_q^\nu(k) = \langle 1-|\gamma^\nu|3-\rangle/s_{13}$ where $k = p_1 + p_3$. Just as in the proof for gluon only amplitudes we compute the ratio of the 3rd to 2nd term in equation (B.4) (the 1st term gives zero):

$$R_3^+ = \frac{i\epsilon_{\mu_1\mu_2\nu_1\nu_2}\epsilon^{\mu_1}(p_2)\epsilon_q^{\mu_2}(k)p_2^{\nu_1}k^{\nu_2}}{-\epsilon_+(p_2)\cdot p_1\epsilon_q(k)\cdot p_2}. \tag{B.18}$$

Using the identities (B.7) and (B.8) it is easy to show $R_3^+ = -1$ and therefore $A_3(\phi, q_1^-, g_2^+, \bar{q}_3^+) = 0$. Similarly, we can show that $R_3^- = +1$ and that the sum of the two terms does indeed match the proposed form of equation (3.43).

In order to extend this method to prove that the n-particle amplitude vanishes we make use of the two currents mentioned before:

$$J_+^\mu(1^+, \ldots, n^+) = \frac{\langle \xi^-|\gamma^\mu\, \not{P}_{1,n}|\xi^+\rangle}{\sqrt{2}\,\langle \xi\, 1\rangle\,\langle 1\, 2\rangle \ldots \langle n\, \xi\rangle}, \tag{B.19}$$

$$S_+^\mu(1_q^-, 2^+, \ldots, n-1^+, n_{\bar{q}}^+) = \frac{\langle \xi^-|\gamma^\mu\, \not{P}_{1,n-1}|\xi^+\rangle}{\langle \xi\, 2\rangle\,\langle 2\, 3\rangle \ldots \langle n-1\, \xi\rangle}. \tag{B.20}$$

We immediately notice that the currents have a very similar form. Indeed since the denominators play no role in making sure the amplitude vanishes, it is obvious that the proof will proceed in the same way as the gluon case. So all that remains is to note:

$$J_+ \cdot S_+ = 0, \tag{B.21}$$

$$\epsilon_{\mu\nu\rho\sigma} J_+^\mu J_+^\nu S_+^\sigma = 0, \tag{B.22}$$

$$\epsilon_{\mu\nu\rho\sigma} J_+^\mu J_+^\nu J_+^\sigma = 0. \tag{B.23}$$

These relations in turn suffice to show that the Feynman vertices coupling ϕ to 3 or 4 gluons, ϕggg and $\phi gggg$, do not contribute to $A_n(\phi, 1^\pm, 2^+, 3^+, \ldots, n^+)$. Terms in these vertices without a Levi-Civita tensor always attach a Minkowski metric $\eta_{\mu_1\mu_2}$ to two currents; their contribution vanishes according to eq. (B.21). (The same is true of the first term in the ϕgg vertex (B.4).) Terms containing the Levi-Civita tensor $\varepsilon_{\mu_1\mu_2\mu_3\mu_4}$ attach it directly to at least three currents; their contribution vanishes according to eqs. (B.22) and (B.23). This leaves just the contributions of the second and third terms in the ϕgg vertex B.4. They cancel against each other, just as in the case of $A_3(\phi, q_1^-, g_2^+, \bar{q}_3^+)$ above. Suppose that the quark current involving gluons 2 to $m-1$ is attached to one leg of the ϕgg vertex, and that the current involving gluons m to $n-1$ is attached to the other leg. Then the ratio analogous to eq. (B.18) is,

$$R_n^+ = \frac{i\epsilon_{\mu_1\mu_2\nu_1\nu_2}\langle\xi^-|\gamma^{\mu_1}\, \not{P}_{1,m-1}|\xi^+\rangle\langle\xi^-|\gamma^{\mu_2}\, \not{P}_{m,n-1}|\xi^+\rangle p_{1,m-1}^{\nu_1} p_{m,n-1}^{\nu_2}}{-\langle\xi^-|\, \not{P}_{m,n-1}\, \not{P}_{1,m-1}|\xi^+\rangle\langle\xi^-|\, \not{P}_{1,m-1}\, \not{P}_{m,n-1}|\xi^+\rangle} \tag{B.24}$$

$$= -1. \tag{B.25}$$

This completes the recursive proof that,

$$A_n(\phi, q_1^-, g_2^+, \ldots, g_{n-1}^+, \bar{q}_n^+) = 0. \tag{B.26}$$

A similar result holds when the quark has positive helicity.

Bibliography

[1] A. D. Martin, R. G. Roberts, W. J. Stirling and R. S. Thorne, *Estimating the effect of NNLO contributions on global parton analyses*, *Eur. Phys. J.* **C18** (2000) 117–126 [hep-ph/0007099].

[2] A. D. Martin, R. G. Roberts, W. J. Stirling and R. S. Thorne, *NNLO global parton analysis*, *Phys. Lett.* **B531** (2002) 216–224 [hep-ph/0201127].

[3] **CTEQ** Collaboration, H. L. Lai *et. al.*, *Global QCD analysis of parton structure of the nucleon: Cteq5 parton distributions*, *Eur. Phys. J.* **C12** (2000) 375–392 [hep-ph/9903282].

[4] G. Altarelli and G. Parisi, *Asymptotic freedom in parton language*, *Nucl. Phys.* **B126** (1977) 298.

[5] S. Moch, J. A. M. Vermaseren and A. Vogt, *The three-loop splitting functions in QCD: The non-singlet case*, *Nucl. Phys.* **B688** (2004) 101–134 [hep-ph/0403192].

[6] A. Vogt, S. Moch and J. A. M. Vermaseren, *The three-loop splitting functions in QCD: The singlet case*, *Nucl. Phys.* **B691** (2004) 129–181 [hep-ph/0404111].

[7] M. E. Peskin and D. V. Schroeder, *An Introduction to quantum field theory.* Addison-Wesley, 1995.

[8] J. Marsden and H. M.J., *Basic Complex Analysis.* Freeman, 1999.

[9] **Particle Data Group** Collaboration, S. Eidelman *et. al.*, *Review of particle physics*, *Phys. Lett.* **B592** (2004) 1.

[10] F. Bloch and A. Nordsieck, *Note on the radiation field of the electron*, *Phys. Rev.* **52** (1937) 54–59.

[11] T. Kinoshita, *Mass singularities of feynman amplitudes*, *J. Math. Phys.* **3** (1962) 650–677.

[12] T. D. Lee and M. Nauenberg, *Degenerate systems and mass singularities*, *Phys. Rev.* **133** (1964) B1549–B1562.

[13] W. T. Giele and E. W. N. Glover, *Higher order corrections to jet cross-sections in e^+e^- annihilation*, *Phys. Rev.* **D46** (1992) 1980–2010.

[14] Z. Kunszt, A. Signer and Z. Trocsanyi, *Singular terms of helicity amplitudes at one loop in QCD and the soft limit of the cross-sections of multiparton processes*, *Nucl. Phys.* **B420** (1994) 550–564 [hep-ph/9401294].

[15] S. Catani, *The singular behaviour of QCD amplitudes at two-loop order*, *Phys. Lett.* **B427** (1998) 161–171 [hep-ph/9802439].

[16] R. E. Cutkosky, *Singularities and discontinuities of feynman amplitudes*, *J. Math. Phys.* **1** (1960) 429–433.

[17] Z. Bern, L. J. Dixon, D. C. Dunbar and D. A. Kosower, *One loop n-point gauge theory amplitudes, unitarity and collinear limits*, *Nucl. Phys.* **B425** (1994) 217–260 [hep-ph/9403226].

[18] Z. Bern, L. J. Dixon, D. C. Dunbar and D. A. Kosower, *Fusing gauge theory tree amplitudes into loop amplitudes*, *Nucl. Phys.* **B435** (1995) 59–101 [hep-ph/9409265].

[19] Z. Bern, L. J. Dixon, D. C. Dunbar and D. A. Kosower, *Recent progress in one loop multiparton calculations*, *Nucl. Phys. Proc. Suppl.* **39BC** (1995) 146–149 [hep-ph/9409214].

[20] Z. Bern, V. Del Duca, L. J. Dixon and D. A. Kosower, *All non-maximally-helicity-violating one-loop seven-gluon amplitudes in $\mathcal{N} = 4$ super Yang-Mills theory*, *Phys. Rev.* **D71** (2005) 045006 [hep-th/0410224].

[21] Z. Bern, L. J. Dixon and D. A. Kosower, *All next-to-maximally helicity-violating one-loop gluon amplitudes in $\mathcal{N} = 4$ super Yang-Mills theory*, *Phys. Rev.* **D72** (2005) 045014 [hep-th/0412210].

[22] Z. Bern and A. G. Morgan, *Massive loop amplitudes from unitarity*, *Nucl. Phys.* **B467** (1996) 479–509 [hep-ph/9511336].

[23] Z. Bern, L. J. Dixon, D. C. Dunbar and D. A. Kosower, *One-loop self-dual and $\mathcal{N} = 4$ super Yang-Mills*, *Phys. Lett.* **B394** (1997) 105–115 [hep-th/9611127].

[24] Z. Bern, A. De Freitas, L. J. Dixon, A. Ghinculov and H. L. Wong, *QCD and QED corrections to light-by-light scattering*, *JHEP* **11** (2001) 031 [hep-ph/0109079].

[25] Z. Bern, L. J. Dixon and D. A. Kosower, *A two-loop four-gluon helicity amplitude in QCD*, *JHEP* **01** (2000) 027 [hep-ph/0001001].

[26] Z. Bern, L. J. Dixon and A. Ghinculov, *Two-loop correction to Bhabha scattering*, *Phys. Rev.* **D63** (2001) 053007 [hep-ph/0010075].

[27] Z. Bern, A. De Freitas and L. J. Dixon, *Two-loop helicity amplitudes for quark gluon scattering in QCD and gluino gluon scattering in supersymmetric Yang-Mills theory*, *JHEP* **06** (2003) 028 [hep-ph/0304168].

[28] Z. Bern, A. De Freitas and L. Dixon, *Two-loop helicity amplitudes for gluon gluon scattering in QCD and supersymmetric Yang-Mills theory*, *JHEP* **03** (2002) 018 [hep-ph/0201161].

[29] Z. Bern, A. De Freitas and L. J. Dixon, *Two-loop amplitudes for gluon fusion into two photons*, *JHEP* **09** (2001) 037 [hep-ph/0109078].

[30] Z. Bern, L. J. Dixon and D. A. Kosower, *Two-loop $g \to gg$ splitting amplitudes in QCD*, *JHEP* **08** (2004) 012 [hep-ph/0404293].

[31] Z.-G. Xiao, G. Yang and C.-J. Zhu, *The rational part of QCD amplitude I: the general formalism*, hep-ph/0607015.

[32] X. Su, Z.-G. Xiao, G. Yang and C.-J. Zhu, *The rational part of QCD amplitude II: the five-gluon*, hep-ph/0607016.

[33] Z.-G. Xiao, G. Yang and C.-J. Zhu, *The rational part of QCD amplitude III: the six-gluon*, hep-ph/0607017.

[34] F. A. Berends, R. Kleiss, P. De Causmaecker, R. Gastmans and T. T. Wu, *Single bremsstrahlung processes in gauge theories*, *Phys. Lett.* **B103** (1981) 124.

[35] P. De Causmaecker, R. Gastmans, W. Troost and T. T. Wu, *Multiple bremsstrahlung in gauge theories at high-energies. 1. general formalism for quantum electrodynamics*, *Nucl. Phys.* **B206** (1982) 53.

[36] R. Kleiss and W. J. Stirling, *Spinor techniques for calculating p anti-p $\to w^{\pm}/z^0$ + jets*, *Nucl. Phys.* **B262** (1985) 235–262.

[37] J. F. Gunion and Z. Kunszt, *Improved analytic techniques for tree graph calculations and the g g q anti-q lepton anti-lepton subprocess*, *Phys. Lett.* **B161** (1985) 333.

[38] Z. Xu, D.-H. Zhang and L. Chang, *Helicity amplitudes for multiple bremsstrahlung in massless nonabelian gauge theories*, *Nucl. Phys.* **B291** (1987) 392.

[39] F. A. Berends and W. Giele, *The six gluon process as an example of weyl-van der waerden spinor calculus*, *Nucl. Phys.* **B294** (1987) 700.

[40] M. L. Mangano, S. J. Parke and Z. Xu, *Duality and multi - gluon scattering*, *Nucl. Phys.* **B298** (1988) 653.

[41] M. L. Mangano and S. J. Parke, *Multiparton amplitudes in gauge theories*, *Phys. Rept.* **200** (1991) 301–367.

[42] E. Witten, *Perturbative gauge theory as a string theory in twistor space*, *Commun. Math. Phys.* **252** (2004) 189–258 [hep-th/0312171].

[43] S. J. Parke and T. R. Taylor, *Perturbative QCD utilizing extended supersymmetry*, *Phys. Lett.* **B157** (1985) 81.

[44] R. Penrose, *Twistor algebra*, *J. Math. Phys.* **8** (1967) 345.

[45] F. Cachazo, P. Svrcek and E. Witten, *MHV vertices and tree amplitudes in gauge theory*, *JHEP* **09** (2004) 006 [hep-th/0403047].

[46] K. Risager, *A direct proof of the CSW rules*, *JHEP* **12** (2005) 003 [hep-th/0508206].

[47] G. Georgiou and V. V. Khoze, *Tree amplitudes in gauge theory as scalar MHV diagrams*, *JHEP* **05** (2004) 070 [hep-th/0404072].

[48] G. Georgiou, E. W. N. Glover and V. V. Khoze, *Non-MHV tree amplitudes in gauge theory*, *JHEP* **07** (2004) 048 [hep-th/0407027].

[49] C.-J. Zhu, *The googly amplitudes in gauge theory*, *JHEP* **04** (2004) 032 [hep-th/0403115].

[50] J.-B. Wu and C.-J. Zhu, *MHV vertices and scattering amplitudes in gauge theory*, *JHEP* **07** (2004) 032 [hep-th/0406085].

[51] J.-B. Wu and C.-J. Zhu, *MHV vertices and fermionic scattering amplitudes in gauge theory with quarks and gluinos*, *JHEP* **09** (2004) 063 [hep-th/0406146].

[52] I. Bena, Z. Bern and D. A. Kosower, *Twistor-space recursive formulation of gauge theory amplitudes*, *Phys. Rev.* **D71** (2005) 045008 [hep-th/0406133].

[53] L. J. Dixon, E. W. N. Glover and V. V. Khoze, *MHV rules for Higgs plus multi-gluon amplitudes*, *JHEP* **12** (2004) 015 [hep-th/0411092].

[54] S. D. Badger, E. W. N. Glover and V. V. Khoze, *MHV rules for Higgs plus multi-parton amplitudes*, *JHEP* **03** (2005) 023 [hep-th/0412275].

[55] Z. Bern, D. Forde, D. A. Kosower and P. Mastrolia, *Twistor-inspired construction of electroweak vector boson currents*, *Phys. Rev.* **D72** (2005) 025006 [hep-ph/0412167].

[56] K. J. Ozeren and W. J. Stirling, *MHV techniques for QED processes*, *JHEP* **11** (2005) 016 [hep-th/0509063].

[57] T. G. Birthwright, E. W. N. Glover, V. V. Khoze and P. Marquard, *Multi-gluon collinear limits from MHV diagrams*, *JHEP* **05** (2005) 013 [hep-ph/0503063].

[58] T. G. Birthwright, E. W. N. Glover, V. V. Khoze and P. Marquard, *Collinear limits in QCD from MHV rules*, *JHEP* **07** (2005) 068 [hep-ph/0505219].

[59] D. A. Kosower, *Next-to-maximal helicity violating amplitudes in gauge theory*, *Phys. Rev.* **D71** (2005) 045007 [hep-th/0406175].

[60] F. A. Berends and W. T. Giele, *Recursive calculations for processes with n gluons*, *Nucl. Phys.* **B306** (1988) 759.

[61] F. A. Berends, W. T. Giele and H. Kuijf, *Exact expressions for processes involving a vector boson and up to five partons*, *Nucl. Phys.* **B321** (1989) 39.

[62] F. A. Berends and W. T. Giele, *Multiple soft gluon radiation in parton processes*, *Nucl. Phys.* **B313** (1989) 595.

[63] R. Roiban, M. Spradlin and A. Volovich, *Dissolving $\mathcal{N} = 4$ loop amplitudes into QCD tree amplitudes*, *Phys. Rev. Lett.* **94** (2005) 102002 [hep-th/0412265].

[64] R. Britto, F. Cachazo and B. Feng, *New recursion relations for tree amplitudes of gluons*, *Nucl. Phys.* **B715** (2005) 499–522 [hep-th/0412308].

[65] R. Britto, F. Cachazo, B. Feng and E. Witten, *Direct proof of tree-level recursion relation in Yang-Mills theory*, *Phys. Rev. Lett.* **94** (2005) 181602 [`hep-th/0501052`].

[66] M.-x. Luo and C.-k. Wen, *Compact formulas for all tree amplitudes of six partons*, *Phys. Rev.* **D71** (2005) 091501 [`hep-th/0502009`].

[67] M.-x. Luo and C.-k. Wen, *Recursion relations for tree amplitudes in super gauge theories*, *JHEP* **03** (2005) 004 [`hep-th/0501121`].

[68] J. Bedford, A. Brandhuber, B. J. Spence and G. Travaglini, *A recursion relation for gravity amplitudes*, *Nucl. Phys.* **B721** (2005) 98–110 [`hep-th/0502146`].

[69] F. Cachazo and P. Svrcek, *Tree level recursion relations in general relativity*, `hep-th/0502160`.

[70] S. D. Badger, E. W. N. Glover, V. V. Khoze and P. Svrcek, *Recursion relations for gauge theory amplitudes with massive particles*, *JHEP* **07** (2005) 025 [`hep-th/0504159`].

[71] S. D. Badger, E. W. N. Glover and V. V. Khoze, *Recursion relations for gauge theory amplitudes with massive vector bosons and fermions*, *JHEP* **01** (2006) 066 [`hep-th/0507161`].

[72] D. Forde and D. A. Kosower, *All-multiplicity amplitudes with massive scalars*, *Phys. Rev.* **D73** (2006) 065007 [`hep-th/0507292`].

[73] C. Quigley and M. Rozali, *Recursion relations, helicity amplitudes and dimensional regularization*, *JHEP* **03** (2006) 004 [`hep-ph/0510148`].

[74] K. J. Ozeren and W. J. Stirling, *Scattering amplitudes with massive fermions using BCFW recursion*, `hep-ph/0603071`.

[75] R. Eden, P. Landshoff, D. Olive and J. Polkinghorne, *The Analytic S-Matrix*. Cambridge University Press, 1966.

[76] R. Britto, F. Cachazo and B. Feng, *Generalized unitarity and one-loop amplitudes in $\mathcal{N}=4$ super Yang-Mills*, *Nucl. Phys.* **B725** (2005) 275–305 [hep-th/0412103].

[77] S. J. Bidder, N. E. J. Bjerrum-Bohr, D. C. Dunbar and W. B. Perkins, *One-loop gluon scattering amplitudes in theories with $\mathcal{N}<4$ supersymmetries*, *Phys. Lett.* **B612** (2005) 75–88 [hep-th/0502028].

[78] R. Britto, E. Buchbinder, F. Cachazo and B. Feng, *One-loop amplitudes of gluons in SQCD*, *Phys. Rev.* **D72** (2005) 065012 [hep-ph/0503132].

[79] S. J. Bidder, D. C. Dunbar and W. B. Perkins, *Supersymmetric ward identities and NMHV amplitudes involving gluinos*, *JHEP* **08** (2005) 055 [hep-th/0505249].

[80] K. Risager, S. J. Bidder and W. B. Perkins, *One-loop NMHV amplitudes involving gluinos and scalars in $\mathcal{N}=4$ gauge theory*, *JHEP* **10** (2005) 003 [hep-th/0507170].

[81] R. Britto, B. Feng and P. Mastrolia, *The cut-constructible part of QCD amplitudes*, *Phys. Rev.* **D73** (2006) 105004 [hep-ph/0602178].

[82] A. Brandhuber, S. McNamara, B. Spence and G. Travaglini, *Loop amplitudes in pure Yang-Mills from generalised unitarity*, *JHEP* **10** (2005) 011 [hep-th/0506068].

[83] S. Giombi, R. Ricci, D. Robles-Llana and D. Trancanelli, *A note on twistor gravity amplitudes*, *JHEP* **07** (2004) 059 [hep-th/0405086].

[84] N. Berkovits and E. Witten, *Conformal supergravity in twistor-string theory*, *JHEP* **08** (2004) 009 [hep-th/0406051].

[85] F. Cachazo, P. Svrcek and E. Witten, *Twistor space structure of one-loop amplitudes in gauge theory*, *JHEP* **10** (2004) 074 [hep-th/0406177].

[86] F. Cachazo, P. Svrcek and E. Witten, *Gauge theory amplitudes in twistor space and holomorphic anomaly*, *JHEP* **10** (2004) 077 [hep-th/0409245].

[87] F. Cachazo, *Holomorphic anomaly of unitarity cuts and one-loop gauge theory amplitudes*, hep-th/0410077.

[88] R. Britto, F. Cachazo and B. Feng, *Computing one-loop amplitudes from the holomorphic anomaly of unitarity cuts*, *Phys. Rev.* **D71** (2005) 025012 [hep-th/0410179].

[89] I. Bena, Z. Bern, D. A. Kosower and R. Roiban, *Loops in twistor space*, *Phys. Rev.* **D71** (2005) 106010 [hep-th/0410054].

[90] A. Brandhuber, B. Spence and G. Travaglini, *One-loop gauge theory amplitudes in $\mathcal{N}=4$ super Yang-Mills from MHV vertices*, *Nucl. Phys.* **B706** (2005) 150–180 [hep-th/0407214].

[91] J. Bedford, A. Brandhuber, B. Spence and G. Travaglini, *A twistor approach to one-loop amplitudes in $\mathcal{N}=1$ supersymmetric Yang-Mills theory*, *Nucl. Phys.* **B706** (2005) 100–126 [hep-th/0410280].

[92] J. Bedford, A. Brandhuber, B. Spence and G. Travaglini, *Non-supersymmetric loop amplitudes and MHV vertices*, *Nucl. Phys.* **B712** (2005) 59–85 [hep-th/0412108].

[93] R. Britto, F. Cachazo and B. Feng, *Coplanarity in twistor space of $\mathcal{N}=4$ next-to-MHV one-loop amplitude coefficients*, *Phys. Lett.* **B611** (2005) 167–172 [hep-th/0411107].

[94] S. J. Bidder, N. E. J. Bjerrum-Bohr, D. C. Dunbar and W. B. Perkins, *Twistor space structure of the box coefficients of $\mathcal{N}=1$ one-loop amplitudes*, *Phys. Lett.* **B608** (2005) 151–163 [hep-th/0412023].

[95] S. J. Bidder, N. E. J. Bjerrum-Bohr, L. J. Dixon and D. C. Dunbar, *$\mathcal{N}=1$ supersymmetric one-loop amplitudes and the holomorphic anomaly of unitarity cuts*, *Phys. Lett.* **B606** (2005) 189–201 [hep-th/0410296].

[96] Z. Bern, L. J. Dixon and D. A. Kosower, *On-shell recurrence relations for one-loop QCD amplitudes*, *Phys. Rev.* **D71** (2005) 105013 [hep-th/0501240].

[97] Z. Bern, L. J. Dixon and D. A. Kosower, *The last of the finite loop amplitudes in QCD*, *Phys. Rev.* **D72** (2005) 125003 [hep-ph/0505055].

[98] Z. Bern, L. J. Dixon and D. A. Kosower, *Bootstrapping multi-parton loop amplitudes in QCD*, *Phys. Rev.* **D73** (2006) 065013 [hep-ph/0507005].

[99] D. Forde and D. A. Kosower, *All-multiplicity one-loop corrections to MHV amplitudes in QCD*, *Phys. Rev.* **D73** (2006) 061701 [hep-ph/0509358].

[100] C. F. Berger, Z. Bern, L. J. Dixon, D. Forde and D. A. Kosower, *Bootstrapping one-loop QCD amplitudes with general helicities*, hep-ph/0604195.

[101] C. F. Berger, Z. Bern, L. J. Dixon, D. Forde and D. A. Kosower, *All one-loop maximally helicity violating gluonic amplitudes in QCD*, hep-ph/0607014.

[102] Z. Bern and G. Chalmers, *Factorization in one loop gauge theory*, *Nucl. Phys.* **B447** (1995) 465–518 [hep-ph/9503236].

[103] Z. Bern, N. E. J. Bjerrum-Bohr, D. C. Dunbar and H. Ita, *Recursive calculation of one-loop QCD integral coefficients*, hep-ph/0507019.

[104] J. F. Gunion, H. E. Haber, G. L. Kane and S. Dawson, *The Higgs Hunter's Guide*. Addison-Wesley, 1990.

[105] P. B. Renton, *Electroweak fits and constraints on the Higgs mass*, hep-ph/0410177.

[106] A. Djouadi, M. Spira and P. M. Zerwas, *Production of Higgs bosons in proton colliders: QCD corrections*, *Phys. Lett.* **B264** (1991) 440–446.

[107] S. Dawson, *Radiative corrections to Higgs boson production*, *Nucl. Phys.* **B359** (1991) 283–300.

[108] D. Graudenz, M. Spira and P. M. Zerwas, *QCD corrections to Higgs boson production at proton proton colliders*, *Phys. Rev. Lett.* **70** (1993) 1372–1375.

[109] M. Spira, A. Djouadi, D. Graudenz and P. M. Zerwas, *Higgs boson production at the LHC*, *Nucl. Phys.* **B453** (1995) 17–82 [`hep-ph/9504378`].

[110] T. Inami, T. Kubota and Y. Okada, *Effective gauge theory and the effect of heavy quarks in Higgs boson decays*, *Z. Phys.* **C18** (1983) 69.

[111] K. G. Chetyrkin, B. A. Kniehl and M. Steinhauser, *Decoupling relations to $\mathcal{O}(\alpha(s)^3)$ and their connection to low-energy theorems*, *Nucl. Phys.* **B510** (1998) 61–87 [`hep-ph/9708255`].

[112] S. Dawson and R. P. Kauffman, *Higgs boson plus multi - jet rates at the SSC*, *Phys. Rev. Lett.* **68** (1992) 2273–2276.

[113] R. P. Kauffman, S. V. Desai and D. Risal, *Production of a Higgs boson plus two jets in hadronic collisions*, *Phys. Rev.* **D55** (1997) 4005–4015 [`hep-ph/9610541`].

[114] V. Del Duca, A. Frizzo and F. Maltoni, *Higgs boson production in association with three jets*, *JHEP* **05** (2004) 064 [`hep-ph/0404013`].

[115] F. Caravaglios and M. Moretti, *An algorithm to compute born scattering amplitudes without Feynman graphs*, *Phys. Lett.* **B358** (1995) 332–338 [`hep-ph/9507237`].

[116] M. L. Mangano, M. Moretti, F. Piccinini, R. Pittau and A. D. Polosa, *ALPGEN, a generator for hard multiparton processes in hadronic collisions*, *JHEP* **07** (2003) 001 [`hep-ph/0206293`].

[117] T. Stelzer and W. F. Long, *Automatic generation of tree level helicity amplitudes*, *Comput. Phys. Commun.* **81** (1994) 357–371 [`hep-ph/9401258`].

[118] F. Maltoni and T. Stelzer, *MadEvent: Automatic event generation with madgraph*, *JHEP* **02** (2003) 027 [`hep-ph/0208156`].

[119] M. T. Grisaru, H. N. Pendleton and P. van Nieuwenhuizen, *Supergravity and the S-matrix*, *Phys. Rev.* **D15** (1977) 996.

[120] M. T. Grisaru and H. N. Pendleton, *Some properties of scattering amplitudes in supersymmetric theories*, *Nucl. Phys.* **B124** (1977) 81.

[121] S. J. Parke and T. R. Taylor, *An amplitude for n gluon scattering*, *Phys. Rev. Lett.* **56** (1986) 2459.

[122] L. J. Dixon, *Recent developments in perturbative QCD*, `hep-ph/0507064`.

[123] V. P. Nair, *A current algebra for some gauge theory amplitudes*, *Phys. Lett.* **B214** (1988) 215.

[124] V. V. Khoze, *Gauge theory amplitudes, scalar graphs and twistor space*, `hep-th/0408233`.

[125] D. A. Kosower, *Light cone recurrence relations for QCD amplitudes*, *Nucl. Phys.* **B335** (1990) 23.

[126] P. Ferrario, G. Rodrigo and P. Talavera, *Compact multigluonic scattering amplitudes with heavy scalars and fermions*, *Phys. Rev. Lett.* **96** (2006) 182001 [`hep-th/0602043`].

[127] G. Rodrigo, *Multigluonic scattering amplitudes of heavy quarks*, *JHEP* **09** (2005) 079 [`hep-ph/0508138`].

[128] L. J. Dixon, Z. Kunszt and A. Signer, *Helicity amplitudes for $\mathcal{O}(\alpha(s))$ production of W^+W^-, $W^\pm Z$, ZZ, $W^\pm\gamma$, or $Z\gamma$ pairs at hadron colliders*, *Nucl. Phys.* **B531** (1998) 3–23 [`hep-ph/9803250`].

[129] S. D. Badger and E. W. N. Glover, *One-loop helicity amplitudes for $H \to$ gluons: The all- minus configuration*, `hep-ph/0607139`.

[130] C. F. Berger, V. Del Duca and L. J. Dixon, *Recursive construction of higgs+multiparton loop amplitudes: The last of the ϕ-nite loop amplitudes*, hep-ph/0608180.

[131] R. K. Ellis, W. T. Giele and G. Zanderighi, *Semi-numerical evaluation of one-loop corrections*, *Phys. Rev.* **D73** (2006) 014027 [hep-ph/0508308].

[132] R. K. Ellis, W. T. Giele and G. Zanderighi, *The one-loop amplitude for six-gluon scattering*, *JHEP* **05** (2006) 027 [hep-ph/0602185].

[133] C. Anastasiou and A. Daleo, *Numerical evaluation of loop integrals*, hep-ph/0511176.

[134] T. Binoth, J. P. Guillet, G. Heinrich, E. Pilon and C. Schubert, *An algebraic / numerical formalism for one-loop multi-leg amplitudes*, *JHEP* **10** (2005) 015 [hep-ph/0504267].

[135] R. K. Ellis, W. T. Giele and G. Zanderighi, *Virtual qcd corrections to higgs boson plus four parton processes*, *Phys. Rev.* **D72** (2005) 054018 [hep-ph/0506196].

[136] W. L. van Neerven, *Dimensional regularization of mass and infrared singularities in two loop on-shell vertex functions*, *Nucl. Phys.* **B268** (1986) 453.

[137] C. R. Schmidt, *$h \to ggg(gq\bar{q})$ at two loops in the large-m(t) limit*, *Phys. Lett.* **B413** (1997) 391–395 [hep-ph/9707448].

[138] D. A. Kosower, *All-order collinear behavior in gauge theories*, *Nucl. Phys.* **B552** (1999) 319–336 [hep-ph/9901201].

[139] Z. Bern, V. Del Duca, W. B. Kilgore and C. R. Schmidt, *The infrared behavior of one-loop QCD amplitudes at next-to-next-to-leading order*, *Phys. Rev.* **D60** (1999) 116001 [hep-ph/9903516].

[140] A. Brandhuber, B. Spence and G. Travaglini, *From trees to loops and back*, *JHEP* **01** (2006) 142 [hep-th/0510253].

[141] Z. Kunszt, A. Signer and Z. Trocsanyi, *One loop helicity amplitudes for all $2 \to 2$ processes in QCD and $\mathcal{N} = 1$ supersymmetric yang-mills theory*, *Nucl. Phys.* **B411** (1994) 397–442 [hep-ph/9305239].

[142] M. Dinsdale, M. Ternick and S. Weinzierl, *A comparison of efficient methods for the computation of born gluon amplitudes*, *JHEP* **03** (2006) 056 [hep-ph/0602204].

[143] C. Duhr, S. Hoche and F. Maltoni, *Color-dressed recursive relations for multi-parton amplitudes*, hep-ph/0607057.

[144] Z. Bern, N. E. J. Bjerrum-Bohr and D. C. Dunbar, *Inherited twistor-space structure of gravity loop amplitudes*, *JHEP* **05** (2005) 056 [hep-th/0501137].

[145] N. E. J. Bjerrum-Bohr, D. C. Dunbar, H. Ita, W. B. Perkins and K. Risager, *MHV-vertices for gravity amplitudes*, *JHEP* **01** (2006) 009 [hep-th/0509016].

[146] N. E. J. Bjerrum-Bohr, D. C. Dunbar and H. Ita, *Six-point one-loop $\mathcal{N} = 8$ supergravity NMHV amplitudes and their IR behaviour*, *Phys. Lett.* **B621** (2005) 183–194 [hep-th/0503102].

[147] Z. Bern, L. J. Dixon and V. A. Smirnov, *Iteration of planar amplitudes in maximally supersymmetric Yang-Mills theory at three loops and beyond*, *Phys. Rev.* **D72** (2005) 085001 [hep-th/0505205].

[148] G. 't Hooft and M. J. G. Veltman, *Regularization and renormalization of gauge fields*, *Nucl. Phys.* **B44** (1972) 189–213.

[149] C. G. Bollini and J. J. Giambiagi, *Lowest order divergent graphs in nu-dimensional space*, *Phys. Lett.* **B40** (1972) 566–568.

[150] J. F. Ashmore, *A method of gauge invariant regularization*, *Lett. Nuovo Cim.* **4** (1972) 289–290.

[151] G. M. Cicuta and E. Montaldi, *Analytic renormalization via continuous space dimension*, *Nuovo Cim. Lett.* **4** (1972) 329–332.

[152] J. C. Collins, *Renormalization.* Cambridge Univ. Press, 1984.

[153] G. Mahlon, *Multi - gluon helicity amplitudes involving a quark loop*, *Phys. Rev.* **D49** (1994) 4438–4453 [hep-ph/9312276].